NAZARBAYEV UNIVERSITY

SCHOOL OF ENGINEERING AND DIGITAL SCIENCES

DEPARTMENT OF CIVIL AND ENVIRONMENTAL ENGINEERING

ENG 400: CAPSTONE II

DESIGN OF 12-STORY HIGH-RISE RESIDENTIAL BUILDING IN LOS ANGELES, CALIFORNIA, USA

Capstone Project II

Group 7 members:

Aidana Ordabayeva	201947442
Kamila Nuraliyeva	202131930
Madiyar Assylkhanov	201992008
Dias Mukhanov	201980346
Aidos Kyrkynbay	201923980
Assylzada Urazova	201971028

Date of Submission: April 25

Spring 2025

DECLARATION

By signing below, we hereby declare that this report entitled "*Design of 12-storey high-rise residential building in Los Angeles, California, USA"* is the result of our own project work except for quotations and citations which have been duly acknowledged. We also declare that it has not been previously or concurrently submitted for any other degree at Nazarbayev University.

Aidana Ordabayeva 

Kamila Nuraliyeva 

Madiyar Assylkhanov 

Dias Mukhanov 

Aidos Kyrkynbay 

Assylzada Urazova 

Date of submission: April 25

Spring 2025

ACKNOWLEDGEMENTS

We express our heartfelt gratitude to everyone who supported us during the completion of this capstone project, *«Design of 12-storey high-rise residential building in Los Angeles, California, USA»*.

We are especially thankful to our academic supervisors and professors, Mert Guney, Dichuan Zhang, Shazim Memon, Chang-Seon Shon, Alfrendo Satyanaga, Sung-Woo Moon, Abid Nadeem, Ferhat Karaca, and Jong Kim, for their guidance and constructive feedback, and to the faculty of the Civil and Environmental Engineering Department for their assistance throughout our coursework and this project.

Sincerely,

Team 7

Date: 25.04.2025

ETHICAL CONSIDERATIONS

Ethical principles played a crucial role in the designing process of this project to meet all the requirements from all parts (structural, geotechnical, environmental and construction management) without compromising integrity. The project adheres strictly to US and international standards. The used regulation codes include International Building Code (IBC 2024), American Concrete Institute (ACI) guidelines, and LEED certification requirements, in order to emphasise accountability in every phase.

During the working process, as a team we recognized the importance of shared responsibility and collaboration. The collaboration and distribution of the work was relatively equal, taking into account the preferences of each member of our team. Thus, each member was responsible for their respective tasks, ensuring the accuracy, reliability and credibility of the work. The individual analysis was balanced with continuous peer review, which in turn enabled us to identify potential issues early and refine our methods collectively. Furthermore, this approach fostered a culture of mutual support and understanding of the project, also enhancing the quality of the work and our learning experience.

In addition, integrity was a crucial part of the team's approach, thus ensuring and requiring transparency in all parts of the project. We ensured that each team member clearly documented their methodologies and assumptions in the work. Furthermore, the plagiarism or misrepresentation of information was strictly avoided by our team.

The collaborative nature of this project didn’t just elevate its overall quality - it also became a valuable learning journey. Through teamwork, we deepened our understanding of ethical responsibility, recognizing the importance to integrate these principles into every aspect of engineering practice. By committing to integrity, transparency, and collaboration, we ensured that this capstone project reflects not only technical excellence but also our dedication to the ethical principles that define responsible engineering practices.

ABSTRACT

This report aims on the design of a 12-story high-rise residential building located at 6435 Wilshire Boulevard in Los Angeles, California. This region is marked by rapid urban growth and significant seismic activity. The project responds to increasing housing demands with a multidisciplinary design strategy that integrates architectural planning, structural analysis, geotechnical investigation, environmental engineering (drainage system), and construction management. The building includes 12 residential levels with one basement level with a total 82 residential units. The structural and geotechnical components were developed in compliance with IBC, ASCE, and local Los Angeles building codes, ensuring the structure can withstand lateral forces from both wind and earthquakes. Site-specific soil properties were evaluated using advanced tools such as PLAXIS and Geo5 to perform liquefaction analysis, site response modeling, and an adequate foundation design. Furthermore, sustainability goals guided the implementation of LEED-compliant features focused on water efficiency, energy performance, and environmental impact mitigation. The project also includes a detailed construction management plan, encompassing cost estimation, scheduling, risk assessment, and safety strategies, with the completion target set for 2026.

Keywords: high-rise building, Wilshire Boulevard, sustainable design, seismic design, structural engineering, foundation analysis, LEED, project planning.

Table of Contents

List of Tables

List of Figures

1. Introduction

This project aims to design a 12-storey high-rise residential building in Los Angeles city. The report will show the step-by-step development, as well as considerations of risks, loads and design specifications. The exact address of the site, where the building will be located is 6435 Wilshire Blvd, Los Angeles, California, USA. The building is located in a strong wind, high seismic area that needs to be considered in the design of the building, especially its structural part. Gravity and lateral loads, including dead, live, snow, wind, and seismic loads, will be assessed by the structural analysis. Additionally, the design seeks to comply with sustainability guidelines set forth by Leadership in Energy and Environmental Design (LEED). Furthermore, considering the seismic characteristics, the foundation design should be appropriately designed from the geotechnical part. Therefore, the study will evaluate different foundation types from a geotechnical standpoint in order to determine which is best for a 12-storey residential project. In addition, the water sewage system will be covered in the environmental part, offering suitable and effective stormwater and drainage systems. A detailed project schedule will be set up, and the scope will be precisely defined from the construction management part. Overall, the project is divided into 4 sections, with people responsible for its completion. The table of responsibilities is presented below:

Table 1.1. Job distribution

Section	Weight	Members responsible
Structural & Architectural	40	Kamila Nuraliyeva Madiyar Assylkhanov
Geotechnical	35	Aidana Ordabayeva Assylzada Urazova
Environmental	15	Aidos Kyrkynbay
Construction Management	10	Dias Mukhanov

1.1. Objectives

The objectives of this project are:

- To perform site response analysis using the PLAXIS2D software;
- To conduct deformation analysis using PLAXIS3D software;
- To design sheet pile by applying Geo5 software;
- To propose a detailed construction procedure;
- To ascertain the building's construction management strategy;
- To demonstrate the building's qualification for LEED Silver through sustainable design;
- To develop a sustainable drainage system that meets environmental and regulatory requirements;

1.2. Problem Statement

Los Angeles' (LA) population is gradually expanding and is estimated to increase up to 4.3 million people by 2029 (Los Angeles City Planning, 2022). The city is undergoing urbanisation of the city planning by replacing most old buildings with new multi-unit housing to accommodate the needs of the local population. According to the report provided by the Department of City Planning, more than half of the new buildings built between the periods of 2010 and 2019 have 50 or more units. This shows the relevance of multifamily residential buildings in LA, which is the exact reason why the project was decided to focus on building the residential building.

2. Architectural Design

2.1. Overview of the Residential Building

The high rise residential building with commercial premises on the first floor and open terrace on the fourth floor. The fourth floor contains a cinema room, fitness section and lounge. The future building will be located in Los-Angeles city, California, USA. The first floor has 7 commercial premises, 9 apartments on 2-3 floors and 8 apartments on 5-12 floors. The total number of apartments is 82.

2.2. Site selection

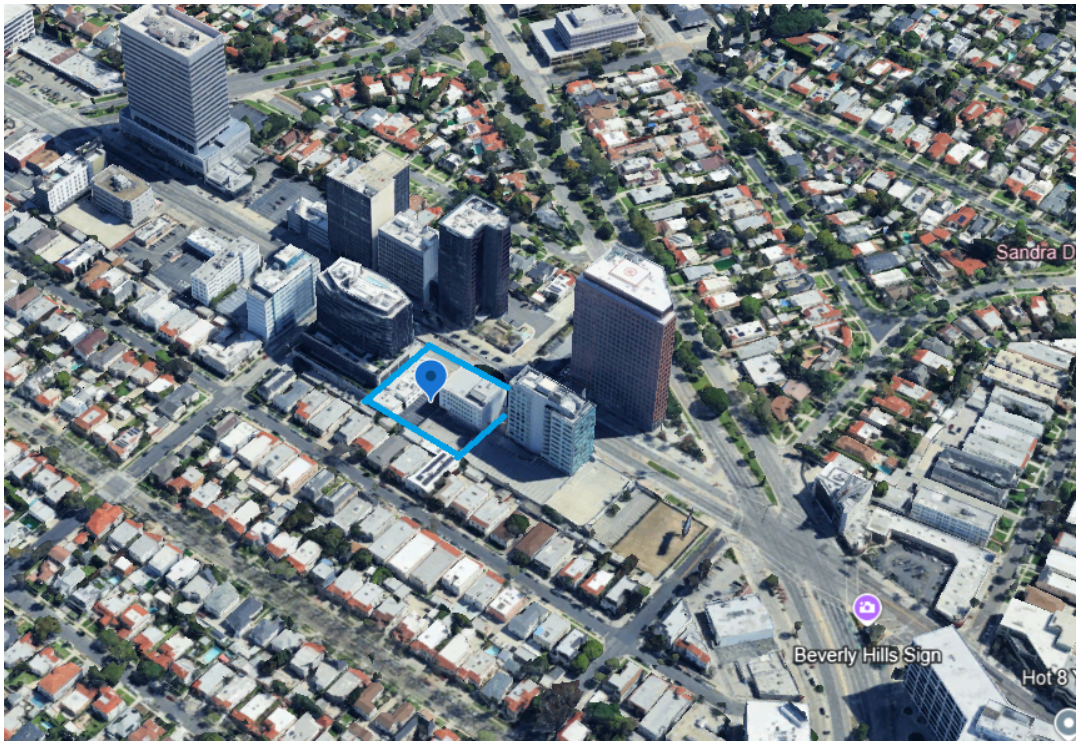

Figure 2.1. Selected site on 3D map (taken from Google Earth)

The site is located at 6435 Wilshire Boulevard, Los Angeles City, California State, USA. In the last few decades, Los Angeles has grown tremendously. It has therefore increased the need for housing within the urban centre.

There are a number of key factors that reveal why this site is in an excellent location for building a 12-story high-rise residential building. Wilshire Street is one of the main streets in Los Angeles, and the site is located in the Mid-Wilshire and Miracle Mile neighbourhoods, which makes the location highly desirable. The area is near the business districts and cultural

landmarks, increasing its appeal to potential residents. Also, Wilshire Blvd is on a major transit route and thus provides easy access to bus lines. The aforementioned aspects have transformed this place into an attractive location for new residential developments. From a broader perspective, population growth coupled with housing shortages thus creates demand conditions such that high-rise building construction becomes requisite to meet the needs of a burgeoning city population.

2.3. Site Analysis

2.3.1. Climate-responsive design and site-specific variables

It is crucial to use climatic data to inform sustainable and energy-efficient architectural design for residential development on Wilshire Boulevard in Los Angeles, assuring comfort while lowering dependency on artificial energy. Los Angeles has a wide range of temperatures throughout the year, which influences design possibilities for thermal comfort and energy efficiency. The warmest months are July and August, with temperatures reaching 39°C, necessitating heat gain-reduction strategies. Whereas the coldest temperatures come in December and January, with the lowest reaching 3°C, effective heating systems are essential to be comfortable. Overall, temperatures range from 11°C to 24°C, emphasising the significance of adaptable thermal design to account for seasonal variations (NOAA, 2023).

According to the Meteoblue (2024), southwesterly winds, particularly warm Santa Ana winds, occur mostly in the autumn and winter. Winds are generally light, however, significant gusts can occur at certain times of the year, altering ventilation strategies. Natural ventilation may be done by arranging building openings to take advantage of prevailing winds, which eliminates the need for mechanical cooling. It should be considered to carefully position landscape and structural obstacles to protect from strong winds and optimize passive cooling.

2.3.2. Historical background

The five-story building located at 6435 Wilshire Blvd, LA, CA was built in 1951. There are also 16-story apartments and 12-story medical buildings being planned to be constructed nearby (Sharp, 2021). The property is located near restaurants and different facilities, which makes this location convenient for residents (LoopNet, n.d.).

Solar access: The duration of the sun is 12 hours 35 minutes and the shadow length during the day is 0.57 m in the noon (SunCalc, 2024). The visual representation of the solar data is given in Figure 2.2.

2.3.3. Orientation

The front of the building is facing south with a slight turn to the southwest, meaning that all sides, except the back, have natural sunlight throughout the day. This should be considered in the design of windows and floors.

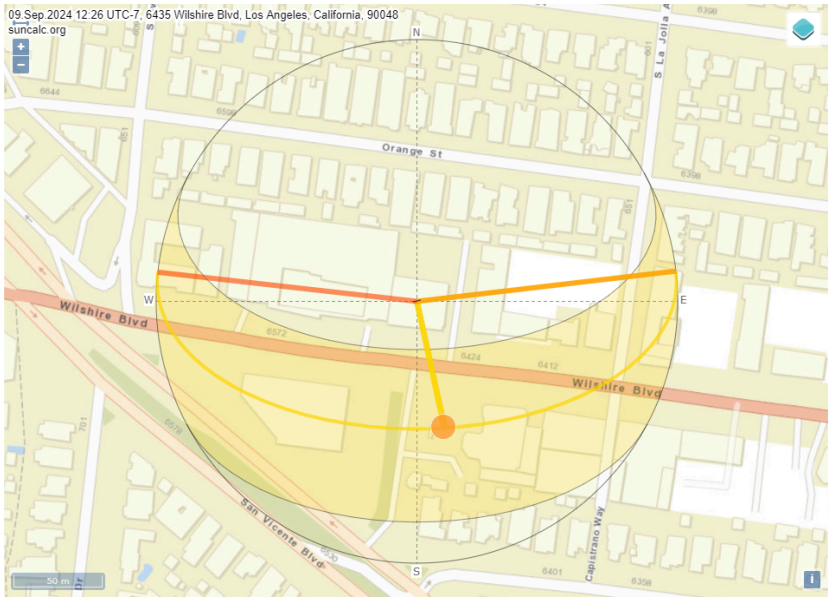

Figure 2.2. The direction of the sun at the chosen location (taken from Suncalc.org)

2.3.4. Cool breeze access

Since LA is located near the ocean, there will always be a sea breeze. The hot weather results in the occurrence of the sea breeze, which cools the air in the nearby area. The land surface heats up faster compared to the water. This results in the shift of the cool air to the sun due to its lighter weight replacing the hot air (NDBC, n. d.).

2.3.5. Site survey

The site is located near several high-rise buildings, with one of them being a 23-storey office building located right across the street. This might create the problem of being

overshadowed by the opposite building but it is located on the southwest side of our site, and overshadowing will most likely occur during the winter evenings. Furthermore, a 12-storey building is located on the right (west) of the site, which might block the light during sunsets. There is a slight slope from north to south of the site (Irvine Geotechnical, 2021). The geotechnical report has indicated that there are two borings, with the fill consisting of sandy clay and alluvium below the fill. Each borehole was drilled up to 18.3 and 24.4 metres (60 and 80 feet), providing information on soil layers for each depth. The soil layers ranged from medium dense to dense and firm to stiff (clay).

2.3.6. Access to transport

Wilshire Boulevard is home to a number of tall buildings, the consulates, and some of the most well-known institutions in an otherwise level city. It also serves as the most prominent "skyline" outside of downtown. Eventually, a subway will traverse the whole length of this multicultural boulevard, carrying passengers from east to west. The figure below represents the availability of transportation to the selected site.

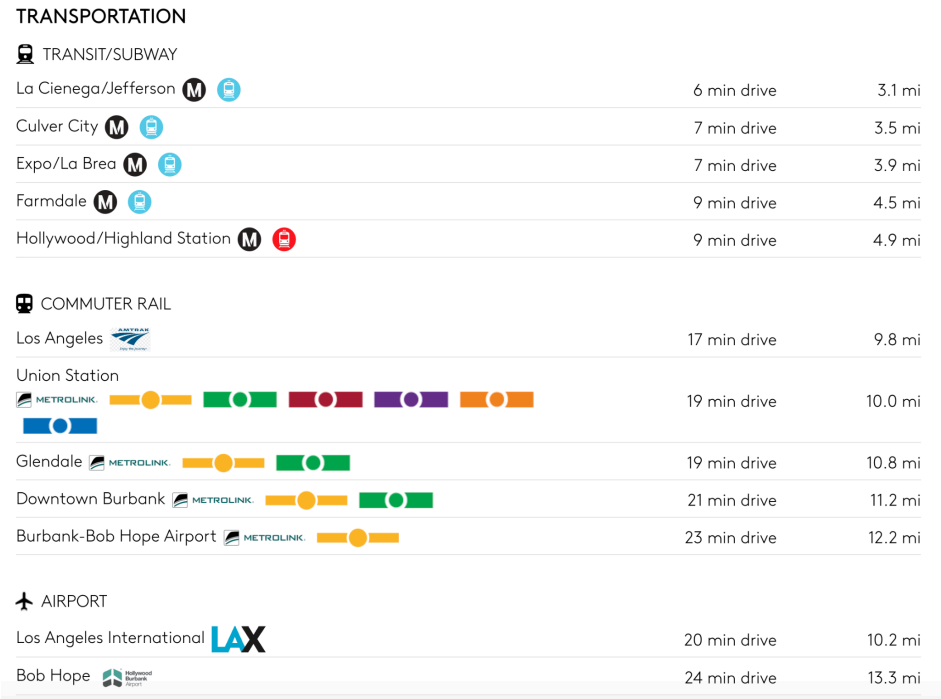

Figure 2.3. Transportation near the area (taken from Loopnet)

2.3.7. Bushfire risks

Urban-wildland interfaces (WUI) are locations that abut urban environments with a higher risk of wildfires. These areas are found mostly in the hills and mountains that surround Los Angeles. This includes regions such as the Santa Monica Mountains and the San Gabriel Mountains. The Mediterranean climate of southern California is usually described as scorching, dry summers and warm, rainy winters. Thus, there is a higher risk of fire during the dry season, particularly when the Santa Ana winds are present and can spread flames quickly.

The California Department of Forestry and Fire Protection, or Cal Fire, reports that there have been several big wildfires in Los Angeles County, especially in 2018 and 2020. In 2018, the Woolsey Fire damaged thousands of houses and scorched over 96,000 acres. In recent times, California has had many megafires that have severely damaged property, human lives, and the state's economy (1). Over 9,600 fires occurred in 2020 alone, costing the economy billions of dollars in damages (2). Apart from the financial and societal consequences, it is estimated that wildland fires are responsible for 32–44% of particulate matter (PM2.5) emissions with an aerodynamic diameter of less than 2.5 μm, making them the primary source of particle contamination in the US (3).

2.3.8. Stormwater drainage

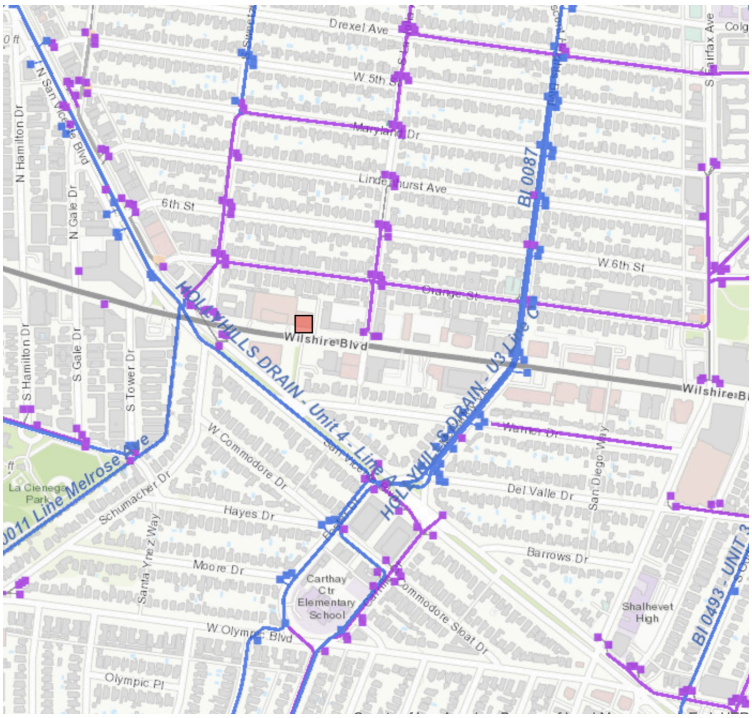

Figure 2.4. Stormwater drainage map (taken from Los Angeles County Public Works)

2.3.9. Services

1. Electricity

   Supplier: Los Angeles Department of Water and Power (LADWP)

   With over 1.5 million users, LADWP is the largest municipal utility in the United States. It provides power to these consumers. Their main areas of attention are energy efficiency and renewable energy projects.

2. Natural Gas

   Supplier: Southern California Gas Company (SoCalGas)

   The biggest distributor of natural gas in the United States is SoCalGas. In addition to offering natural gas for cooking, heating, and hot water, they also support renewable and energy-efficient gas initiatives.

3. Water

   Supplier: Los Angeles Department of Water and Power (LADWP)

   Water supplied by LADWP comes from nearby aqueducts and reservoirs. They are in charge of encouraging water saving initiatives and preserving the quality of the water.

   The Mono Lake Basin, the east slopes of the southern Sierra, and reservoirs are the sources of water for the aqueducts constructed by the City of Los Angeles. Water from the eastern Sierra's Owens River is transported by a 223-mile aqueduct that was finished in 1913 and is a key source of water supply for Los Angeles. The water system gained an additional 50% capacity in 1970 with the completion of a second aqueduct. An average of 430 million gallons are delivered to the city daily by the two aqueducts(4).

4. Sewage

   Supplier: City of Los Angeles Bureau of Sanitation

   Overview: The sewage and wastewater systems of Los Angeles are overseen by the Bureau of Sanitation. They guarantee that wastewater is properly treated and disposed of in order to safeguard the environment and public health.

5. Telephone and Internet

   Supplier: Various providers, including AT&T, Verizon, and Spectrum.

   Overview: Internet, mobile, and landline services are provided in the region by several telecom providers. Availability could differ depending on the supplier.

2.4. Leadership in Energy and Environmental Design (LEED)

The U.S. Green Building Council created LEED as an international green building evaluation system for structures across the globe. The LEED rating system helps buildings maintain environmentally beneficial construction by promoting efficient land use and preserving resources while respecting environmental protection provisions. The project seeks to incorporate sustainability practices through high-impact measures focused on operations and design along with construction implementation for both environmental and LEED standards. However, mere certification will not be enough; actual sustainability comes through efficient energy management, high-performance materials, and state-of-the-art water-saving techniques.

2.4.1. Key Sustainable Design Features

The proposed building design meets LEED requirements by implementing various environmental strategies from different categories.

1) Energy Efficiency:

LED lighting together with daylight sensors along with Energy-efficient HVAC systems were installed to reduce energy consumption. Energy monitoring systems implemented in the building provide time-based information analysis. The tower will get its supply of renewable energy from the rooftop solar panels installed on top.

2) Water Conservation:

Building water efficiency takes shape through the installment of low-flow toilets as well as faucets and showerheads. A drip irrigation system delivers water specifically to native and drought-tolerant plants in outside land areas. The use of reclaimed water provides non-potable requirements that reduces the overall quantity of water needed.

3) Sustainable Site Planning:

Placing the structure in a dense urban core with adjacent shops and educational institutions and public transportation services allows residents to reduce their dependence on car travel. Bicycle facilities available together with a minimal parking area promote eco-friendly transportation choices. The property area offers open fields alongside facilities for collecting rainwater.

4) Materials and Resources:

Materials selected for the construction met environmental footprint requirements along with preferences toward recycled and locally available products. The site implements a waste management system that works to decrease landfill requirements during the construction stage.

5) Indoor Environmental Quality:

Volatile organic compounds (VOC) materials in the building remain at very low levels to improve internal air quality. Design elements of this project enhance natural light exposure along with improved temperature conditions while providing residents with outdoor scenery views. Real ventilation systems should take preference over artificial air cooling when available.

2.4.2. Site and Community Impact

The development lies within a developed Los Angeles neighborhood that also has commercial, residential, and retail areas. This reduces urban sprawl and optimizes the usage of existing infrastructure. Public transport links such as numerous nearby bus stations make it readily accessible for the dwellers to commute to the rest of the city with the added benefit of lower vehicle emissions.

The design of the site incorporates accessible green space to encourage interaction with the external environment while retaining a small building footprint. Such decisions promote the health of the inhabitants and the external environment.

2.4.3. Key Considerations for LEED Certification

To qualify for LEED certification, a development must comply with specific prerequisites and earn points for its performance in terms of sustainability. There are four levels in the certification scheme:

Table 2.1. LEED Certification Levels and Point Requirements

	Points Required	Focus Areas
Certified	40-49 points	Basic sustainability measures
Silver	50-59 points	Enhanced energy and resource efficiency
Gold	60-79 points	High-level sustainability integration
Platinum	80+ points	Cutting-edge sustainable design and performance

This project aims for at least Gold certification by optimizing energy and water use, enhancing indoor environmental quality, and utilizing sustainable materials.

2.4.4. Water Efficiency and Rainwater Management in LEED

Water efficiency is a significant component of LEED, and it keeps water use efficient, conserves water, and lessens the overall environmental impact of a building. All buildings with LEED certification must utilize state-of-the-art water-saving techniques, such as low-flow devices, rainwater harvesting, and reuse of greywater.

Table 2.2. Water Efficiency Strategies and LEED Credit Contribution

Water Efficiency Strategy	Description	LEED Credit Contribution
Low-Flow Fixtures	Installing water-efficient toilets, faucets, and showerheads to reduce consumption	Indoor Water Use Reduction
Rainwater Harvesting	Capturing and reusing rainwater for irrigation and non-potable uses	Rainwater Management
Greywater Recycling	Reusing wastewater from sinks and showers for toilet flushing and irrigation	Water Reuse and Management
Smart Irrigation Systems	Using weather-based irrigation controllers to minimize water waste	Outdoor Water Use Reduction

By incorporating such efficient use of water, such a project can save a significant portion of potable water, reduce operational costs, and work towards higher LEED certification levels.

2.4.5. Critical Analysis of LEED's Energy Performance

While LEED-certified buildings have become universally acknowledged for having a positive impact on the environment, studies have shown mixed levels of actual efficiency in terms of energy consumption. According to some studies, LEED buildings don't necessarily outpace non-LEED buildings, and therefore, a thoughtful selection of LEED credits with direct impact on energy performance is imperative.

Table 2.3. Critical Analysis of LEED's Energy Performance

LEED Energy Credit	Potential Benefit	Challenges
Optimized Energy Performance	Reduces energy use and operational costs	Requires high upfront investment
Onsite Renewable Energy	Enhances sustainability and reduces carbon footprint	Site constraints may limit feasibility
Enhanced Commissioning	Ensures systems operate at peak efficiency	Requires ongoing monitoring and maintenance
Building Envelope	Reduces heating/cooling	Performance depends on material

Improvements	demands	selection

To maximize real savings in terms of actual energy, this project will prioritize post-construction performance tracking, such that energy strategies yield real efficiency improvements and not mere LEED credits.

2.4.6. Performance and Certification Outcome

LEED certification approved the building because of its achievements in water efficiency (10 points), indoor environmental quality (10 points) and energy systems (21 points). The membership of a LEED-accredited individual on the team resulted in one bonus point though innovation points remained unexplored. There were no restrictions on the pursuit of regional priority points by this project operating within the Los Angeles area.

The building reached LEED Silver Certification through its 52 points total scoring. The project demonstrates its commitment to both sustainable building design and decreased energy intake and enhanced comfort of interior spaces for building occupants.

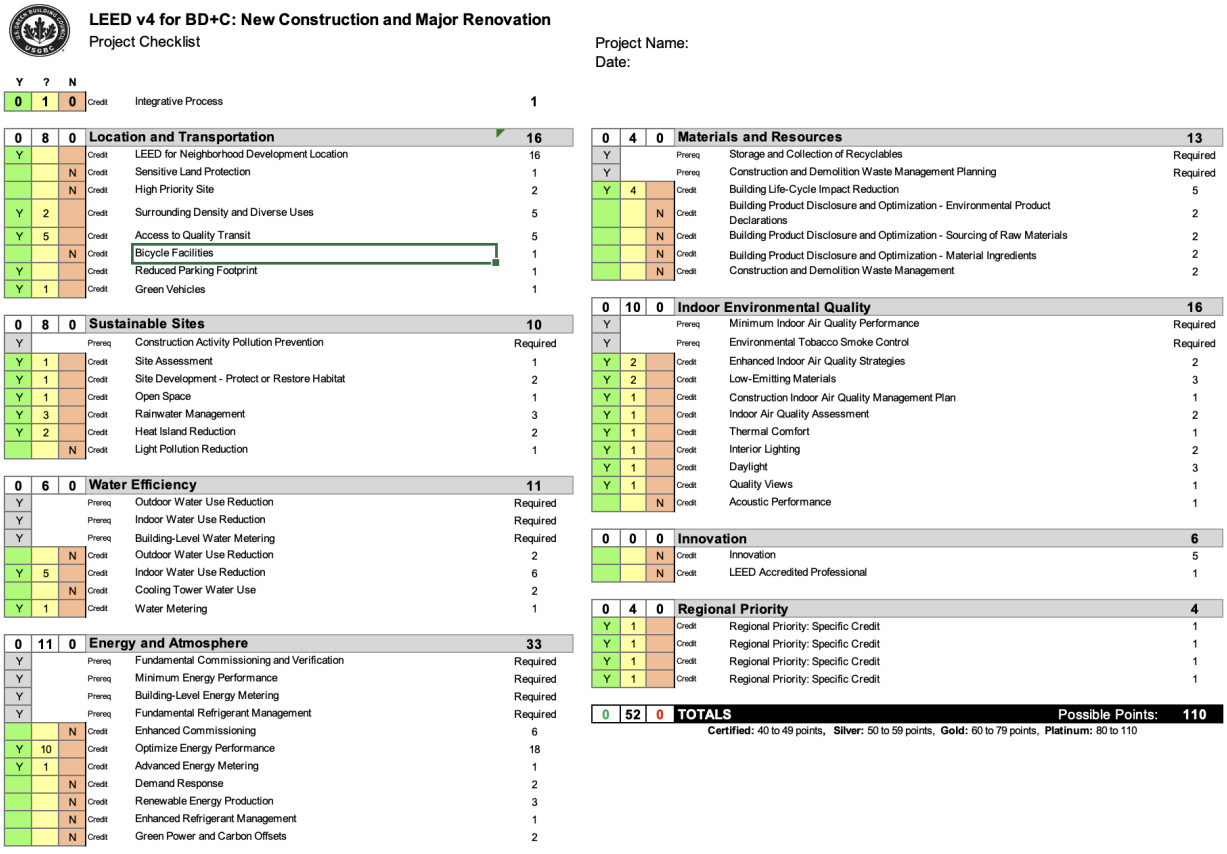

LEED v4 for BD+C: New Construction and Major Renovation
Project Checklist

Project Name:
Date:

Y	?	N			
0	1	0	Credit	Integrative Process	1

0	8	0	**Location and Transportation**		16
Y			Credit	LEED for Neighborhood Development Location	16
		N	Credit	Sensitive Land Protection	1
		N	Credit	High Priority Site	2
Y	2		Credit	Surrounding Density and Diverse Uses	5
Y	5		Credit	Access to Quality Transit	5
		N	Credit	Bicycle Facilities	1
Y			Credit	Reduced Parking Footprint	1
Y	1		Credit	Green Vehicles	1

0	8	0	**Sustainable Sites**		10
Y			Prereq	Construction Activity Pollution Prevention	Required
Y	1		Credit	Site Assessment	1
Y	1		Credit	Site Development - Protect or Restore Habitat	2
Y	1		Credit	Open Space	1
Y	3		Credit	Rainwater Management	3
Y	2		Credit	Heat Island Reduction	2
		N	Credit	Light Pollution Reduction	1

0	6	0	**Water Efficiency**		11
Y			Prereq	Outdoor Water Use Reduction	Required
Y			Prereq	Indoor Water Use Reduction	Required
Y			Prereq	Building-Level Water Metering	Required
		N	Credit	Outdoor Water Use Reduction	2
Y	5		Credit	Indoor Water Use Reduction	6
		N	Credit	Cooling Tower Water Use	2
Y	1		Credit	Water Metering	1

0	11	0	**Energy and Atmosphere**		33
Y			Prereq	Fundamental Commissioning and Verification	Required
Y			Prereq	Minimum Energy Performance	Required
Y			Prereq	Building-Level Energy Metering	Required
Y			Prereq	Fundamental Refrigerant Management	Required
		N	Credit	Enhanced Commissioning	6
Y	10		Credit	Optimize Energy Performance	18
Y	1		Credit	Advanced Energy Metering	1
		N	Credit	Demand Response	2
		N	Credit	Renewable Energy Production	3
		N	Credit	Enhanced Refrigerant Management	1
		N	Credit	Green Power and Carbon Offsets	2

0	4	0	**Materials and Resources**		13
Y			Prereq	Storage and Collection of Recyclables	Required
Y			Prereq	Construction and Demolition Waste Management Planning	Required
Y	4		Credit	Building Life-Cycle Impact Reduction	5
		N	Credit	Building Product Disclosure and Optimization - Environmental Product Declarations	2
		N	Credit	Building Product Disclosure and Optimization - Sourcing of Raw Materials	2
		N	Credit	Building Product Disclosure and Optimization - Material Ingredients	2
		N	Credit	Construction and Demolition Waste Management	2

0	10	0	**Indoor Environmental Quality**		16
Y			Prereq	Minimum Indoor Air Quality Performance	Required
Y			Prereq	Environmental Tobacco Smoke Control	Required
Y	2		Credit	Enhanced Indoor Air Quality Strategies	2
Y	2		Credit	Low-Emitting Materials	3
Y	1		Credit	Construction Indoor Air Quality Management Plan	1
Y	1		Credit	Indoor Air Quality Assessment	2
Y	1		Credit	Thermal Comfort	1
Y	1		Credit	Interior Lighting	2
Y	1		Credit	Daylight	3
Y	1		Credit	Quality Views	1
		N	Credit	Acoustic Performance	1

0	0	0	**Innovation**		6
		N	Credit	Innovation	5
		N	Credit	LEED Accredited Professional	1

0	4	0	**Regional Priority**		4
Y	1		Credit	Regional Priority: Specific Credit	1
Y	1		Credit	Regional Priority: Specific Credit	1
Y	1		Credit	Regional Priority: Specific Credit	1
Y	1		Credit	Regional Priority: Specific Credit	1

0	52	0	**TOTALS**	Possible Points:	110

Certified: 40 to 49 points, **Silver:** 50 to 59 points, **Gold:** 60 to 79 points, **Platinum:** 80 to 110

Figure 2.5. LEED v4.1 BD+C analysis of the building

2.5. Design Conditions

The following considerations for design were included in the building design:

- High seismicity
- Strong wind exposure

The building location was in a seismically active zone in Los Angeles, California. As per site location (6435 Wilshire Blvd), seismic requirements for design exhibited high seismic factors to be taken into consideration. Short period response acceleration (Ss) and 1-second period response acceleration (S1) values for the site were 2.34g and 0.84g, respectively. The site was in Seismic Design Category D with such high acceleration values.

For wind, the site location was in an urban zone with a level of exposure of category B. The basic wind velocity for a 50-year return period was 42 m/s (94 mph), a value over a region and one that required specific consideration in the structure's design. The seismic and wind both presented distinctly high values and played an important role in defining the direction of structure design.

2.5.1. Design concept

The initial form of our building was rectangular in all directions, however, after brainstorming with the group, we decided to add a terrace on the 4th floor. This led us to change plan views for further floors with another structure of apartments. Moreover, the primary plan for outside parking space was a bit small, therefore the decision on adding more parking lots on the right side of the building was made.

Figure 2.6. Development of the plan

Figure 2.7. Front view of the draft building

2.5.2. Architectural Design Considerations

2.5.2.1. Occupancy load for residential and commercial spaces and occupancy classification

According to Chapter 3 of IBC 2024, the residential floors are considered as R-2, and the commercial and fourth floor are classified as B (Business Group) and A (Assembly), respectively. In order to calculate the total occupancy, the occupant load was calculated per residential and commercial floors. For residential areas occupant load is typically 1 person per 200 square feet and for commercial is 1 person per 150 square feet. By taking the average area as 135 m^2 (1453 ft^2), occupants per floor for residential floor 2-3 is 65, and for residential floors 5-12 is 58 occupants per floor. The total occupancy load is 594 occupants.

2.5.2.2. Corridors

In both residential and commercial floors the minimum corridor width is 3700 mm, which satisfies the minimum corridor width of 1117.6 mm (44 inches) per IBC 2024 section 1020.2. Referring to the IBC 2024 Section 1207.2 the minimum ceiling height should be at least 2286 mm (7 ft 6 in) for habitable spaces and corridors. The buildings floor-to-floor height is shown below:

- First and fourth floors: 3590 mm (compliant)
- Floors 2-3 and 5-12: 3116 mm (compliant)

All clear heights and corridor widths exceed the minimum requirements.

2.5.2.3. Parking Spaces

The building accommodated residential and commercial parking spaces both in basements and outdoors. The demand for parking in terms of 2022 California Building Code (CBC 2022) for residential and commercial occupancies with respective parking requirements for residential (R-2) occupancies 1.5 spaces for dwelling unit and visitor unit, respectively, under the code, and for commercial occupancies 1 for 250 square feet (23.225 m²) of occupiable floor area under the code, was necessitated. The detailed car parking calculations were:

Residential Parking Requirements

- ➢ Floors 2-3 accommodated 9 apartments in each (18 in all)
- ➢ Floors 5-12 contained 8 apartments in each (a total of 64 apartments)
- ➢ Total residential unit: 82 apartments
- ➢ Required residential parking = 82 × 1.5 = 123 spaces

Commercial Parking Requirements

- ➢ Ground floor commercial accommodation included 7 individual premises
- ➢ Total commercial square meterage = 869 m² (9,353 ft²
- ➢ Required commercial parking spaces = 38 (rounded up from 37.4

Accessibility Requirements: CBC 2022 Section 11B-208 requirements for accessibility were met in work:

- ➢ 2% of parking spaces have been designed for use as accessible spaces
- ➢ Total provided parking spaces: 161 (123 residential and 38 commercial spaces

- ➢ Required accessible spaces = 4 spaces (rounded up from 3.22
- ➢ Van-accessible spaces have been incorporated at a 1:6 accessible spaces proportion

Parking Access and Traffic Circulation: In its parking complex, the following have been incorporated:

- ➢ A two-way entrance and exit ramp between street level and basement
- ➢ The main entrance and exit ramp was designed with a 1:12 (8.33%) slope, in conformance with CBC maximum allowable slope for parking structures
- ➢ Separate entry and exit ramps at basement level for free flow of traffic
- ➢ Clear directional signage and markings
- ➢ Adequate turning radii for conventional passenger cars
- ➢ Emergency exits and lights in compliance with code requirements

2.5.2.4. Fire Safety and Evacuation Systems

2.5.2.4.1. Stairs

The building accommodated two stairways positioned diagonally in relation to each other in a configuration designed to maximize efficiency in an emergency evacuation scenario. According to Section 1005.3.1 of the International Building Code (IBC 2024), one 250 occupancies' stairway in Residential Occupancy was required. With an occupant count determined at 594 (594 ÷ 250 = 2.3), two stairways met minimum requirements for safe exiting under IBC 2024 codes. With a diagonally positioned configuration, in an emergency scenario in case one of the two stairways became inoperative, occupants in a building could have an alternative escape route at a significant distance.

The stairway width was calculated at 1500 mm, in excess of IBC 2024 Section 1009.3.2 minimums of 1219 mm (48 inches) minimums between handrails. Added width accommodated increased circulation during both ordinary use and in an emergency situation. Stairways were encircled with fire-rated construction and consisted of emergency lights, ventilation, and visibly conspicuous exit signage at all floors. Stairways both began at the basement level and extended through to the roof, providing full vertical access through the structure with ongoing fire separation between floors.

2.5.2.4.2. Elevator

The building housed four centrally positioned elevators in the building core. Two service and two passenger elevators made up the elevator system, both larger in dimensions than the minimum 1370 mm × 2030 mm (54 in × 80 in) for residential and mixed-use buildings over four stories. Central positioning of the elevator bank helped in efficient vertical circulation and maintained relatively uniform travel distance between all residential spaces and the elevators. Positioning maximized access in twelve-story buildings and adhered to multi-story residential building codes, necessitating a minimum of two elevators for buildings over four stories.

2.5.3. Architectural software design

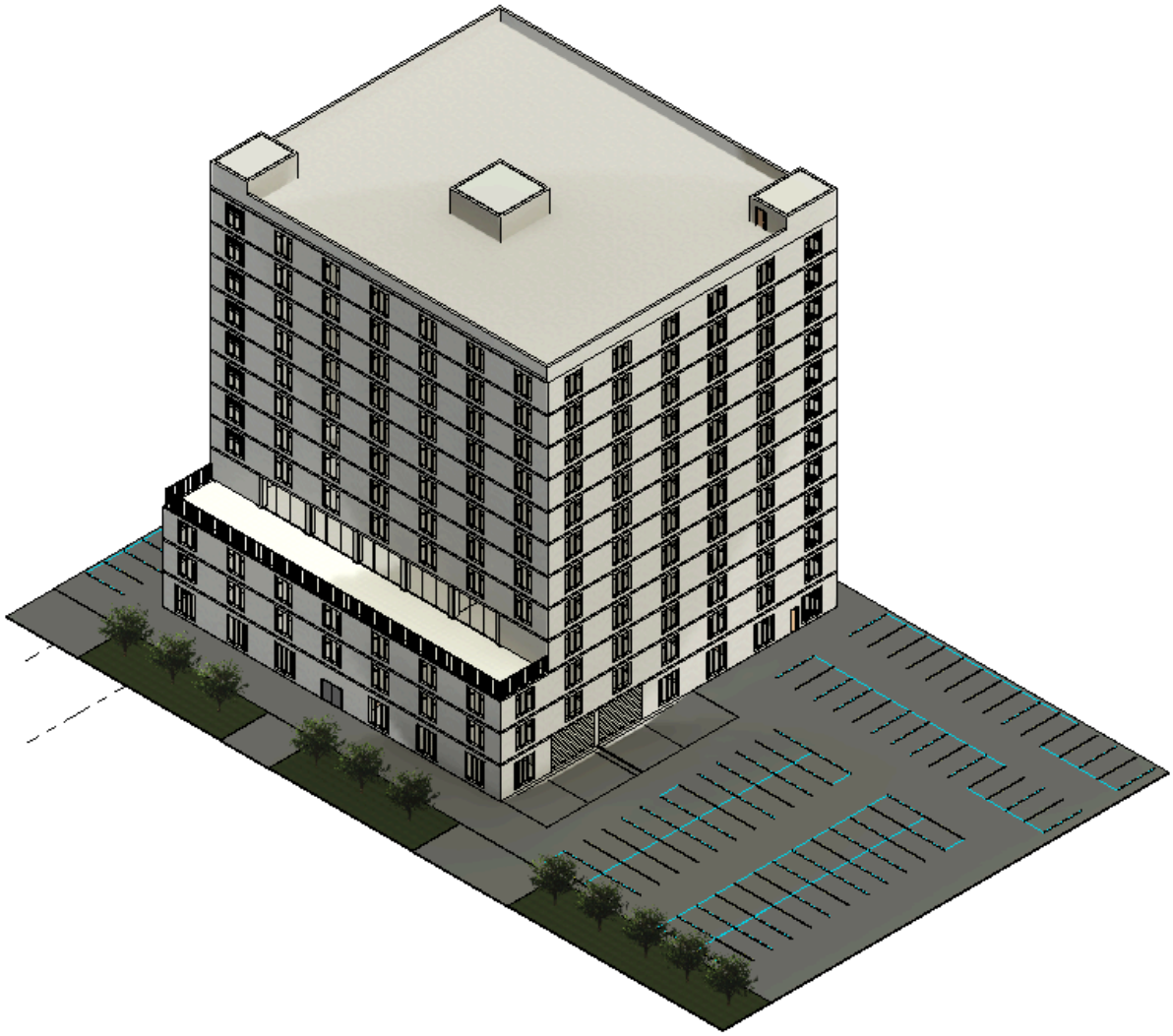

Figure 2.8. 3D plan of the building

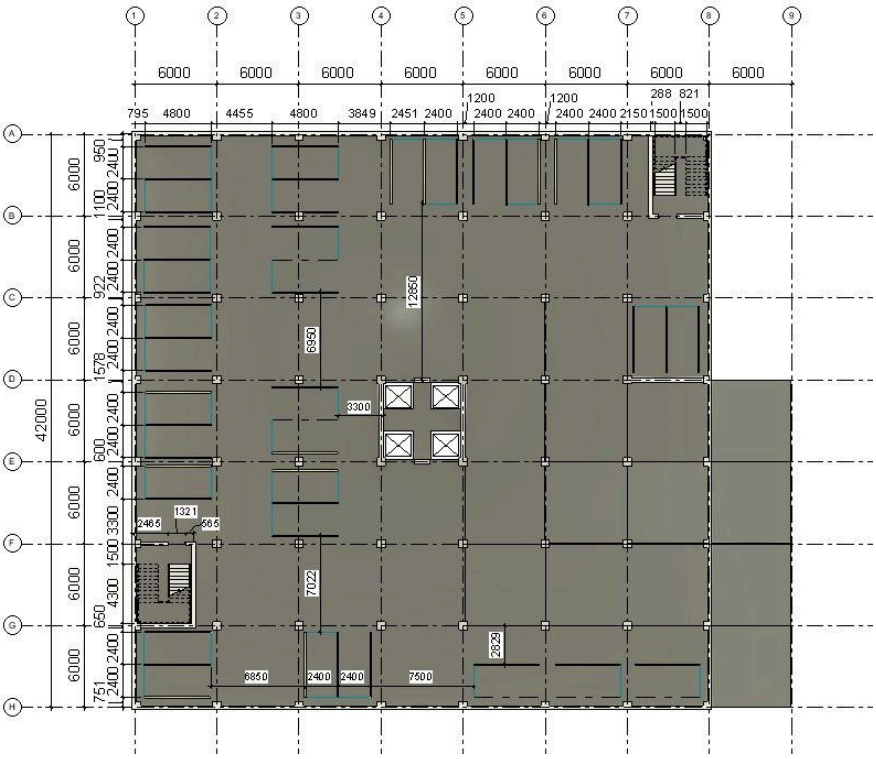

Figure 2.9. Floor plan for Basement

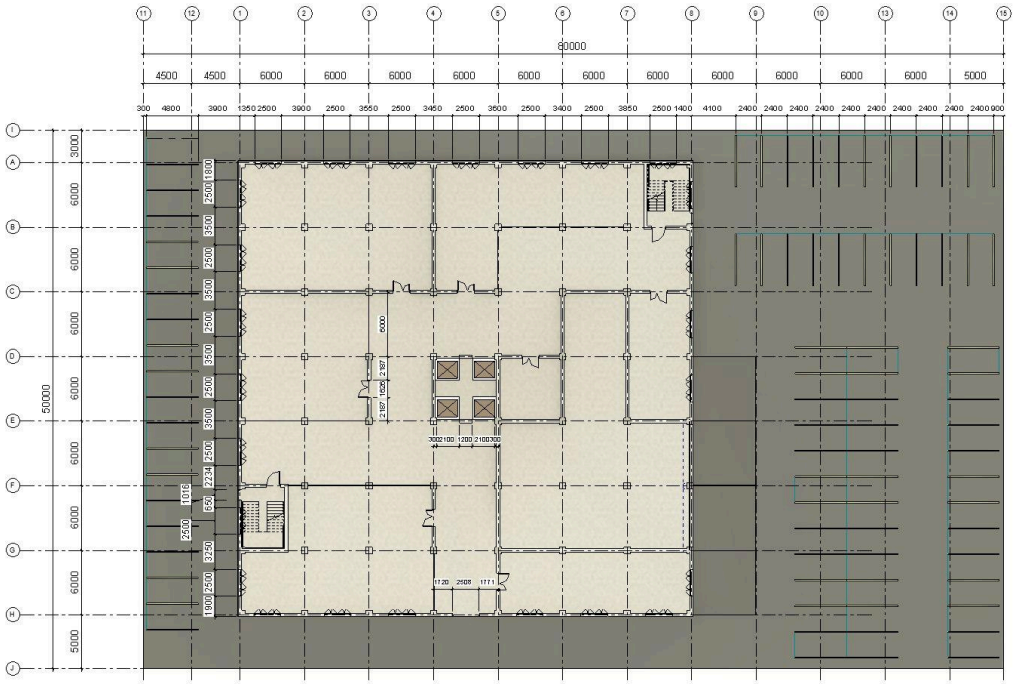

Figure 2.10. Floor plan for Ground Level (Commercial)

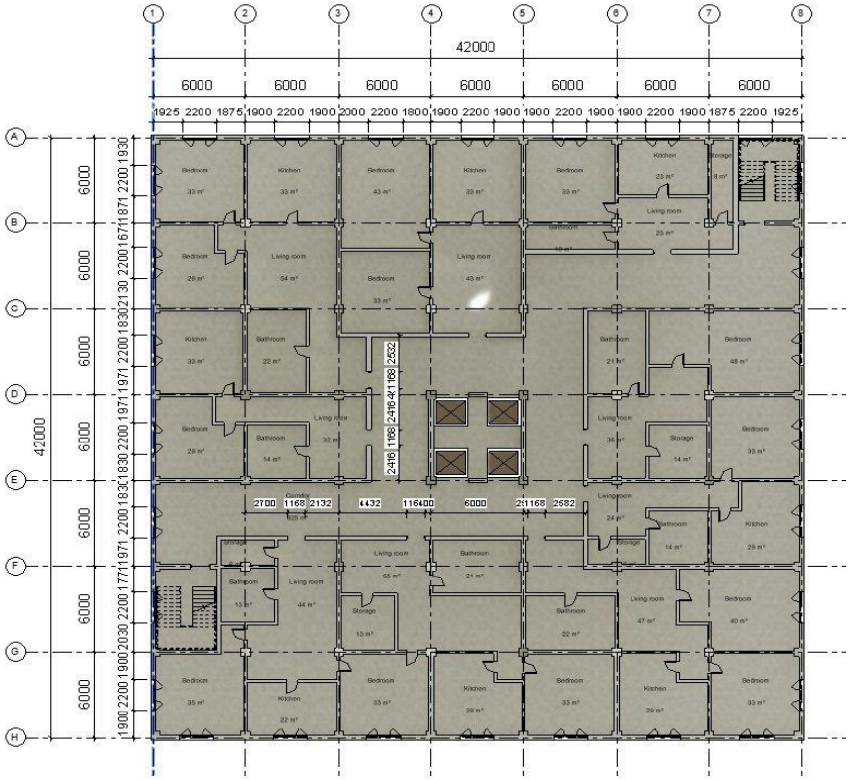

Figure 2.11. Floor plan for Level 2

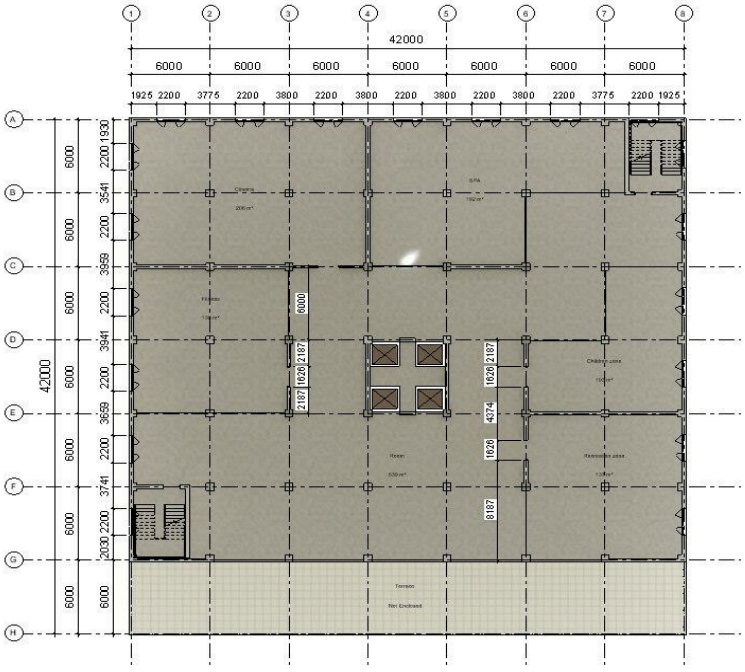

Figure 2.12. Floor plan for Level 5 (Terrace)

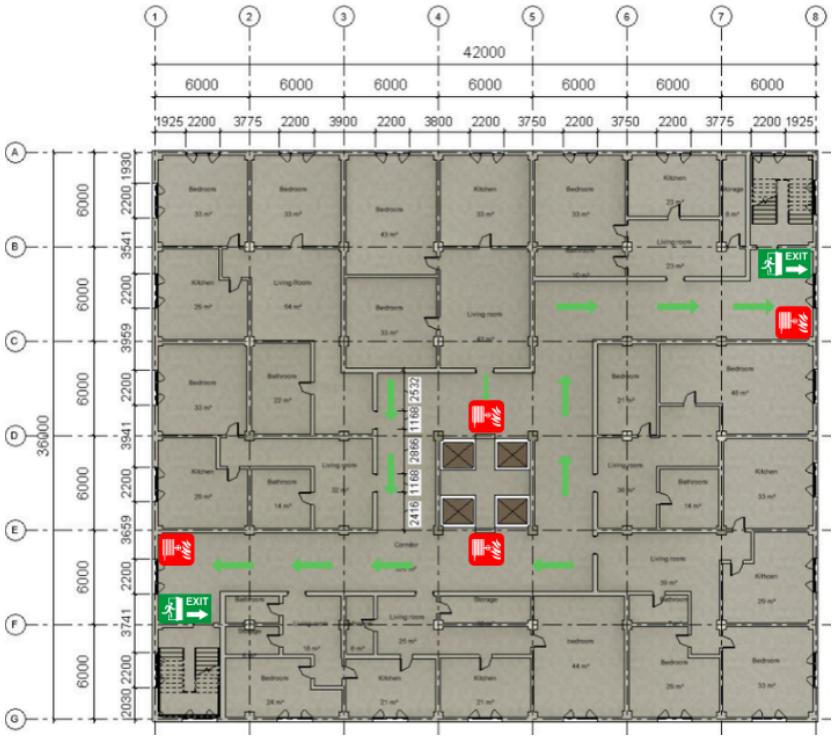

Figure 2.13. Emergency plan for level 6-13

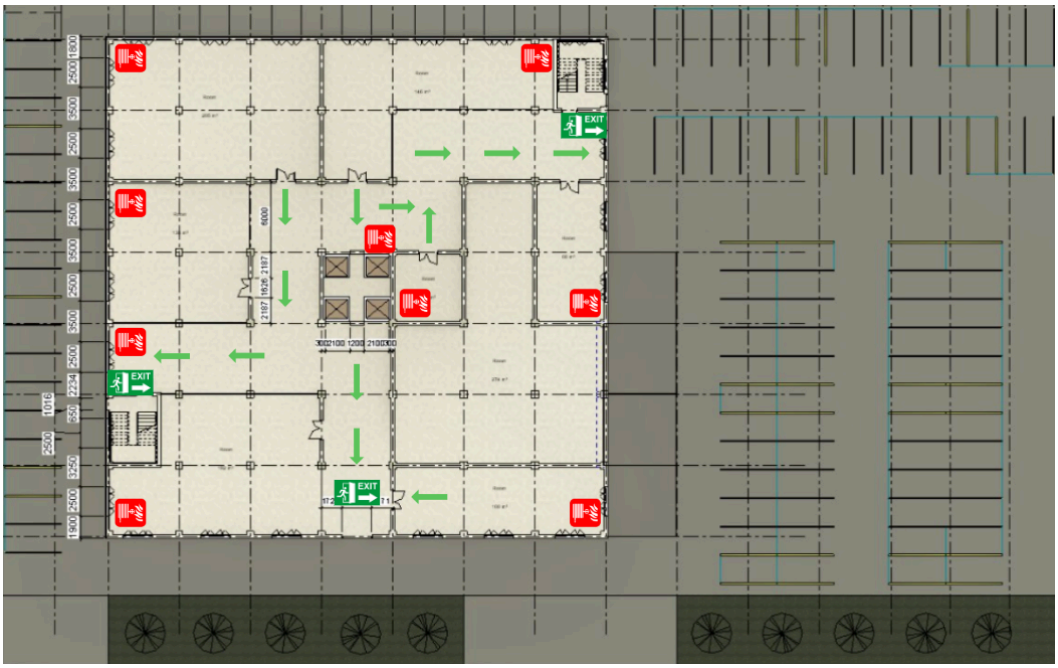

Figure 2.14. Emergency plan for level 1

Figure 2.15. From view of the building with foundation

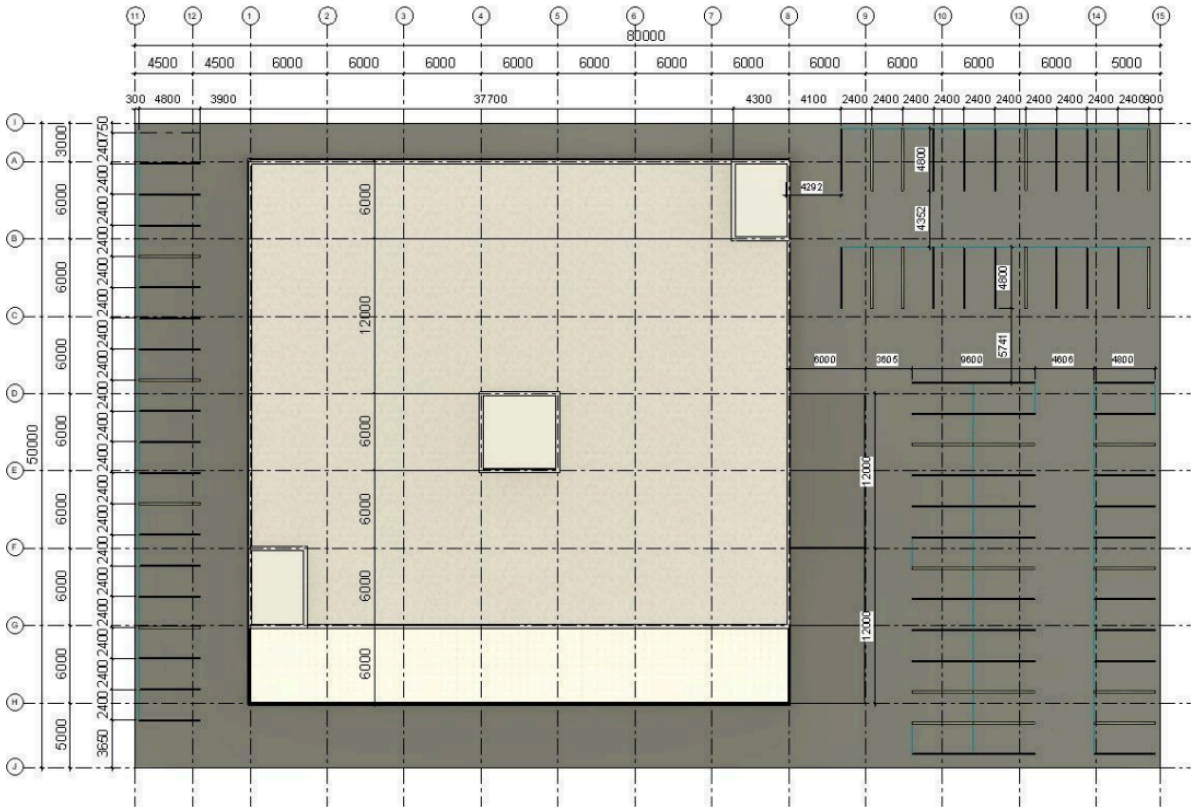

Figure 2.16. Site Layout

The design conditions and concept led us to the final helicopter view of our building with outside parking lots and enlarged territory for construction site and drainage system, as everything shown in Figure 15.

2.5.4. Life Cycle365

2.5.4.1. Concrete mixture

Base case: w/c ratio 0.42, fly ash 0%, silica fume 0%, slag 0%
Alternative 1: w/c ratio 0.35, fly ash 15%, silica fume 0%, slag 5% + black steel
Alternative 2: w/c ratio 0.30, fly ash 10%, silica fume 5%, slag 5% + Stainless steel
Alternative 3: w/c ratio 0.36, fly ash 20%, silica fume 10%, slag 0% + black steel

To further regulate the setting time and avoid calcium nitrite infitration, the Calcium Nitrite inhibitor of SL/m' has been added (Ann et al, 2006). Additionally, in order to determine

their impact on the concrete's life cycle, the membrane and sealers were applied in various mixes.

2.5.4.2. Life cycle cost

The life cycle cost was also incorporated based on the software actual data. The following material cost figures were applied:

- Concrete - $200/m3
- Black steel - $5.6/kg
- Membrane - $50/m2
- Sealer - $15/m2
- Inhibitor - $1.5/L
- Repair - $400/m2

Additionally, by entering the location of Los Angeles City, the software automatically included the temperature and chloride exposure. The temperature ranged between 13.8°C and 21.4°C, and the chloride exposure was 0.68% of the weight of the concrete.

Table 2.1 shows the life cycle costs. It is evident that although other building costs stay the same, the addition of barriers raises life cycle expenses.

Table 2.4. Total life cycle costs.

Name	Construction Cost	Barrier Cost	Repair Cost	Life Cycle Cost
Base case	$384,635	$0	$5,694,430	$6,079,065
Alternative 1	$384,635	$0	$4,287,821	$4,672,456
Alternative 2	$1,428,923	$0	$0	$1,428,923
Alternative 3	$384,635	$0	$3,647,769	$4,032,404

2.5.4.3. Service life

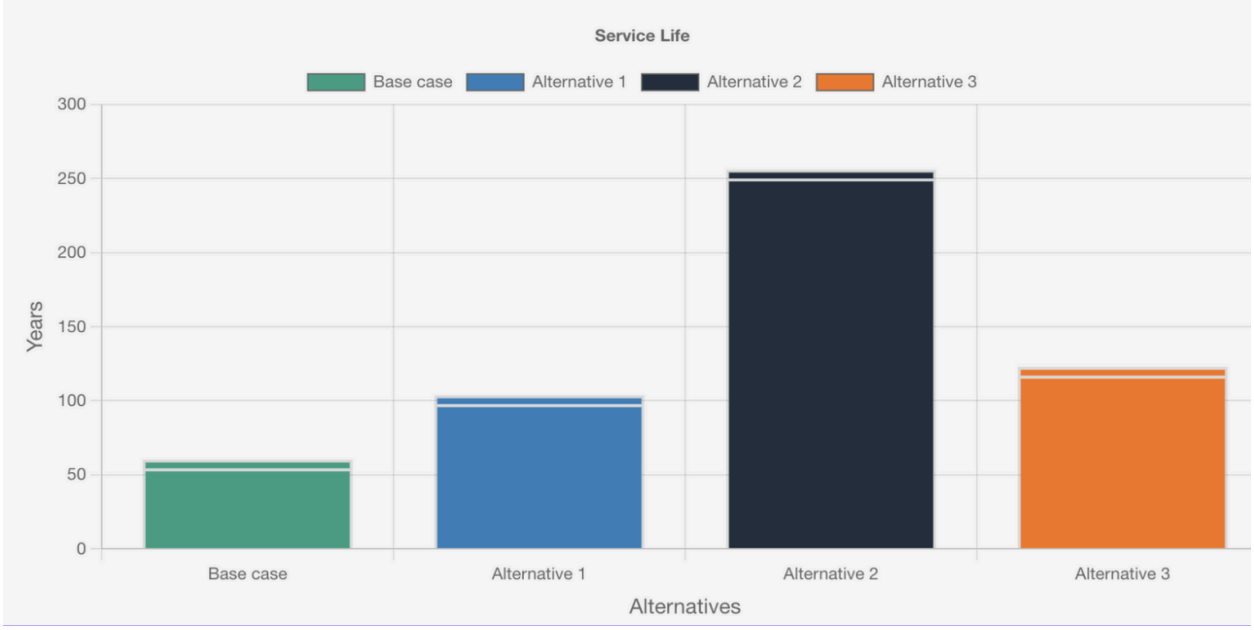

Figure 2.17. Service life

Figure 2.17 displays the service life of each mixture as determined by LCC. The Alternative 2 has the longest service life, as can be observed.

2.5.4.4. Corrosion prevention

The proper application of cementitious ingredients in concrete mixtures is essential to preventing corrosion. Whereas silica fume, usually added at a concentration of 5% to 10% by weight of cementitious ingredients, improves impermeability and resistance to chloride penetration, Portland cement serves as a binder. Utilized at 15% to 30%, fly ash strengthens the durability of concrete by lowering permeability and reacting with calcium hydroxide. 30% to 50% doses of blast furnace slag increase resistance to alkali-silica reaction and sulfate assault. To further reduce corrosion, corrosion inhibitors such as calcium nitrite in 5L/m' may be added. To stop chloride ions from penetrating the structure, a sealer may also be used.

3. Structural Design

3.1. Material Selection

Table 3.1. Material selection

Structural element	Construction material	Features
Column	Reinforced concrete	● High compressive strength ● Durability ● Cost-effective
Beam	Partially prestressed concrete	● Improved crack control ● Balanced Tension and Compression Capacity ● Reduced Deflection
Wall	Concrete masonry	● Fire resistance ● Moisture resistance ● Sound insulation
Roof	Two-way concrete, uniform thickness slab	● Even load distribution ● Greater Flexibility in Column Placement ● Good for Large, Open Areas
Foundation	Pile foundation	● Versatility in Different Soil Conditions ● Resistance to Lateral Forces ● Allows Construction in Limited Space

Reinforced concrete is good for residential buildings due to its advanced power, durability, and hearth resistance. Unlike timber, it doesn't rot, warp, or entice pests, imparting long-term structural integrity. It additionally withstands harsh climate conditions, which include hurricanes and earthquakes, higher than substances like metal or brick.

Reinforcement with metallic bars (rebar) complements its tensile strength, allowing for bendy designs and larger spans. Additionally, strengthened concrete presents outstanding thermal mass, assisting to alter indoor temperatures and improve strength efficiency, making it a reliable and fee-effective preference for houses (Mathai, 2020).

3.2. Non-structural Materials Selection

3.2.1. Floor finishing

The materials used for floor finishing were selected based on their aesthetic appeal, market availability, and use in residential constructions. According to the International Building Code's (2020) standards, the floor finishing's overall thickness, excluding the structural slab, was determined to be 95 mm. It was mostly composed of the following layers, arranged from top to bottom

- Cover - ceramic tile on a 13-mm mortar bed
- Leveling - cinder concrete screed
- Water-proofing - single-ply sheet
- Rigid insulation
- Structural slab - reinforced concrete

3.2.2. Ceiling

The ceiling will consist of two layers and will have a thickness of 165 mm:

- Mechanical duct allowance
- Gypsum board

3.2.3. Partition and exterior walls

For the design of partition walls, a hollow concrete masonry unit was chosen. The advantages of a hollow concrete masonry unit include its high thermal insulation and structural capabilities, lightweight properties, flexibility and high resistance to fire. Moreover, the partition walls consist of proper insulation and cement plaster.

The external covering was already mentioned and it will be constituted of fiber cement cladding.

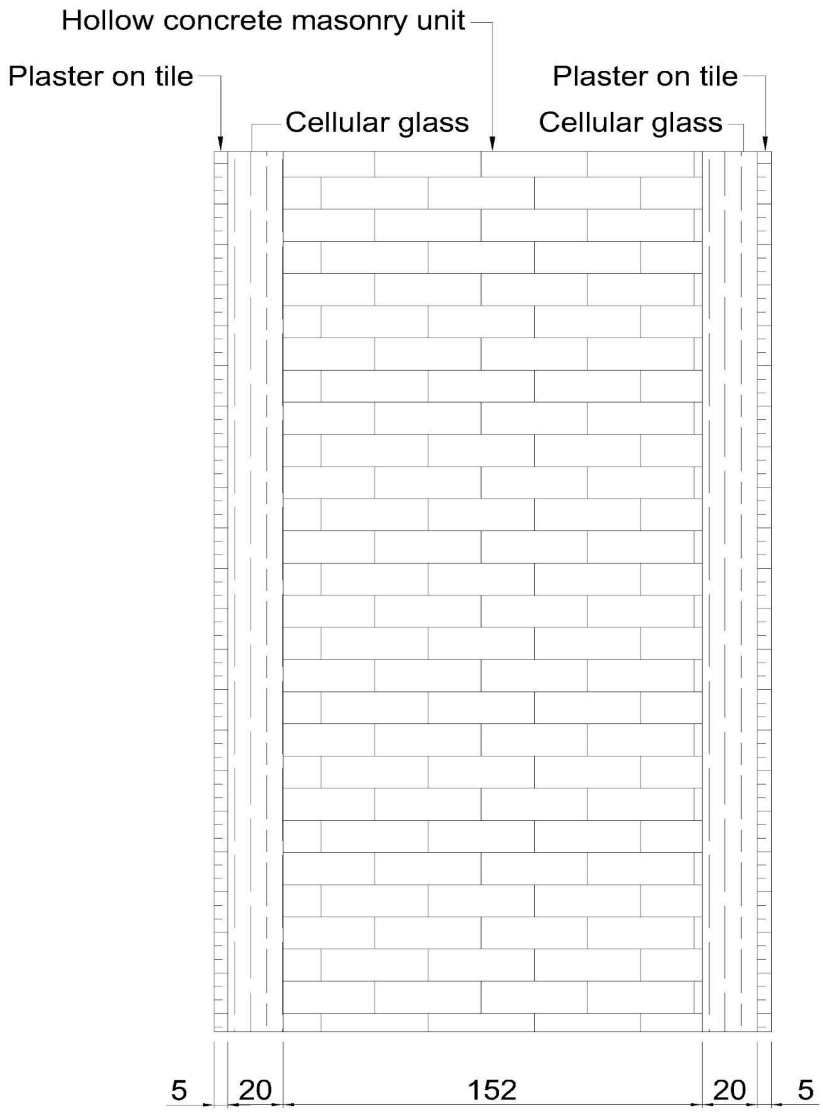

Figure 3.1. Interior wall - sectional view

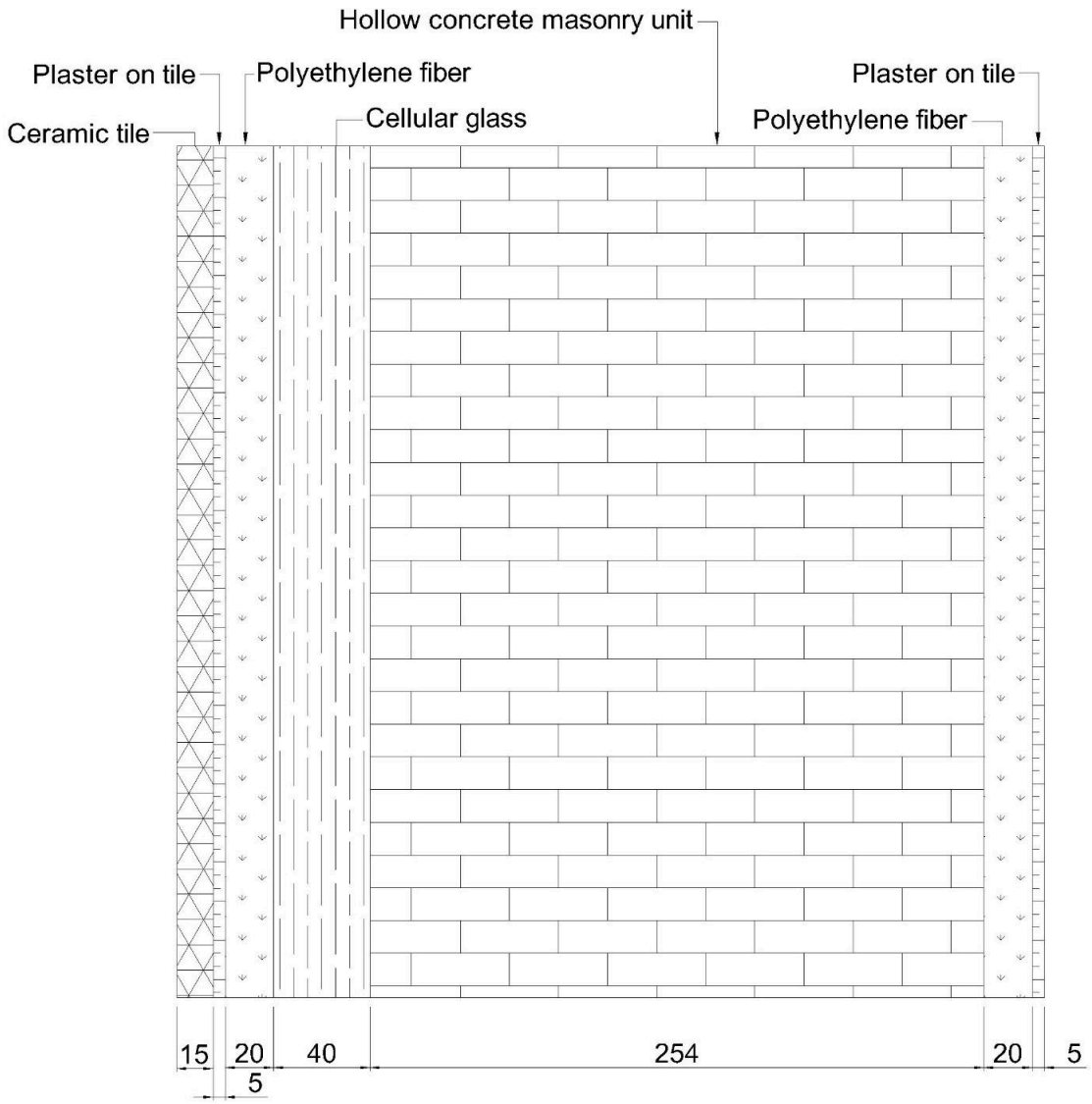

Figure 3.2. Exterior wall - sectional view

3.2.4. Roof parapets

A height of one metre was selected for the parapet design since the International Building Code (2020) stipulates that the minimum height of a roof's parapets must be 762 mm. The autoclaved aerated concrete used to make the roof parapets will have a thickness of 240 mm. The external glazing will be composed of the same fibre cement cladding, and the inside side will have a 5 mm layer of cement screed laid. In the end, 250 mm was found to be the parapets' thickness.

3.3. Analysis and Design of Gravity Load Resisting System (GLRS)

3.3.1. Calculation of Dead, Live, and Snow Loads

3.3.1.1. Calculation of Dead Loads

Dead loads calculation include floor loads, ceiling, stairs, and exterior walls with interior. According to the ASCE 7-10 code the floor loads were calculated in several levels, as the building has different plan structures with different material types. The final calculations are shown in the next 3 tables.

Table 3.2. Dead Load of Corridors/First floor

Corridors/First floor		
Material type	**Thickness (mm)**	**Load (kN/m^2)**
Ceramic tile	19	0.77
Mortar bed	13	
Cinder concrete screed	40	0.68
Single-ply sheet	10	0.03
Rigid insulation	13	0.04
RC concrete - stone (including gravel)	150	3.54
Mechanical duct allowance	150	0.19
Gypsum board	15	0.12
Total	410	5.37

Table 3.3. Dead Load of Apartments

Apartments		
Material type	**Thickness (mm)**	**Load (kN/m^2)**
Linoleum	6	0.05
Cinder concrete screed	40	0.68
Single-ply sheet	10	0.03
Rigid insulation	13	0.04
RC concrete - stone (including	150	3.54

gravel)		
Mechanical duct allowance	150	0.19
Gypsum board	15	0.12
Total	384	4.65

Table 3.4. Dead Load of Roof

Roof		
Material type	**Thickness (mm)**	**Load (kN/m^2)**
Three-ply ready roofing	20	0.96
Perlite	80	0.12
Bituminous, smooth surface	0	0.07
Lightweight concrete	50	0.75
RC concrete - stone (including gravel)	150	3.54
Mechanical duct allowance	170	0,19
Gypsum board	15	0.12
Total	485	5.56

Furthermore, the calculations of walls were done with the help of two methods, using the hole span of the building as one for the interior walls, and using span between columns, which is 6 m. The second method infers more efficient calculations for exterior walls as they are located only on the edges of the building where only edge beams and columns support them.

Table 3.5. Dead Load of Exterior Wall

Exterior Wall							
Material type	Material type	Thickness (mm)	Height (mm)	Span (mm)	Volume (m3)	Density (kg/m3)	Mass (kg)
Exterior finish	Ceramic tile	15	3500	6000	0.315	2400	756
Cement plaster	Plaster on tile	5	3500	6000	0.105	1400	147
Air infiltration barrier	Polyethylene fiber	20	3500	6000	0.42	950	399

Insulation	Cellular glass	40	3500	6000	0.84	143	120.12
Autoclaved aerated concrete block	Hollow concrete masonry unit	254	3500	6000	5.334	1350	7200.9
Air infiltration barrier	Polyethylene fiber	20	3500	6000	0.42	950	399
Cement plaster	Plaster on tile	5	3500	6000	0.105	1400	147
	Total	359					9169.02
						Weight (kN)	89.9480862

Table 3.6. Dead Load of Interior Walls of 2-3 floors

Interior wall (between and inside the apartments) typical floor (2-3)							
Material type	Material type	Thickness (mm)	Height (mm)	Span (mm)	Volume (m3)	Density (kg/m3)	Weight (kg)
Cement plaster	Plaster on tile	5	3500	474000	8.295	1400	11613
Insulation	Cellular glass	20	3500	474000	33.18	143	4744.74
Autoclaved aerated concrete block	Hollow concrete masonry unit	152	3500	474000	252.168	1350	340426.8
Insulation	Cellular glass	20	3500	474000	33.18	143	4744.74
Cement plaster	Plaster on tile	5	3500	474000	8.295	1400	11613
	Total	202			335.118		373142

Table 3.7. Dead Load of Interior Walls of 5-12 floors

Interior wall (between and inside the apartments) floor 5-12							
Material type	Material type	Thickness (mm)	Height (mm)	Span (mm)	Volume (m3)	Density (kg/m3)	Weight (kg)
Cement plaster	Plaster	5	3500	435000	7.6125	1400	10657.5
Insulation	Cellular glass	20	3500	435000	30.45	143	4354.35
Autoclaved aerated concrete block	Hollow concrete masonry unit	102	3500	435000	155.295	1350	209648.25

Insulation	Cellular glass	20	3500	435000	30.45	143	4354.35
Cement plaster	Plaster	5	3500	435000	7.6125	1400	10657.5
	Total	152			231.42		239672

Table 3.8. Dead Load of Parapets

Parapetes							
Material type	Material type	Thickness (mm)	Height (mm)	Span (mm)	Volume (m3)	Density (kg/m3)	Weight (kg)
Autoclaved aerated concrete block	Autoclaved aerated concrete	250	1700	128366	55	580	31642.219

Table 3.9. Dead Load of Stairs

Stairs							
Material type	Material type	Riser height (mm)	Thread (mm)	Width (mm)	Volume (m3)	Density (kg/m3)	Weight (kg)
Reinforced concrete	Concrete	190	280	1500	3.264	2408	7859.9528
		Slab height (mm)	Landing height (mm)	Waist (mm)			
		200	200	150		Load	77.1061
		Slab width (mm)	Landing width (mm)	Length (mm)			
		600	1000	3760			
		Slab length (mm)	Landing length (mm)				
		2200	2750				

Floor area = 1656 m2

3.3.1.2. Calculation of Live Loads

For the residential building the minimum uniformly, distributed loads based on ASCE 7-16 and 7-10 were identified and shown below (American Society of Civil Engineers, 2017):

- Private rooms and corridors serving them: $L_0 = 1.92\ kN/m^2$
- Public rooms: $L_0 = 4.79\ kN/m^2$
- Corridors serving public rooms: $L_0 = 4.79\ kN/m^2$
- Ordinary flat roofs: $L_0 = 0.96\ kN/m^2$
- Stairs and exit ways: $L_0 = 4.79\ kN/m^2$

Live load discount should be implemented for all the uniformly dispersed load except public rooms in step with ASCE 7-16. The discount for ground dead load ought to be carried out using the following components:

$$L = L_0(0.25 + \frac{4.57}{\sqrt{K_{LL}A_T}}) \quad (3.1)$$

Live load element factor, K_{LL}, for the structural members will be:

- Interior columns: $K_{LL} = 4$
- Exterior columns without cantilever slabs: $K_{LL} = 4$
- Corner columns: $K_{LL} = 4$
- Edge beams without cantilever slabs: $K_{LL} = 2$
- Interior beams: $K_{LL} = 2$

The floor live load calculations for each structural member can be seen in Table x.

Table 3.10. Floor live load calculations.

			Space (m)	Span (m)	A_T (m^2)	K_{LL}	Reduction	L_0 (kN/m^2)	L (kN/m^2)
Typical floor	Private rooms and corridors serving them	Exterior columns	6	6	18	4	0.631	1.92	1.21
		Interior columns	6	6	36	4	0.631	1.92	1.21
		Corner	3	3	9	4	1	1.92	1.92

		columns							
		Edge beams	3	6	9	2	1	1.92	1.92
		Interior beams	3	6	18	2	1	1.92	1.92
	Stairs and exit ways	Interior columns	6	6	36	4	0.631	4.79	3.02
		Exterior columns	6	6	18	4	0.631	4.79	3.02
		Interior beams	3	6	18	2	1	4.79	4.79
		Edge beams	3	6	9	2	1	4.79	4.79
First floor		Exterior columns	6	6	18	4	0.631	4.79	3.02
		Interior columns	6	6	36	4	0.631	4.79	3.02
		Corner columns	3	3	9	4	1	4.79	4.79
		Edge beams	3	6	9	2	1	4.79	4.79
		Interior beams	3	6	18	2	1	4.79	4.79

Whereas, for roof live load, the following reduction should be applied:

$$L_r = L_0 R_1 R_2 \quad \text{where } 0.58 \leq L_r \leq 0.96$$

The reduction factor R_1 can be determined as follows:

$$R_1 = \begin{cases} 1 & \text{for } A_T \leq 18.58\ m^2 \\ 1.2 - 0.011 A_T & \text{for } 18.58\ m^2 < A_T < 55.74\ m^2 \\ 0.6 & \text{for } A_T \geq 55.74\ m^2 \end{cases} \quad (3.2)$$

The reduction factor R_2 for ordinary flat roofs is 1.

The roof live load calculations for each structural member can be seen in Table 3.11.

Table 3.11. Roof live load calculations.

	Space (m)	Span (m)	A_T (m^2)	K_{LL}	R_1	R_2	L_0 (kN/m^2)	L (kN/m^2)
Exterior columns	6	6	36	4	0.804	1	0.96	0.77
Interior columns	6	6	36	4	0.804	1	0.96	0.77
Corner columns	3	3	9	4	1	1	0.96	0.96
Edge beams	3	6	9	2	1	1	0.96	0.96
Interior beams	3	6	18	2	1	1	0.96	0.96

3.3.1.3. Calculation of Snow Loads

According to ASCE 7-16, Los Angeles did not experience any snowfall. Therefore, snow loads are not calculated for design projects (American Society of Civil Engineers, 2017).

3.4. Estimation of Member Sizes

3.4.1. Determination of Structural Layout

To provide more space for residential buildings, the distance between the poles was thus set to 6 meters. According to IBC code, pole spacing should be in the range of 2.5 m to 7.5 m, so a spacing of 6 m is suitable (International Code Council, 2024).

Three potential GLRS layouts and the more suitable layout from those was chosen based on the cost of materials, which was determined by calculating the volumes of structural members.

1. Major beams and a two-way slab
2. One-way slab with major beams and one minor beam
3. Two-way slab with major beams and two minor beams

There was done preliminary member size estimation for the further analysis based on the followings statements from ACI 318-19 Chapters 7-10 (American Concrete Institute, 2022):

- The thickness of major beams under a two-way slab without any interior beams is equal to 10% of its span.
- The width of major beams under a two-way slab without any interior beams is equal
- The thickness of major beams under a slab with interior beams is equal to 8% of its span.
- The width of major beams under a slab with interior beams is equal $b = h/2$.
- The thickness of simply supported minor beams is equal to $h = l/16$.
- The thickness of a simply supported one-way slab is equal to $h = l/20$.

3.4.1.1. Option 1: Two-way slab

The lengths of the slab and of the beam were taken as 6 m . As it was mentioned earlier, the thickness of major beam (h) is equal to 10% of its length, whereas its width (b) is equal to $b = \frac{h}{1.5}$.

$$h_{major} = 10\%L = 0.1 * 6 = 0.6\,m$$

$$b_{major} = \frac{h}{1.5} = 0.4\,m$$

To determine the thickness of the floor slab the moment of inertia of the beam and strip and the elastic modulus should be calculated. Concrete grade C40 is selected for slabs and beams. Because they are often used on parts that support heavier structures with heavier weight. The following calculations were done:

$$f_{cb} = f_{cs} = 40\,MPa$$

The modulus of elasticity can be calculated using the following equation:

$$E_b = E_s = 4700\sqrt{f_c} \tag{3.3}$$

$$E_b = E_s = 4700\sqrt{f_c} = 29725.41\,MPa$$

$$I_{b,cr} = \frac{1}{12}\cdot b\cdot h^3\cdot 0.35 = \frac{1}{12}\cdot 0.4\cdot 0.6^3\cdot 0.35 = 2.52\times 10^{-3}\,m^4$$

$$I_{s,cr} = \frac{1}{12}\cdot L\cdot h^3\cdot 0.25 = \frac{1}{12}\cdot 6\cdot 0.150^3\cdot 0.25 = 4.22\times 10^{-4}\,m^4$$

After calculating the members' moments of inertia the stiffness ratio should be calculated:

$$\alpha_{fm} = \frac{E_{cb} I_{b,cr}}{E_{cs} I_{s,cr}} \quad (3.4)$$

$$\alpha_{fm} = \frac{29725.41 \cdot 2.52 \times 10^{-3}}{29725.41 \cdot 4.22 \times 10^{-4}} = 5.972$$

$$\alpha_{fm} = 5.972 > 2$$

The minimum thickness of slab should be calculated using the formula:

$$h = \frac{l_n(0.8 + f_y/200{,}000)}{36 + 9\beta} \leq h \leq 3.5\ in. \quad (3.5)$$

where

$$\beta = L_{yn}/L_{xn} = 1$$

And the clear span is:

$$l_n = L - \frac{b_{major}}{2} - \frac{b_{major}}{2} = 6 - 0.2 - 0.2 = 5.6\ m$$

$$h = \frac{5.6(0.8 + 60000/200{,}000)}{36+9} = 0.137\ m > 0.09\ m\ (3.5\ in.)$$

For conventional design of slab, h = 0.15 m should be taken. Accordingly, the volume can be calculated as following:

$$V(slab) = 6 \cdot 6 \cdot 0.15 = 5.4\ m^3$$

$$V(beam) = 0.6 \cdot 0.4 \cdot 6 \cdot 4 = 5.76\ m^3$$

$$V_{total,\ option\ 1} = 5.4 + 5.76 = 11.16\ m^3$$

3.4.1.2. Option 2: Two-way slab with minor beams

The same procedure was repeated for this option. Thickness of major beam was assumed to be 8% of its length, whereas thickness of simply-supported minor beam is equal to $\frac{l}{16}$. Thickness of slab was assumed to be 0.150 m.

$$h_{major} = 8\% * L = 0.08 * 6 = 0.48\ m$$

$$b_{major} = 0.48/2 = 0.24\ m$$

$$h_{minor} = L/16 = 6/16 = 0.375\ m$$

$$b_{major} = 0.375/2 = 0.188\ m$$

Then, the moment of inertia and stiffness ratio was calculated.

$$I_{b,major} = \frac{1}{12} * 0.240 * 0.48^3 * 0.35 = 7.74 \times 10^{-4}\ m^4$$

$$I_{b,minor} = \frac{1}{12} * 0.188 * 0.375^3 * 0.35 = 2.88 \times 10^{-4}\ m^4$$

$$I_s = \frac{1}{12} * 3 * 0.150^3 * 0.25 = 2.11\times10^{-4}\, m^4$$

$$\alpha_{f,major} = 3.668 \quad \text{and} \quad \alpha_{f,minor} = 1.365$$

$$\alpha_{fm} = \frac{\alpha_{f,major} + \alpha_{f,minor}}{2} = 2.517 > 2$$

Then, the clear span of slabs with beams measured in long direction, and subsequently, the ratio of clear span in long to short directions of slab was found.

$$\beta = \frac{L_{yn}}{L_{xn}} = \frac{3\,m}{3\,m} = 1$$

$$l_n = L - \frac{b_{major}}{2} - \frac{b_{major}}{2} = 3 - 0.24 - 0.188 = 2.786\,m$$

Based on the calculated values, the minimum thickness of slab was found using the equation:

$$h = \frac{2.786(0.8+60000/200{,}000)}{36+9} = 0.068\,m < 0.09\,m\ (3.5\,in.)$$

The minimum thickness of slab should be 0.09 m, thus the initial assumed thickness of slab, 0.150 m was taken. Subsequently, the volumes of members were calculated:

$$V(slab) = 3{\cdot}3{\cdot}0.150{\cdot}4 = 5.4\,m^3$$

$$V(major\ beam) = 0.48{\cdot}0.24{\cdot}6{\cdot}4 = 2.765\,m^3$$

$$V(minor\ beam) = 0.4{\cdot}0.2{\cdot}6{\cdot}2 = 0.96\,m^3$$

$$V_{total,\,option\,2} = 5.4 + 2.765 + 0.96 = 9.125\,m^3$$

3.4.1.3. Option 3: One-way slab with minor beam

For this last case, the dimensions of major and minor beams were found the same way as in the previous option.

$$h_{major} = 0.48\,m;\ b_{major} = 0.24\,m$$

$$h_{minor} = 0.375\,m \simeq 0.4\,m;\ b_{major} = 0.188\,m \simeq 0.2\,m$$

The thickness of simply supported one-way slab is equal to $\frac{l}{20}$.

$$h_{slab} = \frac{L}{20} = \frac{3}{20} = 0.15\,m$$

Accordingly, the volumes of members can be calculated as:

$$V(slab) = 3{\cdot}6{\cdot}0.15{\cdot}2 = 5.4\,m^3$$

$$V(major\ beam) = 0.48{\cdot}0.24{\cdot}6{\cdot}4 = 2.765\,m^3$$

$$V(minor\ beam) = 0.4 \cdot 0.2 \cdot 6 = 0.48\ m^3$$

$$V_{total,\ option\ 1} = 5.4 + 2.765 + 0.48 = 8.645\ m^3$$

Based on the calculations of measurements and add up to volumes of basic individuals, the format that comes about within the most reduced volume, and appropriately, the least fetched was chosen as the layout framework for the full building, for our case it is a one-way slab with a minor beam.

Table 3.12. Total volumes of slab options

Option	Member	L, m	h, m	b, m	V_{total}, m^3
Two-way slab	Slab	6.00	0.15	6.00	11.16
	Major beam	6.00	0.48	0.24	
Two-way slab with minor beams	Slab	3.00	0.15	3.00	9.125
	Major beam	6.00	0.48	0.24	
	Minor beam	6.00	0.40	0.20	
One-way with minor beam	Slab	6.00	0.15	3.00	8.645
	Major beam	6.00	0.48	0.24	
	Minor beam	6.00	0.40	0.20	

3.4.2. Estimation of Size Dimensions of Columns

After the calculation of size dimensions of slab, we can calculate major and minor beams' dimensions with columns using the self-weight of structural members and dead and live loads.

Self-weight of beams:

$$SW_{major\ beam} = \rho_{RC} \cdot V_{beam}(major) = 2400\ kg/m^3 \cdot (0.48 \cdot 0.24 \cdot 6) m^3 = 1659\ kg$$

$$SW_{minor\ beam} = \rho_{RC} \cdot V_{beam}(minor) = 2400\ kg/m^3 \cdot (0.4 \cdot 0.2 \cdot 6)\ m^3 = 1152\ kg$$

Load combination was applied to estimate the dimensions of columns:

$$w_u = 1.2D + 1.6L + 0.5L_r \tag{3.6}$$

Self-weights of major and minor beams transferred to interior column will be:

$$D_{beams} = \frac{(2 \cdot 1659 + 4 \cdot 1152)\ kg}{36\ m^2} \cdot 9.81\ m/s^2 = 2.16\ kN/m^2$$

Total dead load transferred to interior column at first floor will be:

$$D_{floor} = D_{beams} + D_{partition\ walls} + D_{finishing,floor} = 2.16 + 2.21 + 5.37 = 9.74\ kN/m^2$$

$$D_{roof} = 5.56\ kN/m^2$$

$$L = 3.02\ kN/m^2 \text{ (critical live load on interior column)}$$

$$L_r = 0.96\ kN/m^2$$

Based on the loads, the load combination on the first floor will be calculated as:

$$w_u = 19(1.2 \cdot 9.74 + 1.6 \cdot 3.02) + 1.2 \cdot 5.56 + 0.5 \cdot 0.96 = 321.032\ kN/m^2$$

Because of the fact that our building is a reinforced concrete structure, we used the ACI 318-19 code to estimate the size (American Concrete Institute, 2022). In addition, the weight of the columns above the first floor was repeatedly added to the columns of each floor. Moreover, our building has a basement. We also calculated the size of the columns in the basement. Note that the floor height above the first floor is 3.5m, and the floor height of the first floor is 4m. This led to the calculations of exterior and corner columns while making primary calculations of the interior ones.

$$P_u = w_u \cdot A_T + w_{columns\ above\ first\ floor} = 321.032\ kN/m^2 \cdot 36\ m^2 + 400\ kN = 11957.152 kN$$

$$\phi P_n = 0.8\phi(0.85 f_c' A_c + f_y A_s) \quad (3.7)$$

Reinforcement ratio was assumed as 1%, hence, $A_s = 0.01 A_c$, $\phi = 0.65$ (based on ACI 318-19), $f_c' = 40\ MPa$, $f_y = 420\ MPa$.

$$\phi P_n = 0.8 \cdot 0.65 \cdot (0.85 \cdot 40000 A_c + 420000 \cdot (0.01 A_c)) = 19864 A_c$$

$$\phi P_n \geq P_u$$

$$19864 A_c \geq 11957.152$$

$$A_c \geq 0.602\ m^2$$

If we assume that we have square columns of size $a = b \geq 0.776\ m$, then our dimensions of interior columns for 1 floor will be 0.80 m.

Table 3.13. Column size estimations for exterior, interior, and corner columns on the 1st floor.

	D	L	A_T, m^2	W_u, kN/m^2	P_u, kN	A_c, m^2	a = b, m	Column size, m
Exterior column	11.32	3.02	18	412.18	8509.21	0.231	0.481	0.50
Interior column	7.74	3.02	36	368.80	13276.94	0.414	0.644	0.65
Corner column	12.789	4.79	9	440.74	5056.60	0.124	0.352	0.40

The same procedure was performed for all 12 floors, including the basement floor.

Table 3.14. Dimensions of columns.

Floors	Column size, m
0-2	0.80
3-4	0.75
5-6	0.70
7-8	0.65
9-10	0.60
11-13	0.55

3.4.3. Assigning Loads to SAP 2000

3.4.3.1. Assigning Loads to Chosen 2D Frame

For the material type, all the structural members were designed with C40 concrete and Grade 60 rebar.

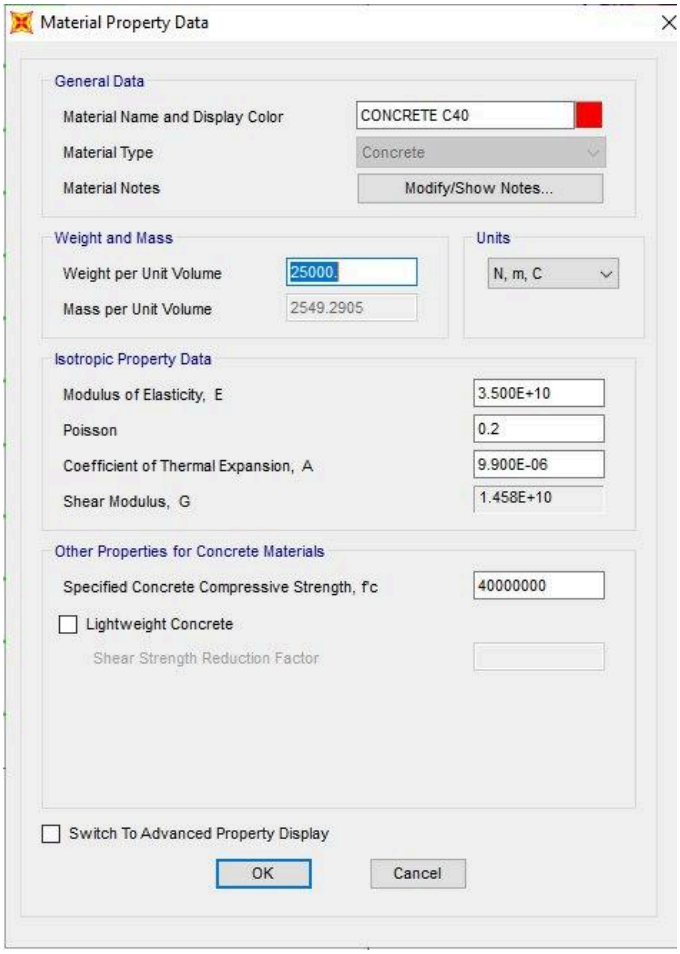

Figure 3.3. Material properties in SAP2000: concrete

The frame components were then defined, specifically the major and minor beams and the varying-sized columns on each floor.

a)

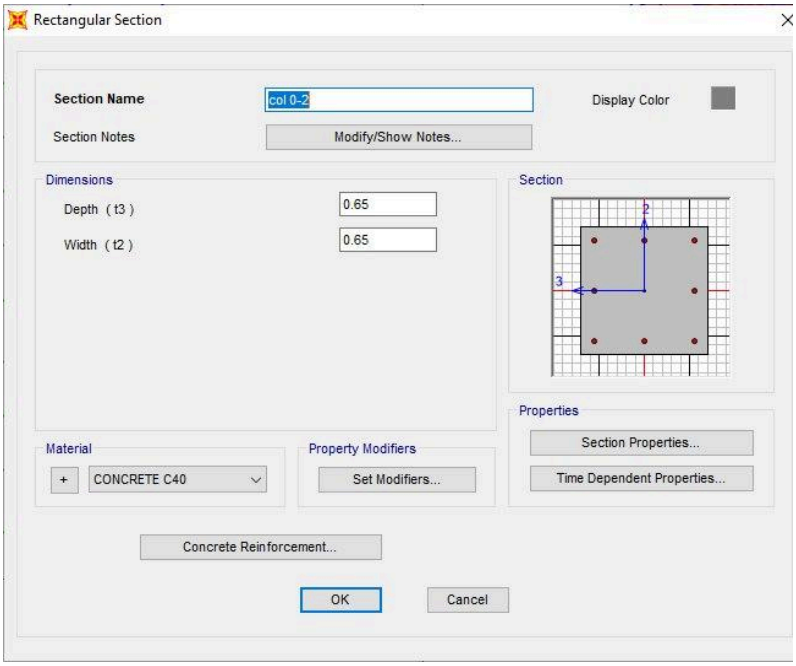
Rectangular Section
Section Name
col 0-2
Display Color
Section Notes
Modify/Show Notes...
Dimensions
Depth (t3)
0.65
Width (t2)
0.65
Section
2
3
Properties
Material
CONCRETE C40
Property Modifiers
Set Modifiers...
Section Properties...
Time Dependent Properties...
Concrete Reinforcement...
OK
Cancel

b)

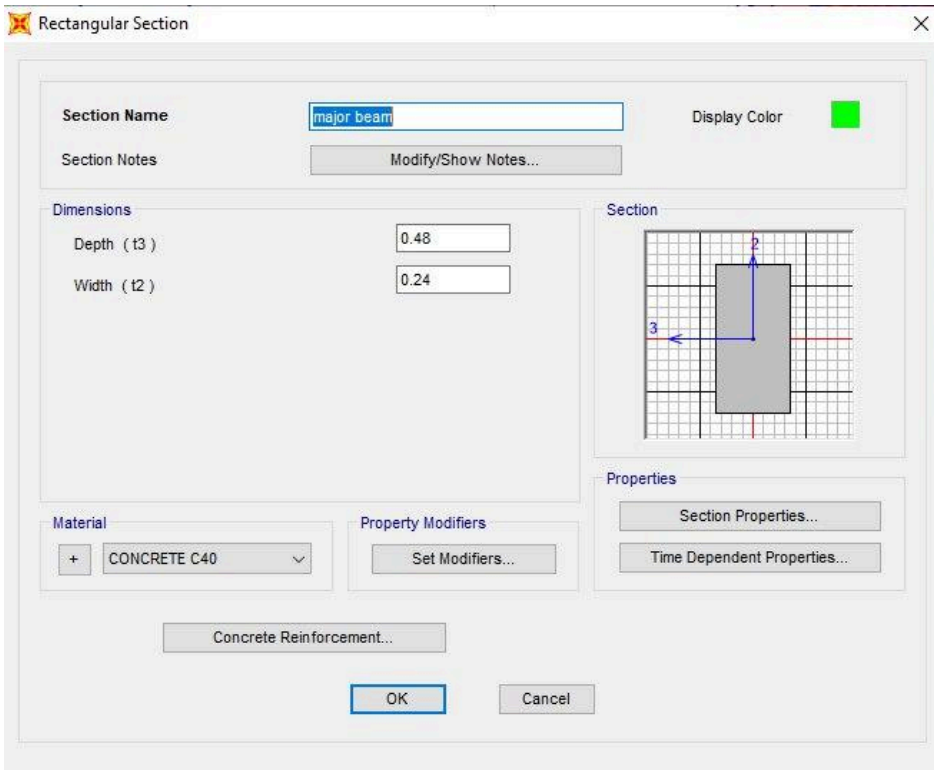
Rectangular Section
Section Name
major beam
Display Color
Section Notes
Modify/Show Notes...
Dimensions
Depth (t3)
0.48
Width (t2)
0.24
Section
2
3
Properties
Material
CONCRETE C40
Property Modifiers
Set Modifiers...
Section Properties...
Time Dependent Properties...
Concrete Reinforcement...
OK
Cancel

c)

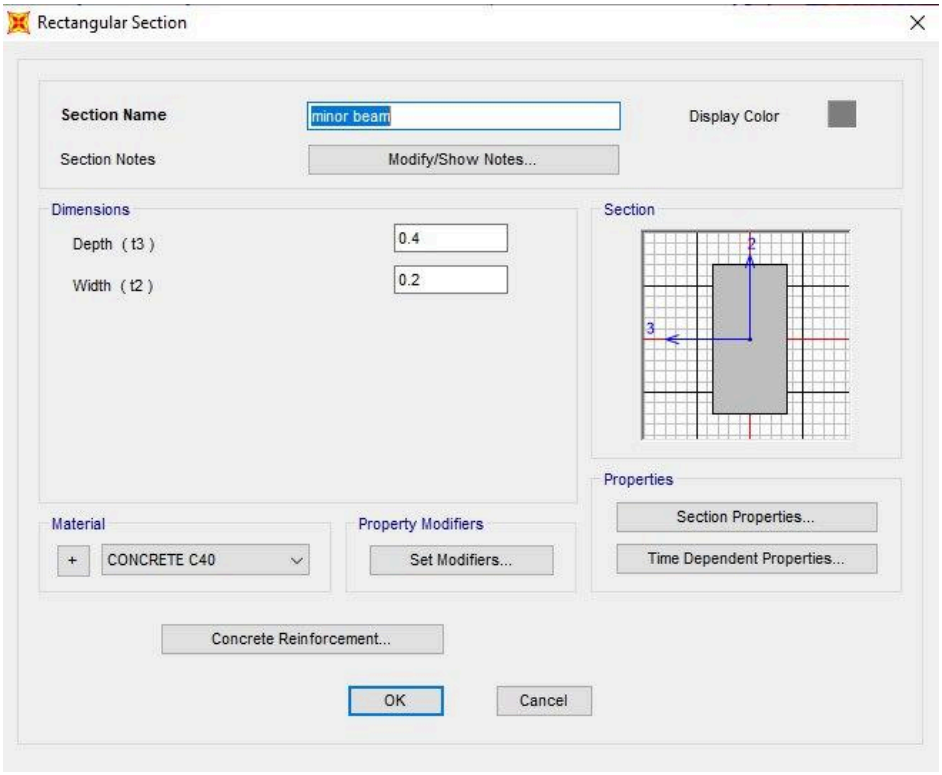

d)

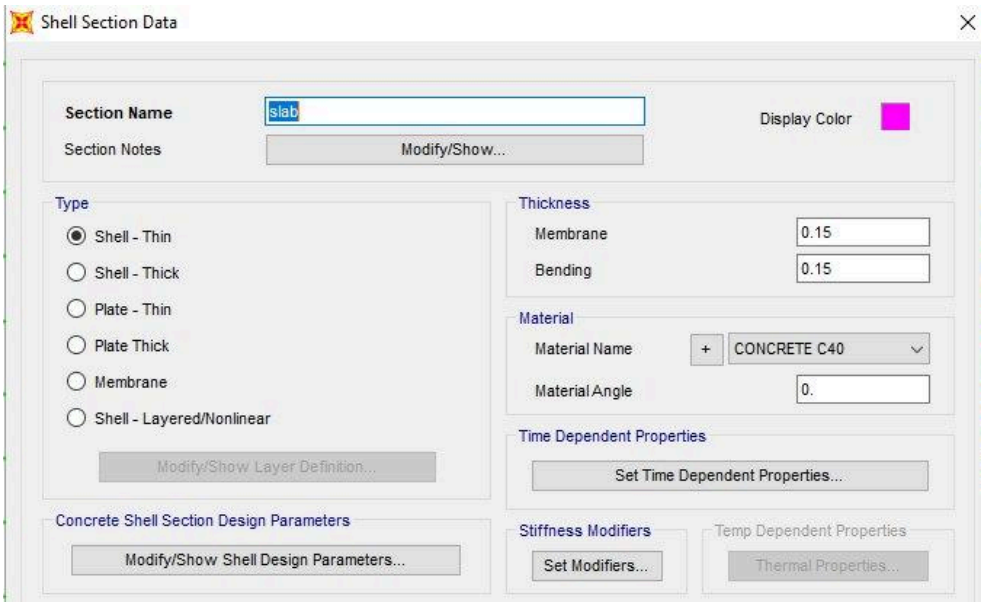

Figure 3.4. Section properties: a) column, b) major beams, c) minor beam, d) slab.

The 2D frame building model was created using the parameter definitions, and unfactored dead, live, and roof live loads were allocated.

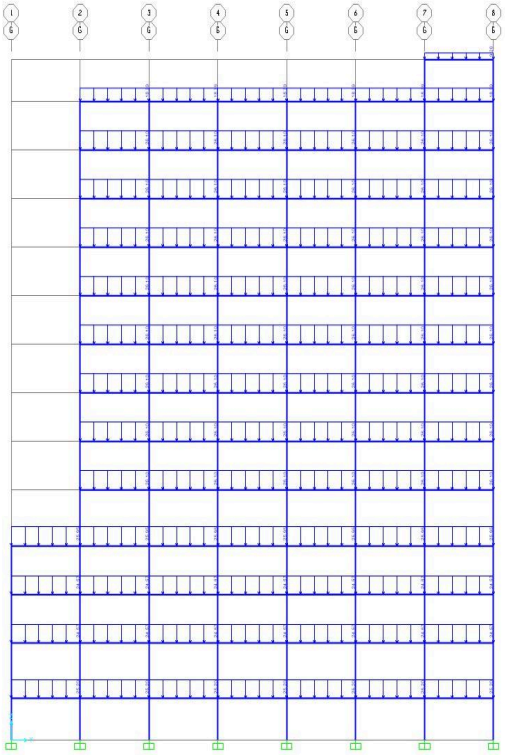

a)

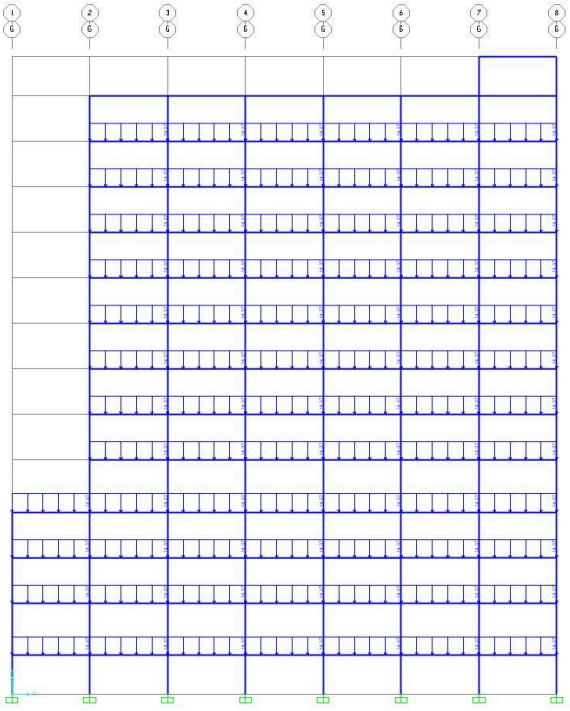

b)

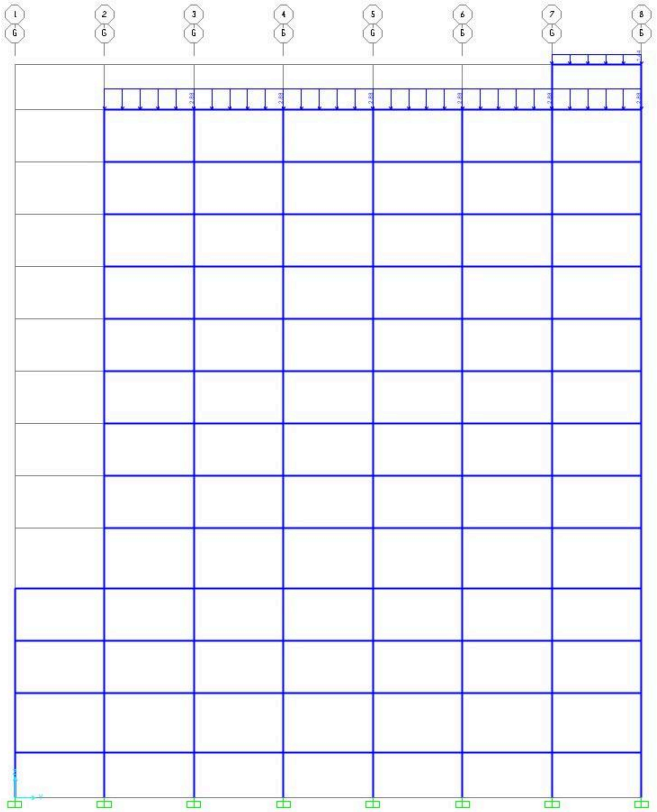

c)

Figure 3.5. Assigned loads on 2D frame in SAP2000: a) dead load, b) live load, c) roof live load.

3.4.3.2. Assigning Loads to 3D Frame

Similarly to the frame sections, materials and constraints, the building structure was designed in 3D in SAP2000.

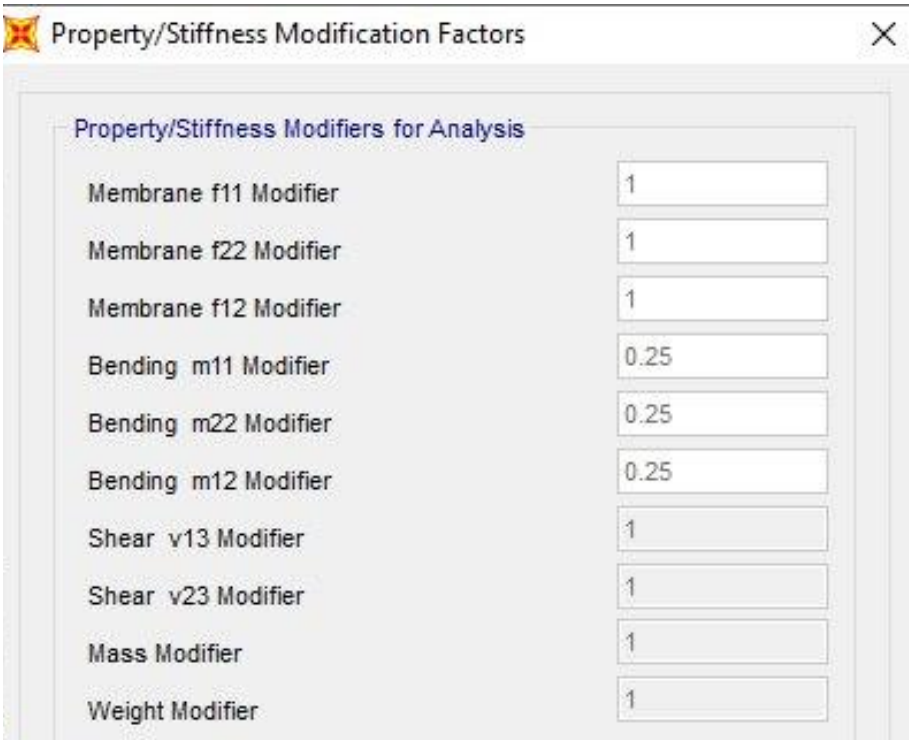

Figure 3.6. Slab section property modifiers.

The loads were then distributed on the slab, and because the elevator shafts and stairs do not have slabs, the loads from the elevators and stairs were distributed on nearby beams according to the one-way slab's load transfer.

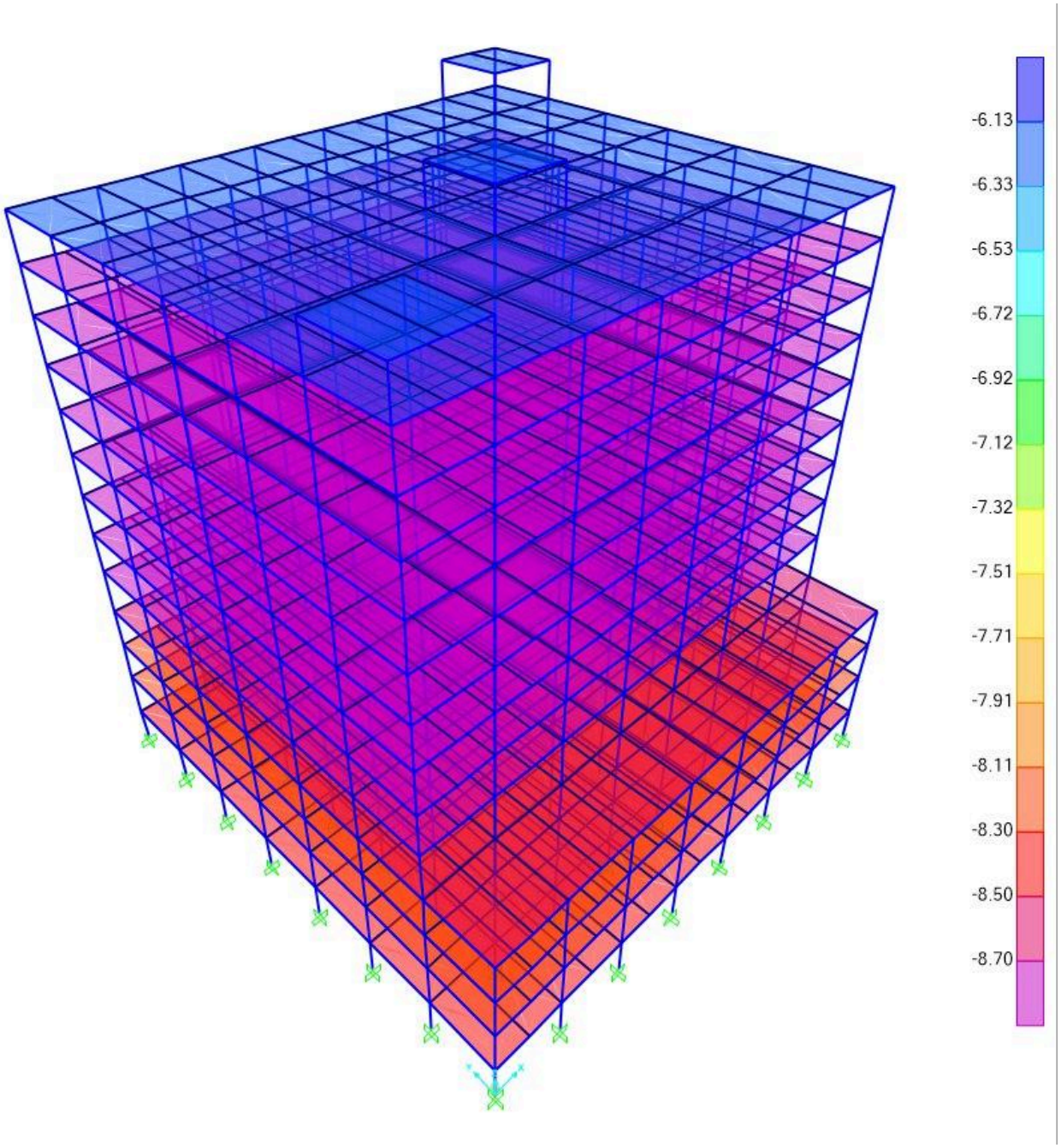

Figure 3.7. Applied dead area loads on a 3D model in SAP2000

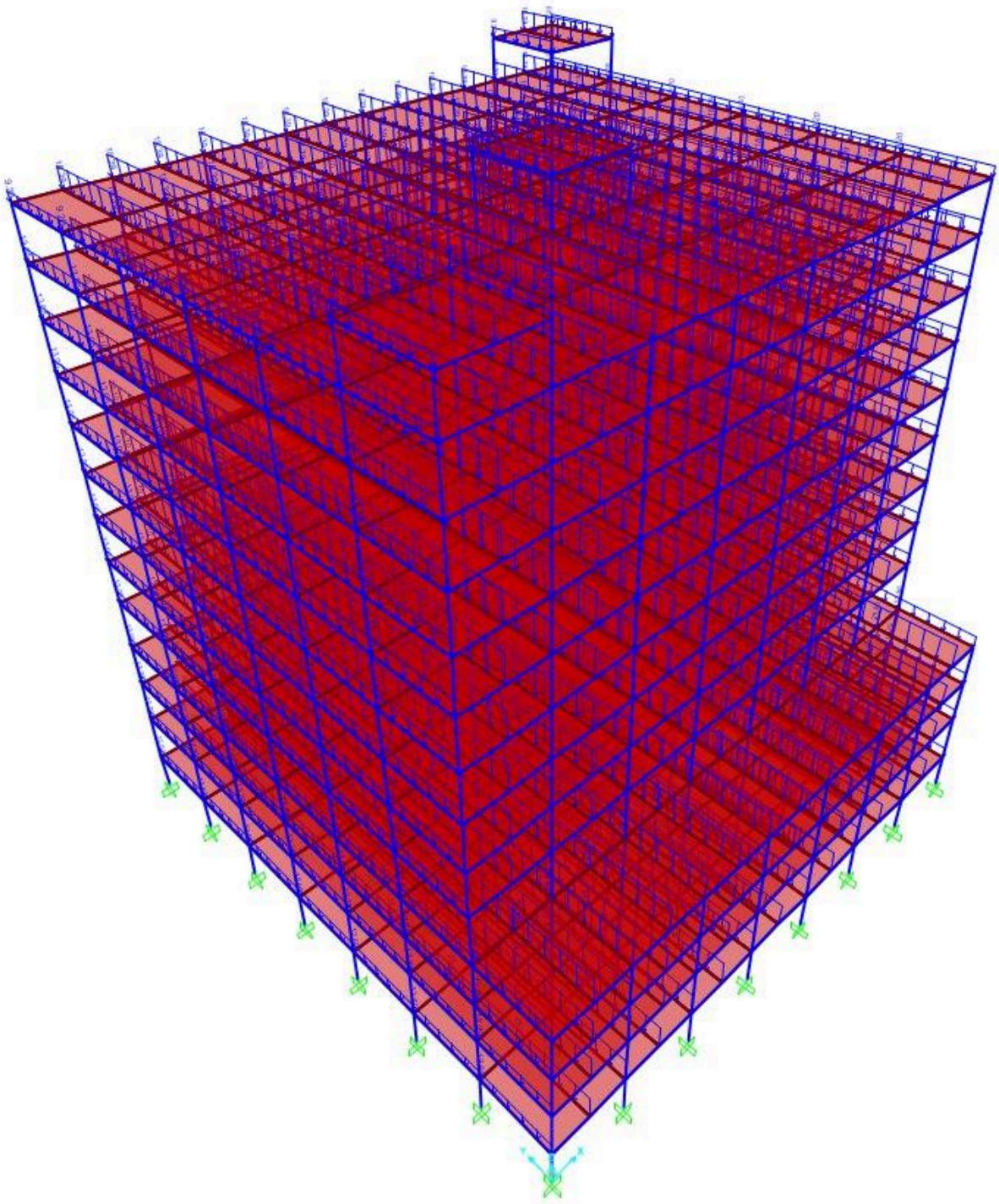

Figure 3.8. Applied dead frame loads on 3D model in SAP2000

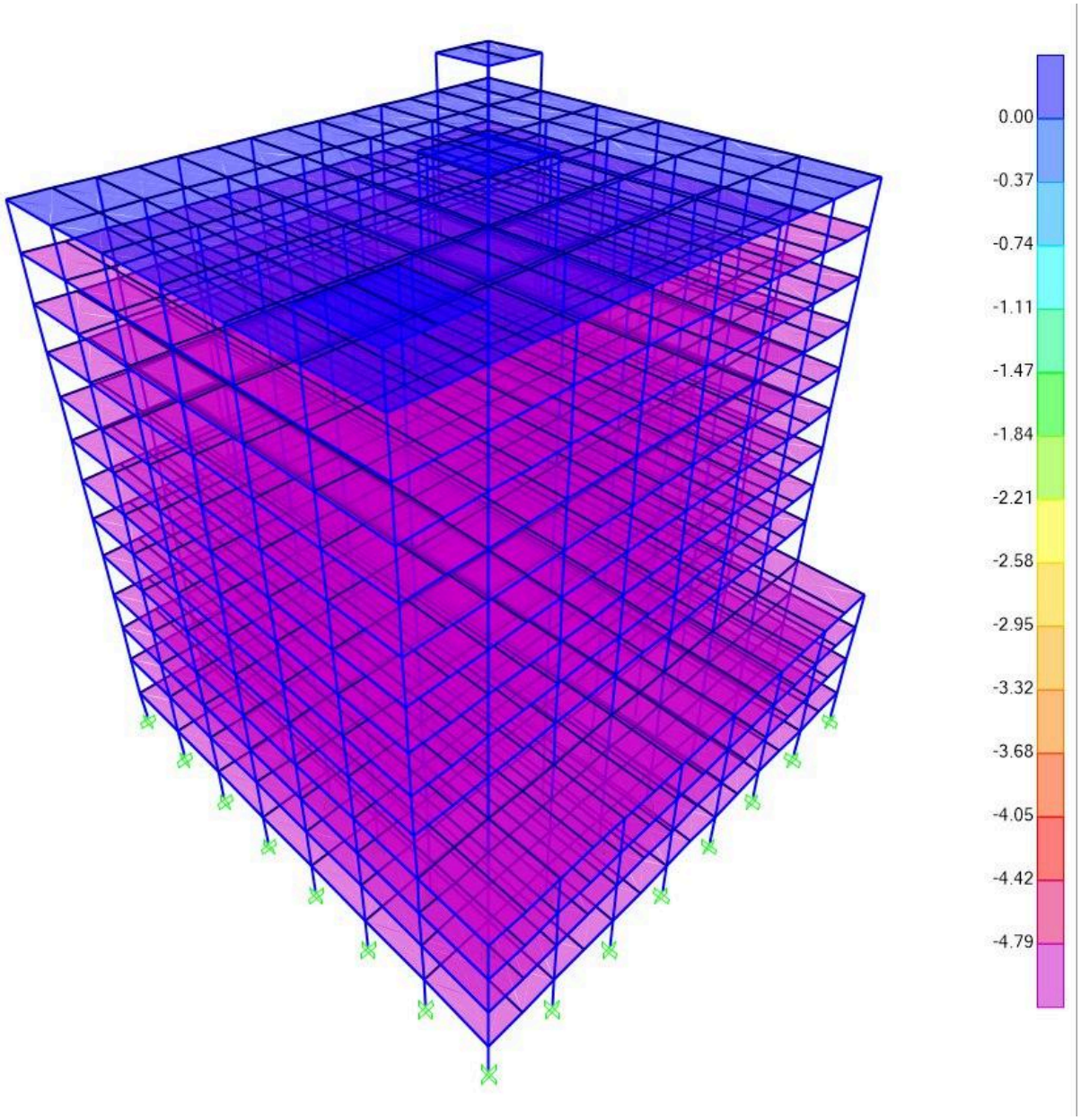

Figure 3.9. Applied live area loads on a 3D model in SAP2000

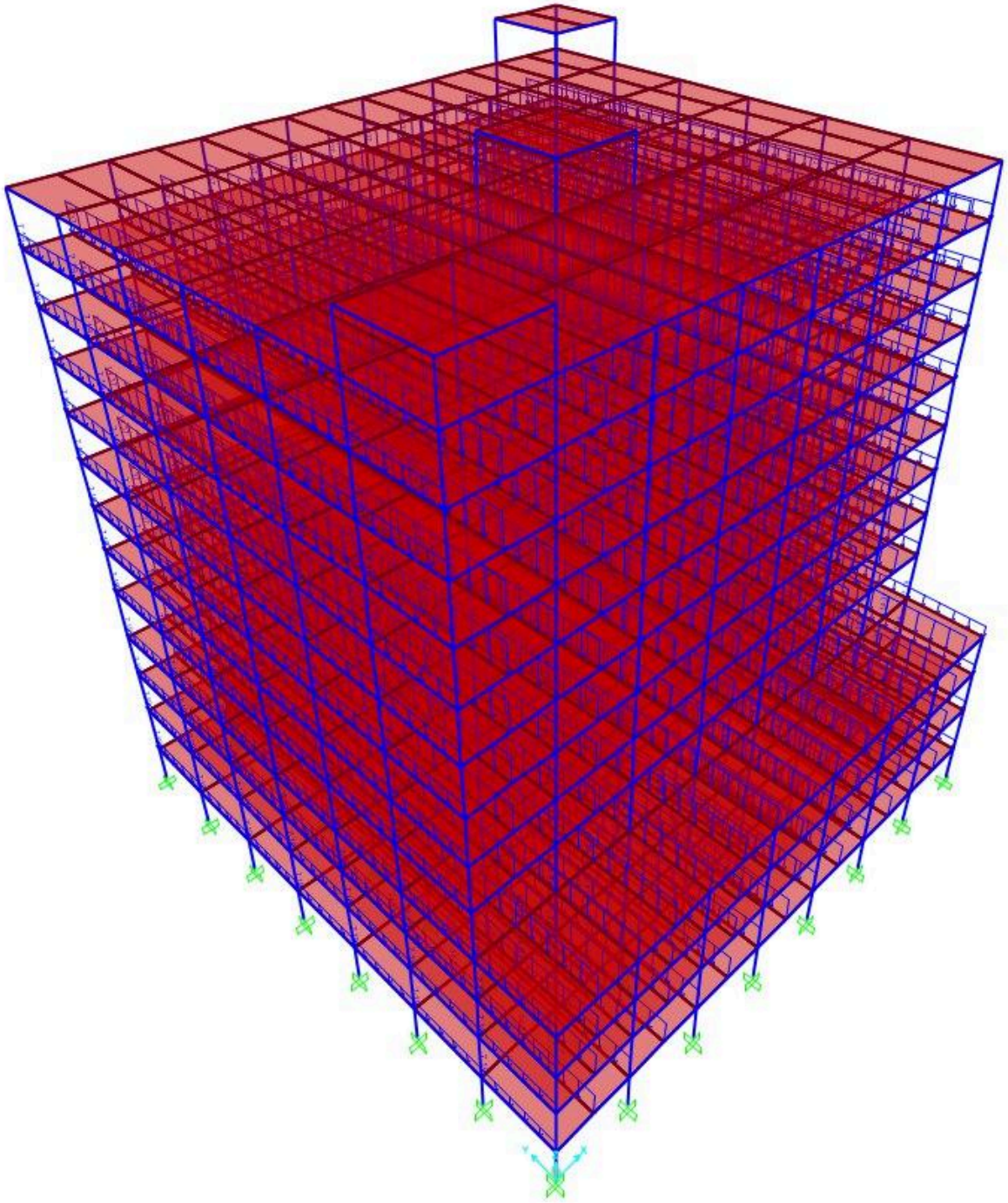

Figure 3.10. Applied live frame loads on 3D model in SAP2000

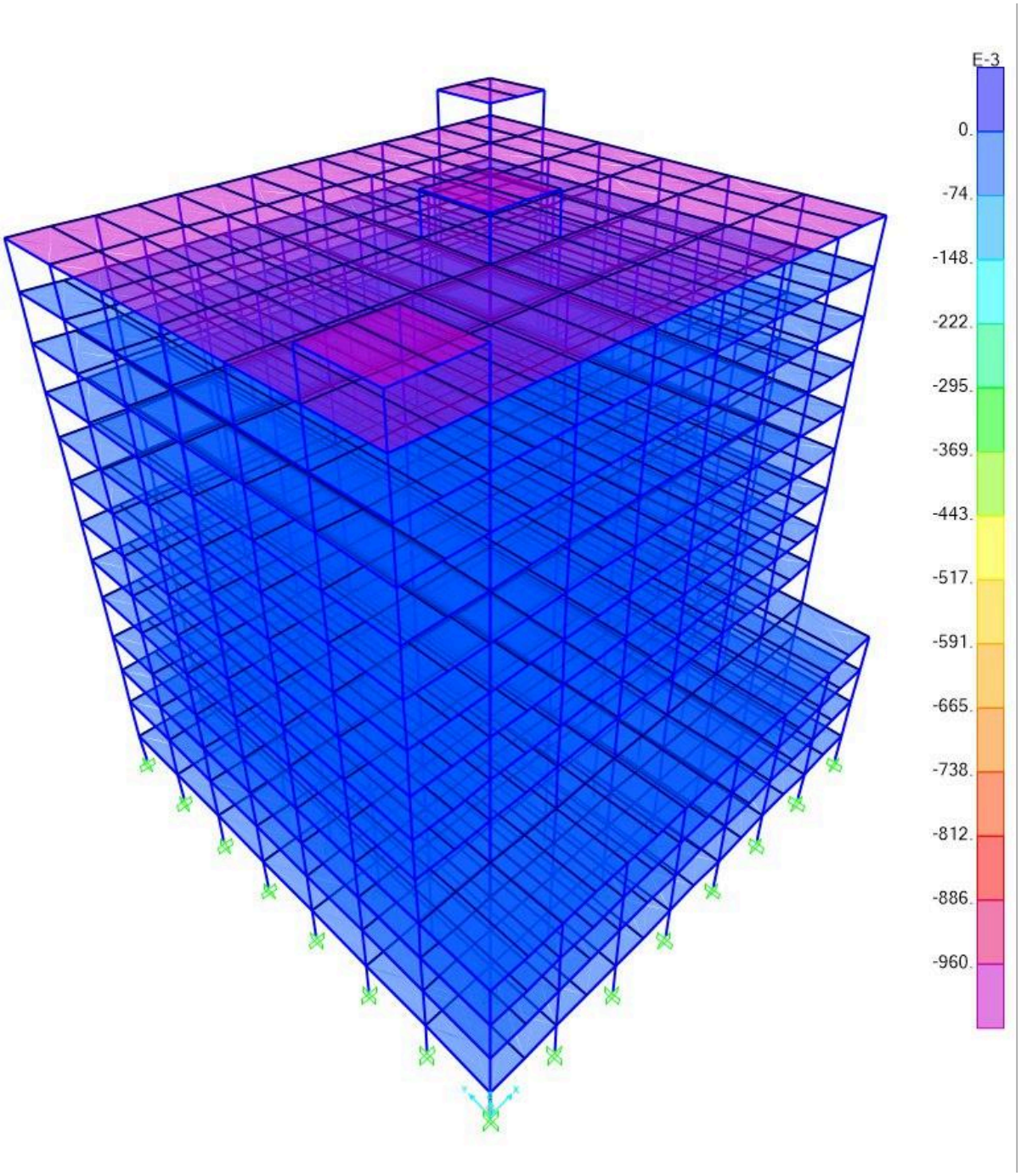

Figure 3.11. Applied roof live area loads on a 3D model in SAP2000

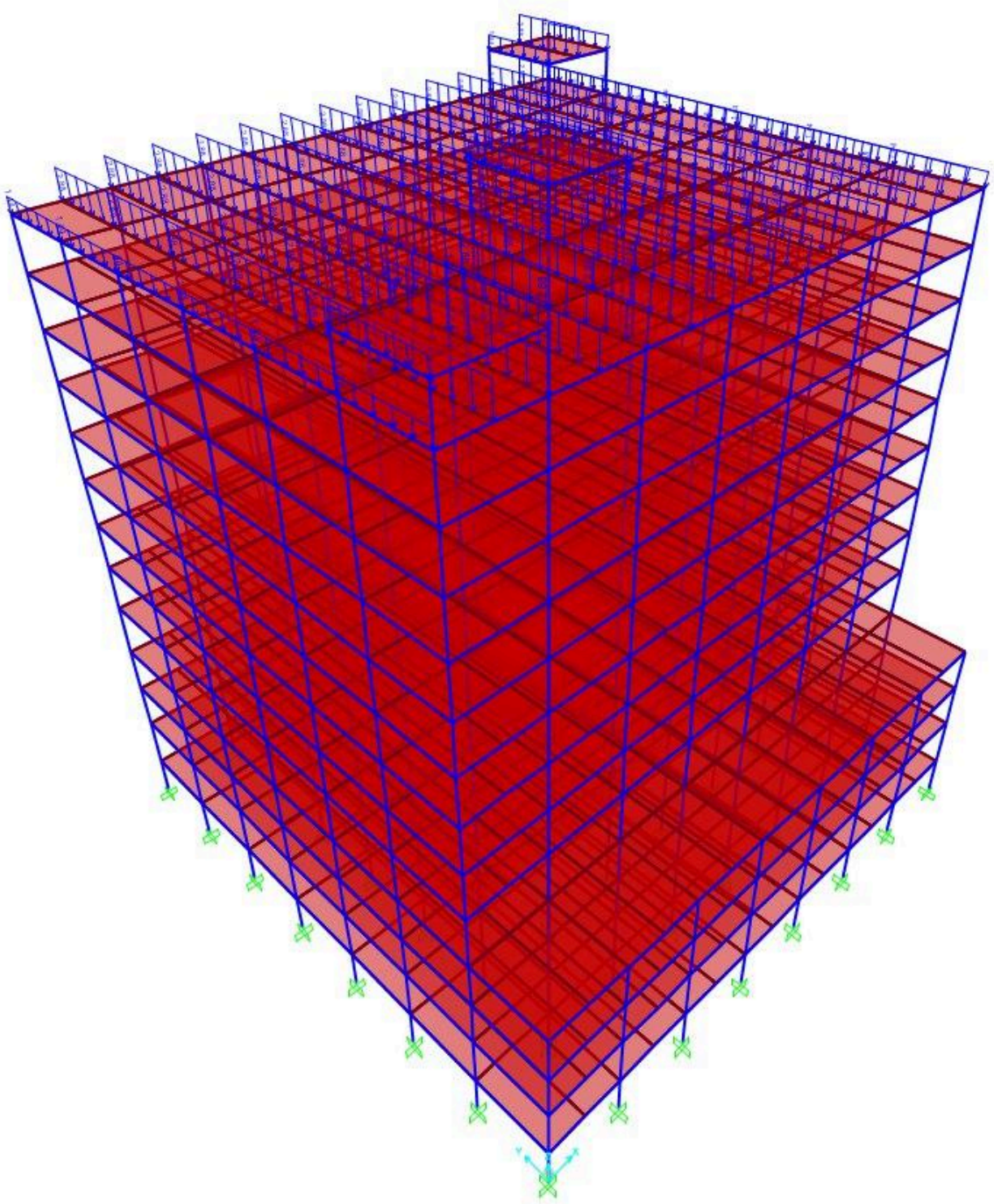

Figure 3.12. Applied roof frame loads on 3D model in SAP2000

3.5. Analysis and Design of Lateral Force Resisting System (LFRS)

3.5.1. Calculation of Wind Loads

3.5.1.1. Wind Loads Including Torsional Effect

According to the ASCE 7-10 basic wind speed in Los Angeles, California was found as $V = 42\ m/s$ This helped to perform calculations on wind load (ASCE Hazard Tool).

- Exposure category B (city)
- Topographical Effect: $K_{zt} = 1$ (flat land)
- Direction Effect: $K_d = 0.85$ (main wind load force resisting system (LFRS))

Table 3.15. Constants fr exposure categories

Exposure	α	z_g (m)	$\hat{a}$	$\hat{b}$	$\bar{\alpha}$	$\bar{b}$	c	ℓ (m)	$\bar{\epsilon}$	z_{min} (m)*
B	7.0	365.76	1/7	0.84	1/4.0	0.45	0.30	97.54	1/3.0	9.14
C	9.5	274.32	1/9.5	1.00	1/6.5	0.65	0.20	152.4	1/5.0	4.57
D	11.5	213.36	1/11.5	1.07	1/9.0	0.80	0.15	198.12	1/8.0	2.13

- Height Effect

The velocity pressure exposure coefficient can be calculated by formula:

$$K_z = 2.01\left(\frac{15}{z_g}\right)^{2/\alpha}, \text{ for } z < 15 \text{ ft} \quad (3.8)$$

$$K_z = 2.01\left(\frac{z}{z_g}\right)^{2/\alpha}, \text{ for } 15 \text{ ft} \le z \le z_g \quad (3.9)$$

The final calculations for Kz values:

Table 3.16. The results for Kz value calculations

Story	h (m)	z (m)	Kz
13	3,5	46,00	1,112
12	3,5	42,50	1,087
11	3,5	39,00	1,060

10	3,5	35,50	1,032
9	3,5	32,00	1,002
8	3,5	28,50	0.969
7	3,5	25,00	0.934
6	3,5	21,50	0.894
5	3,5	18,00	0.850
4	3,5	14,50	0.799
3	3,5	11,00	0.739
2	3,5	7,50	0.662
1	4	4	0.807

- Gust effect

The Gust effect was calculated considering 2 possible wind directions.

For case 1: $B = 37.2\,m,\ L = 43.2\,m,\ \ m\,(number\ of\ frames) = 7$

For case 2: $B = 43.2\,m,\ L = 37.2\,m,\ \ m\,(number\ of\ frames) = 8$

Therefore, the Gust effect is calculated for two cases with consideration of different gust effects on different layouts.

Case 1 (Y-axis)

Since H = 46 m > 18 m, the building is not a "low-rise". In order to estimate the Gust factor for the reinforced concrete frames, these equations were comprised:

$$n_a = 43.5/h^{0.9} = 43.5/150.919 = 0.476 < 1 \text{ Hz: a flexible building.}$$

$$\bar{z} = 0.6h = 0.6 \cdot 46 = 27.6 > z_{min} = 9.14\,m$$

$$I_{\bar{z}} = c\left(\frac{10}{\bar{z}}\right)^{\frac{1}{6}} = 0.3\left(\frac{10}{27.6}\right)^{\frac{1}{6}} = 0.271$$

$$\overline{V}_{\bar{z}} = \bar{b}\left(\frac{\bar{z}}{10}\right)^{\bar{\alpha}} V = 0.45\left(\frac{27.6}{10}\right)^{0.25} \cdot 42 = 24.36\,m/s$$

$$n_1 = n_a = 0.476,\ L_{\bar{z}} = l\left(\frac{\bar{z}}{10}\right)^{\bar{\epsilon}} = 97.54\left(\frac{27.6}{10}\right)^{0.33} = 136.36 \text{ m}$$

$$N_1 = \frac{n_1 L_{\bar{z}}}{\overline{V}_{\bar{z}}} = \frac{0.476 \cdot 136.36}{24.36} = 2.664$$

$$R_n = \frac{7.47 N_1}{(1+10.3N_1)^{5/3}} = \frac{7.47 \cdot 2.664}{(1+10.3 \cdot 2.664)^{5/3}} = 0.075$$

$$\eta_h = \frac{4.6 n_1 H}{\overline{V_z}} = \frac{4.6 \cdot 0.476 \cdot 46}{24.36} = 4.13$$

$$R_h = \frac{1}{\eta_h} - \frac{1}{2\eta_h^{\,2}} \left(1 - e^{-2\eta_h}\right) = 0.213$$

$$\eta_b = \frac{4.6 n_1 B}{\overline{V_z}} = \frac{4.6 \cdot 0.476 \cdot 37.2}{24.36} = 3.344$$

$$R_b = 0.254$$

$$\eta_L = \frac{15.4 n_1 L}{\overline{V_z}} = \frac{15.4 \cdot 0.476 \cdot 43.2}{24.36} = 12.99$$

$$R_L = 0.074$$

$$R = \sqrt{\frac{R_n R_h R_b (0.53 + 0.47 R_L)}{\beta}} = \sqrt{\frac{0.075 \cdot 0.213 \cdot 0.254 \cdot (0.53 + 0.47 \cdot 0.074)}{0.02}} = 0.339$$

$$g_R = \sqrt{2ln(3600 n_1)} + \frac{0.577}{\sqrt{2ln(3600 n_1)}} = \sqrt{2ln(3600 \cdot 0.476)} + \frac{0.577}{\sqrt{2ln(3600 \cdot 0.476)}} = 4.009$$

$$g_v = g_Q = 3.4$$

$$Q = \sqrt{\frac{1}{1 + 0.63 \left(\frac{B+h}{L_z}\right)^{0.63}}} = \sqrt{\frac{1}{1 + 0.63 \left(\frac{37.2+46}{136.36}\right)^{0.63}}} = 0.827$$

$$G_f = 0.925 \left(\frac{1 + 1.7 I_z \sqrt{g_Q^{\,2} Q^2 + g_R^{\,2} R^2}}{1 + 1.7 g_v I_z}\right) = 0.925 \left(\frac{1 + 1.7 \cdot 0.271 \sqrt{3.4^2 \cdot 0.827^2 + 4.009 \cdot 0.339^2}}{1 + 1.7 \cdot 3.4 \cdot 0.271}\right) = 0.841$$

L/B=37.2/43.2=0.861<1

External pressure coefficient C_p:

Windward = 0.8 and Leeward = -0.5

Case 1 (X-axis)

The same calculations were performed for this case, but only *L* and *B* were changed.

$$G_f = 0.925 \left(\frac{1 + 1.7 I_z \sqrt{g_Q^{\,2} Q^2 + g_R^{\,2} R^2}}{1 + 1.7 g_v I_z}\right) = 0.864$$

L/B=43.2/37.2=1.161>1

External pressure coefficient C_p:

Windward = 0.8 and Leeward = -0.3 (Using Interpolation)

Here are other formulas for calculating pressure and force on each floor:

Velocity pressure calculation

$$q_z = 0.613 K_z K_{zt} K_d V^2 \quad (3.10)$$

Design wind pressure calculation

$$P = q_z GC_{p,windward} - q_h GC_{p,leeward} \quad (3.11)$$

Force at top floor

$$F_{21} = (B/number\ of\ frames) \cdot h_{21}/2 \cdot P_{21} \quad (3.12)$$

Force at i_{th} floor

$$F_i = (B/number\ of\ frames) \cdot (P_{i+1} \cdot h_{i+1}/2 + P_i \cdot h_i/2) \quad (3.13)$$

Table 3.17. Y-axis wind force calculations on each frame (Case 1)

Story	h (m)	z (m)	Kz	q (Pa)	Gf	Pw, Pl (Pa)	P (Pa)	Fi (kN)	F per frame (kN)
13	3,5	46,00	1,112	1021,66	0.841	719,46	1159,06	75,46	10,78
12	3,5	42,50	1,087	998,82	0.841	703,37	1142,98	149,86	21,41
11	3,5	39,00	1,060	974,59	0.841	686,31	1125,92	147,71	21,10
10	3,5	35,50	1,032	948,76	0.841	668,12	1107,73	145,41	20,77
9	3,5	32,00	1,002	921,03	0.841	648,60	1088,20	142,95	20,42
8	3,5	28,50	969	891,05	0.841	627,48	1067,09	140,31	20,04
7	3,5	25,00	934	858,31	0.841	604,42	1044,03	137,43	19,63
6	3,5	21,50	894	822,11	0.841	578,93	1018,54	134,27	19,18
5	3,5	18,00	850	781,41	0.841	550,28	989,88	130,75	18,68
4	3,5	14,50	799	734,60	0.841	517,31	956,92	126,74	18,11
3	3,5	11,00	739	678,85	0.841	478,05	917,66	122,03	17,43
2	3,5	7,50	662	608,48	0.841	428,50	868,10	116,25	16,61
1	4	4	807	741,75	0.841	522,34	961,95	128,08	18,30

Table 3.18. X-axis wind force calculations on each frame (Case 1)

Story	h (m)	z (m)	Kz	q (Pa)	Gf	Pw, Pl (Pa)	P (Pa)	Fi (kN)	F per frame (kN)
13	3,5	46,00	1,112	1021,66	0.864	706,17	965,06	72,96	9,12
12	3,5	42,50	1,087	998,82	0.864	690,38	949,28	144,72	18,09
11	3,5	39,00	1,060	974,59	0.864	673,64	932,53	142,26	17,78
10	3,5	35,50	1,032	948,76	0.864	655,78	914,67	139,65	17,46
9	3,5	32,00	1,002	921,03	0.864	636,62	895,51	136,85	17,11
8	3,5	28,50	969	891,05	0.864	615,89	874,79	133,83	16,73
7	3,5	25,00	934	858,31	0.864	593,26	852,16	130,56	16,32
6	3,5	21,50	894	822,11	0.864	568,24	827,13	126,95	15,87
5	3,5	18,00	850	781,41	0.864	540,11	799,01	122,94	15,37
4	3,5	14,50	799	734,60	0.864	507,76	770,00	118,62	14,83
3	3,5	11,00	739	678,85	0.864	469,22	770,00	116,42	14,55
2	3,5	7,50	662	608,48	0.864	420,58	770,00	116,42	14,55
1	4	4	807	741,75	0.864	512,70	771,59	124,88	15,61

These calculations were part of the first case out of four, described in ASCE-7. The equations and the wind direction is shown in Figure x.

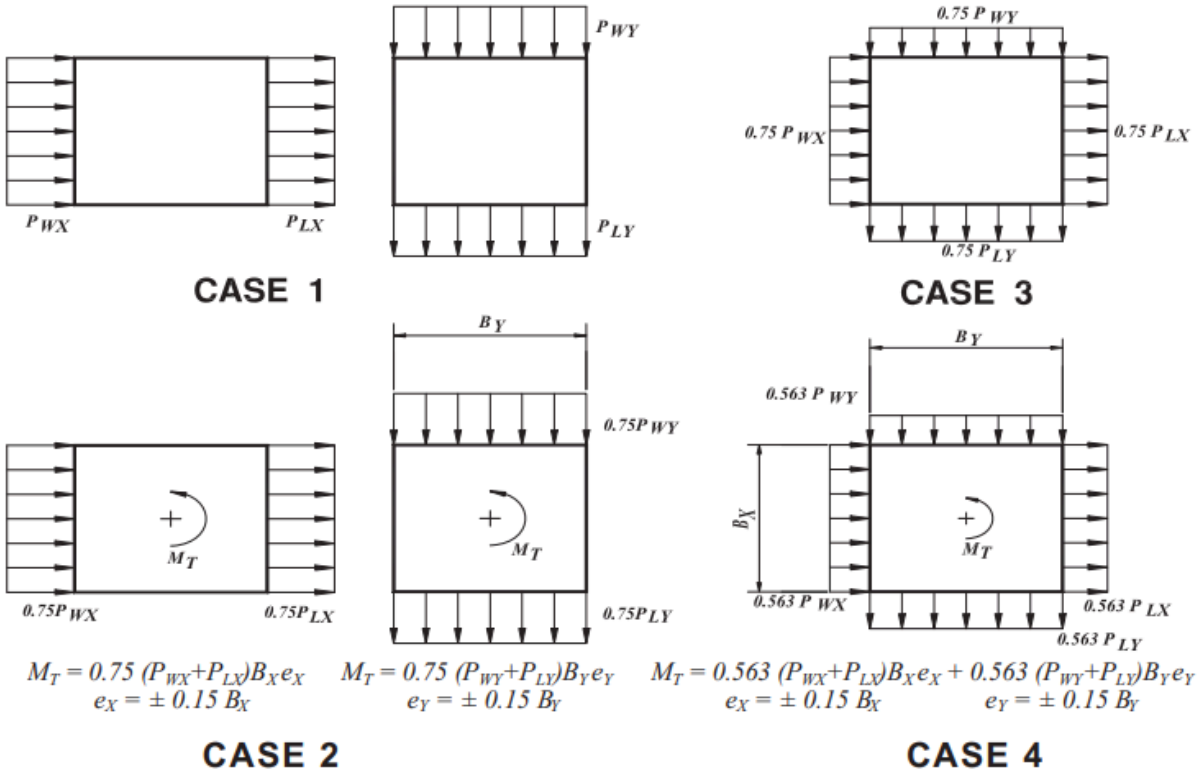

Figure 3.13. Wind load cases description

The further estimations include Case 2 with its torsional effect acting on each floor and each frame.

$$e_x = 0.15 \cdot B \tag{3.14}$$

$$e_x = 0.15 \cdot 37.2 = 5.58$$

Table 3.19. Direct force component for Case

Story	Pw, Pl (Pa)	MT (kN-m)	0.75Fi (kN)	F,direct (kN)
13	719,46	180,45	56,59	8,08
12	703,37	177,94	112,40	16,06
11	686,31	175,29	110,78	15,83
10	668,12	172,45	109,06	15,58
9	648,60	169,41	107,22	15,32
8	627,48	166,13	105,23	15,03

7	604,42	162,54	103,08	14,73
6	578,93	158,57	100,71	14,39
5	550,28	154,11	98,06	14,01
4	517,31	148,97	95,05	13,58
3	478,05	142,86	91,53	13,08
2	428,50	135,15	87,19	12,46
1	522,34	149,76	96,06	13,72

$$e_y = 0.15 \cdot L \tag{3.15}$$

$$e_y = 0.15 \cdot 43.2 = 6.48$$

Table 3.20**.** Direct force component for Case 2 (X-axis)

Story	Pw, Pl (Pa)	MT (kN-m)	0.75Fi (kN)	Fdirect (kN)
13	706,17	202,62	54,72	6,84
12	690,38	199,30	108,54	13,57
11	673,64	195,79	106,70	13,34
10	655,78	192,04	104,74	13,09
9	636,62	188,01	102,64	12,83
8	615,89	183,66	100,38	12,55
7	593,26	178,91	97,92	12,24
6	568,24	173,66	95,22	11,90
5	540,11	167,75	92,20	11,53
4	507,76	160,96	88,96	11,12
3	469,22	152,87	87,32	10,91
2	420,58	142,66	87,32	10,91
1	512,70	162,00	93,66	11,71

Table 3.21. Direct force component for Case 3 (Y-axis)

Story	0.75F1 (kN)	F1 per frame (kN)	0.75F2 (kN)	F2 per frame (kN)
13	56,59	8,08	54,72	7,82
12	112,40	16,06	108,54	15,51

11	110,78	15,83	106,70	15,24
10	109,06	15,58	104,74	14,96
9	107,22	15,32	102,64	14,66
8	105,23	15,03	100,38	14,34
7	103,08	14,73	97,92	13,99
6	100,71	14,39	95,22	13,60
5	98,06	14,01	92,20	13,17
4	95,05	13,58	88,96	12,71
3	91,53	13,08	87,32	12,47
2	87,19	12,46	87,32	12,47
1	96,06	13,72	93,66	13,38

Table 3.22. Direct force component for Case 4 (Y and X-axis)

Story	Pw, Pl (Pa) - x axis	Pw, Pl (Pa) - y axis	MT (kN-m)	0.563F1 (kN)	0.563F2 (kN)	F1 direct (kN)	F2 direct (kN)
13	719,46	706,17	287,55	42,48	41,08	6,07	5,87
12	703,37	690,38	283,18	84,37	81,48	12,05	11,64
11	686,31	673,64	278,55	83,16	80,09	11,88	11,44
10	668,12	655,78	273,61	81,87	78,62	11,70	11,23
9	648,60	636,62	268,31	80,48	77,05	11,50	11,01
8	627,48	615,89	262,58	78,99	75,35	11,28	10,76
7	604,42	593,26	256,31	77,38	73,50	11,05	10,50
6	578,93	568,24	249,39	75,60	71,48	10,80	10,21
5	550,28	540,11	241,61	73,61	69,21	10,52	9,89
4	517,31	507,76	232,66	71,35	66,78	10,19	9,54
3	478,05	469,22	222,00	68,71	65,55	9,82	9,36
2	428,50	420,58	208,54	65,45	65,55	9,35	9,36
1	522,34	512,70	234,02	72,11	70,31	10,30	10,04

Direct and torsional influence of wind load makes the total force acting on the frame, so using the frame stiffness we calculate the total force.

Table 3.23. Calculation of wind force on each frame including the torsional effect on the first floor (Case 2)

Case 2 (X-axis)				**Case 2 (Y-axis)**			
Frame	**Ftorsion (kN)**	**Fdirect (kN)**	**Ftotal (kN)**	**Frame**	**Ftorsion (kN)**	**Fdirect (kN)**	**Ftotal (kN)**
A	-0.2345	10,67	8,89	1	-28,019	13,45	10,01
B	-0.0753	10,67	9,04	2	-22,415	13,45	10,57
C	-0.0236	10,67	9,19	3	-16,812	13,45	11,13
D	0.0056	10,67	9,35	4	-11,208	13,45	11,69
E	0.0236	10,67	9,35	5	-5,604	13,45	12,25
F	0.0753	10,67	9,35	6	3.789	13,45	12,81
G	0.2345	10,67	9,35	7	5,604	13,45	13,37
				8	11,208	13,45	13,93

Table 3.24. Calculation of wind force on each frame including the torsional effect on the first floor (Case 4)

Transverse				Longitudinal			
Frame	Ftorsion (kN)	Fdirect (kN)	Ftotal (kN)	Frame	Ftorsion (kN)	Fdirect (kN)	Ftotal (kN)
1	-2.5003	10.04	7.54	1	-0.7501	10.3	9.55
2	-1.7859	10.04	8.26	2	-0.5358	10.3	9.77
3	-1.0715	10.04	8.97	3	-0.3215	10.3	9.98
4	-0.3572	10.04	9.69	4	-0.1072	10.3	10.19
5	0.3572	10.04	10.4	5	0.1072	10.3	10.41
6	1.0715	10.04	11.12	6	0.3215	10.3	10.62
7	1.7859	10.04	11.83	7	0.5358	10.3	10.84
8	2.5003	10.04	12.54	8	0.7501	10.3	11.05

3.5.1.2. Calculation of Seismic Loads

To calculate seismic loads applied on our building, an equivalent lateral force procedure will be applied (American Society of Civil Engineers 2017).

From the report of site investigation, the class of soil was found as classification D which will be adopted for investigating the seismic design parameter for the site. To identify the seismic parameters of the size, the online map tool was utilised, namely asce 7 hazard tool.online. Since the building is for residential complex, accordingly, the risk category II has been applied on the site. Based on the result showing from map tool, the mapped acceleration parameters were founded as:

$$S_s = 2.34\ g, S_1 = 0.84\ g$$

Accordingly, based on the site class, the soil condition correction coefficients were used to find the adjusted parameters:

$$F_a = 1, F_v = 1.5$$

$$S_{MS} = F_a S_s \tag{3.16}$$

$$S_{M1} = F_v S_1 \tag{3.17}$$

$$S_{MS} = 1 \cdot 2.34 = 2.34\ g$$

$$S_{M1} = 1.5 \cdot 0.84 = 1.26\ g$$

Next, the maximum considered earthquake parameters were adjusted for design acceleration parameters:

$$S_{DS} = \frac{2}{3} S_{MS} \tag{3.18}$$

$$S_{D1} = \frac{2}{3} S_{M1} \tag{3.19}$$

$$S_{DS} = \frac{2}{3} \cdot 2.34 = 1.56\ g$$

$$S_{D1} = \frac{2}{3} \cdot 1.26 = 0.84\ g$$

The seismic design category was calculated to be E from the calculations of seismic design parameters (American Society of Civil Engineers, 2017). With this category, the Lateral Force Resisting System was found to be Special Reinforced Concrete Moment Frame with the following parameters:

Response modification coefficient, R = 8

Overstrength factor, $\Omega = 3$

Design amplification factor, $C_d = 5.5$

Importance factor, $I_e = 1$

Furthermore, the periods of design spectrum were calculated:

$$T_L = 8\ s$$

$$T_0 = 0.2\frac{S_{D1}}{S_{DS}} \tag{3.20}$$

$$T_0 = 0.2\frac{0.84}{1.56} = 0.0108\ s$$

$$T_s = \frac{S_{D1}}{S_{DS}} \tag{3.21}$$

$$T_s = \frac{0.84}{1.56} = 0.538\ s$$

Approximate fundamental period was calculated using the following equation:

$$T_a = C^t h_n{}^x \tag{3.22}$$

Where,

T_a - approximate fundamental period

C^t and x - approximate period parameters defined in ASCE 7-16, 2016

h_n - building height above the ground to its highest point (in our building, $h_n = 46\ m$)

From Table 12.8-2 in ASCE 7-16, for concrete moment-resisting frames, $C^t = 0.0466,\ x = 0.9$ (American Society of Civil Engineers, 2017). Accordingly, the approximate fundamental period can be calculated as:

$$T_a = 0.0466 \cdot 46^{\ 0.9} = 1.462\ s$$

Fundamental period of the structure was calculated by:

$$T = C_u T_a \tag{3.23}$$

Where,

C_u - coefficient for upper limit on calculated period defined in Table 12.8-1. For our building it is 1.4.

$$T = 1.4 \cdot 1.462 = 2.046\ s$$

Because modal analysis in SAP 2000 was not performed so as to find the T*, it is assumed that the period will be an approximate fundamental period, which can be used for regular design procedures ($T = T_a = 1.462\ s$).

The seismic base shear were calculated for ELFr:

$$V = C_s W \tag{3.24}$$

Where,

C_s - seismic response coefficient

W - effective seismic weight of the building

Firstly, to calculate the seismic response coefficient, the following equation was used:

$$C_s = \frac{S_{DS}}{(\frac{R}{I_e})} \tag{3.25}$$

$$C_s = \frac{1.56}{(\frac{8}{1})} = 0.195$$

However, there are limitations for the coefficient values: (1) it should not exceed the following:

$$C_s = \frac{S_{D1}}{T(\frac{R}{I_e})} \quad \text{for } T \leq T_L \tag{3.26}$$

$$C_s = \frac{0.84}{1.462(\frac{8}{1})} = 0.072 > 0.195 \rightarrow C_s = 0.072 \text{ (controlled)}$$

And it should not be less than:

$$C_s = 0.5 S_1/(R/I_e) \quad \text{for } S_1 \geq 0.6 \text{ g} \tag{3.27}$$

$$C_s = 0.5 \cdot 0.84/(8/1) = 0.0525 > 0.041 \rightarrow C_s = 0.0525 \text{ (controlled)}$$

The subsequent step was the calculation of the effective seismic weight, which was calculated by adding weights of columns, beams, slab, floor finishing, stairs, and exterior and partition walls. For calculation, the weights of slab, floor finishing, and exterior and partition walls were given in kPa and were multiplied by floor area, which is 1656 m2. Whereas, other weights were given in kN. The weights for each floor including roof and exit floor can be seen in Table 3.25.

Table 3.25. Effective seismic weight calculations

Floors	**Floor**	**Column**	**Beam**	**Exterior/partition**	**Stairs (kN)**	**Floor**

	finishing and slab	weight (kN)	weight (kN)	walls, (kN/m2)		weight (kN)
1	5,37	3584,00	2475,42	2,97	308,428	20178,9
2	5,37	3584,00	2475,42	2,97	308,428	20178,9
3	5,37	3150,00	2475,42	2,97	308,428	19744,9
4	5,37	3150,00	2475,42	2,97	308,428	19744,9
5	5,37	2744,00	2475,42	2,97	308,428	19338,9
6	5,37	2744,00	2475,42	2,97	308,428	19338,9
7	5,37	2744,00	2475,42	2,97	308,428	19338,9
8	5,37	2366,00	2475,42	2,97	308,428	18960,9
9	5,37	2366,00	2475,42	2,97	308,428	18960,9
10	5,37	2016,00	2475,42	2,97	308,428	18610,9
11	5,37	2016,00	2475,42	2,97	308,428	18610,9
12	5,37	1694,00	2475,42	2,97	308,428	18288,9
13	0	1694,00	2475,42	2,97	308,428	9396,2
Roof	5,56	0	0	46		9283,5
					Effective seismic weight	249976,3

Since effective seismic weight and the seismic response coefficients are known, the seismic base shear can be calculated:

$$V = C_s W = 0.0525 \cdot 249976.3 = 13123.8\,kN$$

Next, the vertical distribution of seismic forces should be calculated using the following equation:

$$F_x = C_{vx} V \tag{3.28}$$

$$C_{vx} = \frac{w_x h_x^k}{\sum_{i=1}^{n} w_i h_i^k} \tag{3.29}$$

Where,

C_{vx} - vertical distribution factor

w_i and w_x - portion of total effective seismic weight at each level i or x

h_i and h_x - height (m) from the ground to level i or x

k - an exponent related to the structure period as following:

- If T ≤ 0.5 s → k = 1
- If T ≥ 2.5 s → k = 2
- T between 0.5 s and 2.5 s should be interpolated as in our case:

  $k = \frac{2-1}{2.5-0.5} \cdot 1.462 + 1 = 1.731$

After a series of calculations for each story, the lateral seismic force at each floor can be seen in Table 3.26. It should be noted that the weight on the roof was added to the 12th floor's weight.

Table 3.26. Lateral seismic force at each floor

Floors	hi, m	Wx, kN	Wx*hx^k	Cvx	Fx, kN
13	46	7898	2290005	0.085767	1046.33
12	42.5	16944.7	4369779	0.16366	1996.6
11	39	17126.7	3888902	0.14565	1776.88
10	35.5	17336.7	3424891	0.128271	1564.87
9	32	17574.7	2977235	0.111505	1360.33
8	28.5	17574.7	2507945	0.093929	1145.91
7	25	17840.7	2096880	0.078534	958.09
6	21.5	18134.7	1704798	0.063849	778.94
5	18	18134.7	1310390	0.049078	598.73
4	14.5	18456.7	968243	0.036263	442.4
3	11	18456.7	643157	0.024088	293.87
2	7.5	18806.7	371673	0.01392	169.82
1	4	18806.7	146515	0.005487	66.94
	Total	204285.3	26700411		

3.5.1.2.1. Seismic Loads Including Torsional Effect

But since our building is prone to torsional effects because of differences in mass centers and stiffness, the torsional effect should be taken into account and the seismic force applied to each frame should be calculated.

First, the center of mass was identified. The slabs, floor finishing, divider, and external walls must all be used to determine the mass center. Since elevators and staircase shafts lack slabs, their areas were subtracted from the mass center of our structure, while all other components were evenly spaced throughout the floor area. It is important to remember that the building is 42 meters long and 59 meters diagonal. Once the origin has been identified in order to determine the mass center, the computations

$$x = 42\ m \text{ (due to symmetrical nature of the building)}$$

$$y = \frac{A_{floor}y_{floor} - A_{elevator\ shaft}y_{elevator\ shaft} - A_{stairs\ shaft,1}y_{stairs\ shaft,1} - A_{stairs\ shaft,2}y_{stairs\ shaft,2}}{A_{floor} - A_{shafts}} \tag{3.30}$$

$$y = \frac{1764 \cdot 21 - 36 \cdot 21 - 25.8 \cdot 3 - 25.8 \cdot 21}{1764 - 25.8 - 36 - 25.8} = 8.24\ m$$

So, mass center: x = 21 m, y = 8.24 m.

The stiffness of the moment frame was then calculated in order to find the stiffness center. First, the following formulas were used to calculate the beams' and columns' cracking moment of inertia:

$$I_{b,cr} = \frac{1}{12}bh^3 \cdot 0.35 \tag{3.31}$$

$$I_{c,cr} = \frac{1}{12}bh^3 \cdot 0.7 \tag{3.32}$$

The following formula can then be used to determine the frame's stiffness:

$$D = \frac{12E}{h^2}\left(\frac{I_{c,cr} * I_{b,cr}}{L * I_{c,cr} + h * I_{b,cr}}\right) \tag{3.33}$$

Force needed to generate an inter-story rotation:

$$C_F = h \cdot D \cdot \#\ of\ columns\ per\ frame \cdot \#\ of\ frames \tag{3.34}$$

The stiffness center can therefore be computed. Appendix A contains detailed computations.

Accordingly, stiffness center: x' = 21 m, y' = 21 m (uniform spacing between columns and major beams).

The eccentricity developed was found to be as:

In x-axis:

$$e_x = 42 - 42 = 0\,m$$

$$e_a = 5\% \cdot L_x = 0.05 \cdot 42 = 2.1\,m$$

$$e_{xt} = e_x + e_a = 2.1\,m$$

In y-axis:

$$e_y = 21 - 8.24 = 0.1\,m$$

$$e_a = 5\% \cdot L = 0.05 \cdot 42 = 2.1\,m$$

$$e_{yt} = e_y + e_a = 4.2\,m$$

Torsion moment, direct force, and torsional force will therefore be computed as follows:

$$T = eF \tag{3.35}$$

$$F_{direct} = \frac{F_x}{\#\ of\ frames} \tag{3.36}$$

$$F_{torsion} = \frac{T * C_f * (x_i\ or\ y_i)}{\sum C_f * (x_i^2\ or\ y_i^2)} \tag{3.37}$$

$$F_{total} = F_{direct} \pm F_{torsion} \tag{3.38}$$

The table 3.27 shows the direct forces and torsion calculations for the longitudinal and transverse axes on each floor. The following table shows an example of the readjusted seismic forces calculated for the longitudinal and transverse axes for each frame on the first level. Appendix A contains the computations for the other floors.

Table 3.27. Direct forces on each frame and torsion for both axes.

	Longitudinal (NS)		**Traverse (NS)**	
Floors	**Fx (kN)**	**Fdirect (kN)**	**Fx (kN)**	**Fdirect (kN)**
13	1046.33	261.58	1046.33	95.12
12	1996.6	499.15	1996.6	181.51
11	1776.88	444.22	1776.88	161.53
10	1564.87	391.22	1564.87	142.26
9	1360.33	340.08	1360.33	123.67
8	1145.91	286.48	1145.91	104.17
7	958.09	239.52	958.09	87.1

6	778.94	194.74	778.94	70.81
5	598.73	149.68	598.73	54.43
4	442.4	110.6	442.4	40.22
3	293.87	73.47	293.87	26.72
2	169.82	42.46	169.82	15.44
1	66.94	16.74	66.94	6.09

Table 3.28. Calculation of seismic force on each frame for the first floor including the torsional effect.

Transverse				**Longitudinal**			
Frame	**Ftorsion, kN**	**Fdirect, kN**	**Ftotal, kN**	**Frame**	**Ftorsion, kN**	**Fdirect, kN**	**Ftotal, kN**
A	8.4796	16.74	25.22	1	-0.6437	6.09	5.44
B	6.0568	16.74	22.79	2	-0.4598	6.09	5.63
C	3.6341	16.74	20.37	3	-0.2759	6.09	5.81
D	1.2114	16.74	17.95	4	-0.092	6.09	5.99
E	-1.2114	16.74	15.52	5	0.092	6.09	6.18
F	-3.6341	16.74	13.1	6	0.2759	6.09	6.36
G	-6.0568	16.74	10.68	7	0.4598	6.09	6.55
				8	0.6437	6.09	6.73

3.5.2. Assigning Forces to SAP 2000 for Lateral Forces

3.5.2.1. Assigning Forces to Chosen 2D Frame

The same procedures were applied for LFRS as for GLRS frame loads including Case 2 and Case 4 for Wind loads and Seismic loads, with F direct forces. The forces were assigned in only a transverse direction showing the procedures in X-direction.

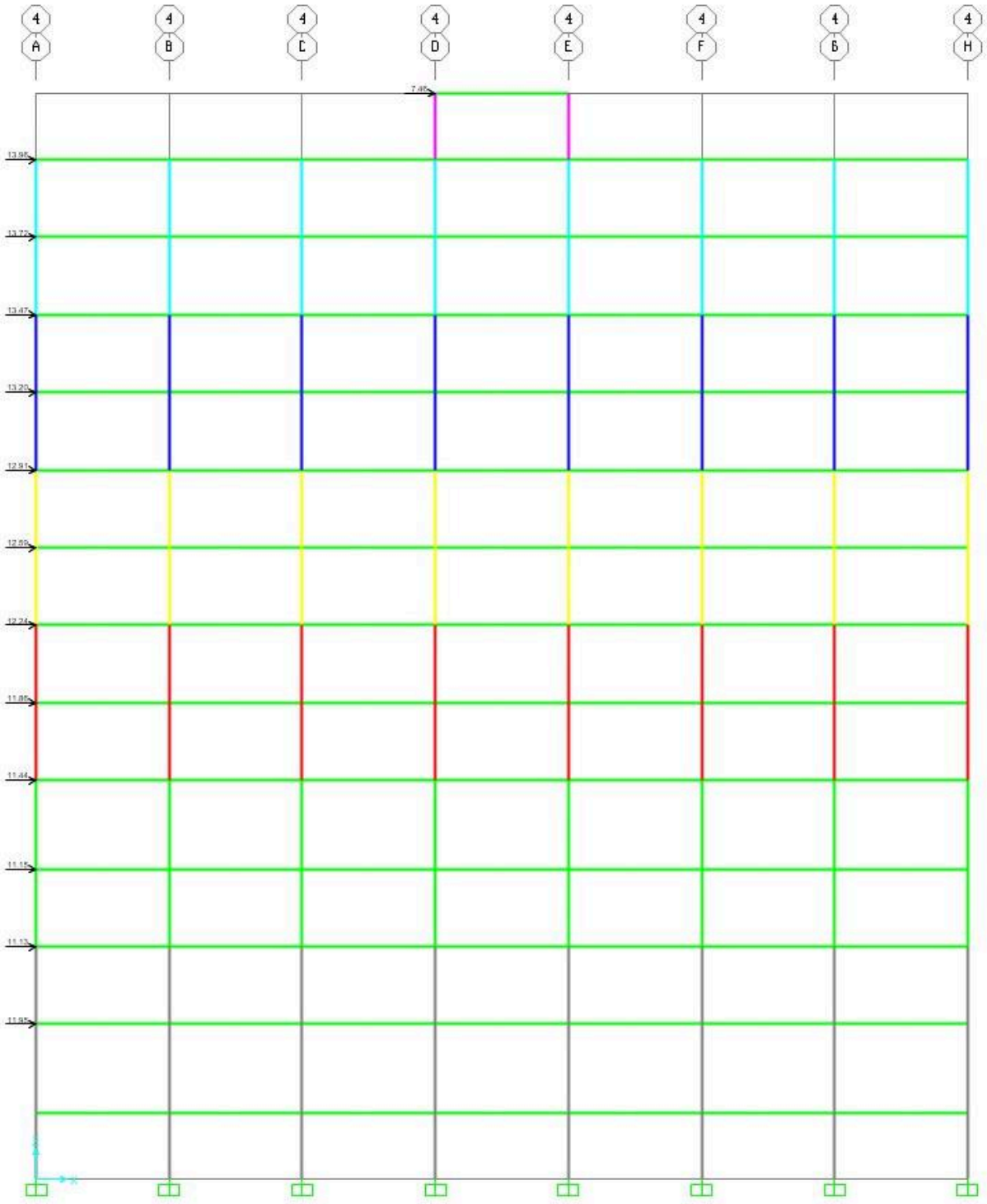
4
A
4
B
4
C
4
D
4
E
4
F
4
G
4
H
7.46
13.96
13.72
13.47
13.22
12.91
12.58
12.24
11.85
11.44
11.15
11.12
11.95

a)

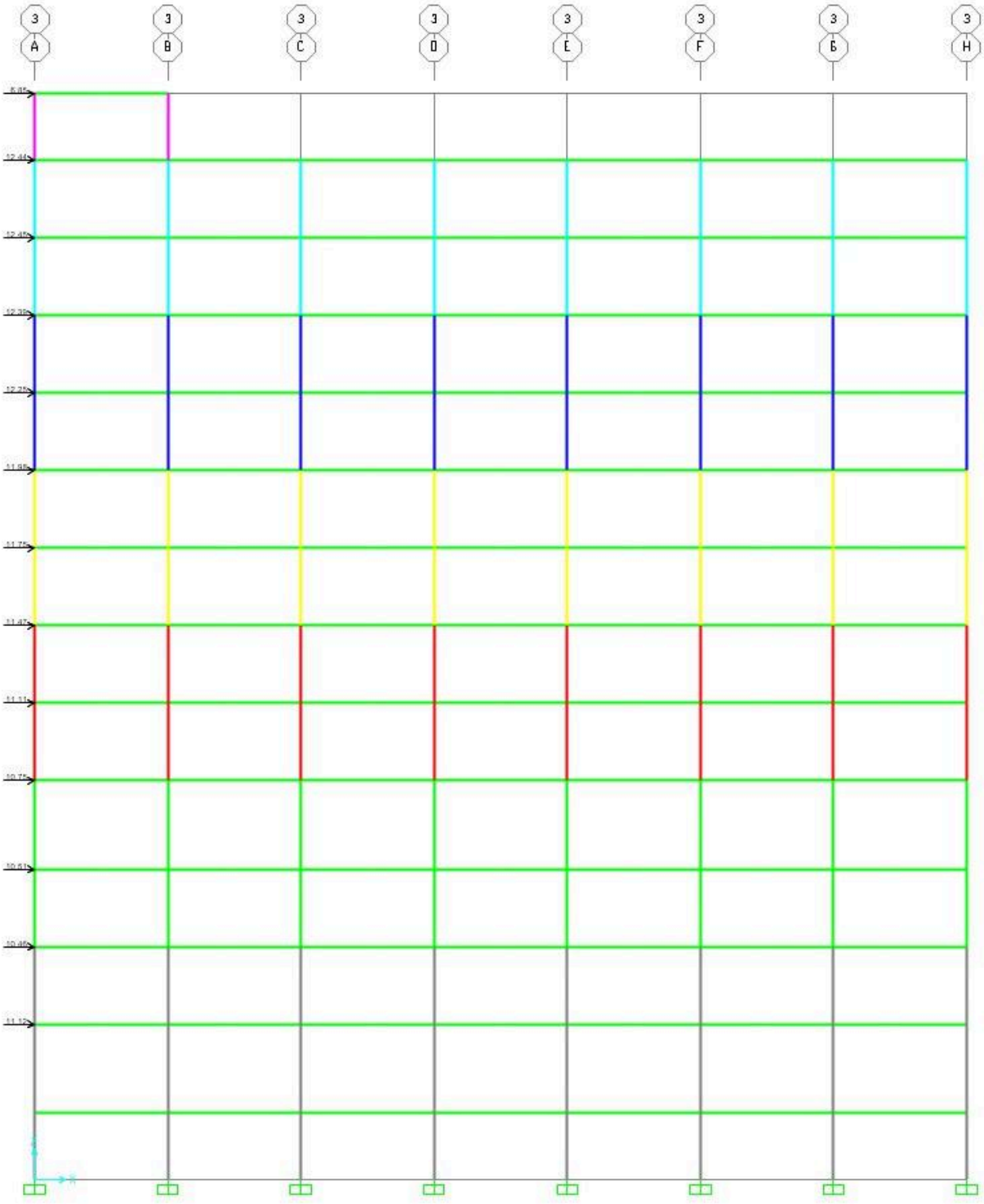

b)

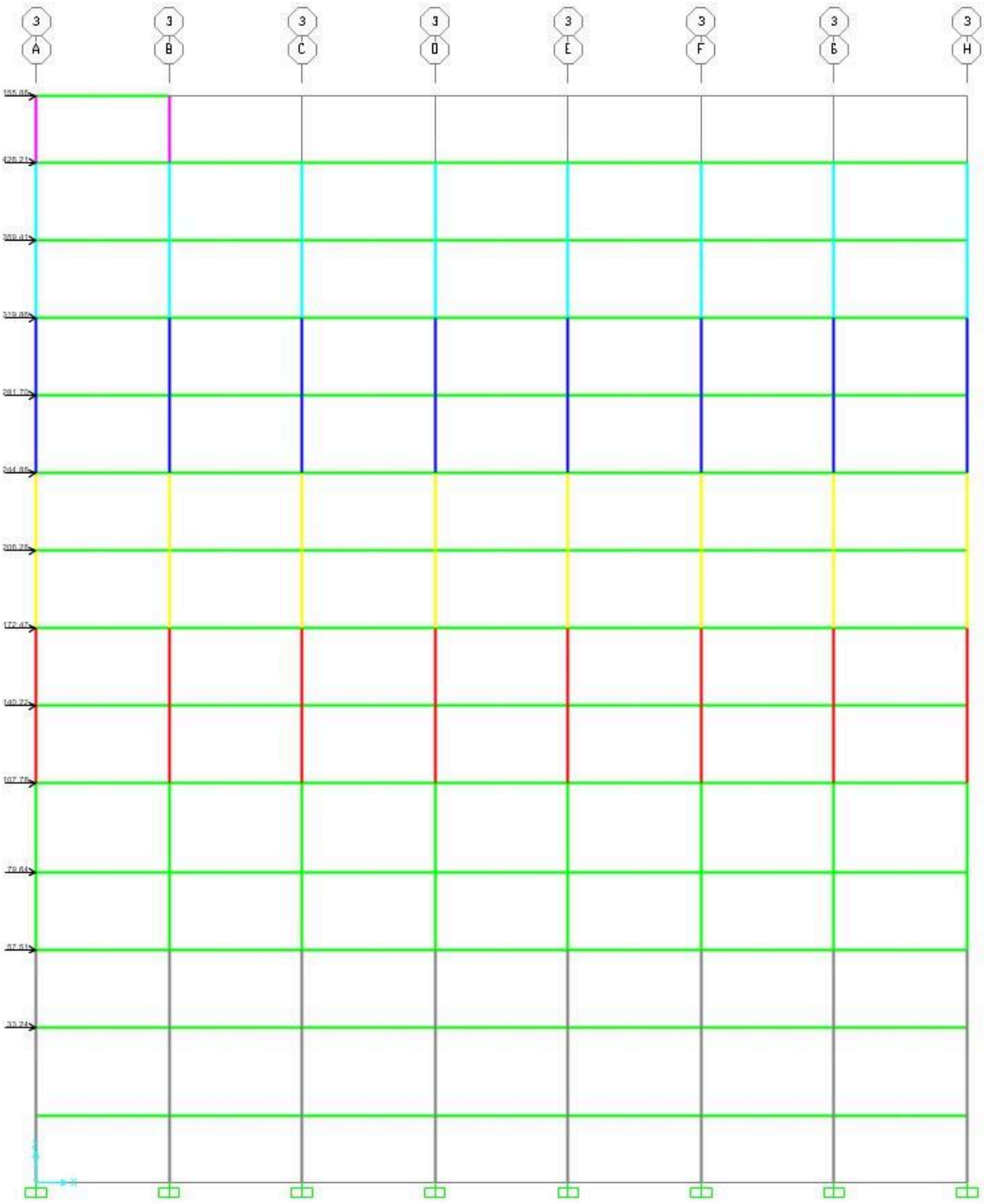

c)

Figure 3.14. Assigned lateral forces on 2D frame in SAP2000: a) wind loads Case 2, b) wind loads Case 4, c) seismic loads.

3.5.2.2. Assigning Forces to 3D Frame

The lateral forces cannot be applied to joints in order to assign them to a 3D frame. Instead, SAP2000 uses its internal functions to execute calculations, and the user can define key parameters for earthquakes, like acceleration periods, fundamental period, response modification, and so on, and for wind, like wind speed, exposure type, Kzt, gust factor, and so on.

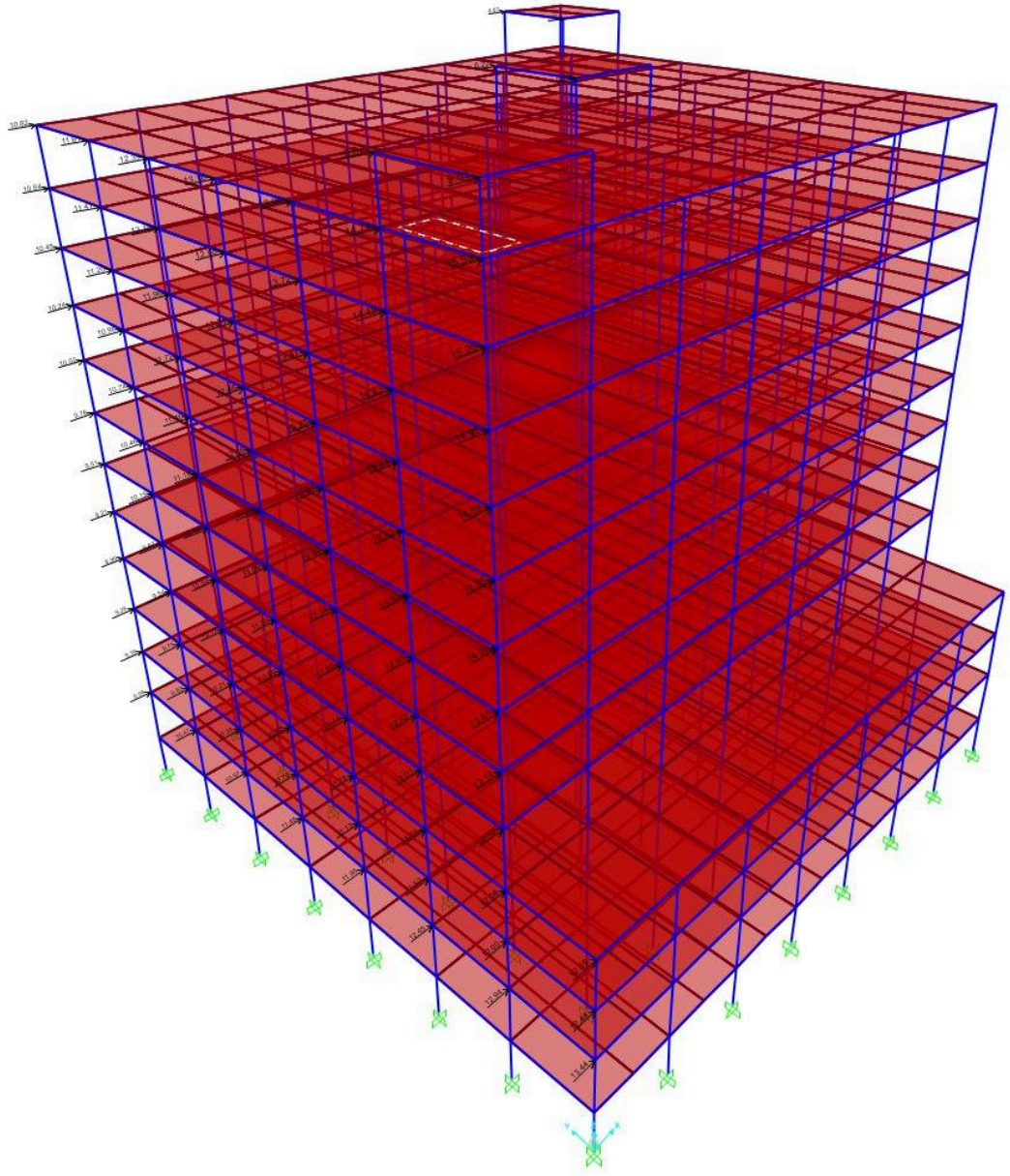

Figure 3.15. Assigned lateral forces on 3D frame in SAP2000 wind loads Case 2

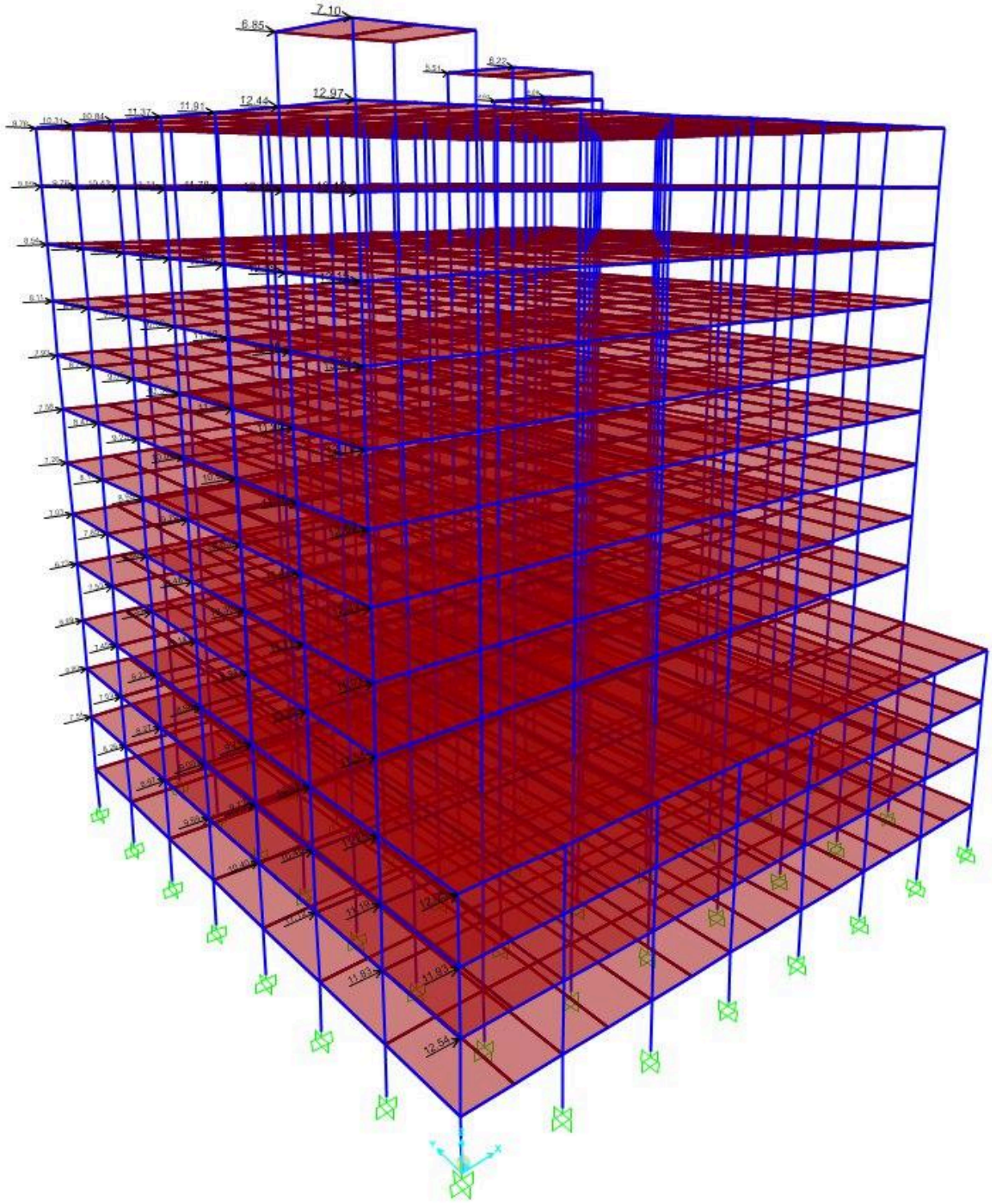

Figure 3.16. Assigned lateral forces on 3D frame in SAP2000 wind loads Case 4.

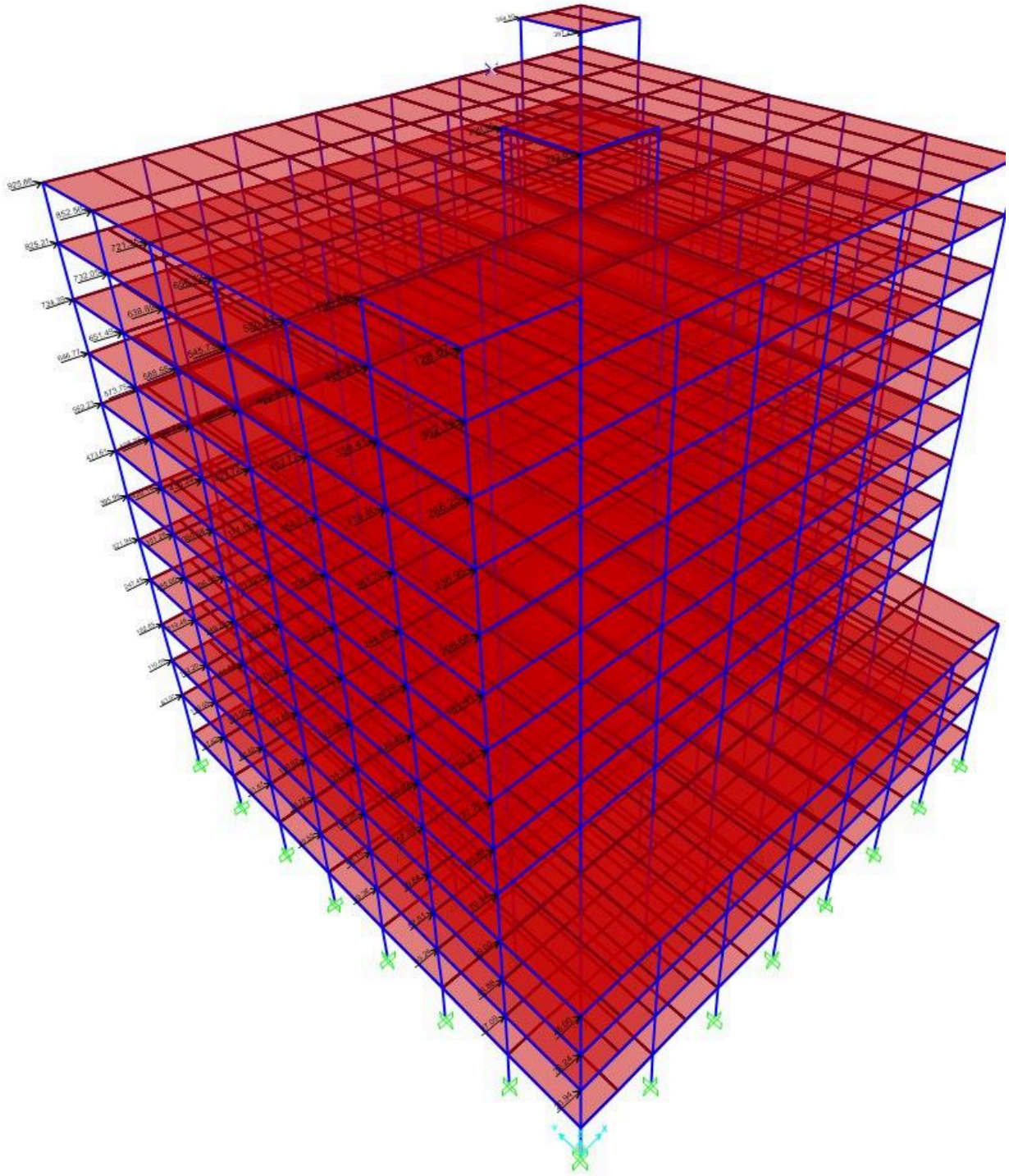

Figure 3.17. Assigned lateral forces on 3D frame in SAP2000 seismic loads

3.6. Lateral drift analysis

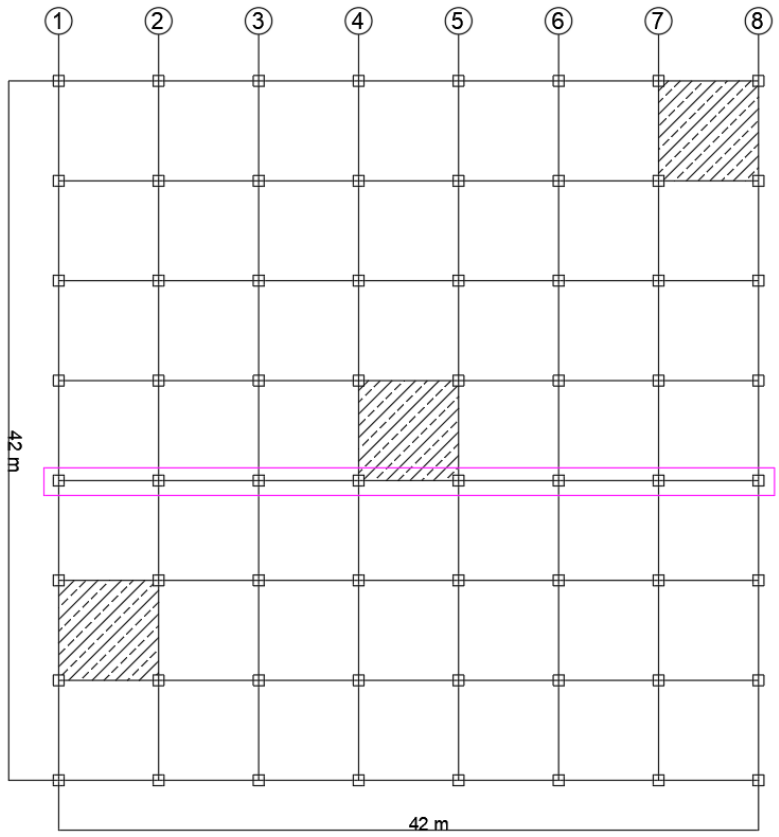

Figure 3.17. Chosen frame for lateral force calculations

3.6.1. Hand calculation for lateral drift analysis under Wind Load

Table 3.29. Shear Drift on Frame A under Wind Load (Longitudinal Direction).

Story	hi (mm)	hi-avg (mm)	Fi (kN)	Vi (kN)	Vi-col (kN)	Vavg (kN)	Ic,cr (mm^4)	Ib,cr (mm^4)	Ic-avg (mm^4)
13	3500	3250,00	9,12	9,12	0,91	0,46	3,65E+09	7,74E+08	3,02E+09
12	3500	3500,00	18,09	27,21	2,72	1,82	3,65E+09	7,74E+08	3,65E+09
11	3500	3500,00	17,78	44,99	4,50	3,61	5,34E+09	7,74E+08	4,49E+09
10	3500	3500,00	17,46	62,45	6,24	5,37	5,34E+09	7,74E+08	5,34E+09
9	3500	3500,00	17,11	79,56	7,96	7,10	7,56E+09	7,74E+08	6,45E+09

8	3500	3500,00	16,73	96,29	9,63	8,79	7,56E+09	7,74E+08	7,56E+09
7	3500	3500,00	16,32	112,60	11,26	10,44	1,04E+10	7,74E+08	8,99E+09
6	3500	3500,00	15,87	128,47	12,85	12,05	1,04E+10	7,74E+08	1,04E+10
5	3500	3500,00	15,37	143,84	14,38	13,62	1,04E+10	7,74E+08	1,04E+10
4	3500	3500,00	14,83	158,67	15,87	15,13	1,40E+10	7,74E+08	1,22E+10
3	3500	3500,00	14,55	173,22	17,32	16,59	1,40E+10	7,74E+08	1,40E+10
2	3500	3500,00	14,55	187,77	18,78	18,05	1,85E+10	7,74E+08	1,62E+10
1	4000	3750,00	15,61	203,38	20,34	19,56	1,85E+10	7,74E+08	1,85E+10

Table 3.30. Shear Drift on Frame A under Wind Load (Longitudinal Direction).

db(mm)	**dc (mm)**	**dt**	**Interstory**	**abs**
0,12	0,02	0,14	0,34	38,43
0,48	0,06	0,54	0,80	38,09
0,96	0,10	1,06	1,30	37,29
1,43	0,12	1,55	1,79	35,99
1,89	0,13	2,02	2,25	34,20
2,34	0,14	2,48	2,70	31,95
2,78	0,14	2,92	3,13	29,25
3,21	0,14	3,35	3,56	26,12
3,62	0,16	3,78	3,98	22,55
4,03	0,15	4,17	4,37	18,57
4,42	0,14	4,56	4,75	14,21
4,80	0,13	4,94	5,96	9,46
6,80	0,19	6,99	3,49	3,49

Table 3.31. Flexural Drift on Frame A under Wind Load (Longitudinal Direction).

Story	M (N-mm)	a=b (m)	A (mm2)	fi	Dqi (rad)	qi (rad)	interstory (mm)	Absolute
13	3,19E+07	0,25	62500	1,06E-10	3,71E-07	5,80E-05	0,20	1,88
12	1,27E+08	0,3	90000	2,93E-10	1,03E-06	5,77E-05	0,20	1,68
11	2,85E+08	0,35	122500	4,83E-10	1,69E-06	5,67E-05	0,20	1,48
10	5,03E+08	0,4	160000	6,53E-10	2,29E-06	5,50E-05	0,19	1,28
9	7,82E+08	0,45	202500	8,02E-10	2,81E-06	5,27E-05	0,18	1,09
8	1,12E+09	0,45	202500	1,15E-09	4,02E-06	4,99E-05	0,17	0,90
7	1,51E+09	0,5	250000	1,26E-09	4,40E-06	4,59E-05	0,16	0,73
6	1,96E+09	0,55	302500	1,35E-09	4,72E-06	4,15E-05	0,15	0,57
5	2,47E+09	0,55	302500	1,69E-09	5,92E-06	3,67E-05	0,13	0,42
4	3,02E+09	0,6	360000	1,74E-09	6,10E-06	3,08E-05	0,11	0,30
3	3,63E+09	0,6	360000	2,09E-09	7,32E-06	2,47E-05	0,09	0,19
2	4,28E+09	0,65	422500	2,11E-09	7,37E-06	1,74E-05	0,06	0,10
1	5,10E+09	0,65	422500	2,51E-09	1,00E-05	1,00E-05	0,04	0,04

Table 3.32. Shear Drift on Frame 4 under Wind Load (Transverse Direction).

Story	hi (mm)	hi-avg (mm)	Fi (kN)	Vi (kN)	Vi-col (kN)	Vavg (kN)	Ic,cr (mm^4)	Ib,cr (mm^4)	Ic-avg (mm^4)
13	3500	3250,00	10,78	10,78	3,59	1,80	3,65E+09	7,74E+08	3,02E+09
12	3500	3500,00	21,41	32,19	10,73	7,16	3,65E+09	7,74E+08	3,65E+09
11	3500	3500,00	21,10	53,29	17,76	14,25	5,34E+09	7,74E+08	4,49E+09
10	3500	3500,00	20,77	74,06	24,69	21,23	5,34E+09	7,74E+08	5,34E+09
9	3500	3500,00	20,42	94,48	31,49	28,09	7,56E+09	7,74E+08	6,45E+09
8	3500	3500,00	20,04	114,53	38,18	34,84	7,56E+09	7,74E+08	7,56E+09

7	3500	3500,00	19,63	134,16	44,72	41,45	1,04E+10	7,74E+08	8,99E+09
6	3500	3500,00	19,18	153,34	51,11	47,92	1,04E+10	7,74E+08	1,04E+10
5	3500	3500,00	18,68	172,02	57,34	54,23	1,04E+10	7,74E+08	1,04E+10
4	3500	3500,00	18,11	190,13	63,38	60,36	1,40E+10	7,74E+08	1,22E+10
3	3500	3500,00	17,43	207,56	69,19	66,28	1,40E+10	7,74E+08	1,40E+10
2	3500	3500,00	16,61	224,17	74,72	71,95	1,85E+10	7,74E+08	1,62E+10
1	4000	3750,00	18,30	242,47	80,82	77,77	1,85E+10	7,74E+08	1,85E+10

Table 3.33. Shear Drift on Frame 4 under Wind Load (Transverse Direction).

db(mm)	dc (mm)	dt	Interstory	abs
0,48	0,07	0,55	1,35	152,85
1,91	0,24	2,14	3,16	151,50
3,79	0,38	4,17	5,15	148,34
5,65	0,48	6,13	7,06	143,19
7,48	0,52	8,00	8,91	136,13
9,27	0,55	9,83	10,71	127,22
11,03	0,55	11,59	12,45	116,51
12,75	0,55	13,31	14,18	104,06
14,43	0,63	15,06	15,86	89,88
16,07	0,59	16,66	17,44	74,02
17,64	0,57	18,21	18,95	56,58
19,15	0,53	19,68	23,74	37,64
27,04	0,76	27,79	13,90	13,90

Table 3.34. Flexural Drift on Frame 4 under Wind Load (Transverse Direction).

Story	M (N-mm)	a=b (m)	A (mm2)	fi	Dqi (rad)	qi (rad)	interstory (mm)	Absolute
13	3,77E+07	0,25	62500	1,25E-10	4,39E-07	6,91E-05	0,24	2,24
12	1,50E+08	0,3	90000	3,47E-10	1,21E-06	6,87E-05	0,24	2,00
11	3,37E+08	0,35	122500	5,71E-10	2,00E-06	6,74E-05	0,24	1,76
10	5,96E+08	0,4	160000	7,74E-10	2,71E-06	6,54E-05	0,23	1,53
9	9,27E+08	0,45	202500	9,50E-10	3,33E-06	6,27E-05	0,22	1,30
8	1,33E+09	0,45	202500	1,36E-09	4,77E-06	5,94E-05	0,21	1,08
7	1,80E+09	0,5	250000	1,49E-09	5,23E-06	5,46E-05	0,19	0,87
6	2,33E+09	0,55	302500	1,60E-09	5,61E-06	4,94E-05	0,17	0,68
5	2,94E+09	0,55	302500	2,02E-09	7,05E-06	4,38E-05	0,15	0,51
4	3,60E+09	0,6	360000	2,08E-09	7,27E-06	3,68E-05	0,13	0,35
3	4,33E+09	0,6	360000	2,50E-09	8,74E-06	2,95E-05	0,10	0,22
2	5,11E+09	0,65	422500	2,51E-09	8,79E-06	2,08E-05	0,07	0,12
1	6,08E+09	0,65	422500	2,99E-09	1,20E-05	1,20E-05	0,05	0,05

3.6.2. Hand calculations for lateral drift analysis under Seismic Load

The same procedure was performed for the drift analysis under Seismic Loading.

Table 3.35. Shear Drift on Frame A under Seismic Load (Longitudinal Direction).

Story	hi (mm)	hi-avg (mm)	Fi (kN)	Vi (kN)	Vi-col (kN)	Vavg (kN)	Ic,cr (mm^4)	Ib,cr (mm^4)	Ic-avg (mm^4)
13	3500	3250,00	261,58	261,58	26,16	13,08	3,65E+09	7,74E+08	1,82E+09
12	3500	3500,00	499,15	760,73	76,07	51,12	3,65E+09	7,74E+08	3,65E+09
11	3500	3500,00	444,22	1204,95	120,50	98,28	5,34E+09	7,74E+08	4,49E+09
10	3500	3500,00	391,22	1596,17	159,62	140,06	5,34E+09	7,74E+08	5,34E+09
9	3500	3500,00	340,08	1936,25	193,63	176,62	7,56E+09	7,74E+08	6,45E+09
8	3500	3500,00	286,48	2222,73	222,27	207,95	7,56E+0	7,74E+0	7,56E+0

							9	8	9
7	3500	3500,00	239,52	2462,25	246,23	234,25	1,04E+10	7,74E+08	8,99E+09
6	3500	3500,00	194,74	2656,99	265,70	255,96	1,04E+10	7,74E+08	1,04E+10
5	3500	3500,00	149,68	2806,67	280,67	273,18	1,04E+10	7,74E+08	1,04E+10
4	3500	3500,00	110,60	2917,27	291,73	286,20	1,40E+10	7,74E+08	1,22E+10
3	3500	3500,00	73,47	2990,74	299,07	295,40	1,40E+10	7,74E+08	1,40E+10
2	3500	3500,00	42,46	3033,19	303,32	301,20	1,85E+10	7,74E+08	1,62E+10
1	4000	3750,00	16,74	3049,93	304,99	304,16	1,85E+10	7,74E+08	1,85E+10

Table 3.36. Shear Drift on Frame A under Seismic Load (Longitudinal Direction).

db(mm)	**dc (mm)**	**dt**	**Interstory**	**abs**
3,48	0,86	4,34	9,82	759,33
13,61	1,69	15,29	22,04	749,51
26,16	2,63	28,79	34,61	727,47
37,28	3,15	40,43	45,37	692,86
47,01	3,29	50,30	54,48	647,49
55,35	3,31	58,66	62,07	593,01
62,35	3,13	65,48	68,28	530,94
68,13	2,95	71,08	73,47	462,66
72,71	3,15	75,87	77,43	389,18
76,18	2,82	78,99	80,08	311,75
78,63	2,54	81,16	81,78	231,68
80,17	2,23	82,40	95,55	149,90
105,74	2,96	108,70	54,35	54,35

Table 3.37. Flexural Drift on Frame A under Seismic Load (Longitudinal Direction).

Story	M (N-mm)	a=b (m)	A (mm2)	fi	Dqi (rad)	qi (rad)	interstory (mm)	Absolute
13	9,16E+08	0,25	62500	3,04E-09	1,06E-05	1,30E-03	4,55	40,70
12	3,58E+09	0,3	90000	8,26E-09	2,89E-05	1,29E-03	4,52	36,14
11	7,80E+09	0,35	122500	1,32E-08	4,63E-05	1,26E-03	4,42	31,62
10	1,34E+10	0,4	160000	1,74E-08	6,08E-05	1,22E-03	4,25	27,21
9	2,02E+10	0,45	202500	2,07E-08	7,24E-05	1,15E-03	4,04	22,95
8	2,79E+10	0,45	202500	2,87E-08	1,00E-04	1,08E-03	3,79	18,91
7	3,66E+10	0,5	250000	3,04E-08	1,06E-04	9,82E-04	3,44	15,12
6	4,59E+10	0,55	302500	3,15E-08	1,10E-04	8,76E-04	3,07	11,69
5	5,57E+10	0,55	302500	3,82E-08	1,34E-04	7,66E-04	2,68	8,62
4	6,59E+10	0,6	360000	3,80E-08	1,33E-04	6,32E-04	2,21	5,94
3	7,64E+10	0,6	360000	4,40E-08	1,54E-04	4,99E-04	1,75	3,73
2	8,70E+10	0,65	422500	4,27E-08	1,50E-04	3,45E-04	1,21	1,99
1	9,92E+10	0,65	422500	4,87E-08	1,95E-04	1,95E-04	0,78	0,78

Table 3.38. Shear Drift on Frame 3 under Seismic Load (Transverse Direction).

Story	hi (mm)	hi-avg (mm)	Fi (kN)	Vi (kN)	Vi-col (kN)	Vavg (kN)	Ic,cr (mm^4)	Ib,cr (mm^4)	Ic-avg (mm^4)
13	3500	3250,00	95,12	95,12	31,71	15,85	3,65E+09	7,74E+08	1,82E+09
12	3500	3500,00	181,51	276,63	92,21	61,96	3,65E+09	7,74E+08	3,65E+09
11	3500	3500,00	161,53	438,16	146,05	119,13	5,34E+09	7,74E+08	4,49E+09
10	3500	3500,00	142,26	580,43	193,48	169,77	5,34E+09	7,74E+08	5,34E+09
9	3500	3500,00	123,67	704,09	234,70	214,09	7,56E+09	7,74E+08	6,45E+09
8	3500	3500,00	104,17	808,27	269,42	252,06	7,56E+09	7,74E+08	7,56E+09
7	3500	3500,00	87,10	895,36	298,45	283,94	1,04E+10	7,74E+08	8,99E+09

6	3500	3500,00	70,81	966,18	322,06	310,26	1,04E+10	7,74E+08	1,04E+10
5	3500	3500,00	54,43	1020,61	340,20	331,13	1,04E+10	7,74E+08	1,04E+10
4	3500	3500,00	40,22	1060,83	353,61	346,91	1,40E+10	7,74E+08	1,22E+10
3	3500	3500,00	26,72	1087,54	362,51	358,06	1,40E+10	7,74E+08	1,40E+10
2	3500	3500,00	15,44	1102,98	367,66	365,09	1,85E+10	7,74E+08	1,62E+10
1	4000	3750,00	6,09	1109,07	369,69	368,67	1,85E+10	7,74E+08	1,85E+10

Table 3.39. Shear Drift on Frame 3 under Seismic Load (Transverse Direction).

db(mm)	dc (mm)	dt	Interstory	abs
4,22	1,05	5,27	11,90	920,40
16,49	2,04	18,53	26,72	908,50
31,71	3,19	34,90	41,95	881,78
45,19	3,82	49,01	54,99	839,83
56,98	3,99	60,97	66,04	784,84
67,09	4,01	71,10	75,24	718,80
75,58	3,80	79,37	82,77	643,57
82,58	3,58	86,16	89,06	560,80
88,14	3,82	91,96	93,85	471,74
92,34	3,42	95,75	97,06	377,88
95,30	3,07	98,38	99,13	280,82
97,17	2,70	99,88	115,82	181,69
128,17	3,58	131,75	65,88	65,88

Table 3.40. Flexural Drift on Frame 3 under Seismic Load (Transverse Direction).

Story	M (N-mm)	a=b (m)	A (mm2)	fi	Dqi (rad)	qi (rad)	interstory (mm)	Absolute

13	3,33E+08	0,25	62500	1,11E-09	3,87E-06	4,73E-04	1,66	14,80
12	1,30E+09	0,3	90000	3,00E-09	1,05E-05	4,69E-04	1,64	13,14
11	2,83E+09	0,35	122500	4,81E-09	1,68E-05	4,59E-04	1,61	11,50
10	4,87E+09	0,4	160000	6,32E-09	2,21E-05	4,42E-04	1,55	9,89
9	7,33E+09	0,45	202500	7,52E-09	2,63E-05	4,20E-04	1,47	8,35
8	1,02E+10	0,45	202500	1,04E-08	3,65E-05	3,94E-04	1,38	6,88
7	1,33E+10	0,5	250000	1,10E-08	3,86E-05	3,57E-04	1,25	5,50
6	1,67E+10	0,55	302500	1,14E-08	4,01E-05	3,18E-04	1,11	4,25
5	2,02E+10	0,55	302500	1,39E-08	4,86E-05	2,78E-04	0,97	3,14
4	2,40E+10	0,6	360000	1,38E-08	4,84E-05	2,30E-04	0,80	2,16
3	2,78E+10	0,6	360000	1,60E-08	5,61E-05	1,81E-04	0,63	1,36
2	3,16E+10	0,65	422500	1,55E-08	5,44E-05	1,25E-04	0,44	0,72
1	3,61E+10	0,65	422500	1,77E-08	7,09E-05	7,09E-05	0,28	0,28

3.6.3. Comparison of lateral drifts for hand, 2D and 3D SAP calculations

Besides the hand calculations, the SAP2000 2D and 3D frames of Frame 4 were developed to compare and contrast the wind and seismic-induced lateral drifts. Furthermore, for seismic resistance, each story must act as different resisting frames (ASCE, 2016). Therefore, the inter-story seismic deflections were amplified to account for the maximum inelastic displacement (δx) using the following equation:

$$\delta_x = \frac{C_d \delta_{xe}}{I_e} \tag{3.39}$$

Where δ_{xe} is an interstory elastic deflection and C_d is the deflection amplification factor (e.g., C_d = 5.5).

$$\Delta_a = 0.020 h_{sx} \tag{3.40}$$

Where h_{sx} is the story height (e.g., for our building the story height is 3500 mm for floors 2-12 and 4000 mm for the first floor).

For wind drifts, the inter-story drift was considered as h/600. All the wind inter-story deflections passed the limit check.

a)

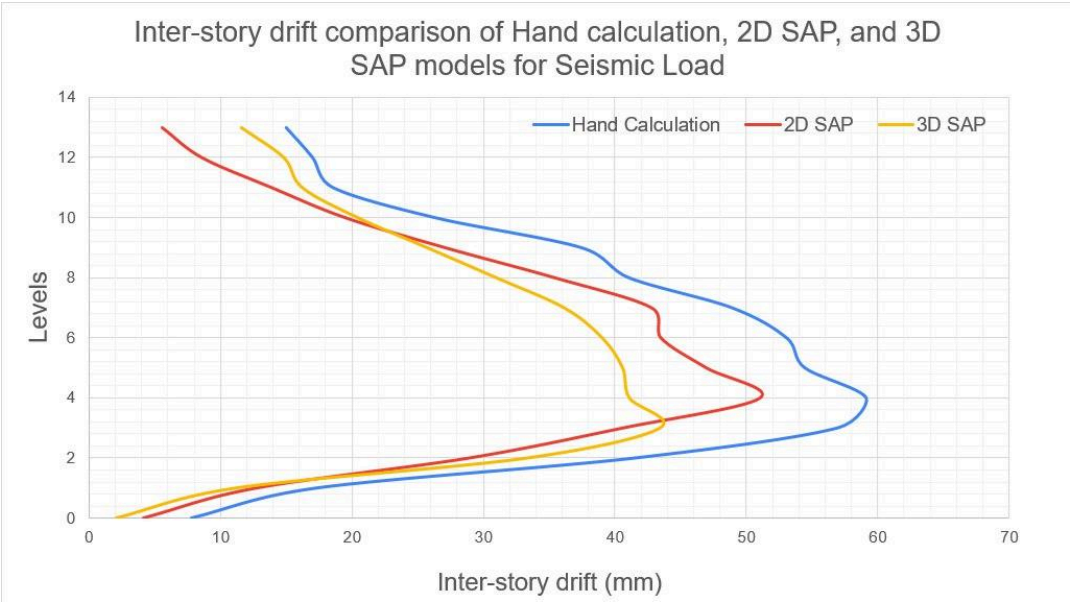

b)

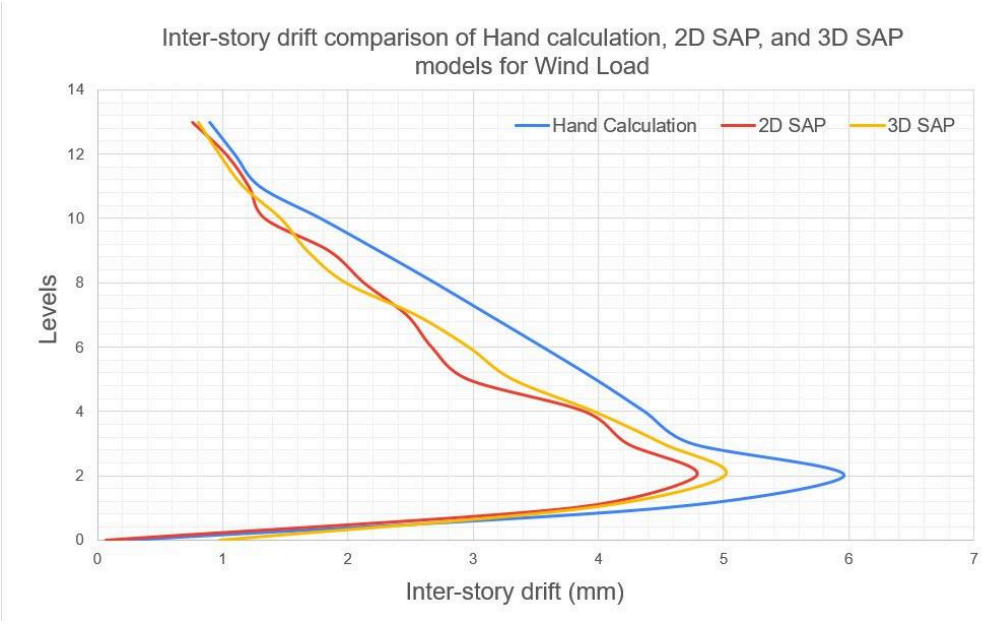

Figure 3.18. Comparison of lateral deflections for Frame 4: (a) seismic; and (b) wind.

We could notice from Figure a) for Frame 4 that deflections by the 2D and 3D calculation are close except for hand calculation. It would be noted that in the 3D SAP2000 model wind loads were specified automatically and, therefore, could be discrepancies from the assumptions applied in hand-calculated wind loads. However, apart from the seismic deflections, all 3D, 2D and hand calculations provided almost the same deflections, which confirms that hand and

SAP2000 calculations are accurate. All drifts were within acceptable drift limits meeting the needs of the structure.

3.6.4. Internal forces calculations

The internal forces calculated by SAP2000 software for the Frame 4 under different loading conditions can be seen below

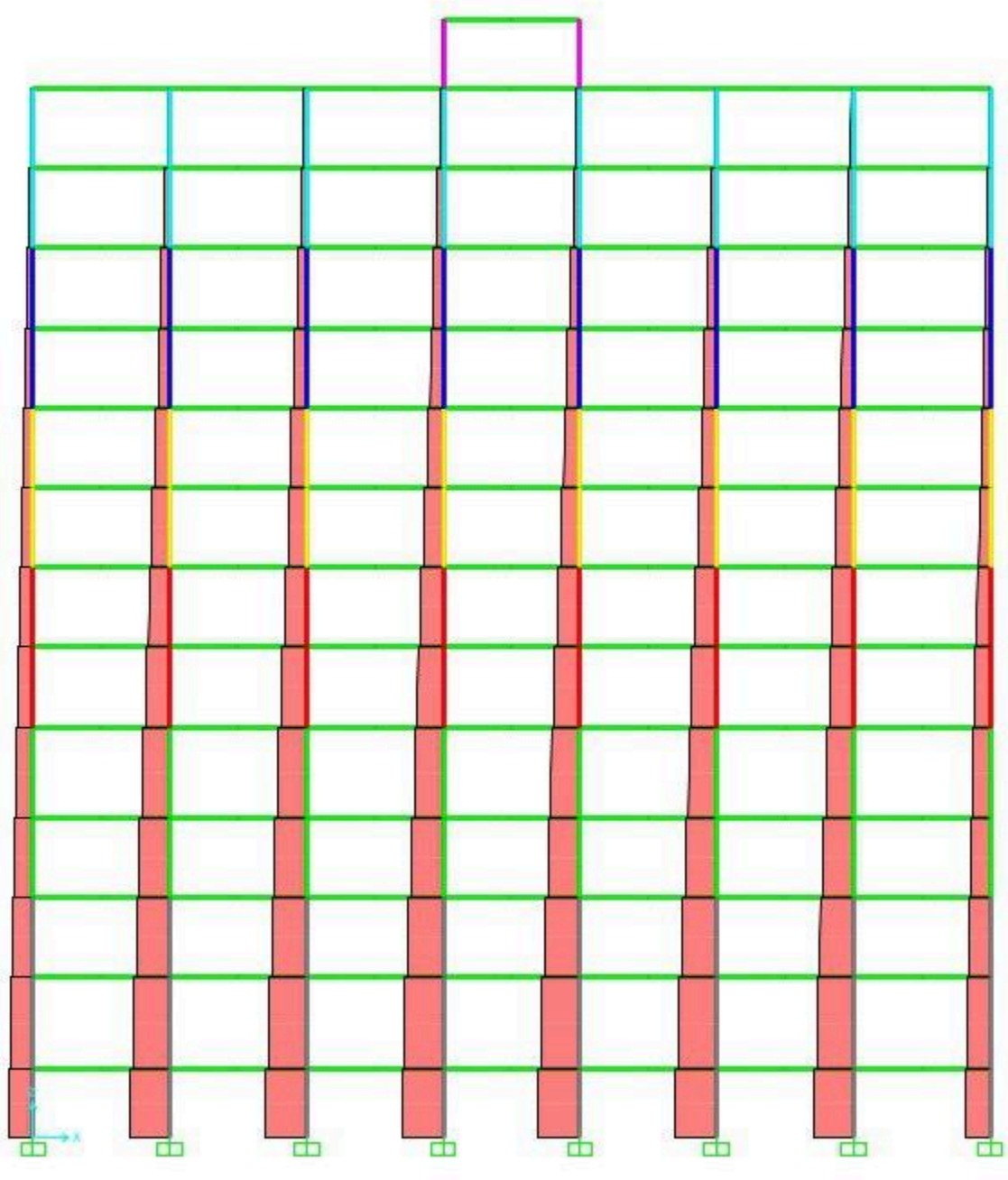

Figure 3.19. Axial force diagram under Dead load in SAP2000.

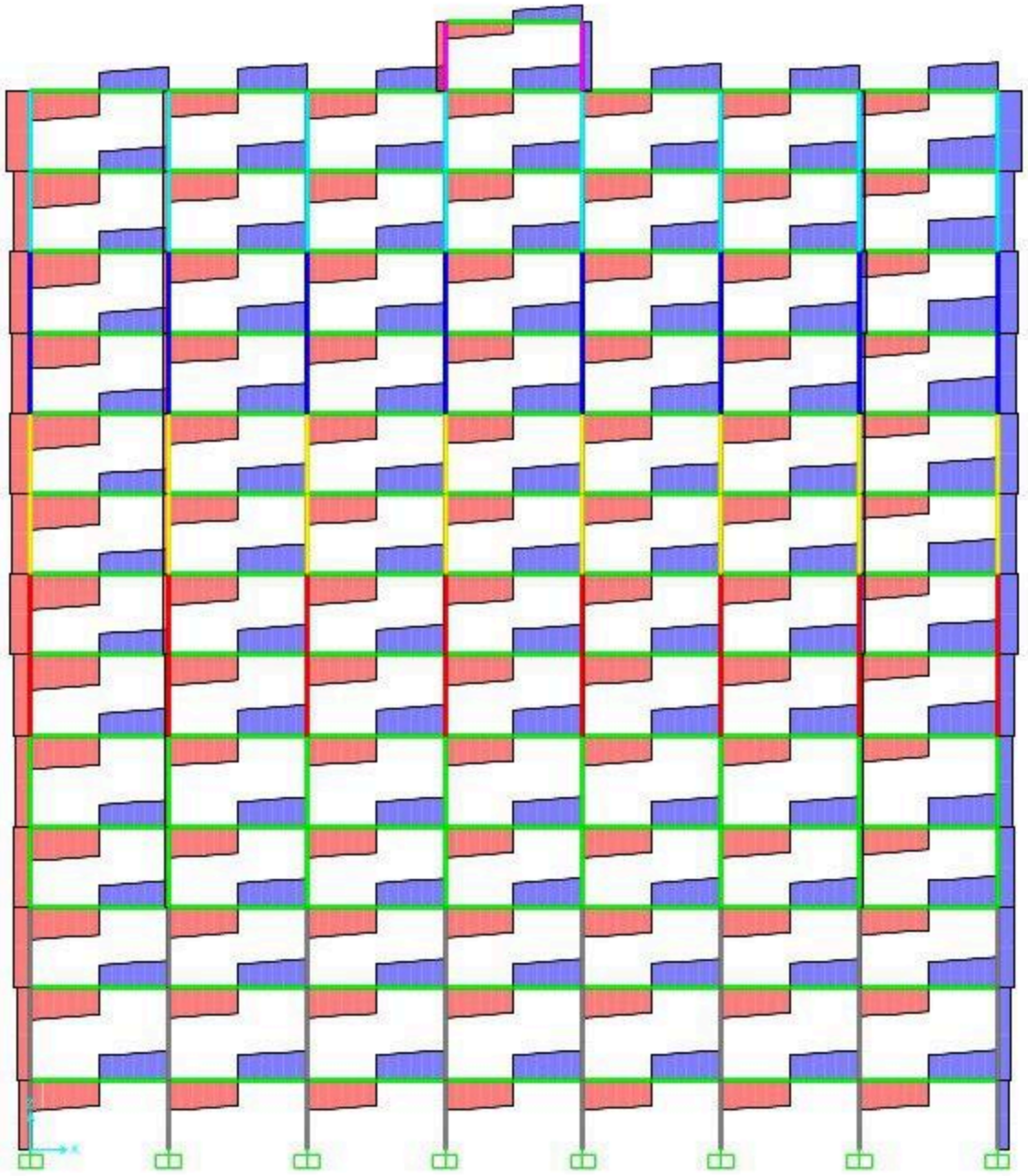

Figure 3.20. Shear force diagram under Dead load in SAP2000.

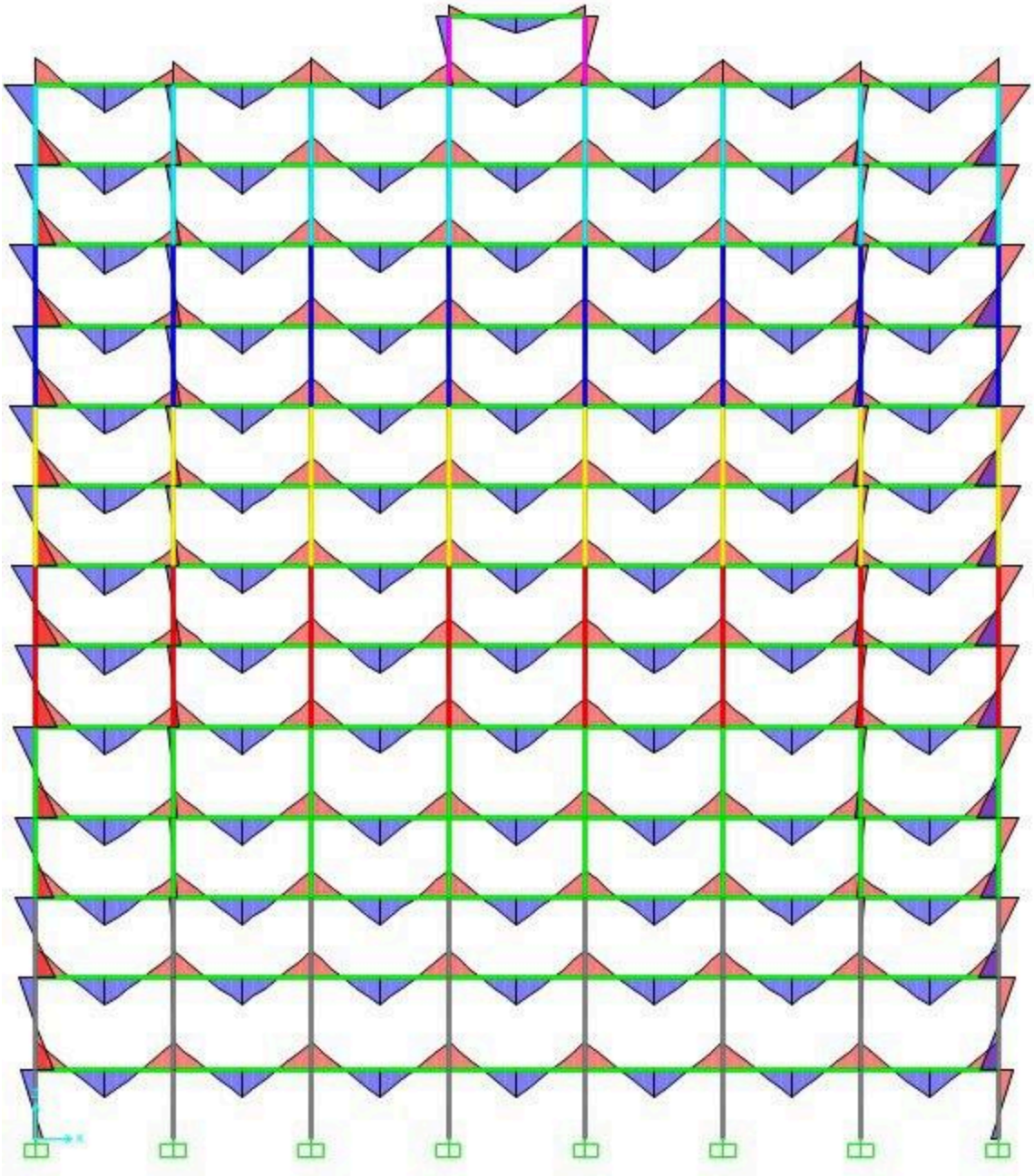

Figure 3.21. Moment diagram under Dead load in SAP2000.

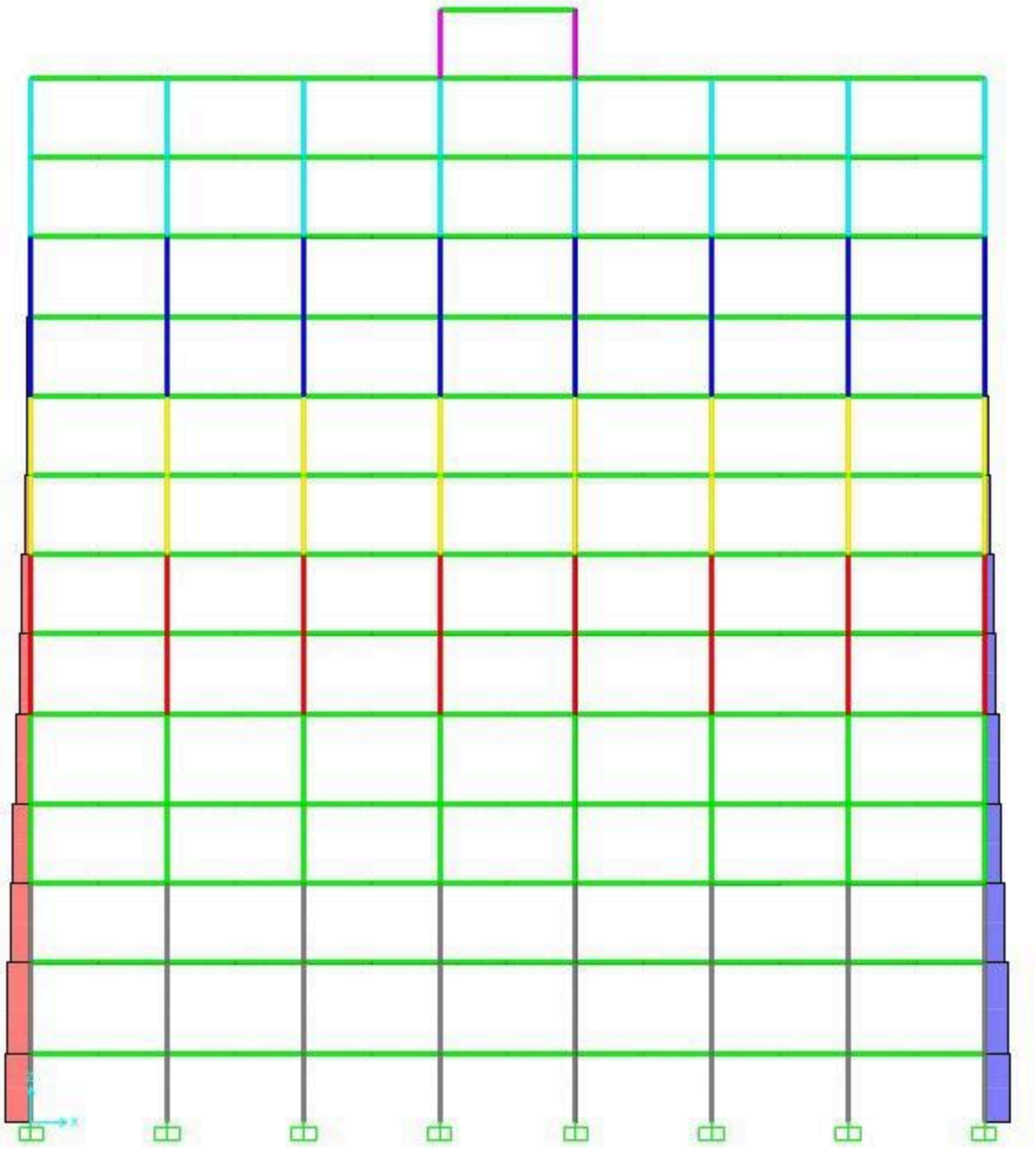

Figure 3.22. Axial force diagram under Wind load in SAP2000.

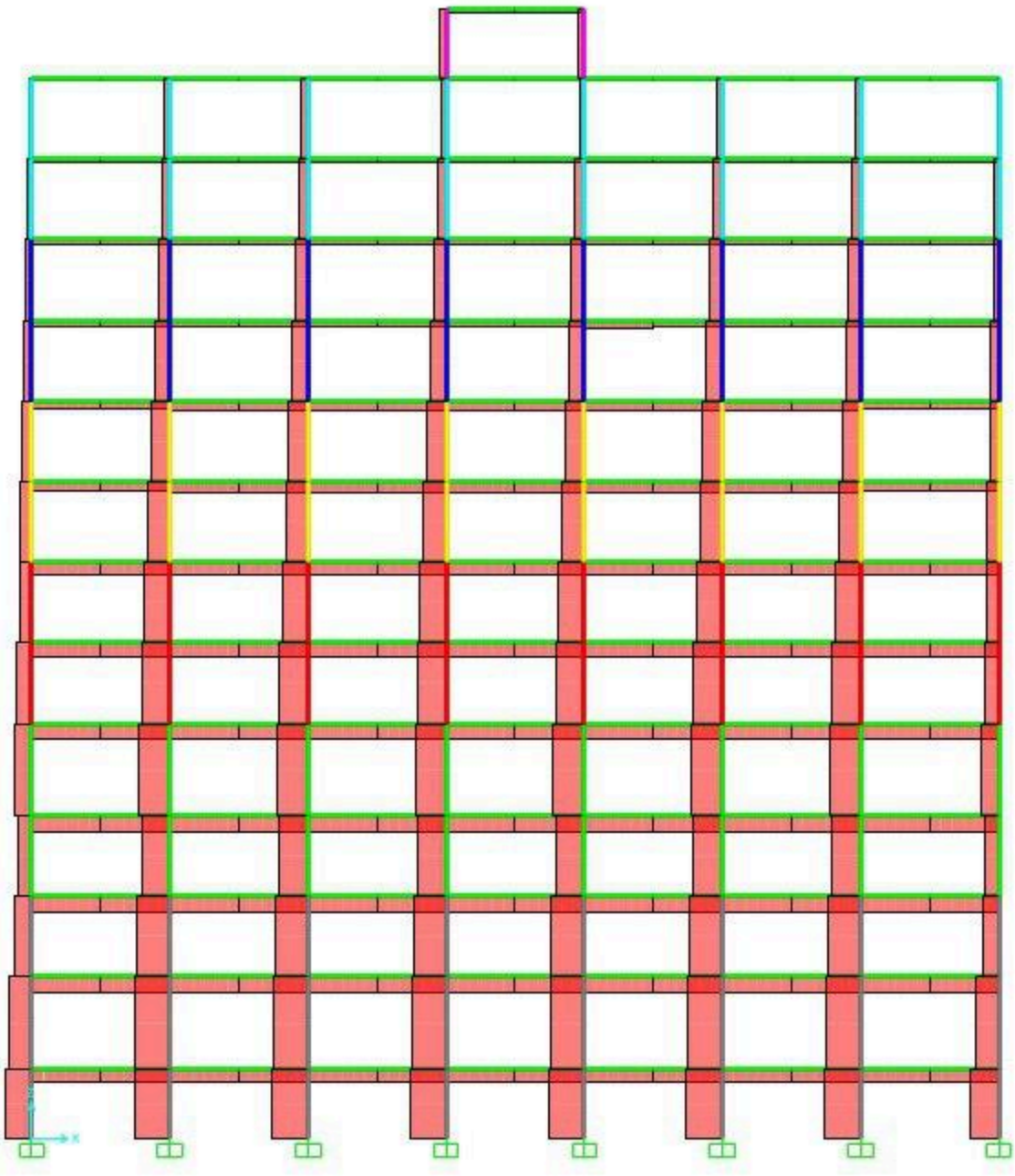

Figure 3.23. Shear force diagram under Wind load in SAP2000.

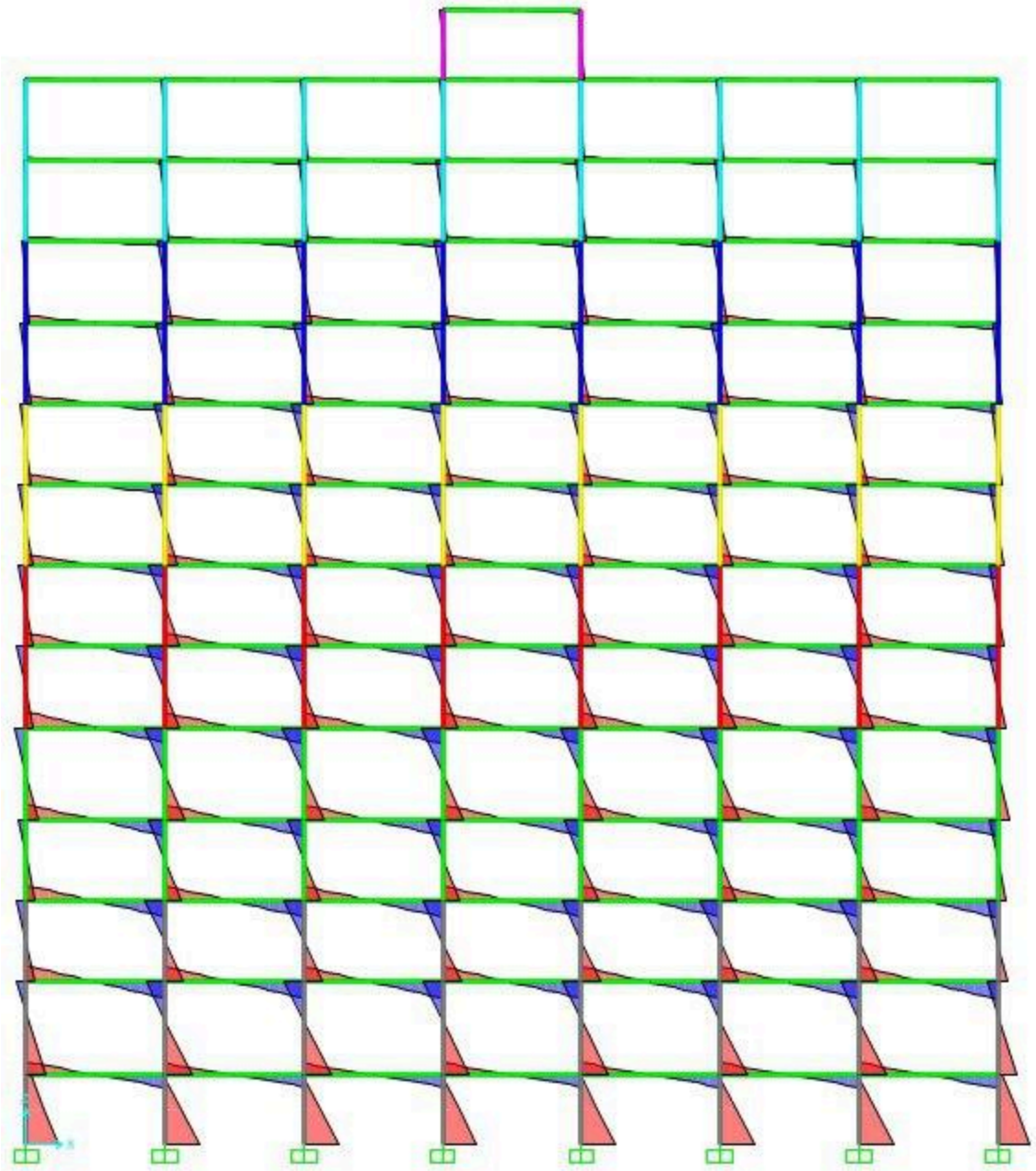

Figure 3.24. Moment diagram under Wind load in SAP2000.

Internal forces verifications under Point Dead load

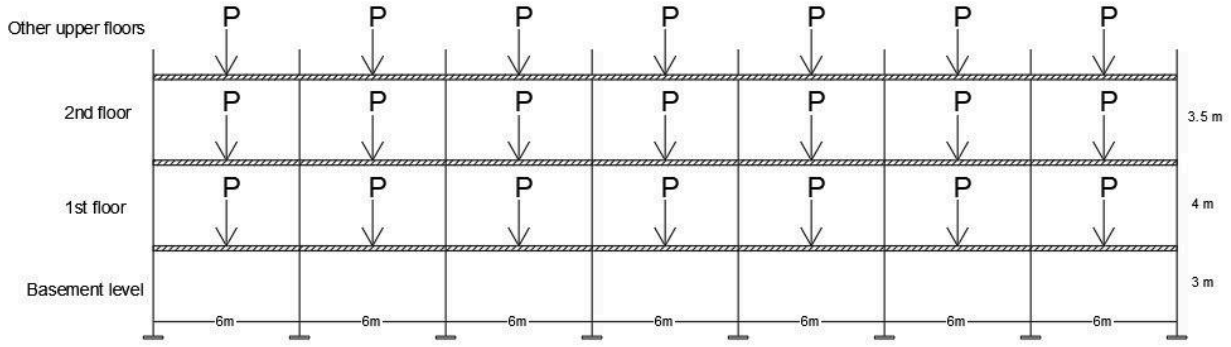

Figure 3.25. Point dead load

Internal forces verifications under Wind load

The internal forces of Frame 4 were calculated for all the floors. The hand calculations process for other floors is presented in Appendix A. The same was followed for the remaining floors and the calculated values were obtained using the spreadsheet. The results for all the floors are presented in Table below.

Table 3.41. The hand calculations of internal forces under wind load.

Story	Internal Column			External Column		
	Axial Force (kN)	Shear Force (kN)	Internal moment (kN-m)	Axial Force (kN)	Shear Force (kN)	Internal moment (kN-m)
12	0,00	3,59	6,29	-1,05	1,80	3,14
11	0,00	10,73	18,78	-5,23	5,36	9,39
10	0,00	17,76	31,09	-13,54	8,88	15,54
9	0,00	24,69	43,20	-25,92	12,34	21,60
8	0,00	31,49	55,12	-42,30	15,75	27,56
7	0,00	38,18	66,81	-62,62	19,09	33,40
6	0,00	44,72	78,26	-86,80	22,36	39,13
5	0,00	51,11	89,45	-114,75	25,56	44,73
4	0,00	57,34	100,35	-146,39	28,67	50,17
3	0,00	63,38	110,91	-181,60	31,69	55,45
2	0,00	69,19	121,08	-220,26	34,59	60,54
1	0,00	74,72	130,76	-262,23	37,36	65,38
0	0,00	80,82	161,64	-314,08	40,41	80,82

(Ground)						

Comparison of internal forces between 2D, 3D and hand calculations

Comparison of internal forces caused by dead load for Frame 4 by hand, 2D, and 3D calculations are shown in Figure x. It can be seen from Figure x that axial and shear forces caused by hand, 2D and 3D calculations are quite close. Although in the bending moment diagram, moment values of the SAP2000 model were marginally different from the ideal due to interaction among various elements' stiffness which contributes to the portion of structure.

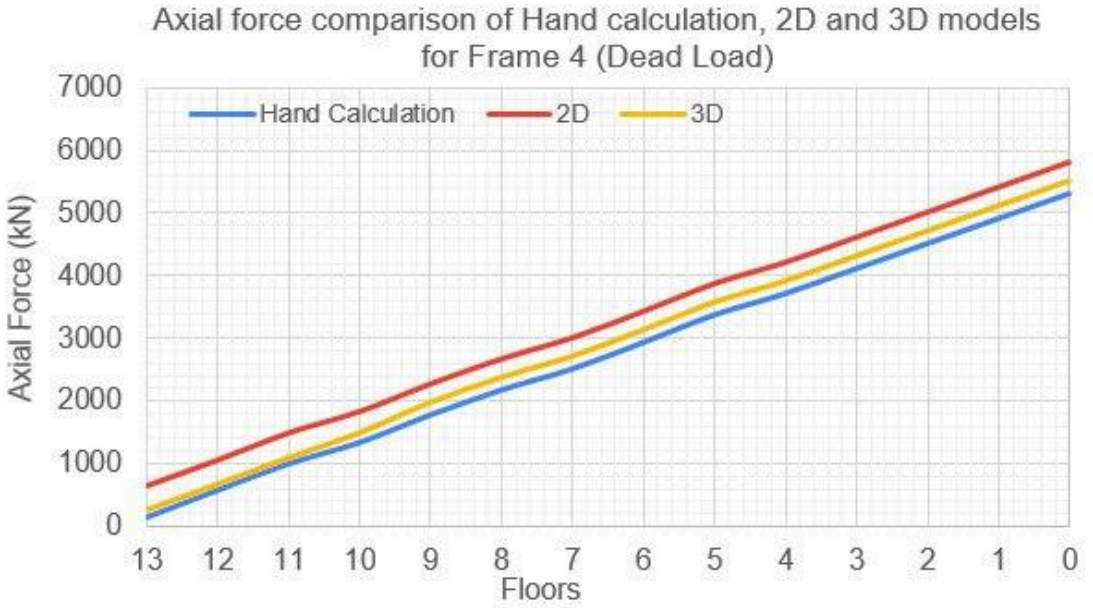

a)

b)

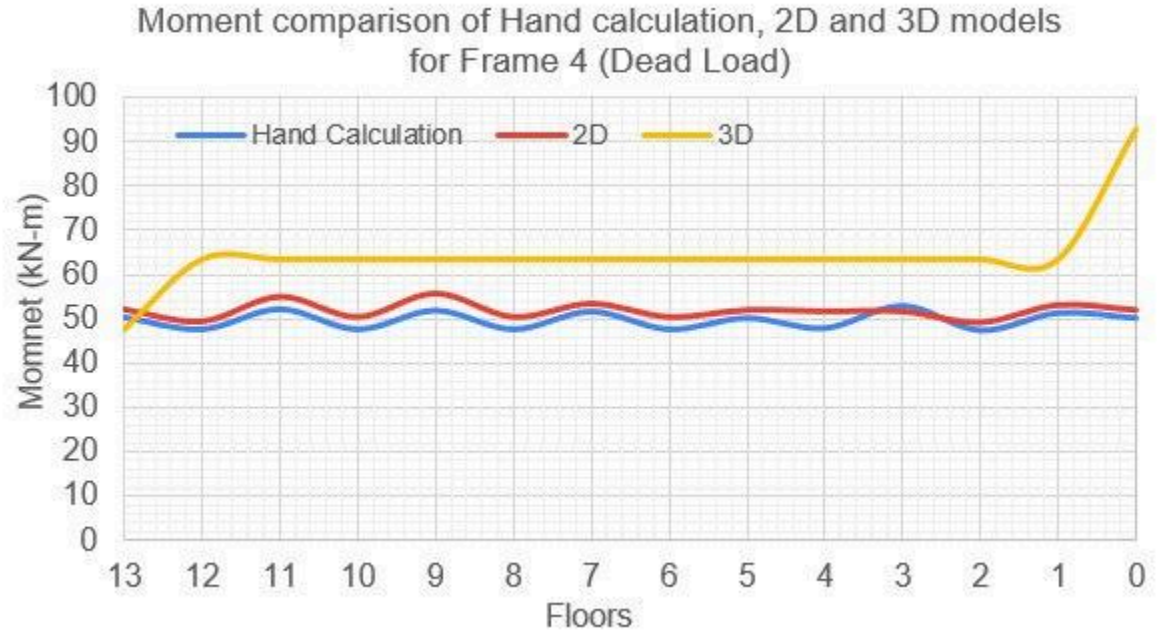

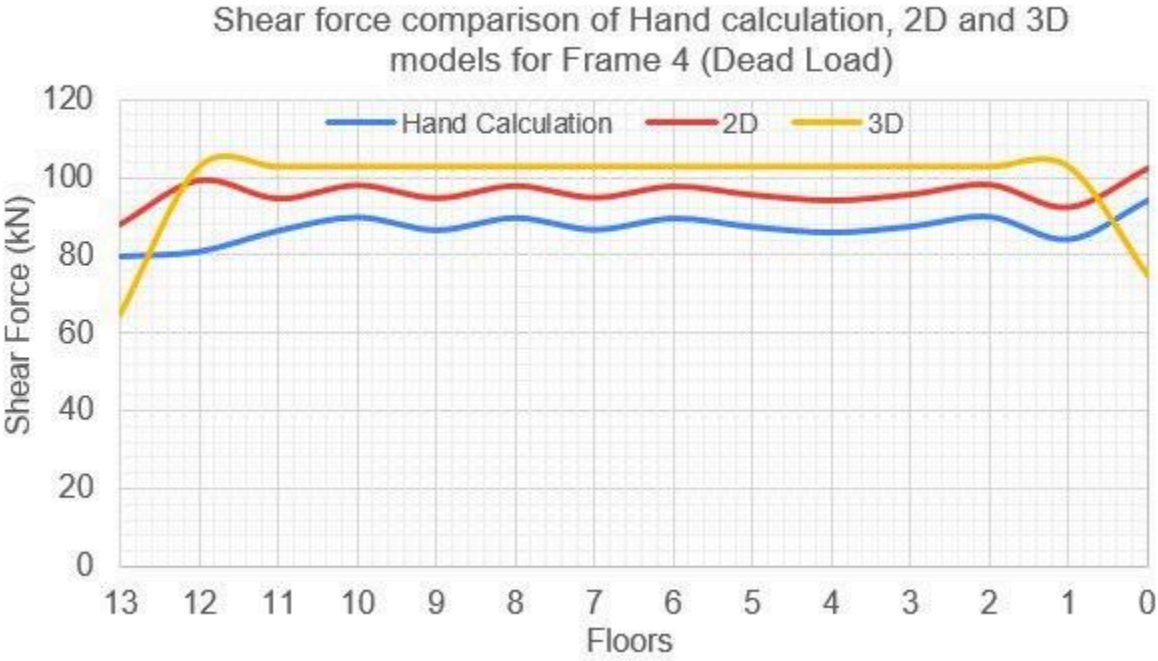

c)

Figure 3.26. Comparison of internal forces for Frame 4 under dead load: (a) axial force; (b) shear force; (c) bending moment.

Likewise, the comparison of internal forces under wind load for Frame 3 can be observed through figures below that the shear and axial force diagrams in all 2D, 3D and hand calculations were consistent with one another. Nonetheless, the moment diagram of hand calculations for lower floors is different because an approximate analysis method was used to calculate the internal forces through hand calculations.

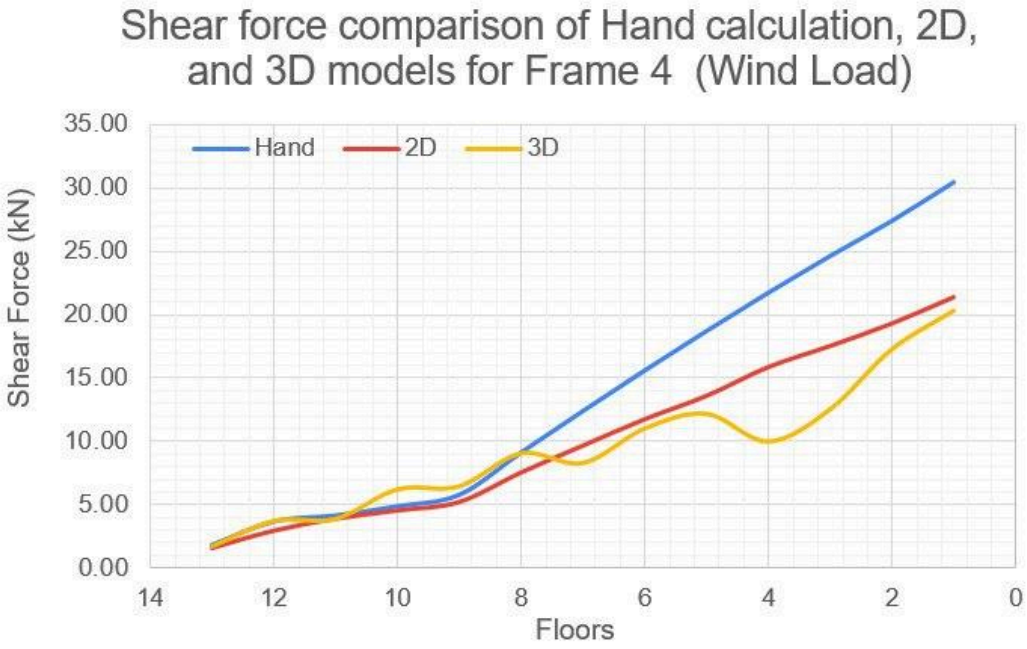

a)

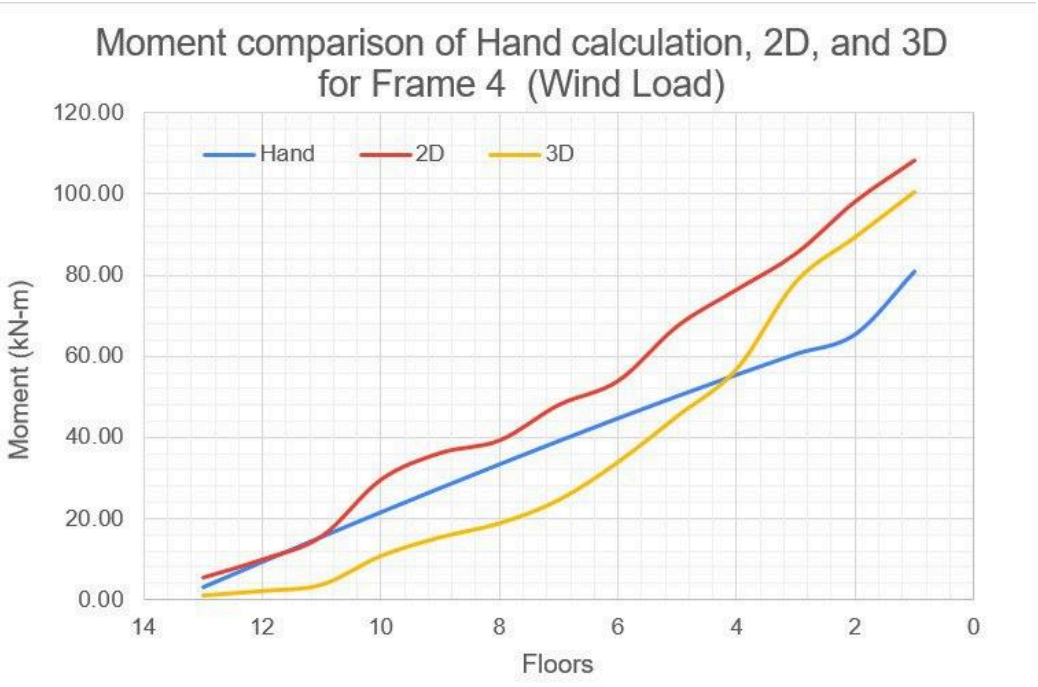

b)

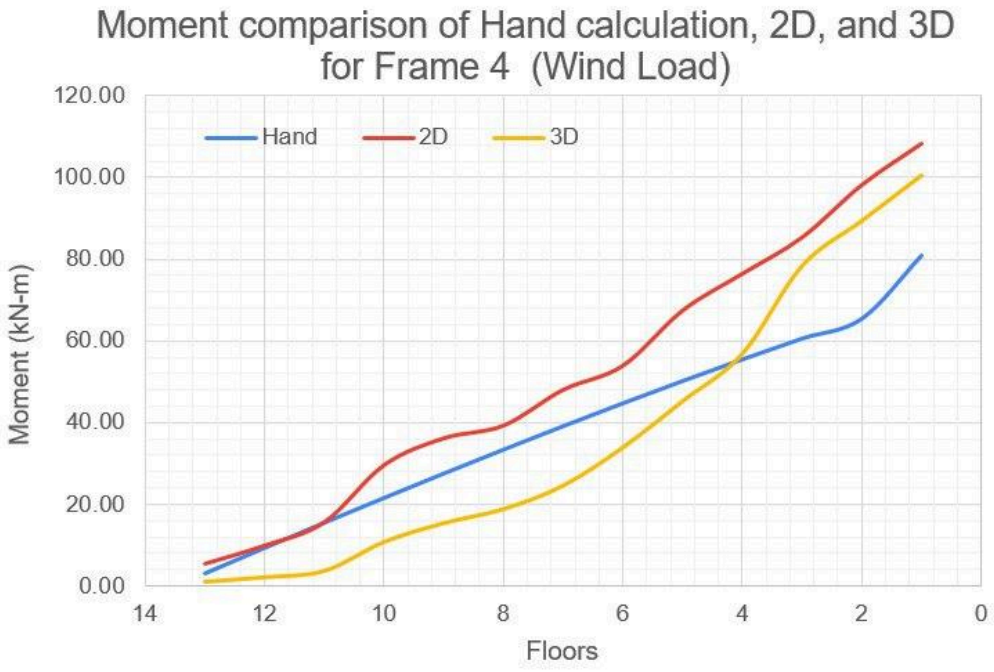

c)

Figure 3.27. Comparison of internal forces for Frame 4 under wind load: (a) axial force; (b) shear force; (c) bending moment.

3.6.5. Load combinations

The load combinations were selected in accordance with ASCE 7-16 Chapter 2. Dead, live, roof live, earthquake, and wind loads are among the load combinations. The structural study and design took into account every scenario involving wind loads. 1.2D + 1L ± 1Ey and 0.9D + 1Ey were found to be the essential load combinations that formed the greatest moments and forces during the analysis.

3.6.6. Structural member design using software

The building's structural design was completed using the SAP2000 software. By using the ACI 318 design code for reinforced concrete, the program can automatically do the analysis and determine the percentages of reinforcement for each individual structural part. The structural design for this project was completed by utilizing SAP2000's capabilities, and it should be confirmed by hand calculations.

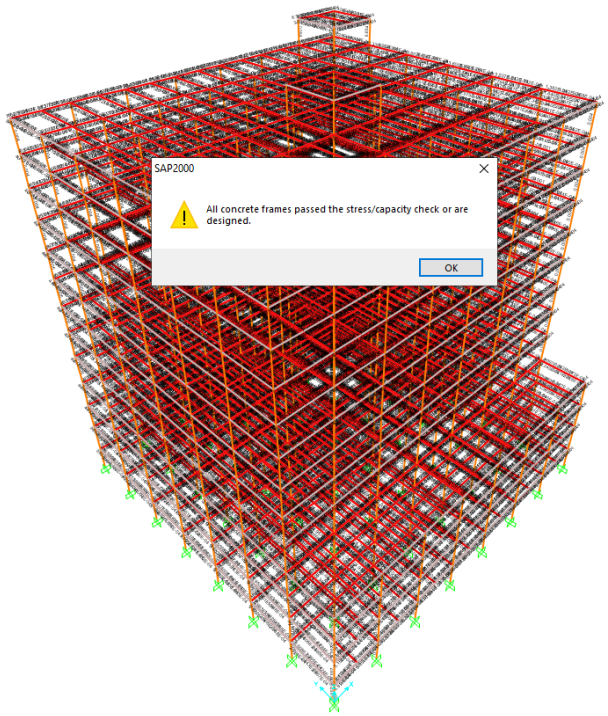

Figure 3.28. The structural design check in SAP2000.

3.6.6.1. Columns

For the column design, the corner column was taken

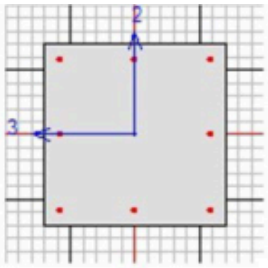

ACI 318-14 COLUMN SECTION DESIGN Type: Sway Special Units: KN, m, C (Summary)

Element : 7656	B=0.800	D=0.800	dc=0.064
Section ID : col 0-2	E=35000000.	fc=40000.000	Lt.Wt. Fac.=1.000
Combo ID : COMB2	L=3.000	fy=413685.473	fys=413685.473
Station Loc : 0.000	RLLF=1.000		

Phi(Compression-Spiral):	0.750
Phi(Compression-Tied):	0.650
Phi(Tension Controlled):	0.900
Phi(Shear):	0.750
Phi(Seismic Shear):	0.600
Phi(Joint Shear):	0.850

AXIAL FORCE & BIAXIAL MOMENT DESIGN FOR PU, M2, M3

Rebar Area	Design Pu	Design M2	Design M3	Minimum M2	Minimum M3
0.006	7972.619	4.769	312.846	312.846	312.846

AXIAL FORCE & BIAXIAL MOMENT FACTORS

	Cm Factor	Delta_ns Factor	Delta_s Factor	K Factor	L Length
Major Bending(M3)	0.419	1.000	1.000	1.000	3.000
Minor Bending(M2)	0.845	1.000	1.000	1.000	3.000

SHEAR DESIGN FOR V2,V3

	Rebar Av/s	Shear Vu	Shear phi*Vc	Shear phi*Vs	Shear Vp
Major Shear(V2)	0.000	88.840	882.825	0.000	0.000
Minor Shear(V3)	0.000	0.615	882.825	0.000	239.545

Figure 3.29. Design information for columns.

3.6.6.2. Major beams

The important positive and negative moments were taken into consideration when designing major beams. It is reasonable to suppose that the seismic forces would dictate the building's structural design because the structure is susceptible to severe earthquake loadings. Thus, from the critical load combinations, both positive and negative moments were extracted. The critical moments were created at the beam's margins as a result of the horizontal seismic loads. Therefore, while the top reinforcement will be placed at the margins of the beams, the bottom reinforcement will be continually designed based on the crucial edge positive moment.

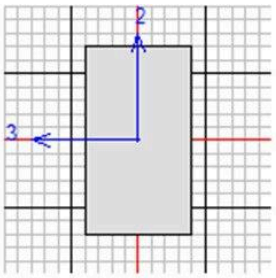

ACI 318-14 BEAM SECTION DESIGN Type:Sway Special Units: KN, mm, C (Summary)

Element : 5745	D=700.000	B=400.000	bf=400.000
Section ID : major beam	ds=0.000	dct=60.000	dcb=60.000
Combo ID : COMB2	E=35.000	fc=0.040	Lt.Wt. Fac.=1.000
Station Loc : 0.000	L=3000.000	fy=0.414	fys=0.414

Phi(Bending):	0.900
Phi(Shear):	0.750
Phi(Seis Shear):	0.600
Phi(Torsion):	0.750

Design Moments, M3

	Positive Moment	Negative Moment	Special +Moment	Special -Moment
	301337.567	0.000	301337.567	0.000

Flexural Reinforcement for Moment, M3

	Required Rebar	+Moment Rebar	-Moment Rebar	Minimum Rebar
Top (+2 Axis)	0.000	0.000	0.000	0.000
Bottom (-2 Axis)	1305.098	1305.098	0.000	974.946

Shear Reinforcement for Shear, V2

Rebar Av/s	Shear Vu	Shear phi*Vc	Shear phi*Vs	Shear Vp
0.000	192.396	201.660	0.000	363.827

Reinforcement for Torsion, T

Rebar At/s	Rebar Al	Torsion Tu	Critical Phi*Tcr	Area Ao	Perimeter Ph
0.000	0.000	100.256	56243.439	161596.229	1844.400

a)

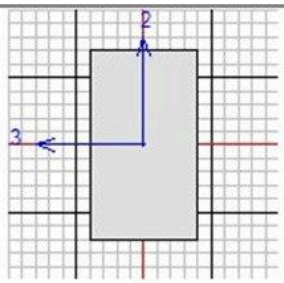

ACI 318-14 BEAM SECTION DESIGN Type:Sway Special Units: KN, mm, C (Summary)

Element : 5933	D=700.000	B=400.000	bf=400.000
Section ID : major beam	ds=0.000	dct=60.000	dcb=60.000
Combo ID : COMB2	E=35.000	fc=0.040	Lt.Wt. Fac.=1.000
Station Loc : 3000.000	L=3000.000	fy=0.414	fys=0.414

Phi(Bending):	0.900
Phi(Shear):	0.750
Phi(Seis Shear):	0.600
Phi(Torsion):	0.750

Design Moments, M3

Positive Moment	Negative Moment	Special +Moment	Special -Moment
156541.508	-313083.016	156541.508	-313083.016

Flexural Reinforcement for Moment, M3

	Required Rebar	+Moment Rebar	-Moment Rebar	Minimum Rebar
Top (+2 Axis)	1357.720	0.000	1357.720	974.946
Bottom (-2 Axis)	890.062	667.546	0.000	890.062

Shear Reinforcement for Shear, V2

Rebar Av/s	Shear Vu	Shear phi*Vc	Shear phi*Vs	Shear Vp
0.080	217.622	201.660	15.961	343.592

Reinforcement for Torsion, T

Rebar At/s	Rebar Al	Torsion Tu	Critical Phi*Tcr	Area Ao	Perimeter Ph
0.000	0.000	9.628	55976.259	161596.229	1844.400

b)

Figure 3.30. Design information for major beams a) critical positive and b) negative moment.

3.6.6.3. Minor beams

Similarly as for major beams, the critical negative and positive moments were chosen.

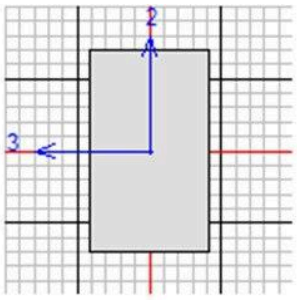

ACI 318-14 BEAM SECTION DESIGN Type:Sway Special Units: KN, mm, C (Summary)

Element	: 829	D=500.000	B=300.000	bf=300.000
Section ID	: minor beam	ds=0.000	dct=60.000	dcb=60.000
Combo ID	: COMB2	E=35.000	fc=0.040	Lt.Wt. Fac.=1.000
Station Loc	: 3000.000	L=6000.000	fy=0.414	fys=0.414

Phi(Bending):	0.900
Phi(Shear):	0.750
Phi(Seis Shear):	0.600
Phi(Torsion):	0.750

Design Moments, M3

Positive Moment	Negative Moment	Special +Moment	Special -Moment
129695.326	-43318.077	26088.712	-43318.077

Flexural Reinforcement for Moment, M3

	Required Rebar	+Moment Rebar	-Moment Rebar	Minimum Rebar
Top (+2 Axis)	356.972	0.000	267.729	356.972
Bottom (-2 Axis)	822.906	822.906	0.000	502.706

Shear Reinforcement for Shear, V2

Rebar Av/s	Shear Vu	Shear phi*Vc	Shear phi*Vs	Shear Vp
0.000	0.034	103.981	0.000	62.429

Reinforcement for Torsion, T

Rebar At/s	Rebar Al	Torsion Tu	Critical Phi*Tcr	Area Ao	Perimeter Ph
0.000	0.000	0.570	22130.314	73765.729	1244.400

a)

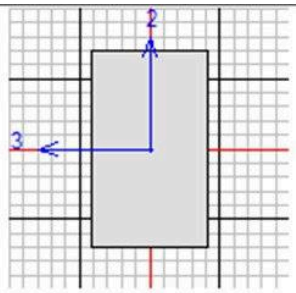

ACI 318-14 BEAM SECTION DESIGN Type:Sway Special Units: KN, mm, C (Summary)

Element : 829	D=500.000	B=300.000	bf=300.000
Section ID : minor beam	ds=0.000	dct=60.000	dcb=60.000
Combo ID : COMB2	E=35.000	fc=0.040	Lt.Wt. Fac.=1.000
Station Loc : 6000.000	L=6000.000	fy=0.414	fys=0.414

Phi(Bending):	0.900
Phi(Shear):	0.750
Phi(Seis Shear):	0.600
Phi(Torsion):	0.750

Design Moments, M3

	Positive Moment	Negative Moment	Special +Moment	Special -Moment
	86534.028	-173068.056	86534.028	-173068.056

Flexural Reinforcement for Moment, M3

	Required Rebar	+Moment Rebar	-Moment Rebar	Minimum Rebar
Top (+2 Axis)	1113.611	0.000	1113.611	502.706
Bottom (-2 Axis)	541.755	541.755	0.000	502.706

Shear Reinforcement for Shear, V2

Rebar Av/s	Shear Vu	Shear phi*Vc	Shear phi*Vs	Shear Vp
0.507	173.162	103.981	69.181	62.429

Reinforcement for Torsion, T

Rebar At/s	Rebar Al	Torsion Tu	Critical Phi*Tcr	Area Ao	Perimeter Ph
0.000	0.000	0.570	22130.314	73765.729	1244.400

Figure 3.31. Design information for minor beams a) critical positive and b) negative moment.

3.6.7. Hand calculations verifications for structural member design

3.6.7.1. Major beams

3.6.7.1.1. Flexural analysis

The following computations were carried out in order to confirm the reinforcement that was supplied in SAP2000 for the main beam. The tension side (top reinforcement at the edges) would be accounted for by the negative moment for the selected frame. It should be mentioned that the center section of the beam span's compression reinforcement was overlooked. Additionally, the design was assumed to be tension-controlled, hence $\phi = 0.9$.

Negative moment

$$M_u = 313.083\ kN - m$$

$$b = 400\ mm,\ h = 700\ mm, d = 700 - 2.5\ in \cdot 25.4\ mm/in = 636.5\ mm \sim 630\ mm$$

$$f'_c = 40\ MPa\ (5801\ psi),\ f_y = 417\ MPa$$

$$R_n = \frac{M_u}{\phi bd^2} = \frac{313.083}{0.9 \cdot 500 \cdot 630} = 1931.98\ kN/m^2$$

$$\rho = \frac{0.85f'_c}{f_y}\left[1 - \sqrt{1 - \frac{2R_n}{0.85f'_c}}\right] = 0.00477$$

$$A_s = \rho bd = 0.0048 \cdot 500 \cdot 630 = 1215.14\ mm^2$$

$$A_s f_y = 0.85f'_c ab \rightarrow a = \frac{1215.14 \cdot 417}{0.85 \cdot 40 \cdot 500} = 37.258\ mm$$

$$\beta_1 = 0.85 - 0.05\left(\frac{5801 - 4000}{1000}\right) = 0.76$$

$$c = \frac{a}{\beta_1} = \frac{37.258}{0.76} = 49.027\ mm$$

$\varepsilon_t = 0.003\left(\frac{d-c}{c}\right) = 0.003\left(\frac{630 - 49.027}{49.027}\right) = 0.0359 > 0.005 \rightarrow$ tension-controlled and ductile

The A_s = 1357.72 mm^2 (2.10 in^2) will be used for bar selection. Accordingly, at the negative moment locations, 3#8 bars will be chosen (A_s = 2.36 in^2). Therefore, the minimum width of the beam should be checked. With the assumption that #3 stirrups will be used at 200 mm for b_{min} = 234.95 mm < b = 400 mm.

Positive moment

$$M_u = 301.337\ kN - m$$

$$R_n = \frac{M_u}{\phi bd^2} = \frac{301.337}{0.9 \cdot 500 \cdot 630} = 1859.498\ kN/m^2$$

$$\rho = \frac{0.85f'_c}{f_y}\left[1 - \sqrt{1 - \frac{2R_n}{0.85f'_c}}\right] = 0.0046$$

$$A_s = \rho bd = 0.0046 \cdot 500 \cdot 630 = 1168.189\ mm^2$$

$$A_s f_y = 0.85f'_c ab \rightarrow a = \frac{1168.189 \cdot 417}{0.85 \cdot 40 \cdot 500} = 35.819\ mm$$

$$\beta_1 = 0.85 - 0.05\left(\frac{5801-4000}{1000}\right) = 0.76$$

$$c = \frac{a}{\beta_1} = \frac{35.819}{0.76} = 47.133\ mm$$

$\varepsilon_t = 0.003\left(\frac{d-c}{c}\right) = 0.003\left(\frac{630-47.133}{47.133}\right) = 0.0375 > 0.005 \rightarrow$ tension-controlled and ductile

The A_s = 1305.098 mm^2 (2.02 in^2) from SAP2000 will be used for bar selection. Based on that, for the bottom reinforcement, 3#8 bars will be used (A_s = 2.36 in^2) for the right end of the beam. The minimum width assuming the #3 stirrups at 200 will be b_{min} = 234.95 mm < b = 400 mm. For midspan and left-end the same procedures were done.

3.6.7.1.2. Shear analysis

V_u = 217.622 kN and λ = 1 (normal-weight), $\phi = 0.75$

$$\phi V_c = \phi \cdot 2\lambda\sqrt{f'_c}\, b_w d = 76.38\ kN$$

Since $V_u > \phi V_c$ ***shear reinforcement is required***

$$V_{c1} = 4\sqrt{f'_c}\, b_w d = 203.68\ kN \text{ and } V_{c2} = 8\sqrt{f'_c}\, b_w d = 407.36\ kN$$

$$V_s = \frac{V_u - \phi V_c}{\phi} = 188.32\ kN < V_{c1} \Rightarrow S_2 = d/2 = 12.53\ in \leq 14\ in$$

$$S_1 = A_v f_{yt} d/V_s = 0.2m$$

$S_2 = d/2 = 0.318\ m$ => #3 stirrups at 200 mm spacing

$$S_3 = A_v f_{yt} d/V_s = 2.959\ m$$

Despite the significant variances, the discrepancies may have been caused by various assumptions about concrete cover and d in SAP2000. On the other hand, Av/s = 1.98 mm should

be utilized for stirrup design. Stirrups will be used for the primary beam shear design #4. #4 stirrups have a 129 mm2 (0.2 in2) area.

3.6.7.1.3. Torsional analysis

From SAP200 T_u = 0.01 kN-m.

$$T_n = \phi\lambda\sqrt{f'_c}\left(\frac{A_{cp}^2}{P_{cp}}\right) = 5.34\,kN - m > T_u$$

Torsional reinforcement is not needed

3.6.7.2. Minor beam

For minor beams similar flexural, shear and torsional analysis were performed.

3.6.7.2.1. Flexural analysis

Negative moment

$$M_u = 173.068\,kN - m$$

$$b = 300\,mm,\ h = 500\,mm, d = 500 - 2.5\,in \cdot 25.4\,mm/in = 436.5\,mm \sim 430\,mm$$

$$R_n = \frac{M_u}{\phi bd^2} = \frac{173.068}{0.9 \cdot 300 \cdot 430} = 3027.798\,kN/m^2$$

$$\rho = \frac{0.85f'_c}{f_y}\left[1 - \sqrt{1 - \frac{2R_n}{0.85f'_c}}\right] = 0.0076$$

$$A_s = \rho bd = 0.0076 \cdot 300 \cdot 430 = 997.40\,mm^2$$

$$A_s f_y = 0.85f'_c ab \rightarrow a = \frac{997.4*417}{0.85 \cdot 40 \cdot 300} = 40.776\,mm$$

$$\beta_1 = 0.85 - 0.05\left(\frac{5801-4000}{1000}\right) = 0.75995$$

$$c = \frac{a}{\beta_1} = \frac{40.776}{0.76} = 53.656\,mm$$

$\varepsilon_t = 0.003\left(\frac{d-c}{c}\right) = 0.003\left(\frac{430-53.656}{53.656}\right) = 0.0214 > 0.005$ => section is tension-controlled and ductile.

As a result, the bar selection will be based on As = 1113.611 mm2 (from SAP2000). Consequently, 4#6 bars will be employed for the top reinforcement negative moment. For the minor beam, b min = 184 mm < b = 300mm is the minimum width needed with the #3 stirrups at 150 mm.

Positive Moment

$$M_u = 129.695\ kN - m$$

$$R_n = \frac{M_u}{\phi bd^2} = \frac{129.695}{0.9 \cdot 300 \cdot 430} = 2268.99\ kN/m^2$$

$$\rho = \frac{0.85f'_c}{f_y}\left[1 - \sqrt{1 - \frac{2R_n}{0.85f'_c}}\right] = 0.0056$$

$$A_s = \rho bd = 0.0056 \cdot 300 \cdot 430 = 738.038\ mm^2$$

$$A_s f_y = 0.85f'_c ab \rightarrow a = \frac{738.038 \cdot 413}{0.85 \cdot 40 \cdot 300} = 30.173\ mm$$

$$\beta_1 = 0.85 - 0.05\left(\frac{5801-4000}{1000}\right) = 0.75995$$

$$c = \frac{a}{\beta_1} = \frac{30.173}{0.76} = 39.71\ mm$$

$\varepsilon_t = 0.003\left(\frac{d-c}{c}\right) = 0.003\left(\frac{430-39.71}{39.71}\right) = 0.03 > 0.005$ => section is tension-controlled and ductile.

According to SAP2000 the As is 822.906 mm2 (1.275 in2). By comparing the minimum steel area, SAP2000 result was taken to identify the reinforcement for the right edge of the selected minor beam. Consequently, the 3#6 bars (A_s = 1.33 in^2) will be used for the bottom reinforcement with #3 stirrups at spacing 150 mm.

3.6.7.2.2. Shear analysis

V_u = 173.162 kN and λ = 1 (normal-weight), $\phi = 0.75$

$$\phi V_c = \phi \cdot 2\lambda\sqrt{f'_c} b_w d = 39.285\ kN$$

Since $V_u > \phi V_c$ shear reinforcement is required

$$V_{c1} = 4\sqrt{f'_c} b_w d = 104.76\ kN \text{ and } V_{c2} = 8\sqrt{f'_c} b_w d = 209.52\ kN$$

$$V_{c1} < V_s = \frac{V_u - \phi V_c}{\phi} = 178.5\ kN < V_{c2} \Rightarrow S_2 = d/4 = 4.3\ in \leq 12\ in$$

$$S_1 = A_v f_{yt} d/V_s = 0.144\ m$$

$S_2 = d/4 = 0.109\ m$ => #3 stirrups at 100 mm spacing

$$S_3 = A_v f_{yt} d/V_s = 3.94\ m$$

3.6.7.2.3. Torsional analysis

From SAP200 T_u = 0.02 kN-m.

$$T_n = \phi\lambda\sqrt{f'_c}\left(\frac{A_{cp}^{\ 2}}{P_{cp}}\right) = 142.2\ kN - m > T_u$$

Torsional reinforcement is not needed

3.6.7.3. Columns

3.6.7.3.1. Slenderness ratio check

The structural design of the building received steel reinforcing for all structural column types. The selected column for verification calculations was a Floor 1 corner column with dimensions 0.8m * 0.8m. The first step requires examination of column slenderness ratio to determine its short or slender classification. Our unsheared columns fail to receive lateral support from the lateral braces or shear walls because of which they are classified as swaying elements. The following calculation shows the slenderness check for sway columns.

Internal column (800 x 800 mm^2)

$$\psi = \frac{\Sigma(EI/l)columns}{\Sigma(EI/l)beams} = 5.97 \Rightarrow k\ (from\ graph) = 2.4$$

$$Max\ kl_u/r = 34$$

$$kl_u/r = 23 < 34 \rightarrow \text{Short Column}$$

Corner column (800 x 800 mm^2)

$$\psi = \frac{\Sigma(EI/l)columns}{\Sigma(EI/l)beams} = 11.94 \Rightarrow k\ (from\ graph) = 3.17$$

$$kl_u/r = 30.4 < 34 \rightarrow \text{Short Column}$$

Edge column (800 x 800 mm^2)

$$\psi = \frac{\Sigma(EI/l)columns}{\Sigma(EI/l)beams} = 7.96 \Rightarrow k\ (from\ graph) = 2.64$$

$$kl_u/r = 25.3 < 34 \rightarrow \text{Short Column}$$

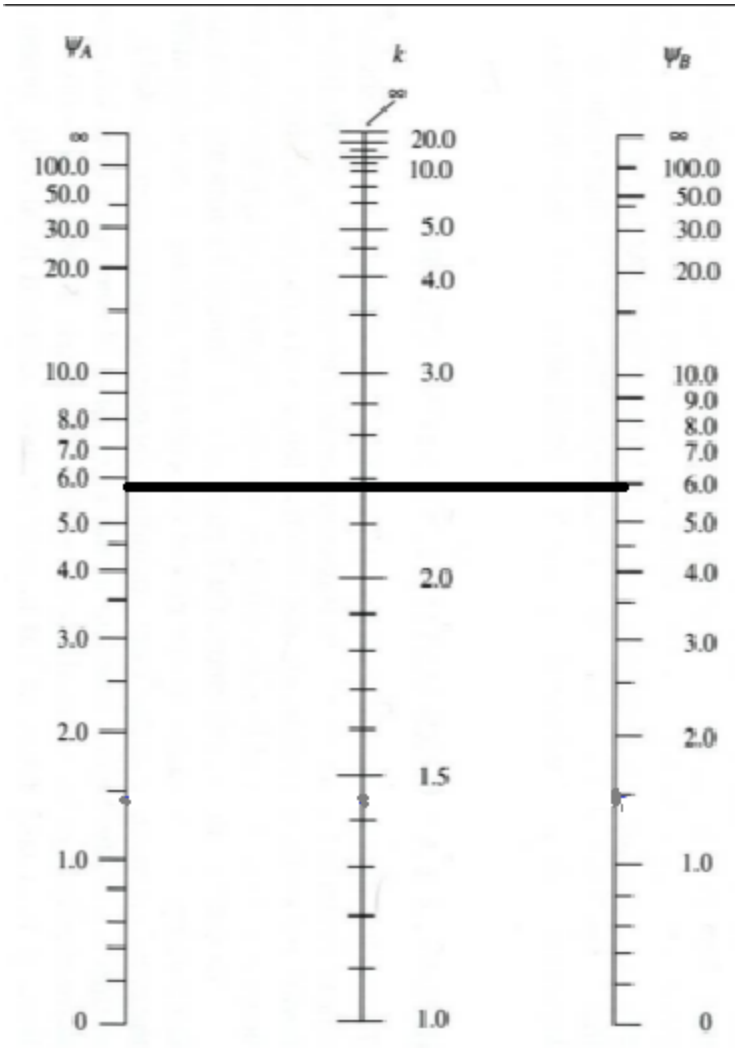

Figure 3.32. Value for k.

The value of k equal to 2.4 was obtained from the chart to calculate slenderness ratios. Results indicate that column slenderness ratio remains below the allowable threshold which means the column needs short-column design subject to both axial and bending loads.

3.6.7.3.2. Axial and moment analysis

The maximum moments and forces acting on the column were found from the SAP2000 software and are equal to:

$$M_u = 312.85\ kN \cdot m$$

$$P_u = 7972.62\ kN$$

Using these values the reinforcement ratio could be identified used the following procedure:

$$P_n = \frac{P_u}{\varphi} = 12265.57\ kN \cdot m$$

$$M_n = \frac{M_u}{\varphi} = 481.3\ kN \cdot m$$

$$e = \frac{M_n}{P_n} = 0.04\ \text{m}$$

$$K_n = \frac{P_n}{A_g f_c'} = 0.479$$

$$\gamma = \frac{0.8-0.07*2}{0.8} = 0.825$$

An interaction diagram for rectangular columns from ACI 318-19 provided the necessary reinforcement ratio information.

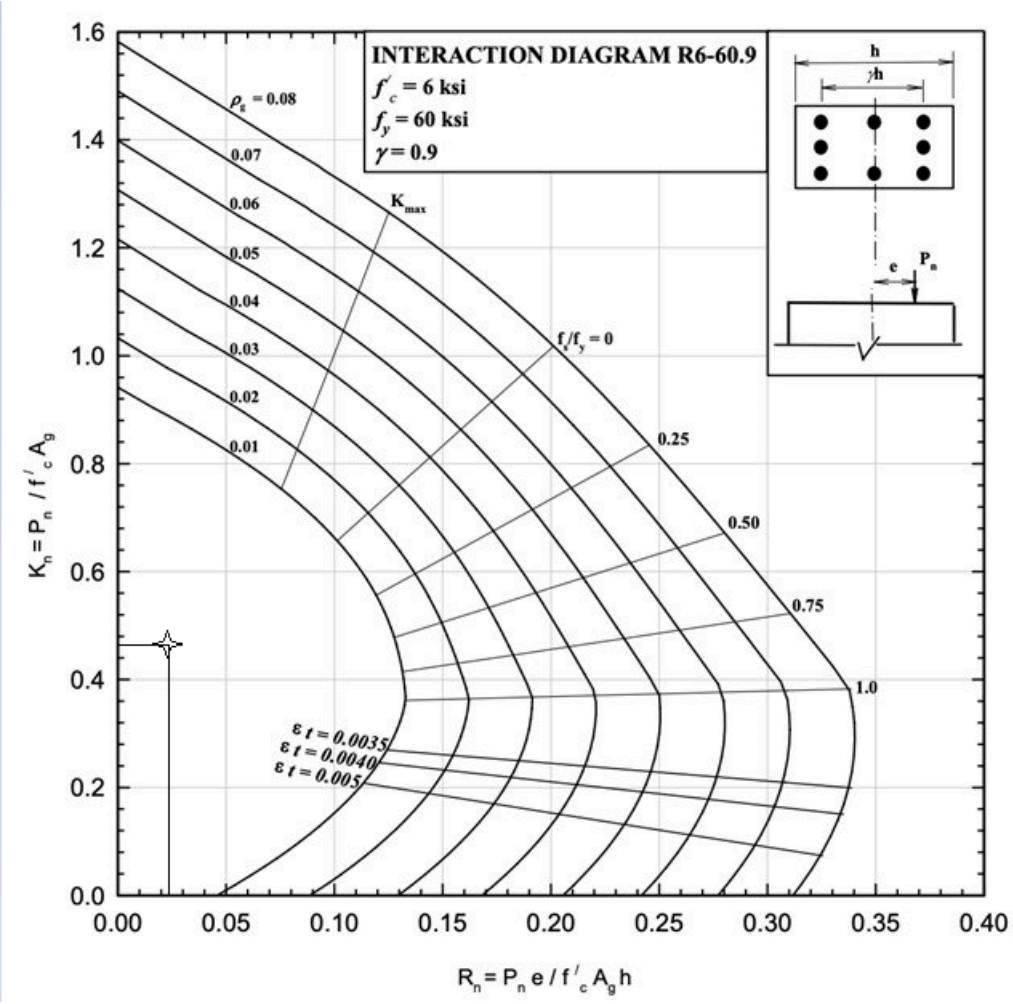

Figure 3.33. Interaction diagram.

According to the values of Kn and Rn, the value of ρ has been found. The same procedure was made for the graph with gamma value equal to 0.8.

$$R_n = \frac{P_n e}{A_g f_c' h} = 0.024 \rightarrow \text{from the graph } \rho = 0.01 = 1\%$$

$$A_s = 0.01 * A_g = 0.0064\, m^2 = 9.92\, in^2 \rightarrow 8\#10 \text{ bar selected}$$

3.6.7.3.3. Shear analysis

In order to check the shear capacity of the column, V_c should be calculated:

$$V_{u1} = 128.1\, kN$$

$$V_{u2} = 1.168\, kN$$

$$V_c = 0.17\left(1 + \frac{P_u}{14A_g}\right)\lambda\sqrt{f_c'}\, b_w d = 1117.67\, kN$$

$\varphi V_c/2 = 439.4\, kN > V_u$ minimum amount of reinforcement is required

Therefore, #4 stirrups at 200 mm spacing

3.6.7.3.4. Biaxial bending analysis

The Bresler Reciprocal Load Method must be used to assess biaxial bending safety of the chosen corner column.

Bending moment values for both axes were obtained using the SAP200 software:

$$M_{ux} = 4.769\, kN \cdot m$$

$$M_{uy} = 312.846\, kN \cdot m$$

$$P_u = 7972.619\, kN$$

The procedure according to Bresler Reciprocal Load Method is summarized below:

$$M_{ny} = \frac{M_{uy}}{0.65} = 481.302\, kN - m$$

$$M_{nx} = \frac{M_{ux}}{\varphi} = 7.339\, kN \cdot m$$

$$P_n = \frac{P_u}{0.65} = 12265.6\, kN$$

$$\gamma_x = \gamma_y = 0.825$$

$$e_x = \frac{M_{nx}}{Pn} = 0.001$$

$$e_y = \frac{M_{ny}}{Pn} = 0.039$$

From the Interaction diagram for rectangular column chart the values obtained for Kn.

$$P_{nx} = \frac{K_{nx} * f_c' * A_g}{\varphi} = 51200\ kN$$

$$P_{ny} = \frac{K_{ny} * f_c' * A_g}{\varphi} = 27569.2\ kN$$

$$P_0 = 0.85 * f_c' * A_g + A_{st}(f_y - 0.85 f_c') = 21764.5\ kN$$

Calculating Pn:

$$\frac{1}{P_n} = \frac{1}{P_{nx}} + \frac{1}{P_{ny}} - \frac{1}{P_0} \rightarrow P_n = 101492\ kN$$

Checking the validity of the method:

$$P_n = 101492\ kN > 0.1P_0 = 2176.25\ kN \rightarrow \underline{\textit{Method is applicable}}$$

$$\varphi P_n = 65969.8 > P_u \rightarrow \underline{\textit{Column is safe against biaxial bending}}$$

3.6.7.4. One-way slab

3.6.7.4.1. Flexural analysis

Design of interior and exterior slab panels occurred through Direct Design Method protocols. The exterior dimensions of these slab panels measure 3000mm*3000mm whereas the column dimensions amount to 800mm*800mm. A minimum limit exists for slab thickness of 200 mm which needs to be checked using corresponding standards.

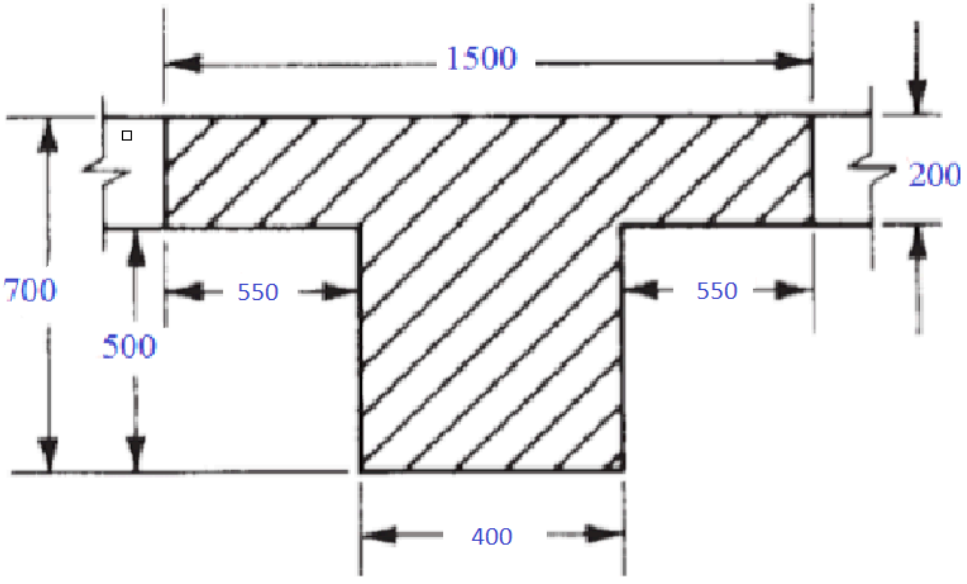

Figure 3.34. Slab model.

$$\bar{y} = \frac{1500*200*200/2+400*400*(200+400/2)}{1500*200+400*400} = 204.35\,mm$$

$$I_{beam} = \frac{1}{12} * 1500 * (200)^3 + 1500 * 200 * (100 - 204.35)^2 + \frac{1}{12} * 400 * 400^3 + 400^2 * (450 - 204.35)^2 = 1.596 * 10^{10} mm^4$$

The moment of inertia of the slab in the long and short direction is:

$$I_{slab} = \frac{1}{12} * 3000 * 200^3 = 2 * 10^9 mm^4$$

$$\alpha_{fm} = \alpha_f = \frac{EI_b}{EI_s} = \frac{1.596*10^{10}}{2*10^9} = 7.98$$

α_{fm} is greater than 2, so the minimum thickness of the slab should be calculated as follows:

$$h_{min} = \frac{l_n(0.8+f_y/200000)}{36+9\beta} = \frac{(3000-800/2)(0.8+420/1400)}{36+9*1} = 63.50\,mm$$

Hence, a thickness of 200 mm satisfies the minimum requirement criteria. Next, factored loads have to be calculated:

$$q_d = 5.37\,kN/m^2$$

$$q_l = 4.79\,kN/m^2$$

$$q_u = 1.2 * 5.37 + 1.6 * 4.79 = 14.108\,kN/m^2$$

Now, the total static moments in the both directions can be calculated:

$$M_o = \frac{q_u l_2 l_n^2}{8} = \frac{14.108*6(6-0.80)^2}{8} = 286.11\,kN-m$$

$$M_n = 0.65M_0 = = 185.97\,kN-m$$

$$M_p = 0.35M_0 = 100.13\,kN-m$$

$$\alpha_{f1} = \alpha_s = 7.98 \geq 1.0$$

$$\frac{l_2}{l_1} = 1.0$$

Table 3.42. Summary of the interior beam-supported panel design.

	Column Strip				Middle Strip	
M	(-ve)	(+ve)	(-ve)	(-ve)	(+ve)	(-ve)
% of moment	75	75	75	25	25	25
Distribution of moment Mu (kN-m)	139.48	75.1	139.48	46.49	25.03	46.49
Mu slab	20.92	11.27	20.92	6.97	3.76	6.97

(kN-m)						
b (m)	1.5	1.5	1.5	1.5	1.5	1.5
Rn (kPa)	575.26	309.75	575.26	191.75	103.25	191.75
Ro	0.0014	0.0007	0.0014	0.0005	0.00025	0.00046
As (m^2)	0.00034	0.00018	0.00034	0.00011	0.00006	0.00011
As (in^2)	0.52718	0.28274	0.52718	0.17472	0.09396	0.17472
Asmin (in^2)	0.837	0.837	0.837	0.837	0.837	0.837
As final (in^2)	1.1744	1.1744	1.1744	1.1744	1.1744	1.1744
Bar Selected	8#3	8#3	8#3	8#3	8#3	8#3
Spacing (m)	0.5	0.5	0.5	0.5	0.5	0.5

The moment of inertia of the slab in the long and short direction is:

$$I_{slab} = \frac{1}{12} * 3000 * 200^3 = 2 * 10^9 mm^4$$

$$\alpha_{fm} = \alpha_f = \frac{EI_b}{EI_s} = \frac{1.596*10^{10}}{2*10^9} = 7.98$$

α_{fm} is greater than 2, so the minimum thickness of the slab should be calculated as follows:

$$h_{min} = \frac{l_n(0.8+f_y/200000)}{36+9\beta} = \frac{(3000-800/2)(0.8+420/1400)}{36+9*1} = 63.50\ mm$$

The minimum requirements regulate the required thickness as 200 mm. It is vital to examine the torsional resistance capability of the effective transverse edge beam which is measured by βt:

$$C = \Sigma(1 - \frac{0.63x}{y})(\frac{x^3y}{3}) = 10.01 * 10^8\ mm^4$$

$$\beta_t = \frac{E_{cb}C}{2E_{cs}I_s} = 0.32$$

Since $\beta_t < 2.5$, the interpolated coefficient should be used for the exterior support.

Table 3.43. Summary of the exterior beam-supported panel design.

	Column Strip			Middle Strip		
M	(-ve)	(+ve)	(-ve)	(-ve)	(+ve)	(-ve)
% of moment	97.29	75	75	2.71	25	25
Distribution of moment Mu (kN-m)	184.43	76.56	142.17	5.13	25.52	47.39
Mu slab	27.66	11.48	21.33	0.77	3.83	7.11

(kN-m)						
b (m)	3.38	3.38	3.38	3.38	3.38	3.38
Rn (kPa)	948.7	393.8	731.33	26.41	131.27	243.78
Ro	0.0023	0.0009	0.0018	0.0001	0.0003	0.0006
As (m^2)	0.00076	0.00031	0.00058	0.00002	0.0001	0.00019
As (in^2)	1.1744	0.4834	0.90232	0.03224	0.1605	0.29858
Asmin (in^2)	1.41244	1.41244	1.41244	1.41244	1.41244	1.41244
As final (in^2)	1.1744	1.1744	1.1744	1.1744	1.1744	1.1744
Bar Selected	6#4	6#4	6#4	6#4	6#4	6#4
Spacing (m)	0.5	0.5	0.5	0.5	0.5	0.5

3.6.7.4.2. Shear analysis

$$d_{shear} = 200 - 20 - 13.675 = 166.325\,mm$$

$$d_{long} = 200 - 20 - 13.675/2 = 173.16\,mm$$

$$d_{short} = 7 - 0.75 - 13.675/2 - 13.675 = 156.18\,mm$$

$$b_0 = 4 * (800 + 166.325) = 3865.3\,mm$$

$$f_c' = 40\,MPa$$

$$f_y = 420\,MPa$$

$$V_u = [l_1 l_2 - (b + d_{avg})(h + d_{avg})] * q_u$$

$$V_u = [3000 * 3000 - (800 + 166.325)^2] * 14.108/10^6 = 113.79\,kN$$

$$\lambda_s = \sqrt{\frac{2}{(1+0.004d_{shear})}} = \sqrt{\frac{2}{(1+166.325*0.004)}} = 0.098 \leq 1,\ thus\ use\ \lambda_s = 1.0$$

$$\varphi V_{c1} = \varphi(0.17\lambda\sqrt{f_c'} + \frac{N_u}{6A_g})b_w d = 256.57\,kN$$

$$\varphi V_{c2} = \varphi(0.66\lambda\lambda_s\rho^{(1/3)}\sqrt{f_c'} + \frac{N_u}{6A_g})b_w d = 134.96\,kN \rightarrow controls$$

$$\varphi V_{c2} = 134.96\,kN > V_u = 113.79\,kN \rightarrow Shear\ criteria\ is\ satisfied$$

3.6.7.5. Joint design

The joint design followed the specifications in Chapter 15 of ACI 318-19. The design book authored by Wight and MacGregor (Wight & MacGregor, 2009) gave the complete calculation procedures. The figure below shows the free body diagram of the interior beam-column joint.

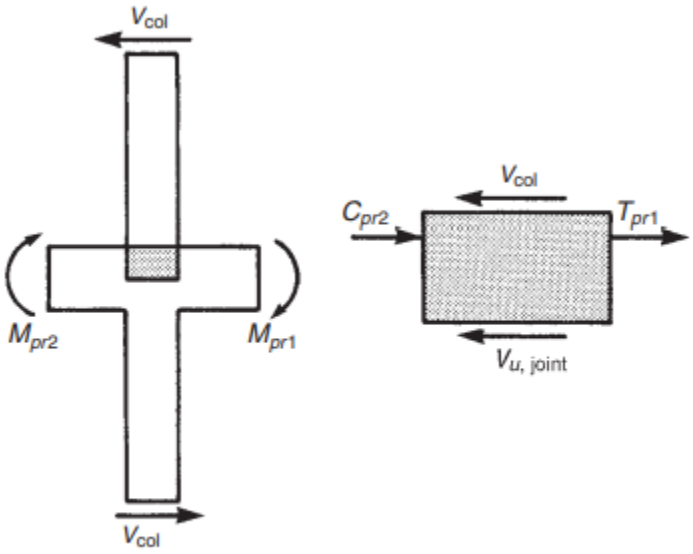

(c) Interior column-beam joint.

(d) Top half of interior column-beam joint.

Figure 3.35. Free body diagram of the beam-column joint.

An interior beam-column joint's shear was calculated according to the following equation:

$$V_{u,joint} = T_{pr1} + C_{pr2} - V_{col} \tag{3.41}$$

The values in the above equation were calculated below:

$$T_{pr1} = \alpha A_s f_y = 1.25 \cdot 2847 \cdot 0.420 = 1494.675\ kN$$

$$C_{pr1} = \alpha A_s f_y = 1.25 \cdot 1764 \cdot 0.420 = 926.1\ kN$$

From SAP2000, the column joint:

$$V_{col} = 465.7\ kN$$

Accordingly, the shear demand on joint:

$$V_{u,joint} = 1494.675 + 926.1 - 465.7 = 1955.075\ kN$$

The first step involved calculating effective joint width as a necessary condition for shear strength determination:

$$b_j = \frac{b_b + b_{col}}{2} = \frac{400+800}{2} = 600\,mm < b_b + h_{col} = 400 + 800 = 1200\,mm$$

$$b_j = 600\,mm < b_b + 2x = 400 + 800 = 1200\,mm$$

A mathematical formula allows the calculation of joint shear capacity:

$$V_n = \gamma\sqrt{f'_c}A_j \tag{3.42}$$

Where γ = 1.7

A_j is the product of b_j and h_{col} and hence:

$$V_n = \gamma\sqrt{f'_c}A_j = 1.7\sqrt{40} \cdot 600 \cdot 800 = 5160.8\,kN$$

The nominal shear strength requirements should be $\phi V_n \geq V_u$. The value of φ can be taken as 0.85 to account for the strain hardening of the reinforcement.

$$0.85 \cdot 5160.8 = 4386.7\,kN \geq V_u = 1955.075\,kN$$

The safe status of the joint against shear forces emerges from this procedure. An equivalent method must be used to evaluate shear safety across other directions and the test results confirmed joint shear limits.

The calculations for spacing requirements followed the method stated in ACI 15.4.2 through this formula:

$$A_v = max(\frac{0.062\sqrt{f'_c}b_c s}{f_{yt}}, \frac{0.35 b_c s}{f_{yt}}) \tag{3.43}$$

$$s = min(\frac{A_v f_{yt}}{0.062\sqrt{f'_c}b_c}, \frac{A_v f_{yt}}{0.35 b_c}) \tag{3.44}$$

Accordingly, the minimum spacing with 3#4 ties:

$$s = min(\frac{2 \cdot 129 \cdot 413.7}{0.062\sqrt{40} \cdot 750}, \frac{2 \cdot 129 \cdot 413.7}{0.35 \cdot 750}) = min(363.3,\ 408) = 363.3\,mm$$

So, 3#4 ties at 360 mm spacing will be provided to meet the code requirements.

The following criteria should be evaluated to ensure the plastic hinges develop in beams instead of columns:

$$\Sigma M_{nc} \geq \frac{6}{5}\Sigma M_{nb} \tag{3.45}$$

$$653.5 + 554.2 = 1207.7\,kN - m \geq \frac{6}{5}(189.3 + 115.6) = 304.9\,kN - m$$

3.6.7.6. Reinforcement detailing

3.6.7.6.1. Bar selection and spacing

Table 3.44. Final selected bars for slab and columns.

Component	**Top reinforcement**	**Bottom reinforcement**	**Stirrups**
One-way slab	6#4	6#4	
		Reinforcement	**Ties**
Column 0-2 floors (800 x 800 mm)		8#10	#4 at 200 mm
Column 3-4 floors (750 x 750 mm)		8#10	#4 at 200 mm
Column 5-6 floors (700 x 700 mm)		8#9	#3 at 200 mm
Column 7-8 floors (650 x 650 mm)		7#9	#3 at 200 mm
Column 9-10 floors (600 x 600 mm)		6#9	#3 at 200 mm
Column 11-13 floors (550 x 550 mm)		8#7	#3 at 200 mm

Table 3.45. Left end reinforcement for major beams.

Floors	Left End Reinforcement (major beam)						Shear Reinforcement
	Compression Reinforcement (bottom)			Tension Reinforcement (top)			
	$A_{SAP2000}$, mm^2	Area, in^2	Selected bar	$A_{SAP2000}$, mm^2	Area, in^2	Selected bar	#3 stirrups at x mm
1	1409.101	2.1840	3#8	807.078	1.2509	3#6	140
2	1409.101	2.1840	3#8	751.068	1.1641	2#7	140
3	1405.895	2.1790	3#8	696.747	1.0799	2#7	150
4	1346.816	2.0874	3#8	667.722	1.0349	2#7	150
5	1251.937	1.9404	2#9	621.061	0.9626	2#7	150
6	1145.058	1.7747	4#6	568.429	0.8810	3#5	150
7	1066.863	1.6535	4#6	529.876	0.8213	3#5	150
8	995.153	1.5424	2#8	494.486	0.7664	3#5	150

9	943.257	1.4620	2#8	468.853	0.7267	4#4	150
10	903.029	1.3996	2#8	448.972	0.6959	4#4	150
11	873.079	1.3532	2#8	434.164	0.6729	4#4	150
12	837.952	1.2987	3#6	416.789	0.6460	4#4	150

Table 3.46. Mid-Span reinforcement for major beams.

Floors	Mid-Span Reinforcement (major beam)						Shear Reinforcement
	Compression Reinforcement (top)			Tension Reinforcement (bottom)			
	$A_{SAP2000}$, mm^2	Area, in^2	Selected bar	$A_{SAP2000}$, mm^2	Area, in^2	Selected bar	#3 stirrups at x mm
1	801.542	1.2423	3#6	1409.101	2.1840	3#8	250
2	769.011	1.1919	3#6	1409.101	2.1840	3#8	250
3	743.105	1.1517	3#6	1409.101	2.1840	3#8	250
4	741.102	1.1486	2#7	1409.101	2.1840	3#8	250
5	721.65	1.1185	2#7	1409.101	2.1840	3#8	250
6	694.964	1.0771	2#7	1409.101	2.1840	3#8	250
7	685.011	1.0617	2#7	1409.101	2.1840	3#8	250
8	667.061	1.0339	2#7	1409.101	2.1840	3#8	250
9	644.025	0.9982	2#7	1409.101	2.1840	3#8	250
10	621.722	0.9636	3#5	1409.101	2.1840	3#8	250
11	587.203	0.9101	3#5	1409.101	2.1840	3#8	250
12	558.486	0.8656	3#5	1409.101	2.1840	3#8	250

Table 3.47. Right end reinforcement for major beams.

Floors	Right End Reinforcement (major beam)		Shear Reinforcement
	Compression Reinforcement (bottom)	Tension Reinforcement (top)	

	$A_{SAP2000}$, mm^2	Area, in^2	Selected bar	$A_{SAP2000}$, mm^2	Area, in^2	Selected bar	#3 stirrups at x mm
1	1409.101	2.1840	3#8	708.422	1.0980	2#7	140
2	1409.101	2.1840	3#8	754.395	1.1692	2#7	140
3	1409.101	2.1840	3#8	807.354	1.2513	3#6	150
4	1409.101	2.1840	3#8	862.153	1.3363	3#6	150
5	1409.101	2.1840	3#8	907.657	1.4068	3#7	150
6	1458.378	2.2604	3#8	960.311	1.4884	3#7	150
7	1510.47	2.3411	3#8	994.159	1.5409	3#7	150
8	1557.509	2.4140	4#7	1024.697	1.5882	3#7	150
9	1587.957	2.4612	2#10	1044.45	1.6188	3#7	150
10	1606.571	2.4900	2#10	1056.52	1.6375	3#7	150
11	1618.036	2.5078	2#10	1063.952	1.6490	3#7	150
12	1648.081	2.5544	2#10	1083.422	1.6792	3#7	150

Table 3.48. Left end reinforcement for minor beams.

Floors	Left End Reinforcement (minor beam)						Shear Reinforcement
	Compression Reinforcement (bottom)			Tension Reinforcement (top)			
	$A_{SAP2000}$, mm^2	Area, in^2	Selected bar	$A_{SAP2000}$, mm^2	Area, in^2	Selected bar	#3 stirrups at x mm
1	707.828	1.0971	3#6	465.444	0.7214	4#4	110
2	730.458	1.1321	3#6	480.106	0.7441	4#4	120
3	746.545	1.1571	3#6	490.521	0.7603	4#4	150
4	776.413	1.2034	3#6	509.838	0.7902	4#4	110
5	781.843	1.2118	3#6	513.347	0.7956	4#4	110
6	787.633	1.2208	3#6	517.088	0.8014	2#6	110

7	791.415	1.2266	3#6	519.531	0.8052	2#6	110
8	793.995	1.2306	3#6	521.198	0.8078	2#6	110
9	794.114	1.2308	3#6	521.275	0.8079	2#6	110
10	790.886	1.2258	3#6	519.19	0.8047	2#6	110
11	791.413	1.2266	3#6	519.53	0.8052	2#6	110
12	791.303	1.2264	3#6	519.459	0.8051	2#6	110

Table 3.49. Mid-Span reinforcement for minor beams.

Floors	Mid-Span Reinforcement (minor beam)						Shear Reinforcement
	Compression Reinforcement (top)			Tension Reinforcement (bottom)			
	$A_{SAP2000}$, mm^2	Area, in^2	Selected bar	$A_{SAP2000}$, mm^2	Area, in^2	Selected bar	#3 stirrups at x mm
1	244.076	0.3783	2#4	557.058	0.8634	2#6	200
2	238.408	0.3695	2#4	546.703	0.8473	2#6	250
3	243.542	0.3775	2#4	547.072	0.8479	2#6	250
4	253.062	0.3922	2#4	567.429	0.8795	2#6	210
5	254.791	0.3949	2#4	571.362	0.8856	2#6	210
6	256.634	0.3978	4#3	572.485	0.8873	3#5	210
7	257.837	0.3996	4#3	574.092	0.8898	3#5	210
8	258.658	0.4009	4#3	575.897	0.8926	3#5	210
9	258.696	0.4010	4#3	577.86	0.8956	3#5	210
10	257.669	0.3994	4#3	580.688	0.9000	3#5	210
11	257.837	0.3996	4#3	581.413	0.9011	3#5	210
12	257.801	0.3996	4#3	584.224	0.9055	3#5	210

Table 3.50. Right end reinforcement for minor beams.

Floors	Right End Reinforcement (minor beam)						Shear Reinforcement
	Compression Reinforcement (bottom)			Tension Reinforcement (top)			
	$A_{SAP2000}$, mm^2	Area, in^2	Selected bar	$A_{SAP2000}$, mm^2	Area, in^2	Selected bar	#3 stirrups at x mm
1	748.217	1.1597	3#6	491.602	0.7619	4#4	110
2	705.695	1.0938	3#6	464.061	0.7193	4#4	120
3	689.094	1.0680	3#6	453.295	0.7026	4#4	150
4	706.396	1.0948	3#6	464.515	0.7200	4#4	110
5	703.476	1.0903	3#6	462.622	0.7170	4#4	110
6	696.004	1.0787	3#6	457.777	0.7095	4#4	110
7	689.791	1.0691	3#6	453.747	0.7033	4#4	110
8	684.469	1.0609	3#6	450.295	0.6979	4#4	110
9	681.349	1.0560	2#7	448.27	0.6948	4#4	110
10	680.223	1.0543	2#7	447.539	0.6936	4#4	110
11	678.593	1.0518	2#7	446.481	0.6920	4#4	110
12	674.405	1.0453	2#7	443.763	0.6878	4#4	110

3.6.7.6.2. Development length

The Development lengths of bars followed computations based on the ACI 318-19 standards. The dimensions of #8 and #9 bars measure db as 1 inch and db as 1.128 inches respectively. The calculation of bar development length in tension depended on the following mathematical formula:

$$l_d = \frac{f_y \psi_t \psi_e \psi_g}{20\lambda\sqrt{f'_c}} d_b \text{ for bars \#7 and larger} \quad (3.46)$$

Reinforcement in Tension:

$$l_{dt} = \frac{f_y \psi_t \psi_e \psi_g}{20\lambda\sqrt{f'_c}} d_b = 44.4\ in\ or\ 1000.5\ mm > 800\ mm(column\ width)$$

→ need to be hooked bars

Accordingly, the developed formula is given:

$$\text{Modified } l_{dh} = \frac{f_y \psi_e \psi_r \psi_o \psi_c}{55\lambda\sqrt{f'_c}} d_b^{1.5} = 358.98 \text{ mm}$$

For the Hook parameters D and r were calculated as follows:

$D = 6d_b = 6\ in\ (152.4\ mm),\ r = D/2 = 3\ in\ (76.2\ mm)$

$12d_b = 12\ in\ (304.8\ mm)$

Reinforcement in Compression:

$$l_{dc} = \left(\frac{f_y \psi_r}{50\lambda\sqrt{f'_c}}\right) d_b = 15.76\ in\ or\ 400.2\ mm \leq 0.0003 f_y \psi_r d_b$$

Since l_{dc} less $0.0003 f_y \psi_r d_b$, use $18\ inch\ or\ 450\ mm$

3.6.7.6.3. Lap splices

The lap splices were also calculated for the beams and columns. For the beam in tension:

$$l_{st} = l_{dh} = \frac{f_y \psi_e \psi_r \psi_o \psi_c}{55\lambda\sqrt{f'_c}} d_b^{1.5} = 358.98\ mm$$

For beam in compression:

$$l_{sc} = 0.0005 f_y d_b = 30\ in\ or\ 762\ mm$$

For column:

$$l_{sc} = 0.0005 f_y d_b = 26.25\ in\ or\ 667\ mm$$

Table 3.51. Lap splices for columns.

Component	Lap splice, mm
Column 0-2 floors (800 x 800 mm)	1059
Column 3-4 floors (750 x 750 mm)	922
Column 5-6 floors (700 x 700 mm)	841
Column 7-8 floors (650 x 650 mm)	841
Column 9-10 (600 x 600 mm)	841
Column 11-13 (550 x 550 mm)	762

3.6.7.7. Special seismic provisions for reinforcement detailing

3.6.7.7.1. Beams

The high seismicity region of the building demands proper attention to seismic detailing. By fulfilling the specified criteria in ACI 318-19 code the clear span together with the width-to-depth ratio achieves compliance. The beams should receive two continuous longitudinal bars at both their upper and lower sections according to ACI. The strength at joint faces derives from the positive moment which exceeds fifty percent of the negative reaction. Transverse reinforcement had to

extend over twice the member depth beginning from the support face and should not exceed d/4, 6db, and 150mm. The first hoop reinforcement received a placement at 50 mm from the primary support position.

3.6.7.7.2. Columns

The seismic aspects concerning columns followed the specifications. The included area for column reinforcement spans from 1% to 6%. The reinforcement crossed the joint's face at distance l_0 from both its sides. Design calculations used the column span to determine l_0 value at one-sixth measurement which yielded 400 millimeters.

3.6.7.7.3. Joints

Beams received their longitudinal reinforcing elements by extending them up to reach the column's far side at the intersections points. The column depth exceeded h>20 db at joints which the longitudinal steel bar crossed through.

$$l_{\text{dh}} \geq \begin{cases} \dfrac{f_y d_b}{65\lambda\sqrt{f_c'}} \\ 8d_b \\ 6 \text{ in.} \end{cases} \tag{3.47}$$

3.6.7.8. Structural serviceability design

3.6.7.8.1. Deflection

The members should undergo deflection testing before determining the serviceability of the building. The structure codes supply tables containing minimal specifications for structural shape thicknesses. The deflection can be ignored if member sizes surpass the minimum requirements of thickness. The required minimum thickness for this beam member with fy = 60000 psi (413.7 MPa) should be calculated through the below mathematical expression.

$$h_b = \frac{L}{21} \tag{3.48}$$

Where L is the span length. For our building, the minimum thickness of the beam is:

$$h_b = \frac{6000}{21} = 286\ mm < 300\ mm \text{ (depth of minor beam)}$$

Deflection calculations can be ignored because the selected members are larger than the minimum beam thickness requirement.

3.6.7.8.2. Crack width

The reinforced concrete design requires effective crack control because it maintains structural safety when subjected to loads. The permit and protection of structures depend on both checking crack widths along with the validation of permissible code-defined limits. The calculation of flexural crack maximum widths follows the below stated equation.

$$w = 0.076\beta_h f_s \sqrt[3]{d_c A} \tag{3.49}$$

w is the estimated crack width (in).

β_h is the ratio of the distance to the neutral axis from the extreme tension concrete face to the distance from the center of the reinforcement.

f_s is the steel stress.

d_c is the cover and A is the effective tension area.

$$d_c = 2.5\ in$$

$$A = \frac{(5\ in)(19.8\ in)}{6} = 15.4\ in^2$$

$$w = 0.076 \cdot 1.2 \cdot (2/3) \cdot 60000 \cdot \sqrt[3]{2.5 \cdot 15.4} = 0.0123\ in$$

The allowable crack width for this building is 0.015 in, where the estimated crack width does not exceed the limit. Therefore, the crack width is satisfactory.

The maximum longitude reinforcing bar spacing can be determined by this specific formula:

$$s = [15(\frac{40}{f_s}) - 2.5C_c] \tag{3.50}$$

$$s = 15(\frac{40}{(2/3)60} - 2.5 \cdot 2.5) = 8.75\ in\ or\ 222.25\ mm$$

Finally, the spacing between longitudinal reinforcement shall be limited to 222.25 mm.

4. Geotechnical Design

4.1. Site characterization

As previously mentioned, the location of residential building is proposed at 6435 Wilshire Boulevard, Los Angeles, California, that is near to the intersection of San Vicente Blvd and Wilshire Blvd, which are one of the main streets in Los Angeles. The site is currently occupied by a 5-story office building and associated exterior 2-level parking structure. The surface elevation of the site is 54 meters above sea level. The geotechnical investigation report proposed a mixed-use residential building 6435 Wilshire Blvd, that was published by Irvine Geotechnical company in 2021 will be used as a main input value for the geotechnical part.

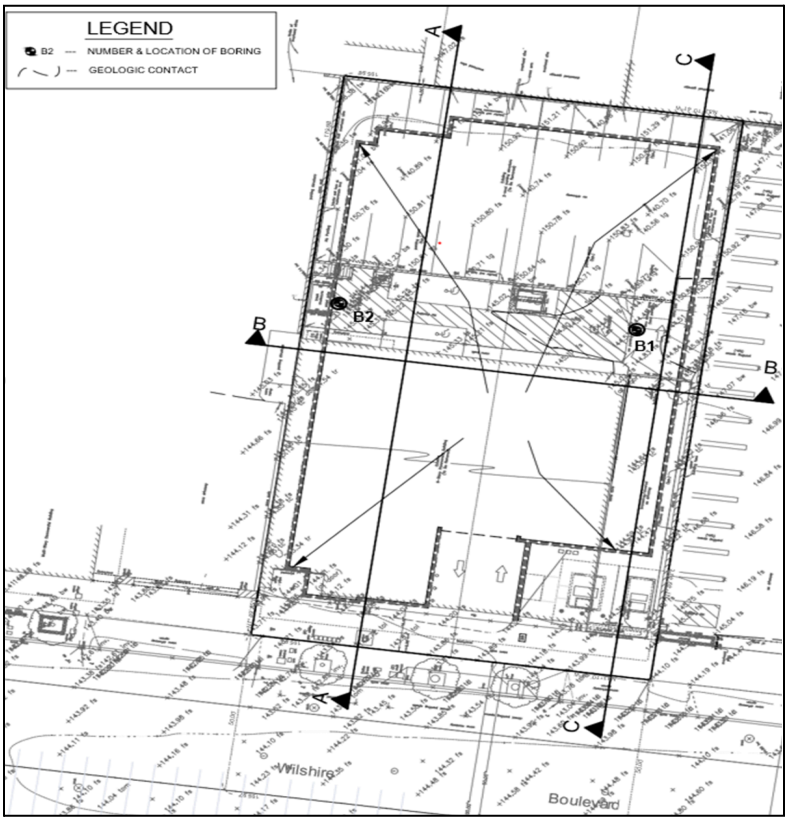

Figure 4.1. Locations of boreholes on the site

The investigation report included 2 boreholes (B-1 and B-2) that were located underneath the building. The location of the boreholes is in the corners of the site along Wilshire Blvd, the distance between the boreholes is 30 m. The geotechnical investigation was conducted using a limited access hollow auger drilling rig, the maximum depth of both borings is 100 feet (30.48 meters). The table provides soil profile data from the borehole B-1. All the soils are classified in

concordance with USCS (Unified Soil Classification System). The standard penetration test (SPT) samples have been retained in special air-tight bags in accordance with ASTMD1586-11.

4.1.1. Shear Wave Velocity

Since the site is in seismically active territory, it is highly significant to take into consideration the dynamic properties of the soil. Therefore, the shear wave velocity will be taken into account. From the geophysical study on the site conducted by GeoDesign company, it was investigated that the average value of the shear wave velocity of the upper 100 feet (30.48 meters) of soils, $V_{s(100)}$ is 923 ft/sec. The graph represents the shear wave velocities and corresponding depths of the soil profile.

Table 4.1. Shear Wave Velocity

Depth (feet)	Shear Wave Velocity, $V_{s(30)}$	
	(feet/sec)	(meters/sec)
0	620.6	189.2
10	620.6	189.2
10	950.6	285.8
17.5	950.6	285.8
17.5	900.6	271.5
22.5	900.6	271.5
22.5	890.7	267.8
32.5	890.7	267.8
32.5	1150.6	320.2
42.5	150.6	320.2
42.5	1230.5	375.1
67.5	1230.5	375.1
67.5	1190.8	362.9
77.5	1190.8	362.9
77.5	1142.6	348.3

100	1142.6	348.3

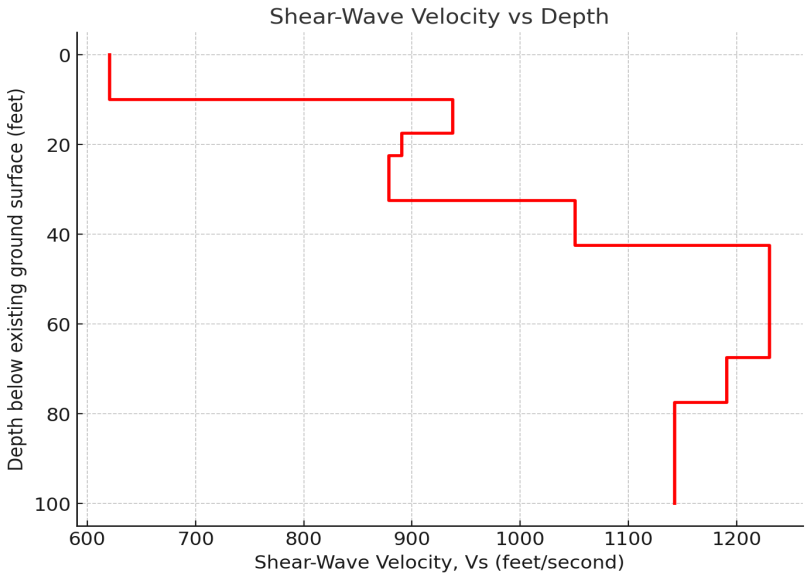

Figure 4.2. Shear Wave Velocity vs. Depth graph

From the Figure 32 is seen that the average shear wave velocity $V_{s(30)}$ is 332.6 m/sec. According to ASCE 7-16 (Table 20.3-1), the $V_{s(30)}$ range for site class D is 180-360 m/sec. Therefore, the Site Class is D - Stiff Soil. The Seismic Design Category is D and the Risk Category II.

For concluding the soil profile part, the physical parameters of the soil, which are elastic modulus, poisson's ratio should be calculated using the SPT results. Furthermore, the friction angle, unit weight, and effective stress were calculated.

4.1.2. Soil profile

Firstly, the N-values from SPT were obtained and adjusted for the field conditions, considering corrections for borehole diameter, rod length, hammer type and sampler, as represented in the equation below:

$$N_{60} = \frac{N\eta_H\eta_B\eta_S\eta_R}{60} \quad (4.1)$$

Where,

N_{60} is a corrected standard penetration number for the field conditions;

η_H is a hammer efficiency;

η_B is a borehole diameter correction;

η_S is a sampler correction;

η_R is a rod length correction;

According to the geotechnical investigation, the hammer efficiency depends on the type of hammer. During the test automatic trip hammer (ATH) was used, the average percentage of hammer efficiency for ATH is 80% (Biringen, 2008). According to ASTM D6066 the values η_B, η_S, η_R equals to 1, 1, 0.75, respectively.

The value of N_{60} can be changed due to effective overburden pressure, therefore N_{60} can be corrected to a standard atmospheric pressure value:

$$(N_{60})_1 = C_N N_{60} \quad (4.2)$$

Where,

C_N, the correction factor is calculated using different relationships:

Table 4.2. Correction Factor Relationships

Liao and Whitman (1986)	Seed et al. (1975)	Peck et al. (1974)
$(C_N)_1 = [\frac{1}{(\frac{\sigma_0'}{p_a})}]^{0.5}$	$(C_N)_2 = 1 - 1.25log(\frac{\sigma_0'}{p_a})$	$(C_N)_3 = 0.77log[\frac{20}{(\frac{\sigma_0'}{p_a})}]$ $\frac{\sigma_0'}{p_a} \geq 0.25$

For cohesionless soil, the unit weight was calculated using the formula below:

$$\gamma = 16 + 0.1 \times N_{60}$$

Formula for calculating the effective overburden pressure:

$$\sigma_0' = \gamma \times H$$

Where, $p_a = 101.33\ kN/m^2$;

The C_N, correction factor is taken as the averaged value of the following three different formulas. Following N_{60} value is calculated. The table below represents the Standard Penetration Test results and calculated corrected values.

Table 4.3. Corrected Values of SPT Results

Sample Depth, m	Soil Type	N	N_{60}	σ_0', kN/m^2	$(C_N)_1$	$(C_N)_2$	$(C_N)_3$	C_N (ave)	$(N_{60})_1$
1.5	Sandy Clay (CL)	35	37	29.55	1.85	1.67	1.41	1.64	61
3.0	Silty Clay (CL)	19	20	54.06	1.37	1.34	1.21	1.31	26
4.6	Sand (SP)	35	37	90.71	1.06	1.06	1.04	1.05	39
5.2	Silty Sand (SM)	14	15	90.94	1.05	0.96	1.04	1.05	16
6.1	Silty Sand (SM)	20	21	110.56	0.96	0.87	0.97	0.96	20
7.6	Clayey Sand with Gravel (SC)	16	17	134.52	0.87	0.85	0.91	0.87	15
10.7	Clayey Sand with Gravel (SC)	28	29	203.03	0.71	0.62	0.77	0.69	21
12.2	Silty Sand (SM)	26	27	228.90	0.67	0.56	0.73	0.65	18
15.2	Silty Clay (CL)	15	16	267.43	0.62	0.47	0.68	0.59	9
18.3	Sandy Clay (CL)	11	12	314.19	0.57	0.39	0.62	0.52	6
21.3	Silty Clay (CL)	19	20	383.79	0.51	0.28	0.56	0.45	9
23.5	Silty Sand (SM)	69	73	548.28	0.43	0.08	0.44	0.32	23
27.4	Silty Sand (SM)	54	57	595.61	0.41	0.03	0.41	0.29	16
30.5	Gravelly Sand (GW)	81	86	750.49	0.37	0.01	0.33	0.20	18

The elastic modulus is calculated by evaluating the average value of three different E_s values. The methods of Kulhawe and Mayne (1990), Bowles (n.d.), Webb (n.d) will be used for calculating the elastic modulus value.

Table 4.4. Elastic Modulus

Soil Type	E_1, MPa	E_2, MPa	E_3, MPa	E_{ave}, MPa
	Kulhawe and Mayne (1990)	Bowles (n.d.)	Webb (n.d.)	
	$E_S = \alpha(N_{60})_1 p_a$ $\alpha = 5$, sand with fines	$E = 500 \times ((N_{60})_1 + 15)$ $E = 300 \times ((N_{60})_1 + 6)$	$E = 358 \times ((N_{60})_1 + 5)$	
Sandy Clay (CL)				45000.0
Silty Clay (CL)				15000.0
Sand (SP)	19820.1	27060.0	15795	20891.7
Silty Sand (SM)	7919.2	6489.1	7385.7	7264.7
Silty Sand (SM)	10345.1	7925.6	9099.9	9123.5
Clayey Sand with Gravel (SC)	7525.4	6255.9	7107.4	6962.9
Clayey Sand with Gravel (SC)	10543.7	8043.2	9240.2	9275.7
Silty Sand (SM)	9107.9	7193.0	8225.7	8175.6
Silty Clay (CL)				15000.0

Sandy Clay (CL)				50000.0
Silty Clay (CL)				15000.0
Silty Sand (SM)	11768.3	8768.3	10105.5	10214.0
Silty Sand (SM)	8337.3	6736.7	7681.2	7585.1
Gravelly Sand (GW)	8904.4	16287.5	8081.8	11091.2

The method of calculation for friction angle is similar to elastic modulus. Firstly, the friction angle will be calculated using three different formulas, and then the average value will be taken as a final value of φ'.

First formula for friction angle, Wolff (1989):

$$\varphi'_1 = 27.1 + 0.3(N_{60})_1 - 0.00054((N_{60})_1)^2 \quad (4.3)$$

Kulhawy and Mayne (1990):

$$\varphi'_2 = tan^{-1}\left(\frac{N_{60}}{12.2+20.3\left(\frac{\sigma'_0}{p_a}\right)}\right)^{0.34} \quad (4.4)$$

Hatanaka and Uchida (1996):

$$\varphi'_3 = \sqrt{15.4(N_{60})_1} + 20 \quad (4.5)$$

Table 4.5. Friction angle calculations

Soil Type	φ'_1, °	φ'_2, °	φ'_3, °	φ'_{ave}, °
Sandy Clay (CL)	43.43	62.36	50.67	52.16
Silty Clay (CL)	34.64	54.29	40.16	43.03
Sand (SP)	38.01	55.50	44.54	46.02

Silty Sand (SM)	31.66	44.47	35.51	37.21
Silty Sand (SM)	33.00	46.36	37.73	39.03
Clayey Sand with Gravel (SC)	31.44	40.58	35.12	35.71
Clayey Sand with Gravel (SC)	33.11	41.05	37.90	37.35
Silty Sand (SM)	32.32	38.06	36.64	35.67
Silty Clay (CL)	29.87	29.48	32.02	30.46
Sandy Clay (CL)	28.92	24.44	29.77	27.69
Silty Clay (CL)	29.78	26.31	31.82	29.30
Silty Sand (SM)	33.78	32.46	38.91	35.05
Silty Sand (SM)	31.89	28.21	35.92	32.01
Gravelly Sand (GW)	32.21	26.86	36.45	31.84

The Poisson's ratio is calculated by using the formula below, according to Das and Sivakugan (2019):

$$\mu_s = 0.1 + 0.3\left(\frac{\varphi' - 25}{20}\right) \quad (4.6)$$

The cohesion values are not provided in the geotechnical investigation report. Therefore, SPT results can be used for estimating the soil cohesion, especially in cohesive soils like clays. In order to get more precise cohesion values, the second method will be also used - correlation from direct shear test.

According to the report, by performing the drained direct shear test in accordance with ASTM D3080/D3080M-11, the peak and ultimate cohesion value were evaluated.

Where,

Peak Cohesion = $41.14\ kN/m^2$.

Ultimate Cohesion = $11.97\ kN/m^2$.

For non-cohesive soil, such as sand, gravels, the cohesion value is taken as 0.

For estimating the cohesion of cohesive soils using SPT N_{60} values, the empirical correlation was used:

$$c' = \frac{N_{60}}{k} \quad (4.7)$$

Where,

k is a empirical correlation factor (range: 10-15)

The table below provides the cohesion values calculated by both methods, and the average value would be taken as a final soil cohesion.

Table 4.6. Cohesion calculations

Soil Type	c_1', kN/m^2	c_2', kN/m^2	c_{ave}', kN/m^2
	From SPT	From Direct Shear Test	
Sandy Clay (CL)	38.6	41.14	39.87
Silty Clay (CL)	9.7	11.97	10.84
Sand (SP)	0	0	0
Silty Sand (SM)	0	0	0
Silty Sand (SM)	0	0	0
Clayey Sand with Gravel (SC)	0	0	0
Clayey Sand with Gravel (SC)	0	0	0
Silty Sand (SM)	0	0	0
Silty Clay (CL)	22.6	11.97	19.29
Sandy Clay (CL)	49.5	41.14	45.32
Silty Clay (CL)	3.1	11.97	7.54
Silty Sand (SM)	0	0	0
Silty Sand (SM)	0	0	0

Gravelly Sand (GW)	0	0	0

Table 4.7. Soil profile with characteristics

Depth, m	SPT Blows/ foot	γ, kN/m^3	Moisture (%)	USCS	c', kN/m^2	φ', °	σ'_0, kN/m^2	E, MPa	Description
0-0.61	61	0	17.4	SC	0	52.16	0	45000.0	Sandy Clay - grey brown, moist, firm to stiff
0.61-2.1	26	15.0	27.9	SC	0	43.03	41.23	6962.9	Clayey Sand - moist to wet, dense
2.1-4.0	39	18.9	6.6	CL	10.84	46.02	54.06	15000.0	Silty Clay - very moist, porous
4.0-4.8	16	16.6	25.9	SW	10.84	37.21	9 .71	20891.7	Sand (medium to coarse) - moist, dense
4.8-6.0	20	16.2	28.0	SM	0	39.03	90.94	7264.7	Silty Sand (medium to coarse) - moist, medium dense
6.0-7.3	15	15.8	24.7	SM	0	35.71	110.56	9123.5	Silty Sand - slightly moist, medium dense
7.3-10.9	21	18.4	23.4	SC	0	37.35	134.52	6962.9	Clayey Sand with some Gravel - moist, medium dense
10.9-14.9	18	17.5	22.1	SC-SM	0	35.67	203.03	9275.78	Clayey Sand with some Gravel & Silty Sand
14.9-17.9	9	16.4	26.4	CL	19.29	30.46	267.43	15000.0	Silty Clay - moist, very dense
17.9-20.1	6	18.0	24.0	CL	45.32	27.69	314.19	50000.0	Sandy Clay - moist, stiff

20.1-21.6	9	17.2	25.2	CL	45.32	29.30	352.10	50000.0	Sandy Clay - moist, stiff
21.6-22.5	23	16.8	27.1	CL-SW	7.54	35.05	383.79	40000.0	Silty Clay & Medium to coarse Sand
22.5-24.4	16	19.2	21.3	SW	0	33.98	548.28	10214.0	Silty Sand - moist, very dense
24.4-28.3	18	15.5	29.1	SM	0	32.80	595.61	7585.1	Silty Sand - moist, very dense
28.3-29.3	32	18.2	25.6	GW	0	32.01	630.54	50000.0	Sandy Gravel - moist, very dense
29.3-30.5	28	17.0	24.3	SW	0	31.84	750.49	11091.2	Gravelly Sand - moist, very dense

The interior group of piles has 9 piles (3 piles on each side). The diameter of the pile is 450 mm. The corner group of piles has 4 piles with a diameter of 400 mm. Whereas, the exterior group of piles consists of 6 piles with the same diameter of 400 mm. The following figure represents the illustration of the soil profile with the group of piles for the inner columns:

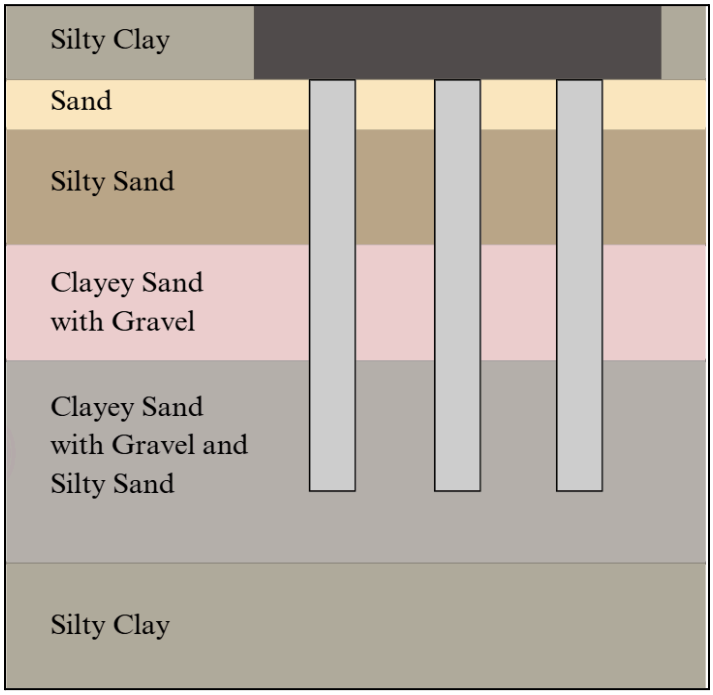

Figure 4.3 Soil Profile Illustration

4.2. Liquefaction and LPI Analysis

Liquefaction is a process, which happens during an earthquake when saturated sediments experience strain reversals repetitively. These reversals lead to a rise in pore water pressure, that in turn, causes an approach of internal pore pressure to overburden pressure. Meanwhile, the shear strength of the soil decreases toward zero. The liquefied soils can lead to the settlement, 3 since it may be subject to excessive strain or flow. Liquefactions affects soil layers below the groundwater table, and particularly include silty sands and loose-dense to medium-dense sands. To prevent possible risks, it is vital to do the analysis of the liquefaction potential. Therefore, to estimate the risks, the Liquefaction Potential Index should be calculated.

According to a geotechnical report, in Boring-1 the depth of the groundwater table is 39.5 feet (13.4 m), and the elevation is 105 feet (32.0 m). In Boring-2 the depth of the groundwater table showed 43 feet, while the elevation is 103 feet. In the area of the site, historically the highest groundwater table equals approximately 18 feet (5.5 m).

Since the soil layers that are higher than the groundwater table have a low moisture content percentage, it can be estimated that the potential liquefaction on the site is moderate. Nevertheless, the LPI (Liquefaction Potential Index) and Liquefaction analysis is provided in the report, the method correlated SPT values. The conducted procedure established by T.L. Youd, et. al. (1996), NCEER-96-0022, SCEC SP117, CGS SP117A, 2008 Guidelines for Evaluating & Mitigating Seismic Hazards & I.M. Idriss & R.W. Boulanger (2008). Overall, included basic analysis of Soil Liquefaction during earthquakes.

The method proposed by Idriss and Boulanger (1971) is correlated with SPT values:

$$(N_{60})_1 = N_m \times C_N \times C_E \times C_B \times C_R \times C_S \quad (4.8)$$

Where,

$(N_{60})_1$ is a corrected N-value of SPT;

N_m is a N-value of SPT;

C_N is a overburden correction factor;

C_E is a energy ratio correction factor (1.30 for auto-hammer);

C_B is a borehole diameter correction factor (1.15 for d=6-8’’);

C_R is a length of rod correction factor (range: 0.75-1.00);

C_S is a samler correction factor (range: 1.00-1.30);

For no sample liner:

$$C_S = 1 + \frac{(N_{60})_1}{100} \quad (4.9)$$

$(N_1)_{60cs}$ value is a normalised blow count of SPT for energy ratio, overburden pressure, and fine content. Mostly, it is adjusted to represent clean sand conditions. The formula below represents the formula of $(N_1)_{60cs}$ value, according to geotechnical report:

$$(N_1)_{60CS} = K_S \times (N_{60})_1 \quad (4.10)$$

Where,

K_S is the fines content correction factor (1 for clean sands);

The values of cyclic stress ratio (CSR) and cyclic resistance ratio (CRR) were taken from the geotechnical report, and represented in the table below. The stress reduction factor, r_d was also provided in the report. The value for MSF (Magnitude Scaling Factor) is 1.5, and the average design magnitude earthquake for our area is 6.36. The procedure by Tokimatsu & Seed, 1987, and modified for spreadsheet by Idriss & Boulanger, 2008.

Horizontal Ground Acceleration = 0.975%;

Analysed Groundwater Depth = 59.06 m;

Average Wet Unit Weight = 18.85 kN/m^3;

Design Magnitude Earthquake = 6.36;

Table 4.8. LPI Calculation by Tokimatsu & Seed (1987)

Depth, m	Soil type	N_{60}	$(N_{60})_1$	$(N_1)_{60CS}$	MSF	r_d	CSR	CRR
1.524 m	Clayey Sand	28.4	47	47	1.5	0.99	0.411	2.000
3.048 m	Silty Clay	15.4	22	22		0.98	0.406	2.000

6.096 m	Silty Clay	26.0	33	44		0.95	0.418	2.000
9.144 m	Clayey Sand	27.3	27	37		0.93	0.488	1.744
12.192 m	Silty Sand	33.8	30	38		0.85	0.494	2.000
15.240 m	Silty Clay	19.5	14	14		0.77	0.478	2.000
18.288 m	Sandy Clay	11.7	8	8		0.69	0.448	1.287
21.336 m	Silty Clay	14.3	9	9		0.60	0.409	2.000
24.384 m	Silty Sand	114.4	80	80		0.52	0.364	2.000
27.432 m	Silty Sand	70.2	46	46		0.44	0.314	2.000
30.480 m	Gravelly Sand	105.3	65	65		0.36	0.261	2.000

The Factor of Safety is calculated using the formula below:

$$FS = \frac{CRR}{CSR} \times MSF \tag{4.11}$$

The LPI was calculated using the formula by Iwasaki et al. (1980) below:

$$LPI = \int_0^{20} F(z) \cdot w(z)dz \tag{4.12}$$

$$F(z) = 1 - F_i \text{, for } F_i < 1.0 \text{;}$$

$$F(z) = 0 \text{, otherwise}$$

$$w_i = 10 - 0.5z$$

Where,

F_i is the factor of safety against liquefaction;

z is the depth from the earth surface;

$w(z)$ is the weight function;

Table 4.9. LPI estimation

Depth, m	Soil type	FC	FS	F_i	LPI
1.524 m	Clayey Sand	0.0	4.87	0	0
3.048 m	Silty Clay	0.0	4.93	0	0
6.096 m	Silty Clay	58.0	4.78	0	0

9.144 m	Clayey Sand	43.9	3.57	0	0
12.192 m	Silty Sand	28.4	4.05	0	0
15.240 m	Silty Clay	0.0	4.18	0	0
18.288 m	Sandy Clay	0.0	2.87	0	0
21.336 m	Silty Clay	0.0	4.89	0	0
24.384 m	Silty Sand	0.0	5.49	0	0
27.432 m	Silty Sand	0.0	6.36	0	0
30.480 m	Gravelly Sand	0.0	7.66	0	0

According to the tables provided above, since the Factor of Safety > 1, and Plasticity Index > 18, the potential for liquefaction is very low.

4.3. Site Response Analysis (SRA)

The site is located in the seismic active region, and as it was mentioned, the site class according to the shear wave velocity is D (stiff soil). The risk category is II, and the seismic design category is D.

The site response analysis was implemented using the Plaxis 2D. For the dynamic multiplier the site related motion data, an accelerogram was used. The data was used from the "Center for Engineering Strong Motion Data" site, Response Spectra Los Angeles La Habra Earthquake. The figure below represents the input data:

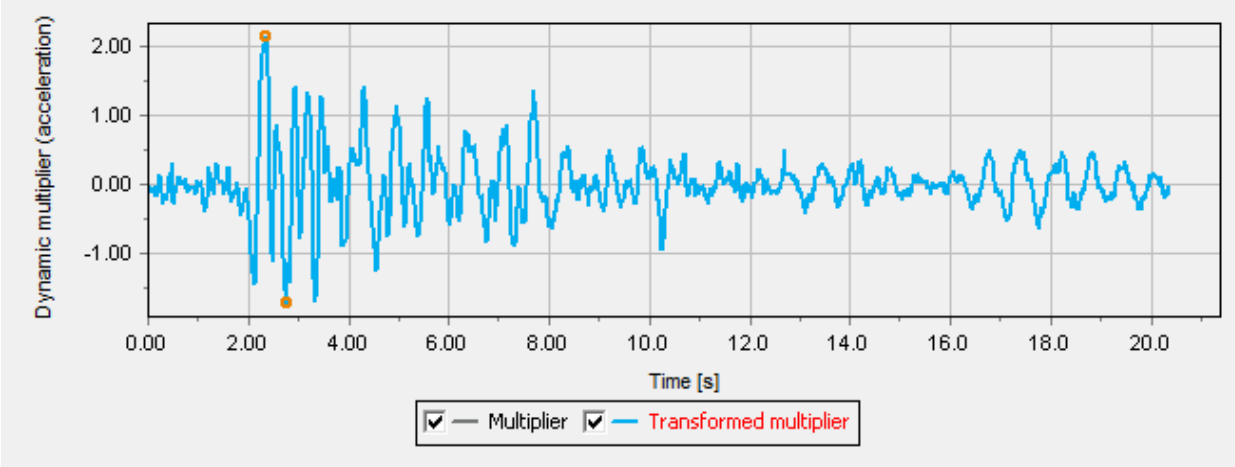

Figure 4.4. Motion data from La Habra earthquake.

After entering the motion data, and assigning the dynamic multiplier the line displacement was set. The displacement was assigned only from x direction (prescribed), whereas the displacement y was fixed:

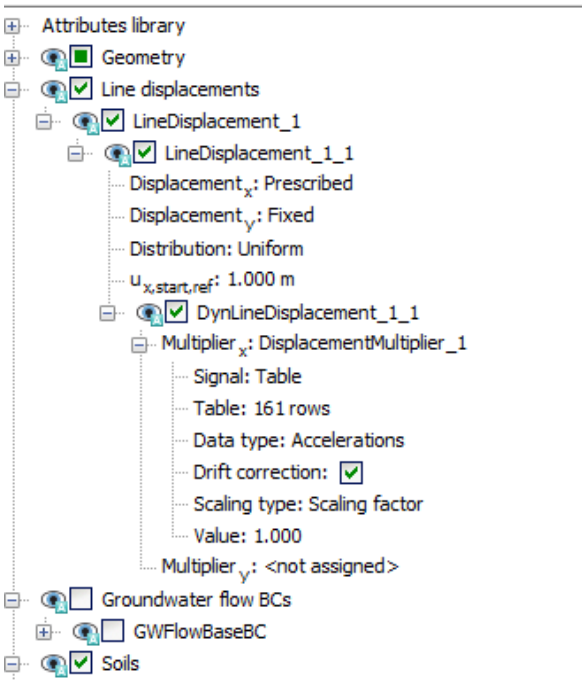

Figure 4.5. Linear displacement set (Plaxis 2D)

The following figure represents the phase stages in plaxis 2D. The calculation type of the second stage was “Dynamic” chosen automatically by program. The dynamic time interval is 20s:

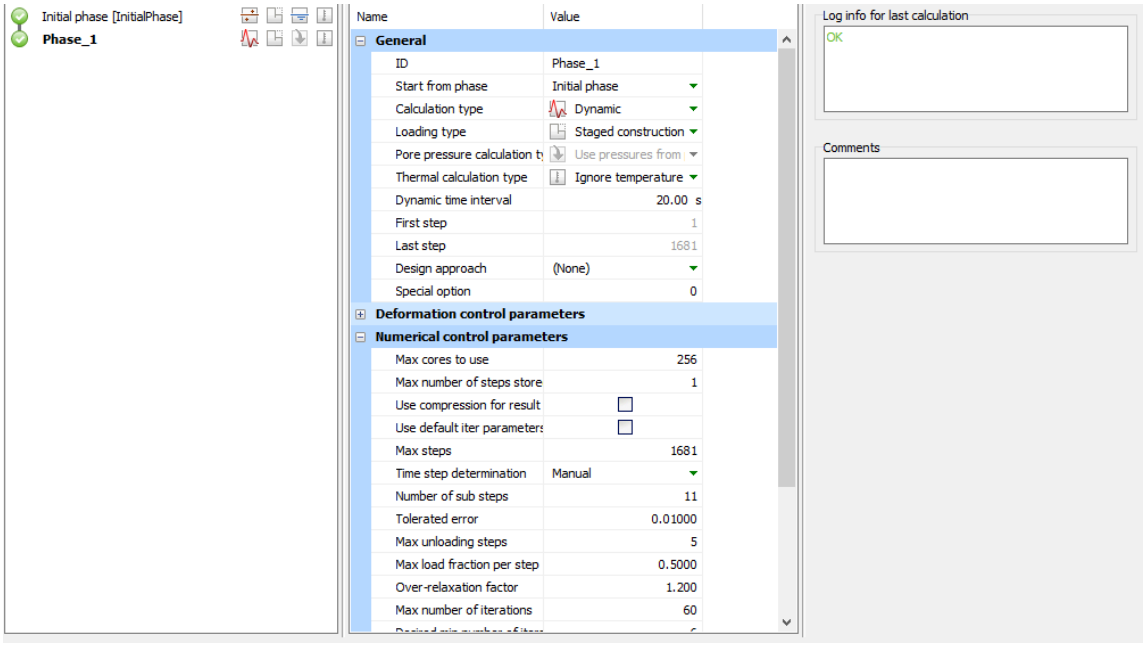

Figure 4.6. Phases of site response analysis in Plaxis 2D.

The figures below represent the results of the site response analysis, which include acceleration chart, fast fourier transformation chart, PSA graph:

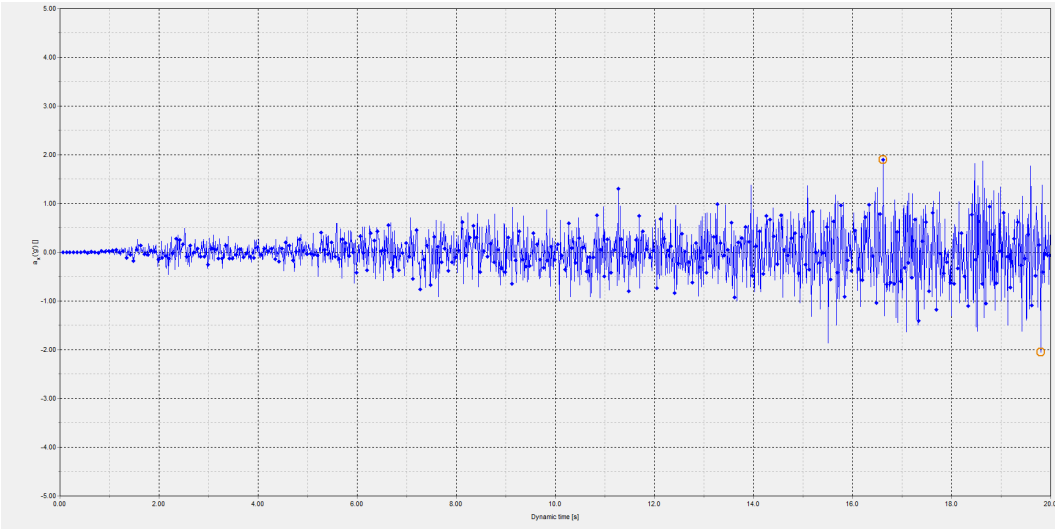

Figure 4.7. Acceleration (x direction) vs time chart.

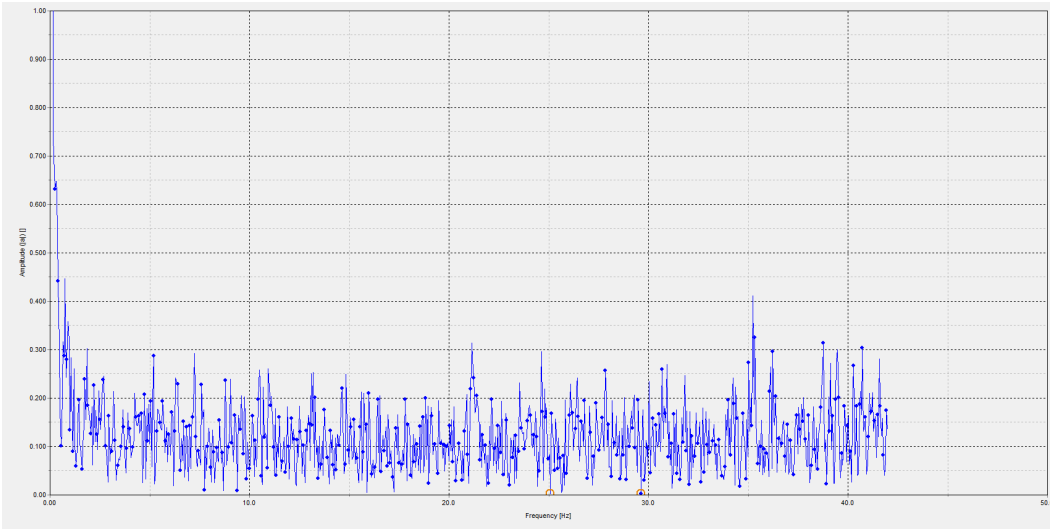

Figure 4.8. Fast fourier transformation chart.

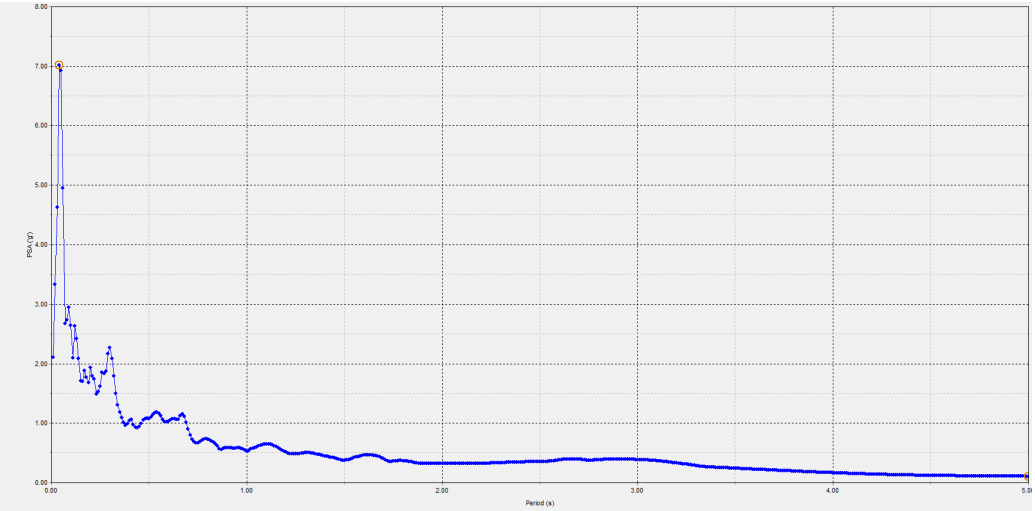

Figure 4.9. PSA vs period graph.

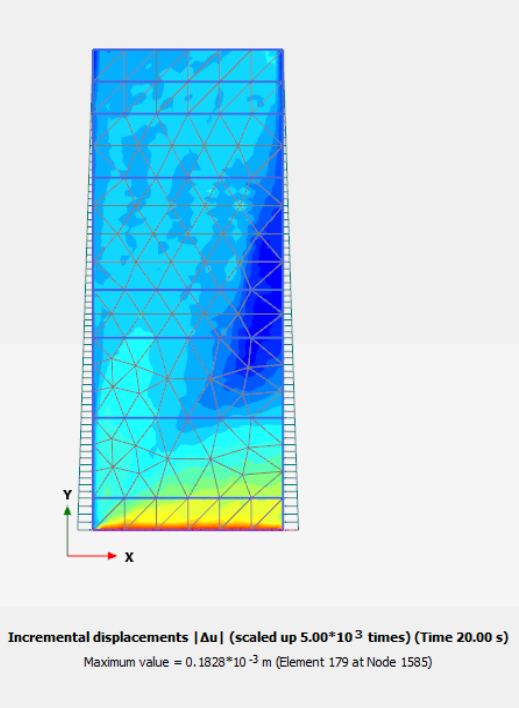

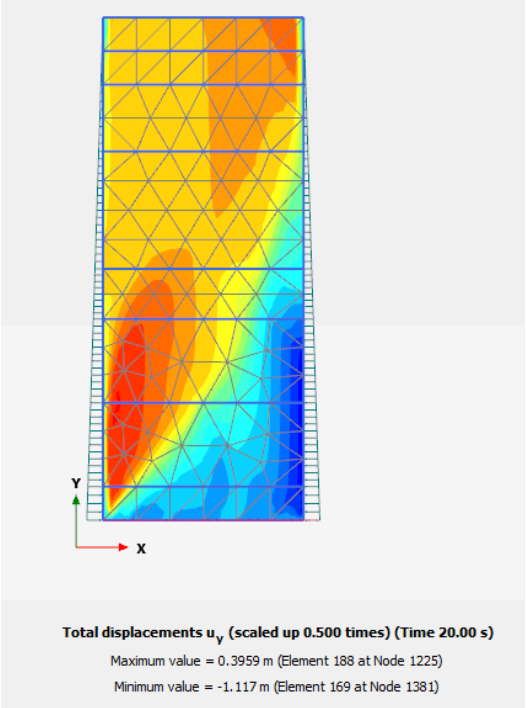

Figure 4.10. Total displacement results.

4.4. Design of the foundation

The foundation design depends on several factors including location, soil profile, design of the building, which determines the most suitable type of foundation for the given conditions. The location of the site determines the soil and seismic considerations. The site is located in LA, which includes both fine and coarse grained soils in the profile and high risk of frequent earthquakes in the area. As it was also mentioned, the project includes 12 storey building with a basement. Moreover, there is a shift from low density soils to denser materials in the soil profile.

Therefore, it was decided to use driven piles in a group. The material for the piles was determined as reinforced concrete, since it is more resistant to corrosion, have high load capacity and perform well in seismic conditions.

Negative skin friction is a critical consideration in pile foundation design, which refers to the downward force exerted on a pile due to the relative settlement of surrounding compressible soils (Das & Sivakugan, 2019). In this case, the upper portion of the soil profile consists of 4 m compressible fill that will be removed during excavation. As this layer will be eliminated, it does not contribute to negative skin friction. Additionally, although another compressible soil stratum exists at a deeper depth, it lies beyond the lateral contact area of the piles and thus does not interact with the pile shaft. As a result, the influence of negative skin friction on the overall axial load-bearing capacity of the piles is deemed minimal and can be reasonably disregarded in design calculations (Das & Sivakugan, 2019).

4.4.1. Shallow foundation

4.4.1.1. Loads Summary

Factored load combination equation in accordance with ASCE-7 is represented below:

$$1.2D + 1.6D + 0.5L_r \quad (4.13)$$

Where,

D, L - Dead and Live load;

L_r - Roof live load;

From the structural part, there are three types of columns (exterior, interior, corner), the following table represents the calculated values of factored load for three types of columns.

Table 4.10. Factored Load for Columns

Geotech unfactored	**Column**	A_t, m^2	$W_u, kN/m^2$	P_u, kN	P_u Whole Area, kN
5,997	Exterior	18	412,18	8509,21	163224
10572,9	Interior	36	368,80	13276,94	238985
3,301	Corner	9	440,74	5056,60	15867
			Critical load for columns	13276,94	238985

4.4.1.2. Pad Foundation

Meyerhof's Bearing Capacity Method is more versatile for varying soil conditions. Moreover, this method considers the shape, depth, and load inclination on the foundation.

For shallow foundation the factor of safety, FS is 3.

The ultimate allowable bearing capacity is evaluated by following formula:

$$q_{all} = \frac{q_u}{FS} \tag{4.14}$$

According to Meyerhof's method the formula for ultimate bearing capacity, q_u is:

$$q_u = c' N_c F_{cs} F_{cd} F_{ci} + qN_q F_{qs} F_{qd} F_{qi} + \frac{1}{2}\gamma B N_\gamma F_{\gamma s} F_{\gamma d} F_{\gamma i} \tag{4.15}$$

Where,

c' - cohesion;

q - effective stress at the bottom of the foundation;

γ - unit weight of soil;

B - width of the foundation;

F_{cs}, F_{qs}, $F_{\gamma s}$ - shape factors;

F_{cd}, F_{qd}, $F_{\gamma d}$ - depth factors;

$F_{\gamma i}$, $F_{\gamma i}$, $F_{\gamma i}$ - inclination factors;

N_c, N_q, N_γ - bearing capacity factors;

For shallow foundation, the foundation shape is square $B \times L$, where $B = L$.

For square shallow foundation, the shape factors are calculated using the formulas below:

$$F_{cs} = 1 + (\frac{B}{L})(\frac{N_q}{N_c}) \tag{4.16}$$

$$F_{qs} = 1 + (\frac{B}{L})tan\varphi' \tag{4.17}$$

$$F_{\gamma s} = 1 - 0.4(\frac{B}{L}) \tag{4.18}$$

For conditions, $\frac{D_f}{B} > 1$ and $\varphi' > 0$, formulas for the depth factors:

$$F_{qd} = 1 + 2tan\varphi'(1 - sin\varphi')^2 atan(\frac{D_f}{B}) \tag{4.19}$$

$$F_{cd} = F_{qd} - \frac{1-F_{qd}}{N_c tan\varphi'} \tag{4.20}$$

$$F_{\gamma d} = 1$$

Load inclination factors are calculated using the formula below:

$$F_{ci} = F_{qi} = (1 - \frac{\beta}{90^{\circ}})^2 \quad (4.21)$$

$$F_{\gamma i} = (1 - \frac{\beta}{\varphi'})^2 \quad (4.22)$$

The formula for vertical effective stress at the bottom of the foundation:

$$q = \gamma D_f \quad (4.23)$$

The bearing capacity factors:

$$N_c = (N_q - 1)cot\varphi \quad (4.24)$$

$$N_q = tan^2(45 + \frac{\varphi}{2})e^{\pi tan\varphi'} \quad (4.25)$$

$$N_\gamma = 2(N_q + 1)tan\varphi' \quad (4.26)$$

The height of the basement level of the building is 4.0 m, and assumed value of embedded depth, D_f is 2m. According to the soil profile table, the bottom of the shallow foundation is on a silty sand layer.

Values of cohesion, friction angle, embedded depth:

$c' = 0$;

$\varphi' = 39.03^{\circ}$;

Calculated bearing capacity values for shallow foundation:

$$N_q = tan^2(45 + \frac{39.03}{2}) \times e^{\pi tan(39.03)} = 163.799$$

$$N_c = (163.799 - 1) \times cot(39.03) = 200.826$$

$$N_\gamma = 2(163.799 + 1)tan(39.03) = 267.191$$

Calculated values of shape factors for shallow foundation:

$$F_{cs} = 1 + 1 \times \frac{163.799}{200.826} = 1.816$$

$$F_{qs} = 1 + tan(39.03) = 1.811$$

$$F_{\gamma s} = 1 - 0.4 \times 1 = 0.6$$

Equation of depth factor, with unknown value B:

$$F_{qd} = 1 + 2tan(39.03)(1 - sin(39.03))^2 tan^{-1}(\frac{2}{B}) = 1 + 0.22tan^{-1}(\frac{2}{B})$$

$$F_{cd} = 1 + 0.22tan^{-1}(\frac{2}{B}) - \frac{0.22tan^{-1}(\frac{2}{B})}{200.826 \times tan(39.03)}$$

$$F_{\gamma d} = 1$$

All factors of inclination equals to 1, since $\beta = 0$:

$$F_{ci} = F_{qi} = F_{\gamma i} = 1$$

Vertical effective stress for the bottom of the foundation is calculated for silty sand (medium dense) layer:

$$\gamma_{SM} = 20.87\ kN/m^3$$

$$q = 20.87\ kN/m^3 \times 2\ m = 41.74\ kN/m^2$$

The equation of the ultimate bearing capacity for shallow square foundation with unknown B, in particular for exterior and corner foundations:

$$q_u = 0 + 41.74 \cdot 163.799 \cdot 1.811 \cdot (1 + 0.22tan^{-1}(\frac{2}{B})) \cdot 1 + \frac{1}{2} \cdot B \cdot 267.191 \cdot 0.6 \cdot 1 \cdot 1$$

$$q_u = 12381.75 + 2723.99tan^{-1}(\frac{2}{B}) + 80.16B$$

For square foundation:

$$q_{load} = \frac{Q}{B^2} \quad (4.27)$$

$$q_{all} = \frac{q_u}{FS} \quad (4.28)$$

The design must meet following condition:

$$q_{load} = q_{all} \quad (4.27)$$

$$\frac{Q}{B^2} = \frac{q_u}{FS} \quad (4.28)$$

The critical value for total load was taken from the interior column, thus the $Q_{load} = 13276.94\ kN$.

$$\frac{12381.75 + 2723.99 \cdot tan^{-1}(\frac{2}{B}) + 80.16B}{3} = \frac{13276.94}{B^2}$$

The calculated foundation length is B=1.66 metres. Although, in accordance with the Building Code in Los Angeles the width of the column satisfies the requirement (B=1.89 m >

472.5 mm), the shallow pad foundation is not suitable for constructing high-rise buildings. This type of foundation has a risk of failure of resistance of dynamic as well as vertical loadings. Therefore, the shallow pad foundation is not suitable for the proposed high-rise residential building.

Table 4.11. Dimensions and Bearing Capacity Results of Pad Foundation

	Interior Column	Exterior Column	Corner Column
B, m	**1.66**	**1.32**	**1.02**
Q_{load}, kN	13276.94	8509.21	5056.60
q_u, kN/m^2	15457.67	15177.29	14906.56
FS	3	3	3
q_{all}, kN/m^2	5152.56	5059.09	4968.85
q_{load}, kN/m^2	4945.56	5085.03	5197.59

The calculated values of the bearing capacity of pad foundation satisfies the requirements. However, there is a possibility that the shallow foundations will not be able to resist dynamic loading. Furthermore, it is not sufficient for horizontal loading. Therefore, these foundations are rarely used for high-rise structure support and construction and are not typically used for residential building design.

4.4.1.3. Mat Foundation

The geotechnical report suggests to use the mat (also known as raft) foundation, since the load can be distributed evenly, however, the suggestion was provided for the construction of an 8-storey building. Since we are designing for a 12-storey building, we would need to calculate the bearing capacity. According to Das & Sivakugan (2018), the mat foundation is usually applied for soils with lower bearing capacity, such as silts and clays, which corresponds to our case. Given that the largest and critical load was calculated to be 13627.97 kN, the load on each of the partial areas divided by 36 internal columns would be 378.55 kN/m^2. For the calculation of bearing capacity, we assume that the embedded depth is 1 m and the foundation lays on the silty sand layer.

The values used to calculate the bearing capacity are:

$c' = 0\ kN/m^2$

$\gamma = 15.80\ kN/m^3$

$\varphi' = 39.03°$

$B = L = 42\ m$

We also calculated bearing capacity factors:

$$N_q = tan^2(45 + \frac{39.03}{2})e^{\pi tan(39.03)} = 56.2$$

$$N_c = \frac{56.2-1}{tan(39.03)} = 68.1$$

$$N_\gamma = 2(56.2 + 1)tan(39.03) = 72.7$$

Shape factors:

$$F_{cs} = 1 + 1 \cdot (\frac{56.2}{68.1}) = 1.82$$

$$F_{qs} = 1 + \frac{B}{L}tan(39.03) = 1.81$$

$$F_{\gamma s} = 1 - 0.4\frac{B}{L} = 0.6$$

Depth factors:

$$F_{cd} = 1 + 0.4 \cdot \frac{1}{42} = 1.01$$

$$F_{qd} = 1 + 2tan(39.03)(1 - sin(39.03))^2\frac{1}{42} = 1.005$$

$$F_{\gamma d} = 1$$

Inclinations factors:

Since the load is purely vertical, $\beta = 0$, which means

$$F_{ci} = F_{qi} = F_{\gamma i} = 1$$

$$q_u = qN_qF_{qs}F_{qd}F_{qi} + \frac{1}{2}\gamma BN_\gamma F_{\gamma s}F_{\gamma d}F_{\gamma i}$$

$q_u = 15.8 \cdot 56.2 \cdot 1.81 \cdot 1.005 \cdot 1 + \frac{1}{2} \cdot 15.8 \cdot 42 \cdot 72.7 \cdot 0.6 \cdot 1 = 16088.36\ kN/m^2$

Using Meyerhof's formula mentioned above, we obtain the ultimate bearing capacity equal to 26510 kN/m^2.

The vertical effective stress is equal:

$$q = 20.87\ kN/m^3 \times 1\ m = 20.87\ kN/m^2$$

The net ultimate capacity:

$$q_{u(net)} = q_u - q = 16067.49\ kN/m^2$$

The allowable bearing capacity can be now calculated:

$$q_{all(net)} = \frac{q_{u(net)}}{FS} = 5355.83\ kN/m^2$$

Although the calculated allowable bearing capacity is meeting the requirement, the settlement should be considered too. Since the mat foundation is located at the sand layers, in accordance with Terzaghi & Peck (1948), the maximum and critical settlement value for mat foundation is 0.05 m.

Net bearing capacity equation considering the settlement:

$$q_{net} = \frac{N_{60}}{0.08} F_d \left(\frac{S_e}{25}\right)$$

Where,

$N_{60} = 20$;

$$F_d = 1 + 0.33\left(\frac{D_f}{B}\right) = 1 + 0.33 * \frac{1}{42} = 1.01$$

$$q_{net} = \frac{20}{0.08} * 1.01 * \frac{50}{25} = 429.25\ kN/m^2$$

The allowable bearing capacity:

$$q_{all(net)} = \frac{q_{(net)}}{FS} = \frac{429.25}{3} = 143.08\ kN/m^2$$

After calculating the net allowable capacity, it is seen that the $q_{all(net)} < q_{load}$. Therefore, the mat foundation will not be considered for a foundation design of our high-rise building.

4.5. Deep Foundation : Pile Foundations

4.5.1. Single Pile

The bearing capacity of a single pile is influenced by many factors, that include the pile geometry, soil properties, installation method etc (Elsamny, 2017). However, one of the main factors influencing the total bearing capacity is the calculated value of bearing capacity at the end of pile and the skin friction. From the practical perspective, the ultimate bearing capacity can be represented by the following equation:

$$Q_u = Q_p + Q_s \quad (4.29)$$

Where,

Q_p - load-carrying capacity of the pile point, kN;

Q_s - skin resistance, kN;

The skin resistance, also known as a frictional resistance can be calculated by soil and pile interface. It will be calculated by implementing α, β, λ methods.

According to the typical dimensions of the concrete circular pipes, the diameter of the pile for high-rise buildings should be 0.61 m. By calculating the area and perimeter of the pipe, the values are $0.2921\ m^2$ and 1.916 m, respectively.

Table 4.12. Single Pile Dimensions

Area, m^2	Perimeter, m	Diameter, m
$\frac{\pi \times D^2}{4}$	$\pi \times D$	
0.2921	1.916	0.61

The material of the single pile foundation is assumed to be reinforced concrete, since it is an acceptable type of material that is used for a construction of high-rise buildings with seismic soil-structures (Sharma, 2020). Furthermore, the D=0.61 m is the typical diameter of the pile foundation of reinforced concrete material.

The bearing capacity of the piles depends on the soil layers, thus on the length of the pile itself. Therefore, both clay and sand layers will be considered as the end of the pile could be

located in either layer. However, the depth of the structure of the building underground including all the elements, such as basement level, slabs, that equals to 3.5 m should be included.

4.5.2. Point-Bearing Capacity

4.5.2.1. Point-Bearing Capacity in Sand Layer

As it was mentioned, the depth of the structure underground should be also considered, therefore the end of the pile with assumed length of 8 m will be located at the depth of 11.5 m. The point-bearing capacity will be calculated by using several methods.

1st Method: Meyerhof's Method for Sand

The formula of Q_p for piles in sand and $c' = 0$:

$$Q_p = A_p q_p = A_p q' N_q^* \leq A_p q_l \tag{4.30}$$

Where, the limiting point resistance, q_l is found by the formula below:

$$q_l = 0.5 p_a N_q^* tan\phi' \tag{4.31}$$

Where,

p_a= 100 kN/m^2 (atmospheric pressure);q'

ϕ' - effective soil friction angle;

The end of the pile will rest in the silty sand layer, from the table 4.5 (Friction angle) the friction angle of the layer is equal to 35.71°. According to the table of interpolated values of N_q^* based on Meyerhof's theory, the N_q^* is equal to 168 for $\phi' = 35.71^\circ$. Considering the values, the limiting point resistance:

$$q' = 1.9 * 18.9 + 0.8 * 16.6 + 1.2 * 16.2 + 1.3 * 15.8 + (10.5 - 7.3) * 18.4$$

$$q' = 148.05\ kN/m^2$$

Calculating for Q_p:

$$Q_p = 0.292\ m^2 * 148.05\ kN/m^2 * 168 = 7262.74\ kN > A_p q_l = 1763.16\ kN$$

$$A_p q_l = 0.292\ m^2 * 0.5 * 100\ kN/m^2 * 168 * tan(35.71^\circ) = 1763.16\ kN$$

The point-bearing capacity for the first method is $Q_p = 1763.16\ kN$.

2nd Method: Vesic's Method

The method proposed by the Vesic (1977) for estimating the point-bearing capacity of the pile is based on the "expansion of cavities" theory. According to the parameters of the effective stress, the formula for Q_p is represented below:

$$Q_p = A_p Q_p = A_p(c'N_c^* + \overline{\sigma_0}'N_\sigma^*) = A_p\overline{\sigma_0}'N_\sigma^* \quad (4.32)$$

The mean effective ground stress at the depth of the pile point is calculated by the following formula:

$$\sigma_0' = (\frac{1+2K_o}{3})q' \quad (4.33)$$

Where,

$K_o = 1 - sin\phi'$ (earth pressure coefficient at rest);

N_c^*, N_σ^* - bearing capacity factors;

According to the Vesic's method, the bearing capacity factor, N_σ^* depends on the reduced rigidity index of the soil that is calculated by the formula below:

$$N_\sigma^* = f(I_{rr}) \quad (4.34)$$

$$I_{rr} = \frac{I_r}{1+I_r\Delta} \quad (4.35)$$

Where,

I_r - rigidity index;

E_s - modulus of elasticity of soil;

μ_s - Poisson's ratio of soil;

Δ - An average value of volumetric strain in the plastic zone that is below the pile point;

$$E_s = m * p_a = 200 * 100 = 20000\,MPa$$

$$\mu_s = 0.1 + 0.3(\frac{\phi'-25}{20}) = 0.1 + 0.3(\frac{35.71^\circ-25^\circ}{20}) = 0.261$$

$$\Delta = 0.005(1 - \frac{\phi'-25}{20})\frac{q'}{p_a} = 0.005(1 - \frac{35.71-25}{20})\frac{148.05}{100} = 0.00232$$

$$I_r = \frac{E_s}{2(1+\mu)*q'*tan(\phi')} = \frac{20000}{2(1+0.261)*148.05*tan(35.71)} = 74.52$$

$$I_{rr} = \frac{I_r}{1+I_r\Delta} = \frac{74.52}{1+74.52*0.00232} = 59.32$$

$$K_o = 1 - sin(35.71) = 0.416$$

$$\sigma_0' = (\frac{1+2K_o}{3})q' == (\frac{1+2*0.416}{3}) * 148.05 = 90.41$$

According to the table of bearing capacity factors proposed by Vesic (1977), and based on the theory of expansion of cavities: $N_c^* = 97.5$ and $N_\sigma^* = 71.9$.

$$Q_p = 0.292\, m^2 * 90.41\, kN/m^2 * 71.9 = 1898.78\, kN$$

3rd Method: Coyle and Costello's Method

According to the analysis proposed by Coyle and Castello (1981), the formula for calculating the point-bearing capacity in sand:

$$Q_p = q'N_q^* A_p \tag{4.36}$$

Where,

N_q^* is a bearing capacity factor obtained from the Variation of N_q^* with L/D graph based on Coyle and Castello (1981);

$$\frac{L}{D} = \frac{7}{0.61} = 11.48$$

For $\phi' = 35.71^\circ$ and L/D = 11.48, the N_q^* The value from the graph is 55. Therefore, the point-bearing capacity:

$$Q_p = 0.292\, m^2 * 148.05\, kN/m^2 * 55 = 2377.68\, kN$$

4th Method: SPT-based using Meyerhof's formula

The Meyerhof's formula (1976) for ultimate point resistance is given by:

$$q_p = 0.4 p_a N_{60} \frac{L}{D} \leq 4 p_a N_{60} \tag{4.37}$$

Where,

$q_p - ultimate\ point\ resistance;$

$p_a - atmospheric\ pressure;$

$N_{60} - corrected\ N - value\ of\ the\ SPT;$

The N_{60} can be obtained using the pile point about 10D above to 4D below:

$$N_{60} = \frac{37+15+21+17+29+27+16}{7} = 23.14 \approx 23$$

To obtain the bearing capacity factor, both sides of the formula should be multiplied by the area of the pile, resulting in:

$$Q_p = A_p \times 0.4 p_a N_{60} \frac{L}{D} \leq A_p \times 4 p_a N_{60}$$

Which gives the value of the bearing capacity factor as:

$$Q_p = 0.292 \cdot 0.4 \cdot 100 \cdot 23 \cdot \frac{7}{0.610} \leq 0.292 \cdot 4 \cdot 100 \cdot 23$$

$$3101.52\ kN \leq 2702.75\ kN$$

Meaning that the value of the bearing capacity equals 2702.75 kN.

5th Method: SPT-based using Briaud's formula

The formula by Briaud et al. (1985) was stated as:

$$q_p = 19.7 p_a (N_{60})^{0.36} \quad (4.38)$$

Which can also be modified to:

$$Q_p = A_p \times 19.7 p_a (N_{60})^{0.36} = 0.292 \cdot 19.7 \cdot 100 \cdot 25^{0.36} = 1524.9 \approx 1525\ kN$$

The point-bearing capacity of the pile with length 7 m was calculated using five different methods. Using the same procedure, the process was repeated for other piles with different lengths (L=8m, 9m, 10m, 11m) with the same diameter D=0.61m. The following table provides the calculation results:

Table 4.13. Results of the Point-Bearing Capacity in Sand

Length of the Pipe, m	Depth, m	Layer	**Meyerhof's Method**	**Vesic's Method**	**Coyle & Costello's Method**	**SPT based on Meyerhof**	**SPT based on Briaud**
7	10.5	Clayey Sand with Gravel	1763.16	1898.78	2377.68	2702.75	1782.46

8	11.5	Clayey Sand with Gravel	2573.89	2482.68	2955.19	3705.87	1783.29
9	12.5	Silty Sand	1729.13	2013.93	3106.23	3769.83	1798.14
10	13.5	Silty Sand	1729.13	2127.20	3461.28	3703.09	1782.46
11	14.5	Silty Sand	1729.13	2296.51	3826.54	3433.33	1716.24

4.5.2.2. Frictional Resistance in Sand Layer

Method 1: Equation 12.15

According to the equation 12.15 (Das & Sivakugan, 2018), the formula for frictional resistance Q_s in soil layer is:

$$Q_s = \Sigma p \Delta L f = \Sigma p \Delta L K \sigma'_0 tan\delta' \quad (4.39)$$

Where,

p - perimeter of the pile, m;

f - frictional resistance;

K - effective earth pressure coefficient (=1.5);

σ'_0–effective vertical stress at the depth under construction;

δ'–soil-pile friction angle;

ΔL–thickness of the soil layer.

Table 4.14. Skin Friction of Sand Layers

Layer	Depth	Z, m	$\sigma,\ kN/m^2$	f	f_{av}	$Q_{s,sand},\ kN$
Clayey Sand	0.61-2.1	1.49	38.74	39.825	61.512	**175.607**
Sand	4.0-4.8	1.8	28.8	24.709	24.357	**84.003**
Silty Sand	4.8-6.0	1.2	26.4	24.005	23.682	**54.450**
Silty Sand	6.0-7.3	1.3	28.6	23.359	44.257	**1100.235**

Clayey Sand	7.3-10.9	3.6	75.6	65.155	63.409	**437.372**
Clayey Sand	10.9-14.9	3.6	75.6	61.663	63.409	**437.372**

The unit frictional resistance for the pile with the length of 7 metres will be equal to:

$$f = 1.5 \cdot 125.12 \cdot tan(28.57°) = 102.3\, kN/m^2$$

The skin friction of the pile is going to be the sum of skin friction in each sand layer, which will give the value of:

$$Q_s = 120 + 74.7 + 39.6 + 92 + 374 + \frac{102+51.4}{2} \cdot 3.2 \cdot \pi \cdot 0.61 = 1171.325\, kN$$

Method 2: Coyle & Costello's Method

Coyle and Costello (1981) suggested the equation below for the calculation of frictional resistance in sand:

$$Q_s = f_{av} pL = (K\overline{\sigma_0'} tan\delta')pL \quad (4.40)$$

Where,

$\overline{\sigma_0'}$ – average effective overburden pressure;

δ' – soil-pile friction angle ($= 0.8\phi'$)

Method 3: Meyerhof's Method

According to Meyerhof (1976) method, the average unit frictional resistance:

$$f_{av} = 0.002 p_a (\overline{N_{60}}) \quad (4.41)$$

Where,

$\overline{N_{60}}$ - average standard penetration resistance;

Method 4: Briaud'd Method

$$f_{av} = 0.224 p_a (\overline{N_{60}})^{0.29} \quad (4.42)$$

Table 4.15. Frictional Resistance in Sand

Depth	Length of the Pile	Layer	**Eq. 12.15**	**Coyle & Costello**	**Meyerhof**	**Briaud**
7.3-10.5	7m	Clayey Sand with Gravel (SC)	1171.33	408.34	2837.99	34160.98
10.9-11.5	8m	Clayey Sand with Gravel (SC)	1140.51	1125.48	3043.31	34225.05
10.9-12.5	9m	Clayey Sand with Gravel (SC)	1267.12	1970.95	3252.40	34332.56
10.9-13.5	10m	Clayey Sand with Gravel (SC)	1423.03	2980.79	3461.27	34439.32
10.9-14.5	11m	Clayey Sand with Gravel (SC)	1606.30	4278.32	3669.26	34542.87

4.5.2.3. Point-Bearing Capacity in Clay Layer

From the soil profile table, the clay layer starts at a depth of 14.9 m. Therefore, for calculating the point-bearing capacity for the clay layer, the length of the pile will be 12 m, thus the end of the pile will be at the depth of 15.5 m.

1st Method: Meyerhof's Method for Clay

$$Q_p = N_c^* c_u A_p = 9 c_u A_p \quad (4.43)$$

Where,

c_u - undrained cohesion of the soil;

The cohesion of the silty clay layer at the depth of 15.5 m was calculated as $c_u = 19.29\ kN/m^2$.

$$Q_p = 9 c_u A_p = 9 * 19.29 * 0.292 = 50.69\ kN$$

2nd Method: Vesic's Method for Clay

According to the proposed method by Vesic (1977), for $\phi = 0$ condition, the net ultimate point bearing capacity of a pile can be calculated by the following equation:

$$Q_p = A_p q_p = A_p c_u N_c^* \quad (4.44)$$

According to the theory of expansion of cavity:

$$N_c^* = \frac{4}{3}(ln\, I_{rr} + 1) + \frac{\pi}{2} + 1$$

$$I_{rr} = I_r = \frac{E_s}{3c_u}$$

$$I_{rr} = \frac{15000}{3*19.29} = 259.21$$

$$N^*_c = \frac{4}{3}(ln(259.21) + 1) + \frac{\pi}{2} + 1 = 11.31$$

$$Q_p = A_p c_u N^*_c = 0.292 * 19.29 * 11.31 = 63.73\, kN$$

The table below represents the results of the point-bearing capacity of the clay layer by proceeding the same procedure for piles with lengths (L=13m, 14m, 15m, 16m, 17m, 18m). The calculated values by both methods showed quite similar results, therefore the average point-bearing capacity was used.

Table 4.16. Results of the Point-Bearing Capacity in Clay

Length of the Pipe, m	Depth, m	Layer	**Meyerhof's Method**	**Vesic's Method**	$Q_{p,\,ave},\ kN$
12	15.5	Silty Clay	50.69	63.73	31.86
13	16.5	Sandy Clay	119.10	155.90	77.95
14	17.5	Sandy Clay	119.10	155.90	77.95
15	18.5	Sandy Clay	119.10	155.90	77.95
16	19.5	Sandy Clay	119.10	155.90	77.95
17	20.5	Sandy Clay	119.10	155.90	77.95
18	21.5	Silty Clay	53.98	75.20	37.60

4.5.2.4. Frictional Resistance in Clay Layer

The skin resistance of piles were determined using several methods: λ-method, α-method, and β-method.

λ-method

According to the method proposed by Vijayvergiya and Focht (1972), the average frictional resistance can be calculated by using the following equation:

$$f_{av} = \lambda(\overline{\sigma_0'} + 2c_u) \quad (4.45)$$

Where,

$\overline{\sigma_0'}$ - mean effective vertical stress;

c_u - mean undrained shear strength;

Since the value of λ decreases with the pile penetration depth, the total skin resistance can be determined by the following formula:

$$Q_s = pLf_{av} \quad (4.46)$$

The mean effective stress for the length of the entire embedment can be found by summation of the areas from the diagrams of the vertical effective stress, and divided by the total length. Thus, the mean effective stress:

$$\overline{\sigma_0'} = \frac{A_1+A_2+A_3+\ldots}{L} = \frac{c_{u1}L_1+c_{u2}l_2+c_{u3}l_3+\ldots}{L}$$

Since it is a calculation of the frictional resistance of the pile in the clay layer, the length of the pile is 12 m and the basement level 3.5 m. Thus, the L = 15.5 m.

$$\overline{\sigma_0'} = \frac{5.184+19.728+26.637+225.216+257.76+((70+9.84)/2*0.6)}{15.5} = 52.66\ kN/m^2$$

According to the variation of λ graph correlated with pile embedment length, the λ for L=12 m pile is 0.227. Thus, the average unit skin resistance:

$$f_{av} = \lambda(\overline{\sigma_0'} + 2c_u) = 0.227(52.66\ kN/m^2 + 2 * 19.29\ kN/m^2) = 410.79\ kN/m^2$$

$$p = \pi * D = 3.14 * 0.61\ m = 1.916\ m$$

$$Q_{s,\,clay} = 1.916\ m * 12\ m * 410.79\ kN/m^2 = 476.279\ kN/m^2$$

The total frictional resistance of the 12 m pile will equal to the sum of the skin resistance of the clay and sand layers:

$$L = 12\ m: \quad Q_s = Q_{s,\,sand} + Q_{s,\,clay}$$

$$Q_{s,\,sand} = 175.607 + 196.414 + 84.003 + 54.450 + 1110.235 + 437.372 + 437.372 = 2319.846\ kN$$

$$Q_s = 2319.846 + 476.276 = 2796.122\ kN$$

Table 4.17. Frictional resistance in Clay by λ-Method

Length, m	Depth, m	Layer	$\overline{\sigma_0'}$	λ	f_{av}	$Q_{s,\,clay}$	$Q_s,\ kN$
12	15.5	Silty Clay	52.660	0.227	20.711	476.279	**2796.119**
13	16.5	Sandy Clay	37.061	0.218	16.489	410.797	**2730.637**
14	17.5	Sandy Clay	38.911	0.209	16.195	434.507	**2754.347**
15	18.5	Sandy Clay	39.531	0.2	26.034	748.346	**3068.186**
16	19.5	Sandy Clay	39.780	0.195	25.432	779.773	**3099.613**
17	20.5	Sandy Clay	40.014	0.189	24.693	804.457	**3124.297**
18	21.5	Sandy Clay	39.794	0.184	23.999	827.846	**3147.686**

α-method

The α-method is a total stress method, and the frictional resistance is expressed the following way:

$$f = \alpha c_u \tag{4.47}$$

$$Q_s = \sum fp\Delta L = \sum \alpha c_u p\Delta L \tag{4.48}$$

The alpha values were identified using the interpolated alpha values based on the Terzaghi (1996) table. Thus, the alpha values for both clay layers:

$Sandy\ Clay$: $\alpha = 0.71$;

$Silty\ Clay$: $\alpha = 0.920$;

$$Q_s = 0.92 * 19.292 * 2 * \pi * 0.61 * (15.5 - 14.9) = 40.79\ kN/m^2$$

$$Q_{s,\,L=12\,m} = Q_{s,\,sand} + Q_{s,\,clay} = 2319.846 + 40.79 = 2360.64\,kN$$

β-method

According to the β-method, the unit frictional resistance for the single pile can be found the following way:

$$f = \beta\sigma_0' \tag{4.49}$$

$$\beta = K \times tan\phi_R'; \tag{4.50}$$

Where,

ϕ_R' - drained friction angle;

K - earth pressure coefficient;

Thus, the frictional resistance load:

$$Q_s = \sum(1 - sin\phi'_R) * tan\phi'_R\sigma'_o\, p\Delta L$$

$$Q_s = (1 - sin\,(30.46)) * tan(30.46) * 267.43 * 1.92 * (15.5 - 14.9) = 89.16\,kN$$

$$Q_{s,\,L=12\,m} = Q_{s,\,sand} + Q_{s,\,clay} = 2319.846 + 89.16 = 2409.01\,kN$$

The following table demonstrates the results of the frictional resistance by proceeding the same procedure for other dimensions of the piles. The final values of the skin resistance was taken as an average of three methods:

Table 4.18. Frictional Resistance in Clay

Length of the Pile	Depth	Layer	λ *method,* Q_s	α *method,* Q_s	β *method,* Q_s	$Q_{s,\,ave}$
12	15.5	Silty Clay	2796.12	2360.66	2409.01	**2521.93**
13	16.5	Sandy Clay	2730.64	2392.15	2583.60	**2568.80**
14	17.5	Sandy Clay	2754.35	2444.64	2758.19	**2652.39**
15	18.5	Sandy Clay	3068.19	2518.64	2971.45	**2852.76**
16	19.5	Sandy Clay	3099.61	2641.96	3178.06	**2973.21**
17	20.5	Sandy Clay	3124.30	2765.28	3384.67	**3091.42**
18	21.5	Sandy Clay	3147.69	2888.61	3595.42	**3210.57**

After completing all the steps for all dimensions of piles, the critical values of point-bearing capacity and frictional resistance were chosen for comparing the bearing capacities with the column loads that are transferred to the foundation. The following table demonstrate the bearing capacities, where the allowable bearing capacity is calculated by using the formula below:

$$Q_{all} = \frac{Q_u}{FS} \quad (4.51)$$

Where, the factor of safety, FS=3;

Table 4.19. Results of Ultimate and Allowable Bearing Capacities for Single Pile

Length of the Pipe, m	Depth, m	Layer	Q_p, kN	Q_s, kN	Q_u, kN	Q_{all}, kN
7	10.5	Clayey Sand with Gravel	2977.68	1171.325	**4549.005**	**1516.34**
8	11.5	Clayey Sand with Gravel	2955.19	1140.509	**5095.699**	**1698.57**
9	12.5	Silty Sand	3106.23	1267.118	**5373.348**	**1791.12**
10	13.5	Silty Sand	3461.28	1423.032	**5884.312**	**1961.44**
11	14.5	Silty Sand	3826.54	1606.300	**6432.840**	**2144.28**
12	15.5	Silty Clay	31.86	2521.93	**3553.79**	**1184.60**
13	16.5	Sandy Clay	77.95	2568.80	**3646.75**	**1215.58**
14	17.5	Sandy Clay	77.95	2652.39	**3730.34**	**1243.45**
15	18.5	Sandy Clay	77.95	2852.76	**3930.71**	**1310.24**
16	19.5	Sandy Clay	77.95	2973.21	**4051.16**	**1350.39**
17	20.5	Sandy Clay	77.95	3091.42	**4169.37**	**1389.79**
18	21.5	Sandy Clay	37.60	3210.57	**4248.17**	**1416.06**

Table 4.20. Applied Loads on the Foundation

Column	A_t, m^2	W_u, kN/m^2	P_u, kN	P_u Whole Area, kN
Exterior	18	412.18	8509.21	163224
Interior	36	368.80	13276.94	238985
Corner	9	440.74	5056.60	15867

By comparing the loads, it is seen that the allowable bearing capacity loads are lower than the applied loads on the foundation, therefore the single piles will not be used for the design of the foundation of our high-rise building.

4.5.2.5. Negative Skin Friction

According to Das and Sivakugan (2019), the negative skin friction, that is a downward drag force, should be considered under certain conditions:

- Clay fill is placed over granular soil, so the fill consolidates and pulls down on the pile.
- Granular fill is placed over soft clay, so the clay consolidates and pulls down on the pile.
- The settlement cause, due to the water table lowering, increases the stress in clay.

Since our soil profile does not include these conditions along the pile, there is no need in calculating the negative skin friction.

4.5.2.6. Group of Piles

In order to calculate the bearing capacity of the group of piles, the group efficiency should be calculated first. By finding the group efficiency, it will be determined whether the piles may act as a block or as individual piles. It can be determined by simplified analysis for friction piles in sand:

$$\eta = \frac{Q_{g(u)}}{\Sigma Q_u} = \left[\frac{2(n_1+n_2-2)d+4D}{pn_1n_2}\right] \quad (4.52)$$

Where,

p- perimeter of the pile;

n_1, n_2- number of piles;

$Q_{g(u)}$ - ultimate bearing capacity (group pile);

Q_u - ultimate bearing capacity (single pile);

The minimum center-to-center pile spacing: d=2.5D;

If center-to-center pile spacing (d) is large, than $\eta > 1$ (piles act as individual piles). Therefore, the ultimate bearing capacity of the group of piles for both cases:

$$\eta > 1: Q_{g(u)} = \Sigma Q_u \text{ (individual piles)}$$

$$\eta < 1: Q_{g(u)} = \eta \Sigma Q_u \text{ (block of piles)}$$

For the high-rise building, it is recommended to design a pile cap including the seismic condition in Los Angeles city. The dimension of the pile cap can be found using the following equations:

$$\text{Width: } B_g = (n_2 - 1)d + 2(D/2)$$

$$\text{Length: } L_g = (n_1 - 1)d + 2(D/2)$$

According to the structural layouts of the building, the total number of the columns is 64. Therefore, the total number of the group of piles is also 64, however in accordance with the load distribution table, the exterior, interior and corner group of piles will have different dimensions.

The diameter of the corner and exterior piles: D = 0.4 m;

The diameter of the interior pile: P = 0.45 m;

Thus, the minimum spacing, d:

$$d = 0.4 * 2.5 = 1\,m\ (exterior\ and\ corner\ piles)$$

$$d = 0.45 * 2.5 = 1.125\,m\ (interior\ piles)$$

By using these equations, the following table contains the calculated preliminary dimensions of the group cap and the group of piles:

Table 4.21. Preliminary Design of the Group Piles

	Corner Column	**Exterior Column**	**Interior Column**
n_1, (x-axis)	2	3	3
n_2, (y-axis)	2	2	3
Diameter of pile, m	0.4	0.4	0.45

Spacing d, m	1	1	1.125
Width B_g, m	2.4	2.4	3.6
Length L_g, m	2.4	3.6	3.6
Length, m	9	9	9
Perimeter, m	1.26	1.26	1.41
Area, m^2	0.13	0.13	0.16

Each type of column will have a different type of group of piles in accordance to the table above. The figure below represents the preliminary layout of the group of piles and its location.

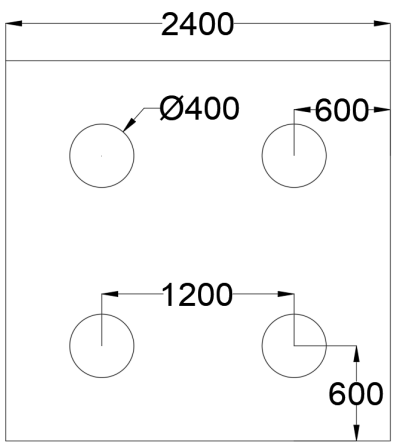

Figure 4.11. Corner Group of Piles

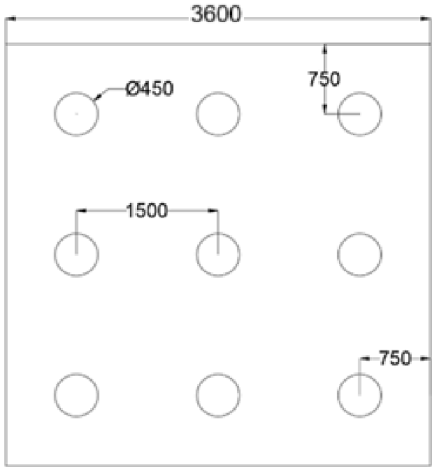

Figure 4.12. Interior Group of Piles

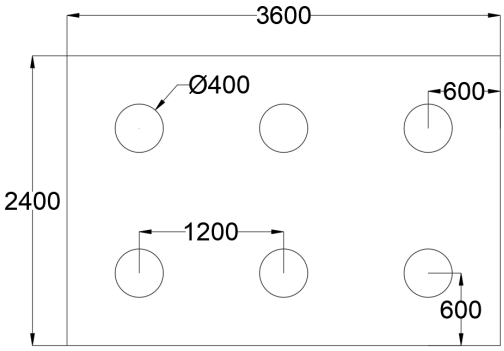

Figure 4.13. Exterior Group of Piles

The point-bearing capacity and the frictional resistance should be calculated for the following dimensions by proceeding the same procedure as the single pile. By choosing the most critical values of the bearing capacity for the group of piles, the point-bearing capacity was calculated by Coyle and Costello (1981) method, and the skin resistance by Meyerhof's (1976).

Table 4.22. Point-Bearing Capacity of Group of Piles

Type of Column	Length, m	Depth, m	L/D	φ', ◦	Nq*	q'	$Q_p,\ kN$
Corner and Exterior	9	12.5	22.5	35.67	50	183.41	**2677.79**
Interior	9	12.5	20.0	35.67	52	183.41	**2784.90**

Table 4.23. Frictional Resistance of Group of Piles

Type of Column	Length, m	N_{60}	$p_a, kN/m^2$	f	$\Delta L,\ m$	p, m	$Q_s,\ kN$
Corner and Exterior	9	23.71	100	4.743	1	1.257	**2270.43**
Interior	9	23.71	100	4.743	1	1.414	**2504.23**

The group efficiency, for each type of pile is calculated next:

$$\eta_{exterior} = [\frac{2(3+2-2)*1+4*0.4}{1.26*3*2}] = 1.01$$

$$\eta_{corner} = [\frac{2(2+2-2)*1+4*0.4}{1.26*2*2}] = 1.11$$

$$\eta_{interior} = [\frac{2(3+3-2)*1.25+4*0.45}{1.57*3*3}] = 0.84$$

The ultimate bearing capacity of the corner group of pile:

$$Q_{u(g)} = \sum(Q_u + Q_s) = 2 * 2 * (2677.79 + 2270.43) = 19792.88\ kN$$

The allowable bearing capacity of the group of piles is calculated by dividing the ultimate bearing capacity to the factor of safety 3:

$$Q_{all(g)} = \frac{Q_{u(g)}}{FS} = \frac{19792.88}{3} = 6597.63\ kN$$

By comparing the number with calculated applied load for the columns, the ultimate bearing capacity of the group of piles is larger, which satisfies the design:

$$Q_{all(g)} = 6597.63\ kN\ > Q_{column} = 5056,60\ kN$$

Table 4.24. Results of the Bearing Capacities of the Group of the Piles

Type of Column	η	$Q_p,\ kN$	$Q_s,\ kN$	$Q_u,\ kN$	$Q_{u(g)},\ kN$	$Q_{all(g)},\ kN$	$Q_{column},\ kN$
Exterior	1.01	2677.79	2270.43	4948.21	29689.28	**9896.43**	**8509.21**
Corner	1.11	2677.79	2270.43	4948.21	19792.85	**6597.62**	**5056.60**
Interior	0.84	2784.90	2504.23	5289.13	47602.16	**15867.39**	**13276.94**

4.6. Design of the foundation: axial loading

4.6.1. Axial bearing capacity : hand calculations

After selecting the proper type of foundation for our building, the hand calculations for the bearing capacities of each pile was calculated in Capstone 1. As it was mentioned, there are three types of group of piles, that differ with dimensions: exterior, interior, corner. The following table represents the loads of the columns presented from the structural parts that transferred to the foundation.

Table 4.25. Column Loads Transferred to Foundation.

Geotech unfactored	**Column**	$A_t,\ m^2$	$W_u, kN/m^2$	$P_u,\ kN$	P_u Whole Area, kN
5,997	Exterior	18	412,18	8509,21	163224
10572,9	Interior	36	368,80	13276,94	238985
3,301	Corner	9	440,74	5056,60	15867
			Critical load for columns	13276,94	238985

According to the given table of the loads acting from the columns, the preliminary design of the group of piles was presented in the previous work. From the preliminary design of the group of piles the minimum spacing between piles was taken as d=1m and d=1.125 m. However, to prevent negative interactions, and excessive settlement, it was decided to increase the spacing.

$$For\ corner\ and\ exterior\colon\ d = 3D = 3 * 0.4 = 1.2$$
$$For\ interior\colon\ d = 3D = 3 * 0.45 = 1.35$$

Generally, increasing the spacing between piles increases the efficiency of the pile group. This is because when piles are placed too close together, their stress zones overlap, reducing their individual load-bearing capacities due to group effects. Thus, the efficiency of each type of pile is $\eta \geq 1$.

As it was mentioned, the bearing capacity of the group piles, $Q_{u(g)}$ depends on the efficiency, which can be calculated using the formulas below:

$$\eta = [\frac{2(n_1+n_2-2)d+4D}{pn_1n_2}]$$

Table 4.26. Efficiency of the Piles.

	Corner Column	Exterior Column	Interior Column
Efficiency, η	1.273	1.167	1.085

Bearing capacity formula:

$$Q_{u(g)} = \eta \sum Q_u = \eta \sum (Q_u + Q_s)$$

Table 4.27. Results of the Bearing Capacities of the Group of the Piles

Type of Column	η	$Q_p,\ kN$	$Q_s,\ kN$	$Q_u,\ kN$	$Q_{u(g)},\ kN$	$Q_{all(g)},\ kN$	$Q_{column},\ kN$
Exterior	1.17	2677.79	2270.43	4948.21	34736.53	**11578.84**	**8509.21**
Corner	1.27	2677.79	2270.43	4948.21	25136.91	**8378.97**	**5056.60**
Interior	1.09	2784.90	2504.23	5289.13	51886.37	**17295.46**	**13276.94**

4.6.2. Hand calculations of settlement

The estimation of total settlement can be done using Vesic's method (1977), by calculating the three components: elastic shortening of the pile ($s_{e(1)}$), settlement of the pile due to the working load at the pile point ($s_{e(2)}$) and the settlement of the pile due to the working load at the pile shaft ($s_{e(2)}$). Therefore, the total elastic settlement of the pile head is given as:

$$s_e = s_{e(1)} + s_{e(2)} + s_{e(3)}$$

Elastic shortening of the pile, $s_{e(1)}$, can be expressed by the following formula:

$$s_{e(1)} = \frac{(Q_{wp} + \xi Q_{ws})L}{A_p E_p} \quad (4.53)$$

Where,

Q_{wp} – working load at the pile point; $= \frac{2677.8}{3} = 892.6\ kN$;

Q_{ws} – working load along the pile shaft, $= \frac{2270.4}{3} = 756.8\ kN$;

A_p – cross-sectional area of the pile point, 0.503 m^2;

L – pile length, = 9 m;

E_p – modulus of elasticity of the pile material; $= 4700\sqrt{27.6} = 24.69\ GPa$;

ξ – constant, 0.67;

The constant ξ is taken as 0.67, since the skin friction increases with depth (Das & Sivakugan, 2019). Thus, the first component is equal:

$$s_{e(1)} = \frac{(892.6 + 0.67 \cdot 756.8)9}{0.503 \cdot 24.69} = 0.001\ m$$

Second component is the magnitude of settlement, $s_{e(2)}$, which is described as:

$$s_{e(2)} = \frac{q_{wp} D}{E_s}(1 - \mu_s^2) I_{wp} \quad (4.54)$$

$$s_{e(2)} = \frac{1774.5 \cdot 0.4}{6962}(1 - 0.285^2)0.85 = 0.0796$$

Where.

q_{wp} – point load per unit area at the pile point; = $\frac{Q_{wp}}{A_p}$;

E_s – modulus of elasticity of soil at/below the pile point;

μ_s – Poisson's ratio of soil for $25° \leq \phi' \leq 45°$; $= 0.1 + 0.3(\frac{\phi'-25}{20})$;

I_{wp} – influence factor; =0.85;

$$\mu_s = 0.1 + 0.3(\frac{37.35-25}{20}) = 0.285$$

Lastly, third component is calculated as:

$$s_{e(3)} = \frac{Q_{ws}D}{pLE_s}(1 - \mu_s^2)I_{ws} \quad (4.55)$$

Where,

p – perimeter of the pile, =1.257 m;

I_{ws} – influence factor;

The influence factor can be calculated as:

$$I_{ws} = 2 + 0.35\sqrt{\frac{L}{D}} = 3.66$$

Therefore:

$$s_{e(3)} = \frac{756.8 \cdot 0.4}{1.257 \cdot 9 \cdot 6962}(1 - 0.285^2)3.66 = 0.003$$

The elastic settlement of the single pile can now be found as a sum of the three components:

$$s_e = s_{e(1)} + s_{e(2)} + s_{e(3)} = 0.001 + 0.095 + 0.003 = 0.099\,m$$

Finally, we can use the following formula to find the elastic settlement of group piles:

$$s_g = \sqrt{\frac{B_g}{D}}s_e;$$

Table 4.28. The values of the settlement for each type of column by Vesic's method (1977)

Type of Piles	$D,\ m$	$B_g,\ m$	$s_e,\ m$	$s_g,\ m$
Corner	0.40	2.4	9.90	22.9
Exterior	0.40	2.4	10.9	24.2

Interior	0.45	4.5	9.90	32.7

Settlement of the group of piles can be calculated by the following formula by Meyerhof:

$$s_{g(e)}(mm) = \frac{0.96q\sqrt{B_g}I}{N_{60}} \quad (4.)$$

Where,

$$q = \frac{Q_g}{L_g B_g};$$

L_g – length of the pile group section, m;

B_g – width of the pile group section, m;

N_{60} – average standard penetration number;

I – influence factor, $= 1 - L/8B_g \geq 0.5$

The calculated values of the settlement for each column is represented in the table below:

Table 4.29. The values of the settlement for each type of column by Meyerhof's method

Type of Column	$L,\ m$	$Q_g,\ kN$	$q,\ kN/m^2$	$L_g,\ m$	$B_g,\ m$	N_{60}	I	$s_g,\ mm$
Corner	9	8378.97	1454.68	2.4	2.4	34	0.53	33.8
Exterior	9	11578.84	1340.14	3.6	2.4	34	0.53	31.1
Interior	9	17295.46	914.016	4.5	4.5	34	0.58	29.8

Table 4.30. Comparison of settlements complicated by software and hand calculations

	Hand calculations		Software calculations	
Type of Piles	Meyerhof	Vesic	Geo 5	Plaxis
Corner	33.8	22.9	22.8	10.5
Exterior	31.1	24.2	25.0	15.6
Interior	29.8	32.7	23.2	21.5

Table 4.31. Comparison of hand calculation and software results

	Exterior		Interior		Corner	
	Geo5	Hand calc	Geo5	Hand calc	Geo5	Hand calc

$Q_{u(g)}$, kN	24024	34736	27909	51886	18653	25136
$Q_{u(s)}$, kN	6107	4948	4580	4948	6616	5289
Q_{all}, kN	-	11579	-	17295	-	8379
FS	3.01	3	3.81	3	3.16	3
s_e, mm	22.8	31.1	23.2	31.4	25	33.8

4.6.3. Analysis of each pile group using Plaxis 3D

The analysis of each pile group was done using Plaxis 3D software. The piles were analysed as embedded beams with Mohr-Coulomb model. The values for the parameters were assumed based on the type of the piles used - reinforced concrete with unit weight of about 25 kN/m^3. Pile caps, basement walls and floors were taken as plate models with respectful values. The following figures represent the total displacement of the soil in the software. The results of the output values are represented in Table … above.

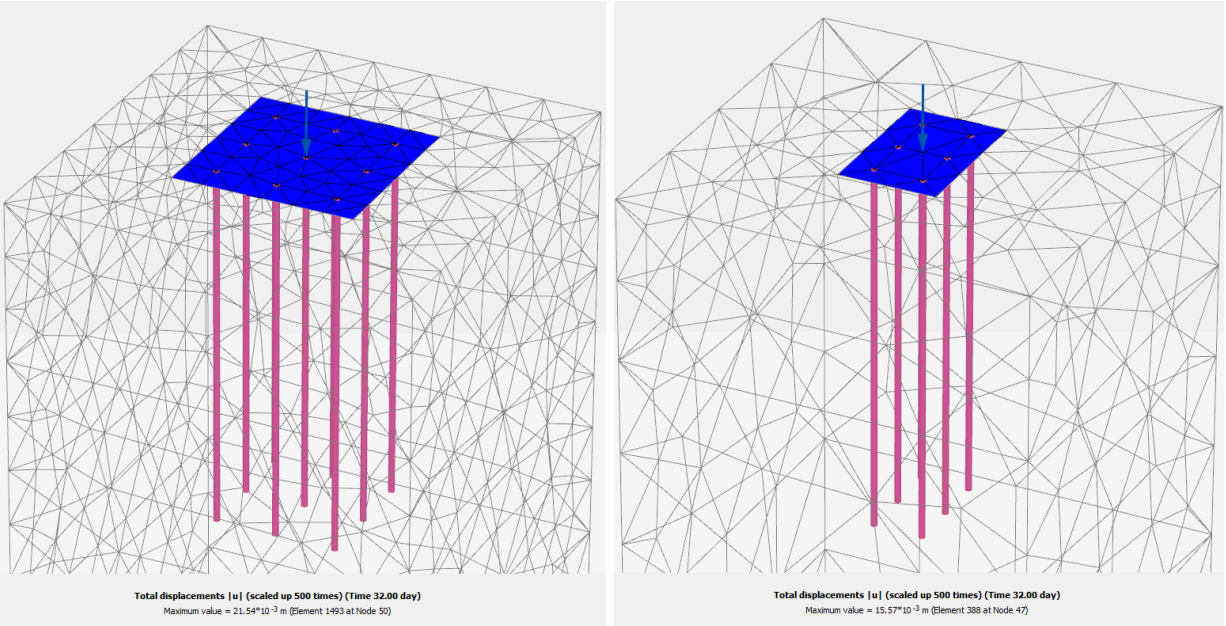

Figure 4.14. Software analysis results of interior (left) and exterior (right) pile groups

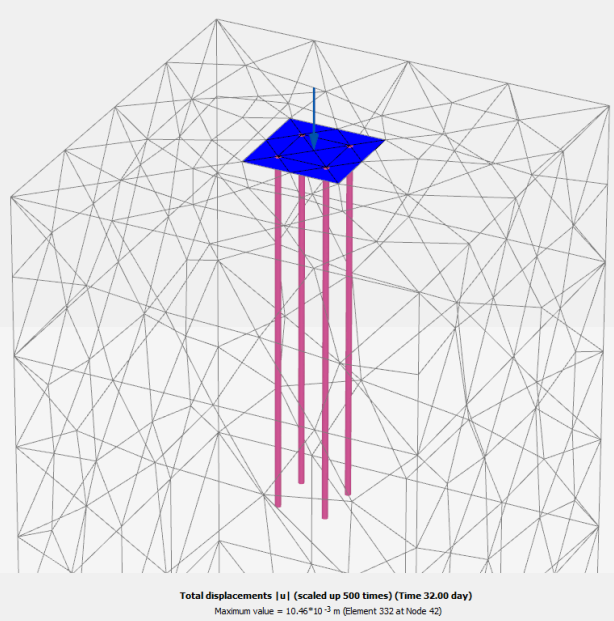

Figure 4.15. Software analysis results of corner pile groups

4.6.4. Analysis of all pile groups using Plaxis 3D

The total deformation of the foundation was determined using the software, consisting of several phases. The analysis was done in 6 stages - excavation (1 and 2), construction of walls and piles, application of loads, and consolidation settlement analysis (5 and 6).

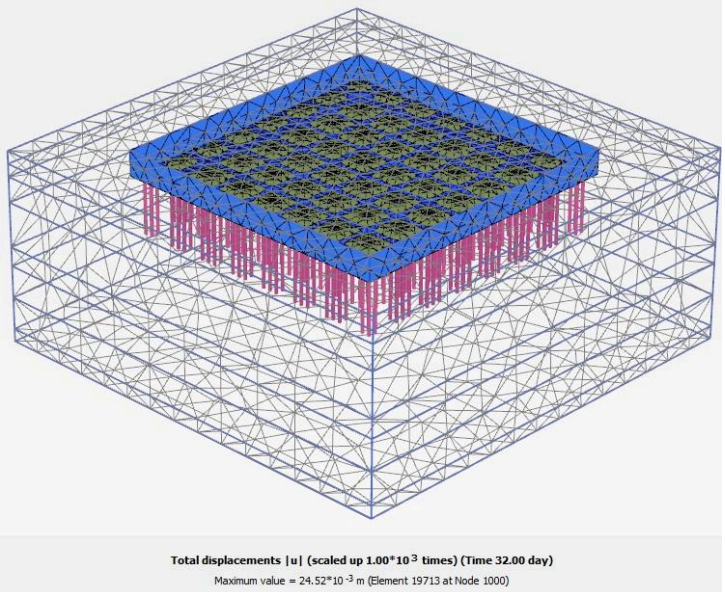

Figure 4.16. Software analysis of all pile groups

4.7. Design of the foundation: lateral loading

4.7.1. Hand calculation of lateral bearing capacity

The calculation of lateral loading of the piles is essential for ensuring the safety of the foundation. Thus, the lateral load of the single pile is calculated, where the horizontal load is chosen as the most critical. From the table below provided by the structural part, it is seen that the corner columns are experiencing largest lateral loads. Whereas, the internal columns vice versa surrounded by other structural elements, so they can be considered as more shielded:

Table 4.32. Lateral loads for each group of piles

Column	Number of piles	Combination of load	$F_x,\ kN$	$F_y,\ kN$	Lateral load of column, kN
Corner	4	1.2D+1E+1L	350.2	420	105.00
Exterior	6		395.2	396.1	66.02
Interior	6	0.9D+1E	382.5	371.7	61.95

Now, the subgrade modulus is calculated using the formula below:

$$k_z = \eta_h * z$$

Where, η_h - modulus of subgrade reaction (constant);

z - depth of the layer;

Table 4.33. Modulus of subgrade for the depth z

Depth, m	Description	η_h	k_z
0.61	Sandy Clay	2000	1220
1.5	Clayey Sand	4000	6000
1.9	Silty Clay	1200	2280
0.8	Sand (medium to coarse)	10000	8000
1.2	Silty Sand (medium to coarse)	16000	19200

1.3	Silty Sand	16000	20800
3.6	Clayey Sand with some Gravel	16000	57600
4	Clayey Sand with some Gravel & Silty Sand	16000	64000

The modulus of elasticity, E_p is calculated using the compressive strength of concrete, f_c':

$$E_p = 4700\sqrt{f_c'}$$

According to the LA building code, for the site with the seismic design category D and the risk category II, the minimum value of compressive strength should be $f_c' = 35\ MPa$.

Whereas, the moment of inertia is calculated using the following way:

$$I_p = \frac{\pi D^4}{64}$$

Then the characteristic length of the pile is calculated using the formula below:

$$T = \sqrt[5]{\frac{E_p I_p}{\eta_h}} = \sqrt[5]{\frac{25500 * 10^3 * 0.00201}{16000}} = 1.26\ m$$

The length of the piles is taken as 9 m, knowing that 5*T=6.31 m < 9m, thus the piles are long.

Rankine passive earth pressure coefficient:

$$K_p = tan^2(45 + \frac{\varphi'}{2})$$

Section modulus of the pile:

$$S = \frac{\pi D^3}{32} = \frac{\pi * 0.45^3}{32} = 8.95 * 10^{-3}$$

Yield moment of the interior pile:

$$M_y = SF_y = 313.25$$

Where, F_y - yield stress of the material of the pile, MPa;

The ultimate lateral resistance is then found using the graph for piles in soils with sand presented by Das & Sivakugan (2019). The ultimate lateral resistance should be found for three types of column (corner, interior, exterior) using the calculated value of yield moment. The graph

and the table of bearing capacities is represented below. Furthermore, the allowable bearing capacity is calculated using the formula below, and the actor of safety is taken as 3:

$$Q_{all} = \frac{Q_{ug}}{FS}$$

As it was mentioned, according to Das & Sivakugan (2019), FoS = 3.

Table 4.34. Comparison of load bearing capacity and lateral load

Column	Q_{ug}, kN	Q_{all}, kN	$Q_{lateral}$, kN
Corner	478.31	159.44	119.56
Exterior	338.16	112.67	56.36
Interior	363.08	121.03	60.51

Now, comparing the values of allowable bearing capacity and the lateral load bearing capacity for the particular type of column, it is seen that $Q_{all} > Q_{lateral}$. Thus, each type of column has a larger value of allowable bearing capacity than the exerted lateral load. Overall, the structure can be considered as satisfactory.

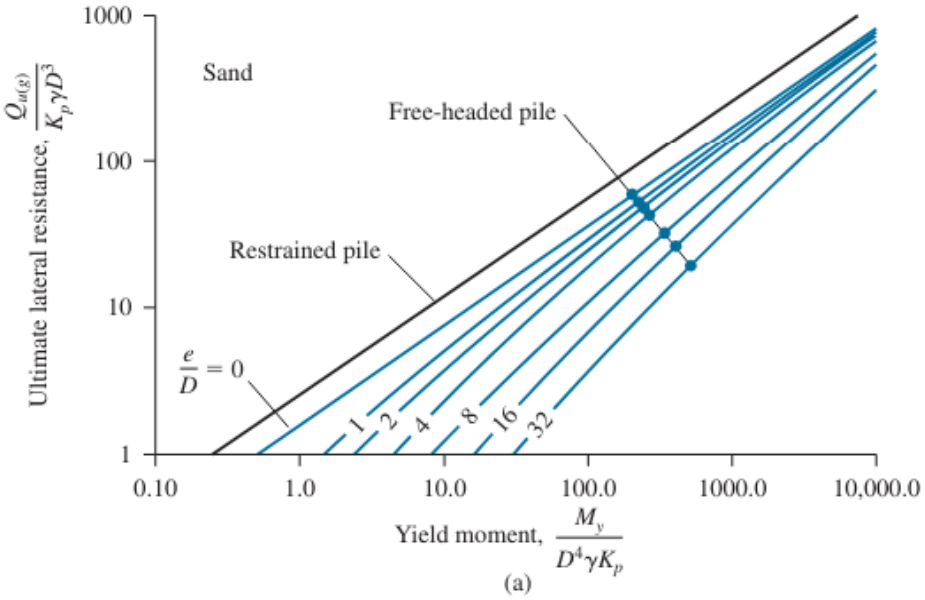

Figure 4.17. Ultimate lateral resistance graph.

4.7.2. Hand calculation of lateral deflection

The elastic method was used for evaluating the lateral deflection of the structure. The lateral deflection of the pile head at Xz at z=0 can be calculated using the formula below:

$$\eta = \sqrt[5]{\frac{\eta_h}{E_p I_p}}$$

For clay:

$$K = \frac{pressure\ (kN/m^2)}{displacement\ (m)}$$

$$\beta = \sqrt[4]{\frac{KD}{4E_p I_p}}$$

Whereas, the pile deflection at any depth can be evaluated using the formula below:

$$x_z(z) = A_x' \frac{Q_g T^3}{E_p I_p} + B_x' \frac{M_g T^2}{E_p I_p}$$

Using the table 12.15 provided by the Das & Sivakugan, that is also in the appendix part, the values of A_x' and B_x' can be found. By applying the values on the formulas above, the calculated lateral deflection of one pile is represented in the table below:

Table 4.35. Lateral load deflection for each pile on different layers

Layer	Depth, m	Description	A_x'	B_x'	$x_z(z)$, mm corner	$x_z(z)$, mm exterior	$x_z(z)$, mm interior
1	0.61	Sandy Clay	2.435	1.623	14.404	14.093	13.270
2	1.5	Clayey Sand	1.496	0.752	7.748	7.581	7.138
3	1.9	Silty Clay	0.142	-0.070	0.100	0.098	0.092
4	0.8	Sand (medium to coarse)	-0.075	-0.089	-0.619	-0.606	-0.570
5	1.2	Silty Sand	-0.05	-0.028	-0.271	-0.266	-0.250

		(medium to coarse)					
6	1.3	Silty Sand	-0.009	0	-0.026	-0.026	-0.024
7	3.6	Clayey Sand with some Gravel	0	0	0	0	0
8	4	Clayey Sand with some Gravel & Silty Sand	0	0	0	0	0

The figure below represents the pile deflection graph for three types of columns with respect to the soil layers. The deflection on x-axis was taken from the table above $x_z(z)$.

Brom's method was used for calculating the deflection of the pile head:

$$Dimensionless\ lateral\ deflection\ = \frac{x_z(EI)^{3/5}(n_h)^{2/5}}{Q_g L}$$

$$Dimensionless\ length\ = \eta * L$$

Since the soil profile on the site is mostly sand, silty sand and sand with some gravel, the graph of the solution of Brom's for estimating deflection of pile head was used in sand and represented in a figure below:

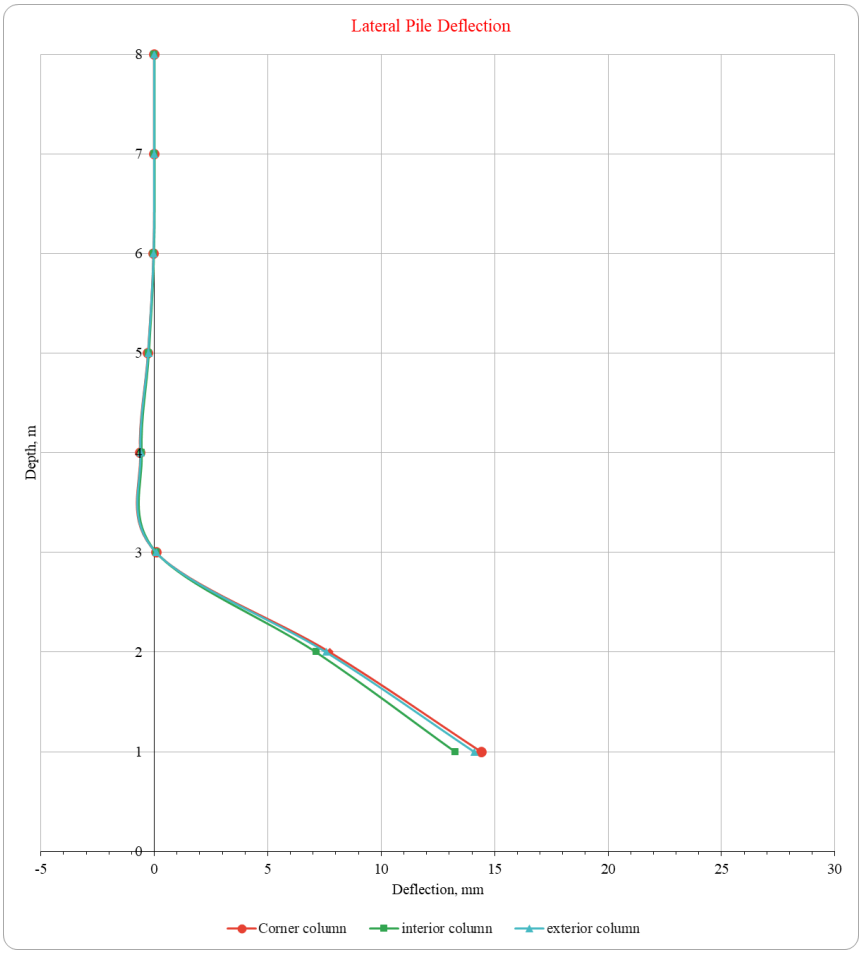

Figure 4.18. Lateral Pile deflection

The deflection of the pile head was calculated using three different methods, which are the elastic method, Brom's method and the Lpile method using Excel. The following tables represent the results obtained:

Table 4.36. Results of the deflection using Elastic method

Corner	Exterior	Interior
14.40	14.09	13.27

Table 4.37. Results of the deflection using Brom's method

Corner	Exterior	Interior
9.60	9.39	8.85

From the results it is seen that the deflections are in allowable range, therefore it can be considered that the design is satisfactory.

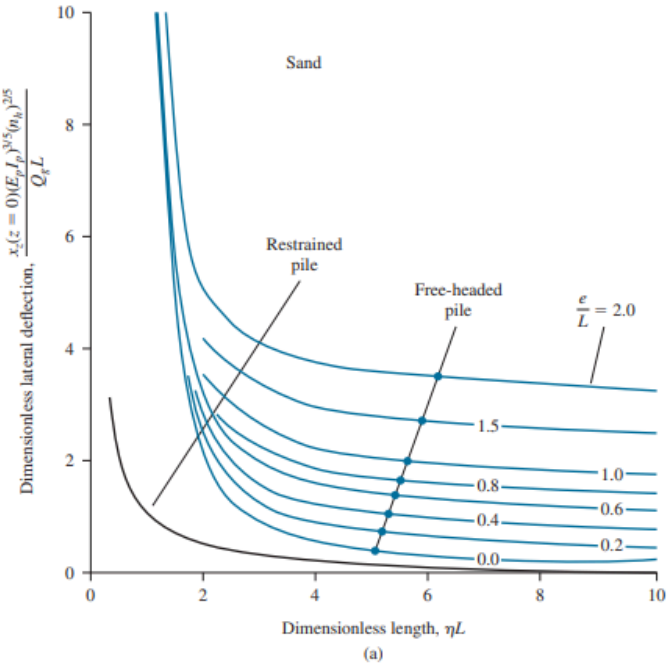

Figure 4.19. Brom's method for estimating deflection of pile for sand

4.8. Design of the Group Piles

Group piles are used when a single pile is insufficient to carry heavy loads, itr i especially common for large span and high-rise buildings (Das, 2010). The load is distributed across multiple elements to ensure structural safety and minimization of the settlement of the structure. Furthermore, group piles are particularly effective in soft or compressible soils where individual pile capacity is limited (Poulos & Davis, 1980). The reinforced pile cap and reinforced piles should be further designed to resist shear and bending load, and meet the acceptable requirements. The design procedure was held according to Ray S. (1994).

4.8.1. Pile cap reinforcement design

The size of the pile cap can be calculated using the formula below:

$$L = d(n_1 - 1) + 2 * 1.5D$$

$$B = d(n_2 - 1) + 2 * 1.5D$$

For the corner and interior group piles the caps are square. The corner spacing, the distance between the center of the pile and the corner of the cap can be calculated using the formula below:

$$h_{min} = 1.5D$$

First, the analysis of loads acting on the pile cap should be done. Particularly, it should include weight of the pile cap:

$$W_{pc} = h * \gamma_{concrete} = 0.675 * 24 = 16.2\ kN/m^2$$

Weight of backfill for interior cap:

$$W_{bf} = h * \gamma_{soil} = 0.5 * 18 = 9.0\ kN/m^2$$

Furthermore, it should contain the weight of the superstructure and columns, the following table represents the loads that act on the pile cap:

Table 4.38. Loads acting on the pile cap

Dead Load, kN	Live Load, kN	$W_{pc}, kN/m^2$	$W_{bf}, kN/m^2$	$W_{sc}, kN/m^2$
90.79	73.73	16.2	9.0	164.52

The total weight, W is calculated first:

$$W = W_{pc} + W_{bf} + W_{load} = 16.2 + 9 + 139.32 = 164.52\ kN/m^2$$

According to Ray S. (1994) and ASCE 7, including both seismic load and wind load, the load combinations are as follows:

$$LC_1 = 1.2D + 1.6L$$

$$LC_2 = 1.2D + 1L + 1W$$

$$LC_3 = 1.2D + 1L + 1E_x$$

Now, by applying the load factors to the dead load, we get:

$$1.2 * W = 1.2 * 164.52 = 197.424\ kN/m^2$$

$$1.4 * W = 1.4 * 164.52 = 230.328\ kN/m^2$$

For interior cap, since the shape is square, the moment sections 1-1 and 2-2 calculation equations are the same and equals to:

1.2W: $M'_{11} = M'_{22} = \frac{4.35 * q * L^2}{2} = \frac{4.35*197.424*1.725^2}{2} = 1277.73\ kNm$

1.4W: $M'_{11} = M'_{22} = \frac{4.35*230.328*1.725^2}{2} = 1490.68\ kNm$

Reaction forces:

$$Q = \frac{P}{R} \pm \frac{M_{xx} y}{I_{xx}} \pm \frac{M_{yy} x}{I_{yy}}$$

Vertical load:

$$P = (1.2\ or\ 1.4)N + W_{pc} + W_{bf}$$

Moment about x-axis:

$$M_{xx} = M_x + Ne_y + H_y h + M_x *$$

Moment about y-axis:

$$M_{yy} = M_y + Ne_x + H_x h + M_y *$$

$$About\ x\text{-}axis: I_{xx} = \sum y^2$$

$$About\ y\text{-}axis: I_{yy} = \sum x^2$$

$$Q_3 = 1131.46\ kN\ \ and\ \ Q_4 = 1005.12\ kN$$

$$M''_{11} = 1.4(Q_3 + Q_4) = 1.4(1031.46 + 1005.12) = 2851.212 kNm$$

$$M''_{22} = 0.5(Q_1 + Q_2 + Q_3) = 1527.44\ kNm$$

Combined bending moments:

$$M_{11} = M'_{11} + M''_{11} = 4159.21\ kNm$$

$$M_{22} = M'_{22} + M''_{22} = 2462.02\ kNm$$

For reinforcement design in the x and y directions, steel bars with diameters of 32 mm and 25 mm, respectively, were used. The concrete is assumed to have a compressive strength of 5 MPa, while the yield strength of the reinforcing steel is 460 MPa. According to ACI 318-19, the minimum concrete cover for structural elements in direct contact with soil is 75 mm. Based on these parameters, the required reinforcement area in the pile cap is found using the equations below:

$$d_x = h_{pile\ cap} - cover - 0.5 * d_{bar} = 700 - 75 - 0.5 * 32 = 609\ mm$$

As it was mentioned, $f_{cu} = 35\ N/mm^2$ and $f_y = 460\ N/mm^2$

$$K = \frac{M_{11}}{f_{cu} bd^2} = \frac{4159.21}{35*3000*609^2} = 0.107$$

$$z = d(0.5 + \sqrt{(0.25 - \frac{K}{0.9})}) \leq 0.95d$$

$$z = 609(0.5 + \sqrt{(0.25 - \frac{0.107}{0.9})}) = 525.014 \leq 0.95d = 578.55$$

$$A_{st} = \frac{M_{11}}{0.87 f_y z} = \frac{4159.21}{0.87*460*525.014} = 28187.21\, mm^2$$

$$\#of\ bars = \frac{A_{st}}{A_{bar}} = \frac{28187.21}{804.2} = 35.05$$

$$Spacing = \frac{4350\, mm}{36} = 120.83\, mm$$

use 33 #32 mm at 120.83 mm spacing

Pile cap design in y direction for the interior column was implemented using the same procedure:

$$d_y = h_{pile\ cap} - cover - 0.5 d_{bar} = 700 - 75 - 32 - 0.5 * 25 = 619.5\, mm$$

$$K = \frac{M_{11}}{f_{cu} bd^2} = \frac{4159.21}{35*3000*619.5^2} = 0.065$$

$$z = d(0.5 + \sqrt{(0.25 - \frac{K}{0.9})}) \leq 0.95d$$

$$z = 619.5(0.5 + \sqrt{(0.25 - \frac{0.065}{0.9})}) = 564.50 \leq 0.95d = 581.875$$

$$A_{st} = \frac{M_{11}}{0.87 f_y z} = \frac{4159.21}{0.87*460*564.50} = 18410.68\, mm^2$$

$$\#of\ bars = \frac{A_{st}}{A_{bar}} = \frac{18410.68}{491.44} = 38$$

$$Spacing = \frac{4350\, mm}{38} = 114.47\, mm$$

use 38 #25 mm at 114.47 mm spacing

By applying the same procedure to other two columns (exterior, corner), the pile cap design reinforcement is represented below:

Table 4.39. The pile cap reinforcement design

Group Piles	h, mm	d_x, mm	d_y, mm	Design in x	Design in y
Exterior	600	512	481	44 #32mm @ 100mm	49 #25mm @ 90mm
Interior	700	620	609	33 #32mm @ 125mm	38 #25mm @ 115mm
Corner	600	512	481	40 #32mm @ 85mm	25 #25mm @ 150mm

Single Pile Reinforcement

The design of the reinforcement in each individual pile is implemented by checking the slenderness first. The slenderness check is evaluated using the procedure below:

$$l_e = \beta l_o = 1.2 * 9 = 10.8\,m$$

Where, $\beta = 1.2$ for piles in pile cap;

$$\frac{l_e}{h} = \frac{10.8}{0.45} = 24 > 10 \quad \text{(slender pile)}$$

$$a = \frac{l_e^{\,2}}{2000h} K = \frac{10.8^2}{2000*0.45} * 1 = 0.13\,m$$

$$M_{add} = Q_{min} * a = 630.33\,kN * 0.13\,m = 81.56 kNm$$

$$M_{mag} = M + M_{add} = 91.98 + 81.56 = 173.54\,kNm$$

$$e = \frac{M_{mag}}{Q_{min}} = \frac{173.54}{630.33} = 0.275\,m$$

$$\frac{e}{R} = \frac{0.275}{0.225} = 1.22$$

$$\frac{M}{h^3} = \frac{173.54}{0.45^3} = 1.904\,kN/m^2$$

$$k = \frac{h_s}{h} = 0.83$$

Thus, the corresponding reinforcement:

$$A_{st} = \frac{A_c * 1}{100} = \frac{\pi * 0.225^2 * 1.6}{100} = 2543.4\,mm^2$$

8 #20mm bars (A=2512 mm^2)

Shear check:

$$\frac{M_{max}}{Q_{max}} = \frac{173.54}{1030.33} = 0.168 < 0.6h = 0.3$$

Since it meets the requirement, there is no need for a shear check.

Table 4.40. Individual pile cup design requirements

Group Piles	D, m	l_e/h	M/h^3	ρ	A_{sc}, mm^2	Design
Exterior	0.4	27	2.76	2.9%	3052.1	12 #20 mm
Interior	0.45	24	1.904	1.6%	2543.4	10 #20 mm
Corner	0.4	27	2.76	2.9%	3815.1	15#20 mm

4.8.2. Pile cap reinforcement design Geo5 check

By applying all the values and selected reinforcement type to the Geo5 software, we get satisfactory results as it is shown in the figures below:

Interior Column:

SHEAR :
SATISFACTORY (8,2%)
BENDING + COMPR. :
SATISFACTORY (6,8%)
Reinforcement ratio :
SATISFACTORY (25,3%)

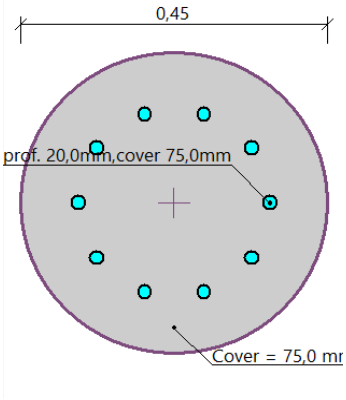

Figure 4.20. Geo5 results of interior reinforced pile.

Exterior Column:

SHEAR :
SATISFACTORY (8,8%)
BENDING + COMPR. :
SATISFACTORY (7,8%)
Reinforcement ratio :
SATISFACTORY (16,7%)

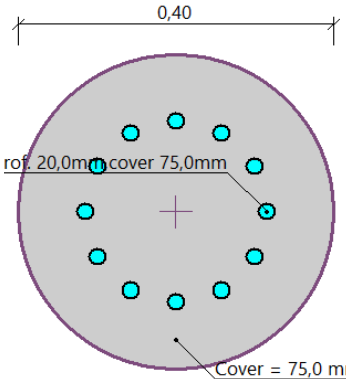

Figure 4.21. Geo5 results of exterior reinforced pile

Corner Column:

SHEAR :
SATISFACTORY (8,2%)
BENDING + COMPR. :
SATISFACTORY (6,7%)
Reinforcement ratio :
SATISFACTORY (13,3%)

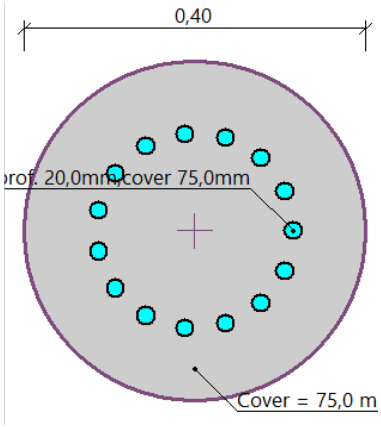

Figure 4.22. Geo5 results of corner reinforced pile

The figure below is visual representation of the reinforced interior group of pile designed in AutoCAD software:

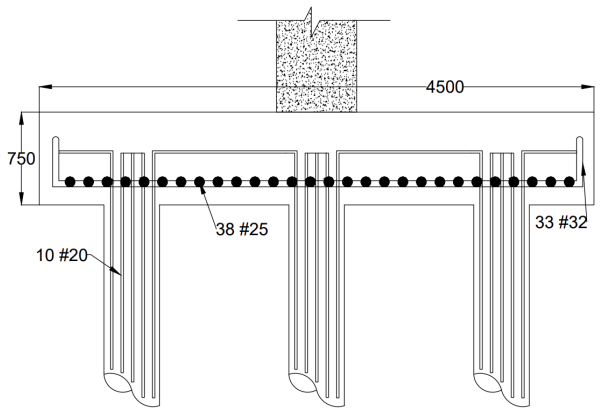

Figure 4.23. Interior pile cap reinforcement design.

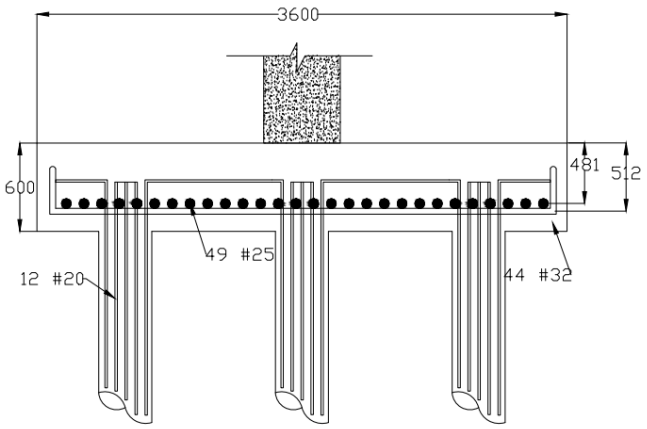

Figure 4.24. Exterior pile cap reinforcement design.

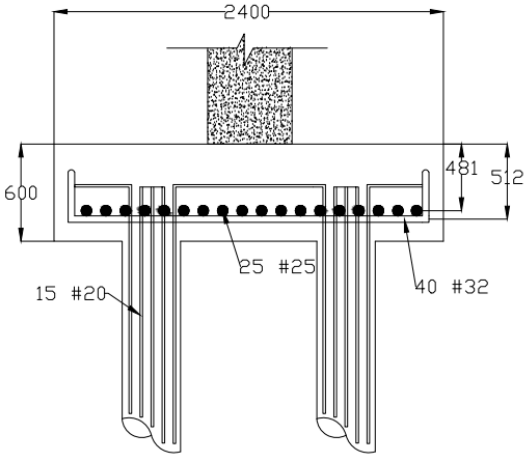

Figure 4.25. Corner pile cap reinforcement design.

4.9. Sheet Pile design

Steel sheet piles were selected as the primary retaining system to resist lateral earth pressures due to their constructability, durability, and cost-effectiveness. In comparison to other retaining walls, for instance, cast-in-place walls, they are installed by driving or pressing into the ground, significantly reducing construction time (Coduto, 2001). Furthermore, according to FHWA (2006), geotechnical and environmental testing revealed low potential for corrosion and sulfate attack, which makes it even more suitable.

An important consideration in the design was the method of installation. Among the two common approaches, which are dredged and backfilled. The backfill method was selected due to

the site's predominantly granular soil conditions. In the backfilled method, sheet piles are installed first to create a stable barrier, and then the excavation is carried out behind the wall. Once the target depth is reached, the excavated area is filled with engineered backfill material, which is typically compacted in layers. This method allows for better control over soil compaction, reduces wall deformation, and enhances overall stability (Terzaghi, Peck, & Mesri, 1996).

Backfilling also provides an opportunity to improve drainage and reduce hydrostatic pressure by incorporating free-draining materials or geosynthetic drainage systems behind the wall. Furthermore, since the site did not require deep excavation below the groundwater table, dewatering challenges were minimized, this in turn making the backfill approach both practical and cost-efficient. Based on these conditions, a cantilever sheet pile system was selected, which does not require anchorage and is effective for moderate wall heights (Tomlinson & Woodward, 2015).

4.9.1. Hand calculations of sheet pile design

In order to design a proper sheet pile design, first the Rankine earth pressure coefficient is calculated.

Active earth pressure coefficient:

$$K_a = tan^2(45 - \frac{\varphi'}{2})$$

Passive earth pressure coefficient:

$$K_p = tan^2(45 + \frac{\varphi'}{2})$$

An excavation depth is 4 m, therefore the minimum length of the sheet pile is 4 m. Using this depth the soil profile details is presented below:

$$\gamma = 16.82\ kN/m^3$$

$$\varphi' = 39.39^\circ$$

Step 1. Using this details of the soil profile the earth pressure coefficients:

$$K_a = tan^2(45 - \frac{39.39}{2}) = 0.224$$

$$K_p = tan^2(45 + \frac{39.39}{2}) = 4.473$$

Step 2. A Factor of safety is applied to the passive earth pressure coefficient to account for soil variability, overestimation risks, construction disturbances, and structural stability. This ensures a conservative and reliable design that prevents failure.

$$K_{p(design)} = \frac{K_p}{FS} = \frac{4.473}{2} = 2.237$$

Step 3. The active pressure at L=4 m:

$$\sigma'_2 = \gamma L K_a = 16.82 * 4 * 0.224 = 15.07\ kN/m^2$$

Step 4. The depth at $\sigma' = 0$:

$$L_3 = \frac{LK_a}{K_{p(design)} - K_a} = \frac{4*0.224}{2.237-0.224} = 0.445m$$

Step 5. The pressure at $L = 4\ m$:

$$\sigma'_5 = \gamma L K_{p(design)} + \gamma L(K_{p(design)} - K_a)$$

$$\sigma'_5 = 16.82 * 4 * 2.237 + 16.82 * 4 * (2.237 - 0.224) = 285.94\ kN/m^2$$

Step 6. The area of the pressure diagram is calculated using the formula below:

$$P = \frac{1}{2}\sigma'_2 L + \frac{1}{2}\sigma'_2 L_3 = \frac{15.07*4}{2} + \frac{15.07*0.445}{2} = 33.49$$

Step 7. The centroid of the pressure diagram is evaluated by this formula:

$$\bar{z} = \frac{L(2K_a - K_{p(design)})}{3(K_{p(design)} - K_a)} = \frac{4(2*0.224-2.237)}{3(2.237-0.224)} = 1.18\ m$$

$$A'_1 = \frac{\sigma'_5}{\gamma(K_{p(design)} - K_a)} = \frac{285.94}{16.82(2.237 - 0.224)} = 8.44$$

$$A'_2 = \frac{8P}{\gamma(K_{p(design)} - K_a)} = \frac{8 \cdot 33.49}{16.82(2.237 - 0.224)} = 7.91$$

$$A'_3 = \frac{6P\left[2\bar{z}\gamma(K_p - K_a) + \sigma'_5\right]}{\gamma^2(K_p - K_a)^2} = \frac{6 \cdot 33.49[2 \cdot 1.18 \cdot 16.82(2.237 - 0.224) + 285.94]}{16.82^2(2.237 - 0.224)^2} = 64.12$$

$$A'_4 = \frac{P\left[6\bar{z}\sigma'_5 + 4P\right]}{\gamma^2(K_p - K_a)^2} = \frac{33.49[6 \cdot 1.18 \cdot 285.94 + 4 \cdot 33.49]}{16.82^2(2.237 - 0.224)^2} = 63.05$$

Step 8. L_4 can be calculated using the following equation:

$$L_4^4 + A'_1 L_4^4 - A'_2 L_4^2 - A'_3 L_4 - A'_4 = 0$$

$$L_4 = 3.27$$

Step 9. D_{theory}:

$$D_{theory} = L_3 + L_4 = 3.715\, m$$

So, the total length of the sheet pile can b evaluated by the sum of the D_{theory} and L, for safety reasons the value is also will be increased to 25-30%. Thus, $L_{total} = 8.03\, m$

Step 10. σ'_3, σ'_4 :

$$\sigma'_3 = L_4(K_p - K_a)\gamma = 3.27(2.237 - 0.224) * 16.82 = 110.72\, kN/m^2$$

$$\sigma'_4 = \sigma'_5 + \gamma L_4 (K_p - K_a) = 285.94 + 16.82 * 3.27(2.237 - 0.224) = 396.66\, kN/m^2$$

Step 11. L_5:

$$L_5 = \frac{\sigma'_3 L_4 - 2P}{\sigma'_3 + \sigma'_4} = \frac{110.72 * 3.27 - 2 * 33.49}{110.72 + 396.66} = 0.58\, m$$

Step 12. Zero shear force, z':

$$z' = \sqrt{\frac{2P}{\gamma(K_p - K_a)}} = 1.406\, m$$

Step 13. Maximum bending moment, M_{max}:

$$M_{max} = P(\bar{z} + z') - \left[\frac{1}{2}\gamma z'^{2}(K_p - K_a)\right](\frac{1}{3})z' = 82.08\,kN \cdot m/m$$

According to the ASTM A328, for traditional sheet pile design using ASD the allowable stress is 170 MPa.

$$S = \frac{M_{max}}{\sigma_{all}} = \frac{72.85}{170000} = 4.28 * 10^{-4} m^3/m\ of\ the\ wall$$

For the sheet pile design, considering the calculated forces and moments, the sheet pile section PZ 27 was chosen. The figure below represents the sheet pile section from the Geo5 software:

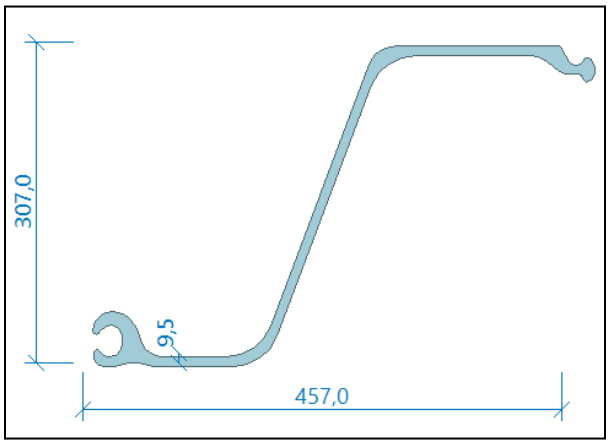

Figure 4.26. Sheet pile section PZ 27

The following table represents dimensions and characteristic details if PZ 27:

Table 4.41. Dimensions and characteristic details for sheet pile PZ27

	Section PZ 27
Width	457.2 mm
Height	304.8 mm
Flange Thickness	9.525 mm
Web Thickness	9.525 mm
Section Modulus	0.000494 m^3/m
Moment of Inertia	0.0000767 m^4
Wall Weight	131.82 kg/m^2

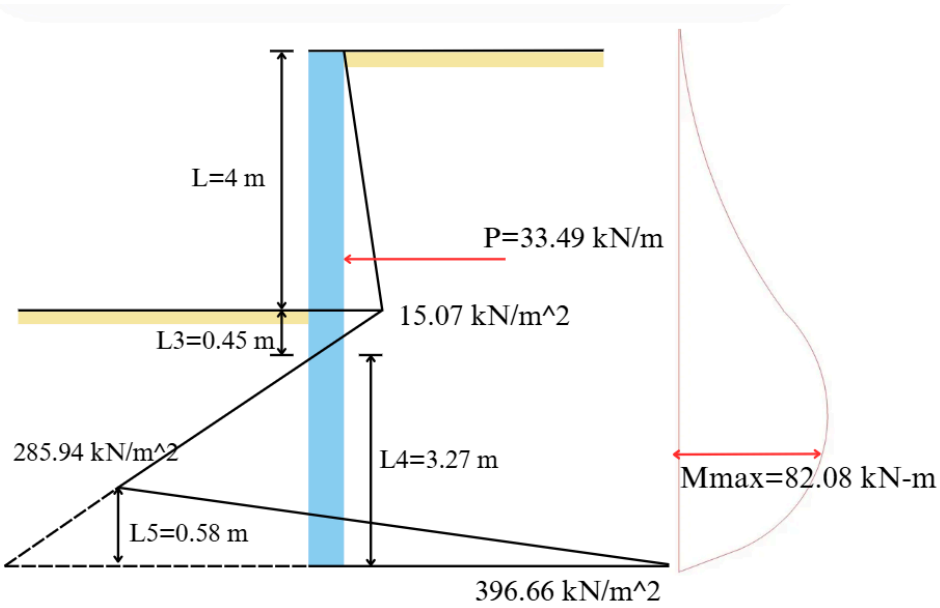

Figure 4.27. Sheet Pile Design.

Table 4.42. Results of Geo5 software analysis

Max. Bending Moment, M_{max}	Total depth, L_{total}	Section modulus, I	All. Stress, σ_{all}	Type of steel	Sheet pile type	Displacement, GEO5
82.08 kN m	8.03 m	0.000494 m^3/m	170 MPa	ASTM A328	PZ 27	4.8 mm

4.9.2. Geo5 software analysis of sheet pile design

For evaluating maximum displacement and maximum pressure, the Geo5 software is used. The excavation process consisted of 4 phases. First, sheet pile installation (section PZ 27) and excavation of the first phase to the depth of 2 m. The second stage included the first layer of anchors at the depth of 1 m. The next stage included another excavation to the further 2 m, total excavation depth is 4 m. The last step is installing the second layer of anchors at the depth of 3 m. The figures below represents the diagram of bending moment and shear force:

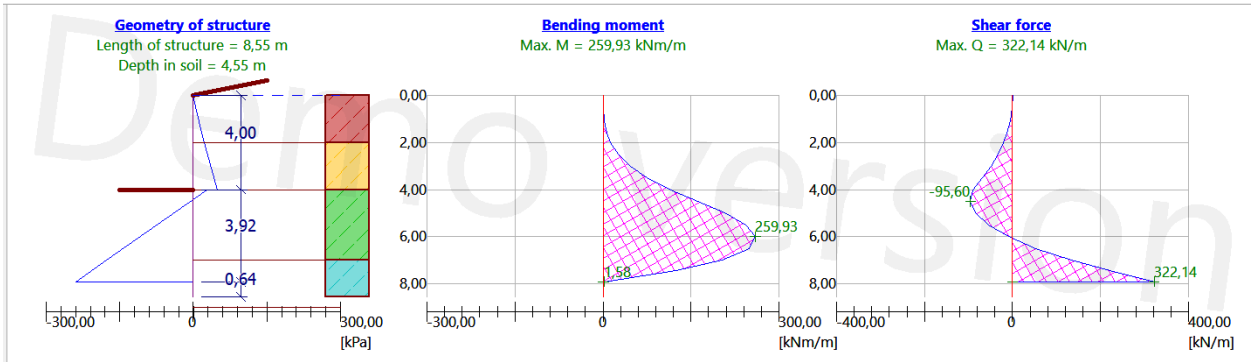

Figure 4.28. Bending moment and shear force diagrams (Geo 5).

In sheeting check section, the maximum displacement and the maximum pressure acting on the structure was evaluated:

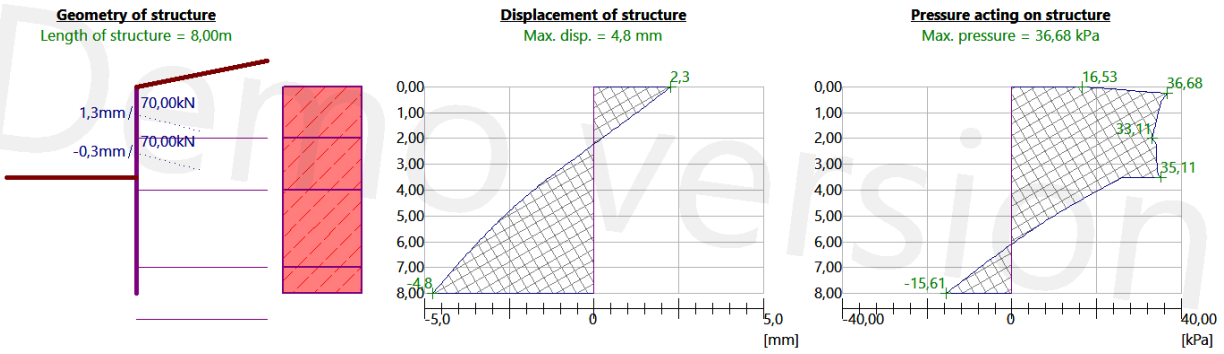

Figure 4.29. Displacement and pressure diagrams (Geo 5).

The following figures represent the details on installed sheet pile PZ 27. Furthermore, the bending and shear check:

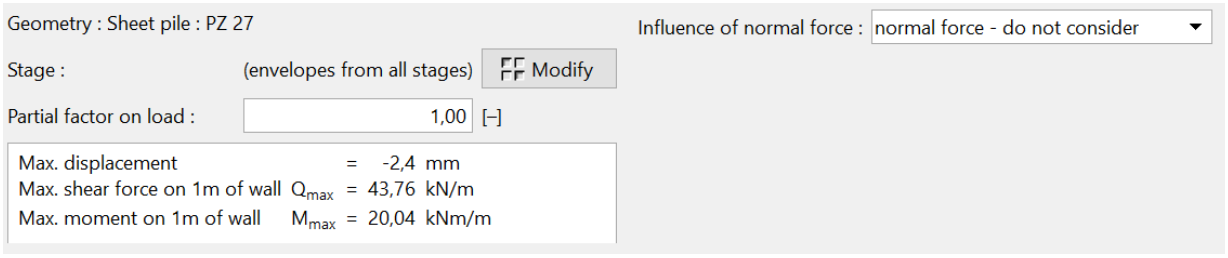

Figure 4.30. PZ 27 sheet pile section details.

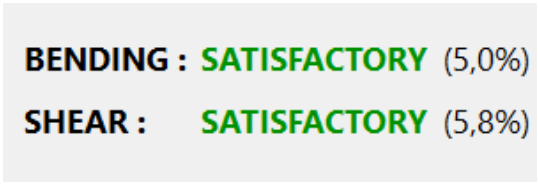

Figure 4.31. Bending and shear check in Geo5.

The following figure represents the visual representation of the anchored wall, sheet pile design in Geo 5 software:

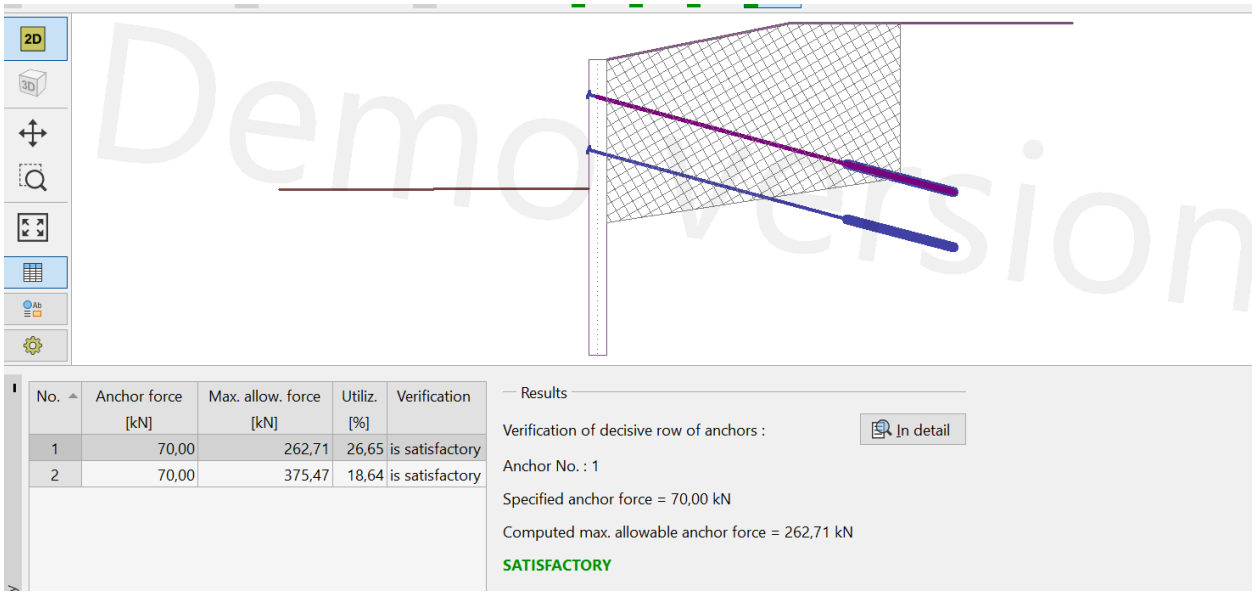

Figure 4.32. Sheeting check in Geo 5.

4.10. Construction Procedure

Every construction process requires adequate site preparation, which in turn will ensure structural integrity, construction efficiency, long-term safety etc. Proper execution at this phase minimizes delays and unexpected costs during later stages of construction (Smith, 2020). These stages are site clearing, surveying, soil testing, site investigation, plan design, excavation process etc. The following sections will provide a more detailed choice of each stage for our construction of the “Ivory residence” residential building in Los Angeles.

Site Clearing

According to Northey & Gribble (2013), this involves the removal of vegetation, debris, existing pavements, or obsolete structures that may obstruct new construction. Removing surface layers also allows engineers to inspect subgrade conditions early. Since the site has an existing old building, it will require demolition and the removal of the existing asphalt sidewalk in front of the building, to ensure a proper site for excavation.

Site Surveying

Surveying defines legal boundaries and marks key locations for excavation, foundation layout, and utility connections. It is vital not only for construction accuracy but also for complying with local zoning codes and building permits (Chudley & Greeno, 2016). Advanced surveying tools like GPS total stations and 3D laser scanning can be used to increase accuracy and speed of this process.

Soil Testing

Geotechnical investigation is essential for evaluating the subsurface conditions. Parameters such as soil strength, compressibility, permeability, and bearing capacity are determined through laboratory and in-situ tests. These results influence the whole foundation design decisions, which include the foundation type, retaining wall type etc. therefore, this stage can be considered one of the most significant, if needed the soil should be improved. For instance, in cases where the native soil is unsuitable, ground improvement techniques such as vibro-compaction or soil stabilization may be used (Das & Sobhan, 2018).

Site Investigation

A multi-phase investigation (preliminary, detailed, and supplementary) is conducted to gather comprehensive data on subsurface geology, groundwater level, and potential hazards such as liquefaction, expansive soils, or contamination. This data supports the design of stable and durable foundations and retaining systems (Craig & Knappett, 2012).

Site Plan Implementation

A well-developed site plan ensures optimal placement of buildings, equipment zones, utilities, and access roads. It also addresses logistics for materials, worker circulation, and environmental considerations like erosion control. Effective site layout reduces equipment idling time and enhances overall productivity (Gould & Joyce, 2009).

Sheet Pile Installation

We decided to go with the vibratory driving method for installing the sheet piles because it suits the conditions of our site—a large-scale excavation with a mixed soil profile of clay and sand, and a depth requirement of around 8 meters. This method stands out as both efficient and cost-effective, especially for layered soils like the ones we're dealing with. One of the biggest advantages is how quickly the piles can be installed, thanks to vibratory hammers that reduce soil resistance during driving (Das & Sobhan, 2018).

While the method does generate some vibration, our site isn’t close to any sensitive structures, so that’s not a major concern. And in case we encounter tougher soil layers, we have options like jetting or predrilling to help with installation (Tomlinson & Woodward, 2015; FHWA, 2006). All

in all, this method gives us a solid balance between performance, speed, and cost, which makes it the right fit for our project.

Excavation

Excavation proceeds once sheet piles are in place. This stage consists of several phases. The first stage of excavation is applied to the depth of 2 m, and the one layer of the inclined anchors is attached to the sheet pile. In the second stage, the site is excavated further to 2 m with a total depth of excavation of 4 m. Since the value of deformation is bigger than allowed, the second layer of anchors is installed. The result of the excavation is shown in Figure X.

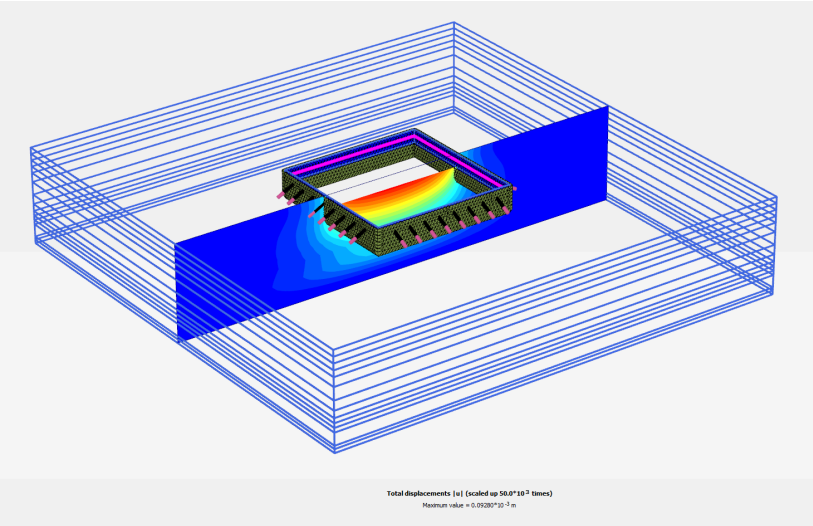

Figure 4.33. Total displacement for excavation

Pile Installation

For our project, we decided to use the vibratory driving method to install the sheet piles. Since the vibratory hammers make the process quicker and more efficient by reducing resistance as the piles are driven into the ground. It's also a cost-effective solution, especially for projects like ours where speed and efficiency matter (Das & Sobhan, 2018). Since our site doesn't have any nearby structures sensitive to vibration, this method won't pose any risk in that regard.

In addition, if we run into tougher soil layers, we can use techniques like jetting or predrilling to help with the installation (Tomlinson & Woodward, 2015; FHWA, 2006). To keep things accurate during construction, we'll also use guide frames for alignment and dewatering systems if needed.

5. Environmental Part

Environmental engineering is a discipline that throws light on different urban challenges in the areas of stormwater management, sustainable construction, and public health. Unlike other engineering streams, such as structural engineering or aerospace engineering, environmental engineering pertains to finding appropriate solutions that can realistically sustain pressing ecological and urban demands. Stormwater management from the perspective of environmental engineering sustainability, water quality, and resilience in cities.

The next part of the project primarily deals with a residential development grading and drainage system. The key objective here will be to develop an effective methodology for stormwater runoff management with due consideration for environmental sensitivity and municipal and state statutes. This project stitches together appropriate technical design, environmental analysis, and regulatory compliance to ensure the project's sustainability for a long period.

5.1. General Information

It is located at 6435 Wilshire Boulevard, Los Angeles, California, a region faced with high sensitivity to urban density and intersectoral environmental issues. Los Angeles enjoys a Mediterranean type climate that includes dry summers and rainy winter seasons. This wide variation in climatic conditions now calls for a stormwater management system able to handle a great deal of rainfall in seasonal periods without erosion and flooding into the urban areas.

The topographical study could tell that the general slope of the natural topography around the site was from north to south. Its elevation, in fact, tumbles down from 45 m to 43 m. This slopes up some opportunities as well as challenges in designing a grading and drainage system. Efficient design of drainage is critical in avoiding water accumulation, protecting the structure of the building, and maintaining regulations.

5.2. Legal Requirements

The drainage system design is carried out in compliance with the ordinance and regulatory requirements of the City of Los Angeles and California State. Regulatory compliance assures the

impending environmental standards that minimize the possible penalties or construction delays on this project. Key regulatory documents include:

Los Angeles Municipal Code, Section 66.03:

- Proper stormwater diversion to avoid the pollution of natural water bodies.
- Implementation of runoff retention systems.
- Compliance with the water quality objectives set by the city.

EPA National Pollutant Discharge Elimination System (NPDES):

- Reduce pollutants in stormwater discharges from construction sites.

Los Angeles County Drainage Design Manual:

- Provides the guidelines for hydrology and drainage calculations.
- Recommends the use of best management practices such as permeable pavements and bioswales.

Thus, these regulations ensure that the drainage system is contributive to environmental sustainability as well as protective of public health.

5.3. Topographical Analysis

The land structure in the site really affects the way we design the storm water system. You can refer to Figure 39 below. It evidences the fact that our project area is lower compared to the land surrounding it. An in-depth assessment as to how water flows evidences that it generally moves towards a place where the building is located. This goes to mean that we have to come up with a drainage system to manage this flow effectively.

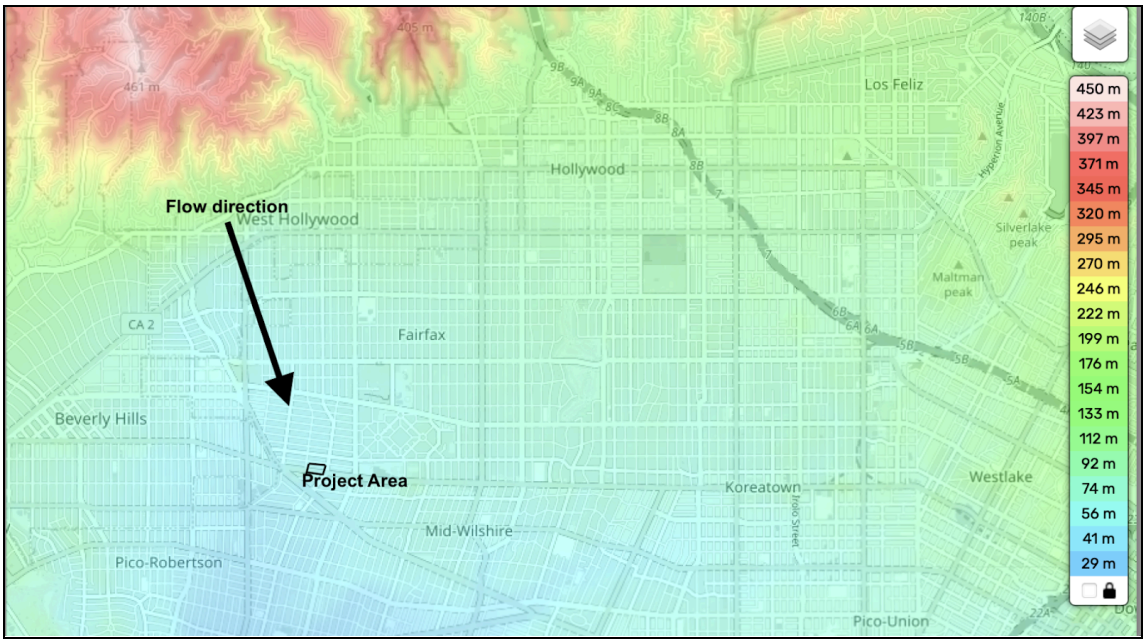

Figure 5.1. Flow Direction and Project Area Topography (taken from Topographic Map)

Site Layout

The site consists of:

- A residential building in a central location.
- Parking lots to the north and east, using permeable materials to recharge the groundwater.
- A south-side terrace and main entrance.
- Clearly defined property boundaries and easements to meet municipal permitting standards.

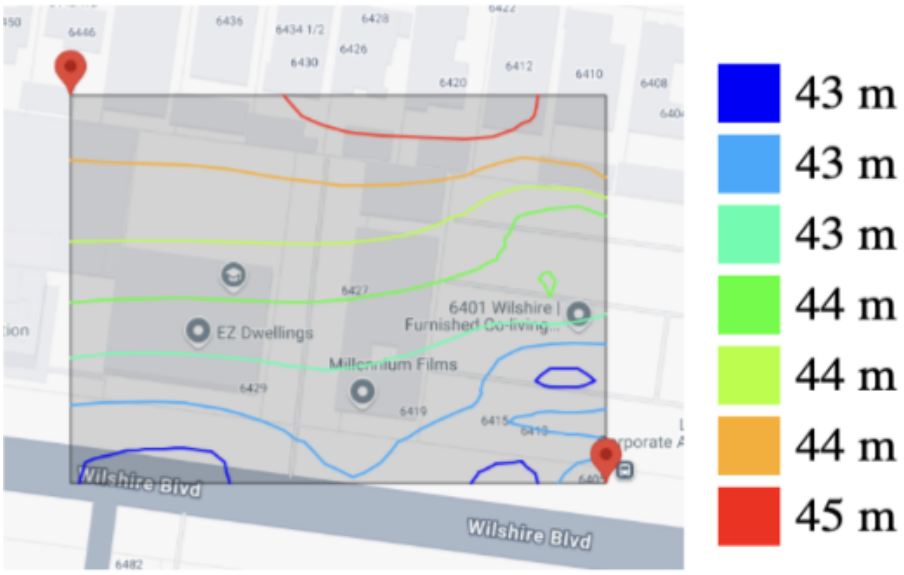

Figure 5.2. Site-Specific Contour Map (taken from Contour Map Creator)

Figure X introduces that the natural slope of the site well will inform where drainage elements and grading adjustments could happen from north at elevation 45 to south at elevation 43. Water flows downhill towards the southern boundary, thereby requiring strategic infrastructure to avoid erosion and overflows.

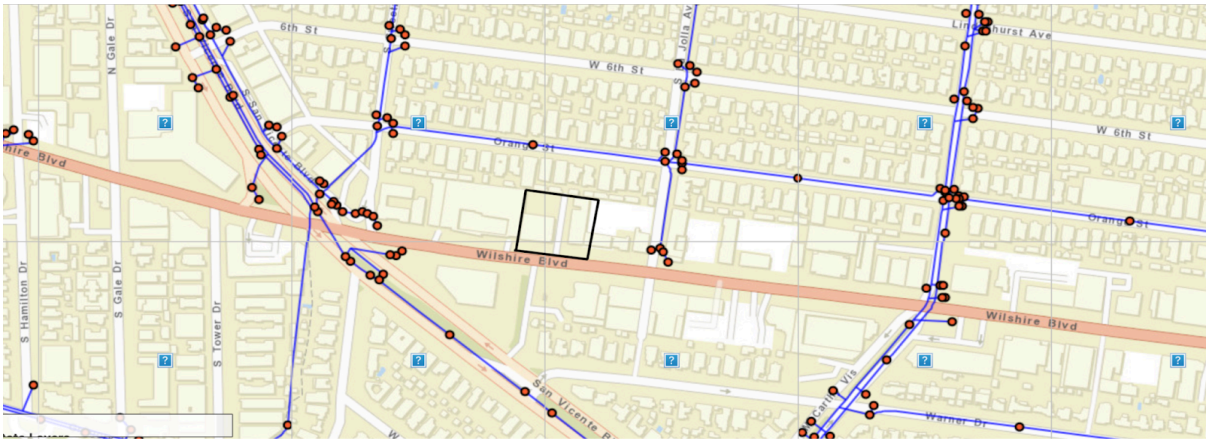

Figure 5.3. Existing Infrastructure and Municipal Drainage System (taken from City of Los Angeles)

Figure X displays the current municipal drainage infrastructure around the area of the project site. More specifically, it gives a close-up view of underground pipes and catch basins that are

hooked up in such a way as to establish a system that handles storm water within the city. This system is of utmost importance in draining water from the urban area, thereby minimizing the chances of the area being flooded and ensuring proper disposal of runoff.

5.4. Grading Plan

Table 5.1. Excavation plan

Site Area	Elevation Range	Action	Explanation
Top Boundary (North)	45	Minor Cut	Use a high point for surface runoff directions.
Building Perimeter	44.8 – 44.5	Fill or Cut	Ensure water flows away from the building, and does not collect near the home foundation.
Parking Lot	44.5 down to 43.0	Fill (upper) & Cut (lower)	Provide a gradual grade to allow surface drainage to the catch basins.
Catch Basin Areas	42.5 – 43.0	Cut	Create local depression to capture water at designated drainage points.
Bottom Boundary (South)	43.0 (or lower)	Cut	Maintain the low elevation in the ground for natural runoff direction.

Grading considerations in planning will control the natural topography of the site in order to divert water away from critical structures. The grading adjustments involve strategic cuts and fills to create appropriate slopes for the management of stormwater.

5.5. Drainage Infrastructure

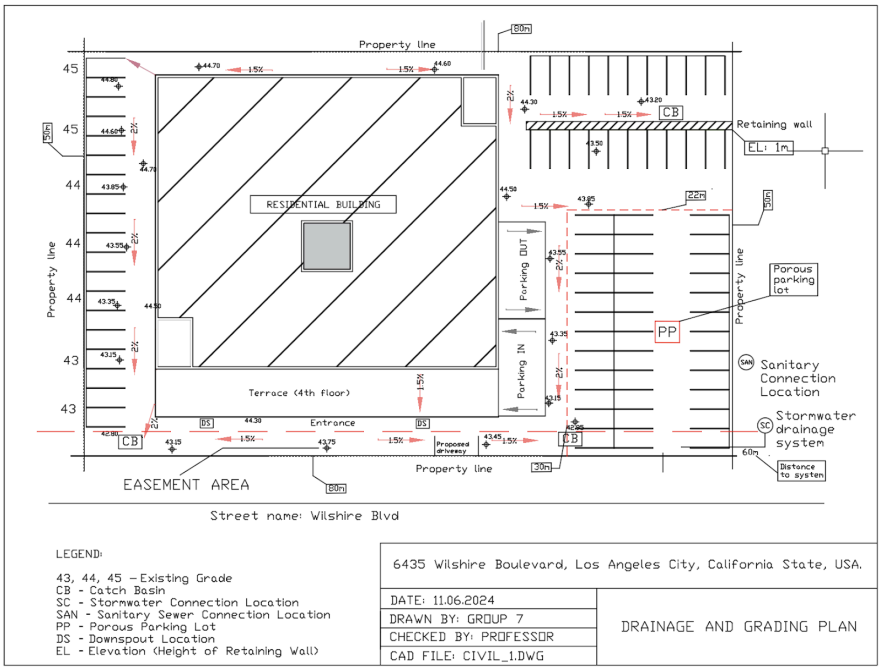

Figure 5.4. Grading and Drainage Plan

The various natural and engineered components of the drainage system merge to handle stormwater in an effective manner. Major elements of a drainage system include:

- Catch Basins (CB): Set at low points for the purpose of catching storm water runoff from parking lots and terraces.
- Downspouts (DS): Around the building, provide for the conveyance of roof runoff into the underground drainage.
- Stormwater and Sanitary Sewer Connections: These are needed to take excess water into the municipality systems in order to dispose of it.
- Porous Parking Lot (PP): Its material is permeable to allow the reduction of surface runoff and increase groundwater recharge.

These features make for easy integration within the municipal infrastructure, hence reducing flood risks and enhancing the effectiveness of water management.

5.6. Structural Elements

- Retaining Wall: Located on the northern edge, it serves the purpose of slope stabilization and erosion control.
- Terrace and Building Entrance: Graded to prevent water accumulation, slopes are terminated at catch basins.

5.7. Design Purpose

This plan is intended to:

1. Capture and convey stormwater through provided infrastructure.
2. Support environmental sustainability through using natural infiltration techniques to reduce runoff.
3. Follow local regulations related to stormwater and wastewater management.
4. Ensure the site is cleared, safe, operational, and ready for construction to start.

5.8. Site Drainage and Runoff Management Plan

The Rational Method serves as a traditional hydrological tool for peak discharge estimation at the project site. A collective analysis of rainfall intensity with ground surface condition together with drainage area permits runoffs to calculate probable totals through this method. Researchers used their findings to create improved stormwater management infrastructure which ups the sustainability level and supports flood reduction while meeting local stormwater standards.

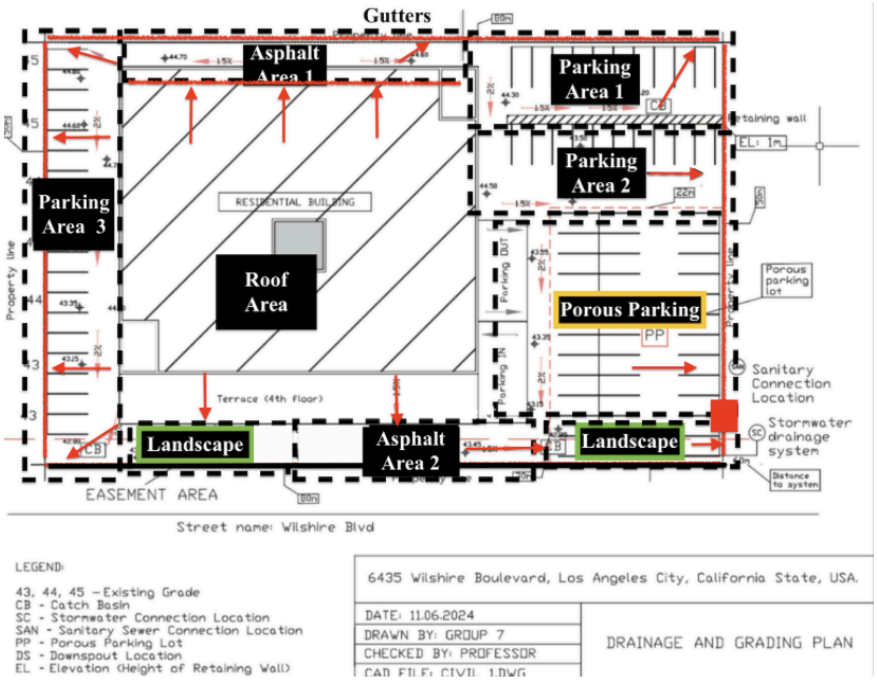

Figure 5.5 . Runoff Management Plan

5.9. Methodology

Calculations followed this procedure:

Classification of Surface Types: Each section of the site is divided into different surface types, as roof areas, areas with asphalt surfaces, parking areas, porous paving.

Determination of Coefficient of Runoff (C): The surface type's permeability ranges a scale from 0.3 for landscaping surfaces to 0.9.

Rain Intensity Calculation: A design rain intensity of 3.132 in/hr was used in a 5-minute, 5-year storm event as per local Los Angeles, California.

Time of Concentration Calculation: Applying Manning's formula and the velocity-based approach, time of concentration for varied sections on the site was calculated.

5.10. Rainfall Intensity Calculation

For a 5-year, 5-minute storm event in Los Angeles, California, the given rainfall depth is 0.261 inches.

The below is the figure from NOAA official site, where rainfall intensity was identified:

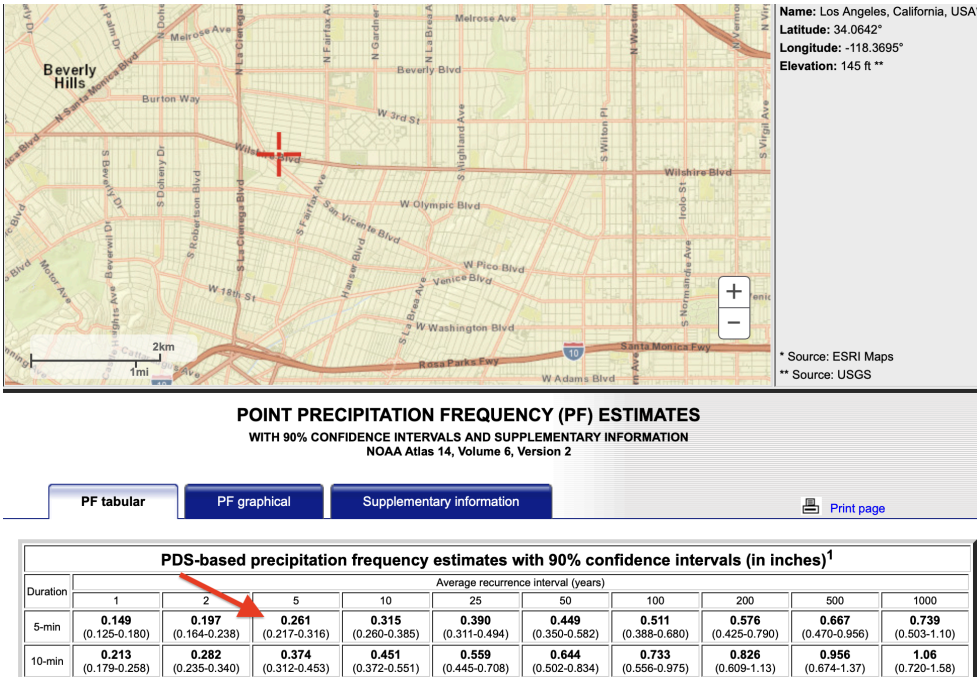

Figure 5.6. Identification of Rainfall Intensity from NOAA

Time of concentration calculation:

1. Sheet Flow Travel Time

$$T_{t1} = \left(\frac{0.933}{I^{0.4}}\right) \times \left[\frac{nL}{\sqrt{S}}\right]^{0.6}$$

I = 3.132 in/hr (rainfall intensity for a 5-year, 5-minute storm)

n = 0.011 (roughness coefficient for smooth asphalt)

L = 50 m (estimated sheet flow length)

S = 0.02 ft/ft (transverse)

2. Shallow Concentrated Flow Travel Time

$$V = 3.28 \times K \times S^{0.5}$$

k = 0.619 (intercept coefficient for paved area)

S = 0.015 ft/ft (longitudinal)

3. Total time:

$$T_T = T_{t1} + V$$

So, calculating for every area we obtain this table:

Table 5.2. Runoff Coefficient Calculation and Total Time of Concentration Table

Surface Type	Length (m)	Width (m)	Area (m²)	Runoff Coefficient (C)	Weighted C	Flow Length (m)	(T_t1)	(T_t2)	(T_c)
Roof Area	42	36	1512	0.9	1360.8	42	1.43	2.81	4.25
Asphalt Area 1	40	5	200	0.9	180.0	40	1.39	2.68	4.07
Asphalt Area 2	20	5	100	0.9	90.0	20	0.92	1.34	2.26
Parking Area 1	35	20	700	0.9	630.0	35	1.28	2.34	3.63
Parking Area 2	30	15	450	0.9	405.0	30	1.17	2.01	3.18
Parking Area 3	25	10	250	0.9	225.0	25	1.05	1.67	2.73
Porous Parking	30	25	750	0.5	375.0	30	8.54	2.01	10.55
Landscape Area 1	10	5	50	0.3	15.0	10	2.91	0.67	3.58
Landscape Area 2	12	6	72	0.3	21.6	12	3.25	0.80	4.05

Using Rational Method Formula:

$$Q = C \times I \times A$$

Q = Peak runoff (CMS or CFS)

C = Runoff coefficient

I = Rainfall intensity (m/hr)

A = Drainage area (hectares)

Table 5.3. Peak Runoff Estimations

Surface Type	Runoff Coefficient (Ç)	Area (ha)	Peak Runoff (CMS)	Peak Runoff (CFS)
Roof Area	0.9	0.1512	0.0109	0.385
Asphalt Area 1	0.9	0.0200	0.0014	0.051
Asphalt Area 2	0.9	0.0100	0.0007	0.025
Parking Area 1	0.9	0.0700	0.0050	0.176
Parking Area 2	0.9	0.0450	0.0032	0.112
Parking Area 3	0.9	0.0250	0.0018	0.063
Porous Parking	0.5	0.0750	0.0030	0.105
Landscape Area 1	0.3	0.0050	0.0001	0.005
Landscape Area 2	0.3	0.0072	0.0002	0.006

So total Peak Runoff for the area (Q) in CFS (Cubic Feet per Second) is 0.928 CFS.

5.11. Trapezoidal Gutter Design

A trapezoidal cross-section was used to manage surface runoff along parking and landscape areas.

Design Parameters:

- Bottom width, b=0.25 m
- Depth, y=0.1 m
- Side slope, z=1
- Slope: 1% (CPC requirement)

Computed Flow Capacity:

- Area, A=0.035 m2
- Wetted perimeter, P=0.533 m

- Hydraulic radius, R=0.0657 m
- Resulting Q=0.038 m3/s

Compliance Check:

- Required peak runoff: 0.0263 m^3/s
- Provided capacity: 0.038 m^3/s — adequate

This confirms the gutter system meets the critical storm event design requirement with a margin of safety.

5.12. Storm Drain Pipe Design

To carry accumulated runoff from the catch basins, a 10 inches internal diameter storm drainage pipe made of HDPE/PVC was chosen.

Design Highlights:

- Pipe Area: A=0.0507 m2
- Wetted Perimeter: P=0.798 m
- Hydraulic Radius: R=0.0635 m
- Manning's n=0.013, Slope S=0.005

Resulting Flow Capacity:

$$Q = \frac{1}{0.013} \times 0.0507 \times (0.0635)^{2/3} \times (0.005)^{1/2} \approx 0.0439\, m^3/s\, (\approx 1.55\, cfs)$$

This exceeds the estimated overall site runoff of 0.928 cfs, which signifies optimal and adequate design.

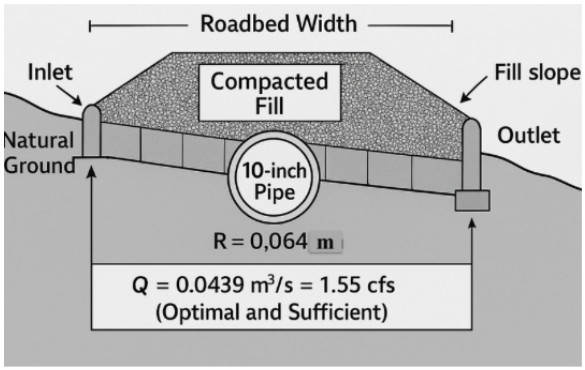

Figure 5.7. Storm drain pipe cross-section

5.13. System Integration and Compliance

Key Major Results include:

- The peak flow design specifications have been successfully achieved for each part.
- The system fulfills drainage requirements specified by CPC together with the specific rules of Los Angeles City.
- PVC/HDPE is the material used in the system which complies with both EPA guidelines and environmental standards.
- Trapezoidal gutter systems successfully collect water runoff before municipal storm drain systems transport it to the public water management facilities.

Design advantages include:

- Additional capacity created through resilience protects structures from flooding events at their most extreme level.
- Drainage systems succeed in preventing soil deterioration while allowing water to enter the soil.
- The cost remains affordable when standard construction processes combined with regular materials are used as the building elements.

A general summary of storm drainage system design parameters is shown in this table together with dimensional specifications and flow capability requirements consistent with CPC and local code.

Table 5.4. Stormwater Conveyance Components and Design Specifications

Component	Size/Type	Slope	Capacity	Compliance
Roof Gutters	6-inch K-style	1/8 in/ft	~1.5 cfs	CPC 1101.12
Downspouts	3 (0.5 cfs each)	Vertical	~1.5 cfs total	CPC 1101.12
Parking Gutters	Trapezoidal (0.25×0.1 m)	1%	1.34 cfs	CPC 1101.7
Inlets	Surface grates	N/A	N/A	Local code
Drain Pipe	10-inch PVC	0.5%	1.55 cfs	CPC 1101.8

5.14. Conclusion

Based on the site topography and existing infrastructure, the environmental section describes how to design a stormwater management system for a residential project. To effectively manage runoff, and prevent water accumulation, we created a complete grading and drainage scheme. Our result is that strategically placed catch basins and permeable pavement mitigate surface runoff and promote groundwater recharge. We ensure that the project meets environmental and functional requirements, complies with regional regulations, and of course, promotes long-term sustainability. These efforts should provide a solid foundation for a sustainable, environmentally friendly stormwater system that supports environmental conservation and urban resilience.

6. Construction Management

6.1. Project charter

Table 6.1. Project charter

General information		
Project title	**12-story high-rise residential-commercial building in Los Angeles, CA, USA**	
Project start date: October 2024		Project end date: September 2026
Purpose	The objective is to build a high-rise residential structure that complies with the most recent structural, geotechnical, and LEED criteria in a Downtown commercial district. **Advantages:** The residence will offer pleasant flats to its occupants. Environmentally conscious building practices. Trade is essential to the downtown region.	
Project scope	The development of an original design incorporating engineering, management, geotechnical, and architectural elements. ● Monitoring and managing the building process. ● Supply and disposal of materials. ● Maintenance of buildings. ● Records	
Project Outcomes	1. A residential structure with 12 stories 2. Patio 3. Parking space available 4. One floor is used for business 5. Rooftop level entry	
Risk and Problems	● Possibility of extra expenditures ● hazards to the environment ● Improvements to the design made during construction ● Unexpected foundation base and soil problems ● Workplace safety risks that arise during building process	
Assumptions	● The structure will be built according to a schedule.	

<table>
<tr><td></td><td colspan="3">Every contractor, worker, and stakeholder completes the project with pleasant outcomes.
The structure's construction will be secure and robust during earthquakes.
Over 150 individuals will be able to live in flats in this skyscraper.
Sales of residences and other commercial activity will finance the project.
There will be sufficient space for safe car movement.</td></tr>
<tr><td>Planned budget</td><td colspan="3">$55,683,354.13</td></tr>
<tr><td rowspan="8">Milestones</td><td>Stage</td><td>Deadline</td><td>Status</td></tr>
<tr><td>Preliminary site evaluation</td><td>15.09.2024</td><td>Done</td></tr>
<tr><td>Financing calculation</td><td>10.10.2024</td><td>Done</td></tr>
<tr><td>Primary construction design and confirmation</td><td>27.12.2024</td><td>Done</td></tr>
<tr><td>Final construction design and confirmation</td><td>07.01.2025</td><td>Pending</td></tr>
<tr><td>Structural part</td><td>23.04.2026</td><td>Pending</td></tr>
<tr><td>Finishing part</td><td>15.07.2024</td><td>Pending</td></tr>
<tr><td>Construction project closure</td><td>27.08.2026</td><td>Pending</td></tr>
<tr><td>Team members</td><td colspan="3">Kamila Nuraliyeva, Madiyar Assylkhanov
Aidana Ordabayeva, Assylzada Urazova,
Aidos Kyrkynbay, Dias Mukhanov</td></tr>
</table>

6.2. Feasibility study

Before starting every construction project a thorough analysis should be undertaken. As a 20-story high-rise residential building is a large and complex project, preliminary investigation should be done, proving that project is viable. A feasibility study below analyzes each aspect of the future project.

Site analysis: The selected site is located in the Downtown business area, meaning there are shopping malls, restaurants and office complexes near. The construction site has enough space to carry out construction processes and place material stockpiles. Also, this space will be used after construction for parking and the courtyard. The building will be located on the south side of the site for safe and quick movement of the vehicles and convenient exit/entrance to main streets.

Design and development plan: From initial stages of construction the preliminary design of the residential building was developed taking into account the future improvements. The 3D design was created using building codes and requirements, particularly California Building Codes and Los Angeles Building Codes, which needs specific approvals. The structural, geotechnical, energy efficiency and LEED standards required to be followed for better quality and maintenance in seismic zone.

Environmental impact assessment: As Los Angeles is in a seismic zone and due to the complexity of residential building the environmental regulations should be complied, according to California Environmental Quality Act. The potential risks related to environmental causes and their mitigation ways were identified. During the construction process the waste materials stockpile was considered, which will be recycled in future. Also, disposal management will be developed for usage of residents to minimize negative impacts from waste materials.

Legal analysis: The legal requirements should be maintained, in order to face all regulations and compliances. As it mentioned design and environmental analysis, at the beginning stages approvals are needed from local government. Also, in the planning phase clear and comprehensive contracts with contractors, property agreements and document approvals should be completed. It needs consultation of legal professionals to follow Los Angeles construction laws. Also, workers safety and rights should be considered according to Labor Laws.

Economic impact analysis: The construction phases of residential building will create jobs both directly and indirectly, including engineers, construction workers, architects, project managers and other services related to material transportation. Also, this construction positively affects infrastructure development in the selected area, contributing to improvement of sector growth. The 20-story residential building will provide more than 400 people with apartments and the first floor will be used for commercial purposes. It is suggested that the minimum rent cost

for one apartment for a month will cost $2700, price per square foot planned to be $900 and area for commercial purposes will be rent starting from $1200 per square foot. The payback period is planned to be in the next few years after construction.

Project schedule and timeline: After determining the project scope the work breakdown structure and scheduling were improved for effective work distribution and organization of project stages. During the creation of timetable potential delay days because of weather conditions, holidays and other non-working days were taken into consideration. Nevertheless, the project will be completed in an approximate time range.

Based on feasibility study the construction project can be completed successfully and serve local residents with high-quality apartments. Also, due to its deliverables and benefits stakeholders, investors and users will be satisfied with the result. The well-chosen location of the 20-story residential building faces all the needs and demands of residents. Thus, this project is viable in every aspect, which is provided through feasibility study.

6.3. Cost/benefit analysis - RS Means

It is important to prepare an accurate cost estimation, thus it is one of the challenges faced in the construction industry. Nowadays, there are sufficient strategies, techniques and softwares to get detailed cost estimation of the project, in order to mitigate the financial losses. To analyze the cost for high-rise residential building the RSMeans (RSM) was used. It is reliable to calculate the construction cost and determine productivity benchmark, which is marketed by the Gordian Group (Nicolas, Monjurul, & Ming, 2018). This software purposed to give up-to-date information about cost to estimate and control general project budget for engineers, architects and contractors. With the help of RSMeans users get an opportunity to find productivity rates overhead and profit rates with a related time and location of the construction project (Nicolas, Monjurul, & Ming, 2018).

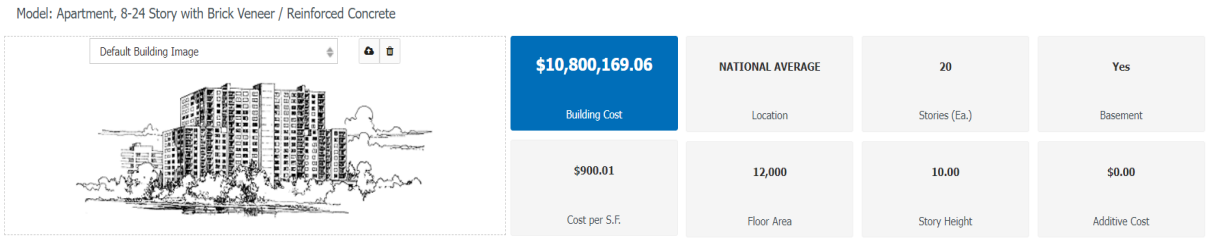

Figure 6.1. Estimated values from RSMeans

A 20-story residential building with a basement overall cost according to RSMeans is shown in the figure above. It seems that cost per square foot of current construction is higher than average cost per square foot in Los Angeles ($550-$700) (Drexell Luxury Homes, 2023). However, taking into consideration the presence of the basement, high quality reinforced materials, location and other benefits and deliverables, which are mentioned in project charter, the cost is appropriate.

After, the materials cost was determined per square foot, taking into account the average cost for cities in the USA.

Table 6.2. Cost Estimation from RSMeans

		Quantity	**% of Total**	**Cost per S.F.**	**Cost**
A	Substructure		5.54%	$37.60	$451,251.65
A1010	Standard Foundations			$0.70	$8,391.72
	Pile caps, 6 piles, 8' - 6" x 5' - 6" x 37", 40 ton capacity, 14" column size, 458 K column	1.65		$0.25	$3,053.79
	Pile caps, 12 piles, 11' - 6" x 8' - 6" x 49", 40 ton capacity, 19" column size, 900 K column	1.24		$0.44	$5,337.93
A1020	Special Foundations			$22.47	$269,621.93
	Steel H piles, 100' long, 400K load, end bearing, 6 pile cluster	1.65		$5.34	$64,055.17
	Steel H piles, 100' long, 800K load, end bearing, 12 pile cluster	1.24		$8.01	$96,082.76
	Grade beam, 30' span, 52" deep, 14" wide, 12 KLF load	542		$9.12	$109,484.00
A1030	Slab on Grade			$0.29	$3,480.00

	Slab on grade, 4" thick, non industrial, reinforced	600		$0.29	$3,480.00
A2010	Basement Excavation			$0.19	$2,280.00
	Excavate and fill, 10,000 SF, 8' deep, sand, gravel, or common earth, on site storage	600		$0.19	$2,280.00
A2020	Basement Walls			$13.96	$167,478.00
	Foundation wall, CIP, 12' wall height, pumped, .591 CY/LF, 28.79 PLF, 16" thick	542		$13.96	$167,478.00
B	Shell		65.94 %	$447.90	$5,374,750.74
B1010	Floor Construction			$80.27	$963,183.26
	Cast-in-place concrete column, 24" square, tied, 900K load, 12' story height, 567 lbs/LF, 4000PSI	1166.47		$18.96	$227,462.24
	Cast-in-place concrete column, 12", square, tied, minimum reinforcing, 150K load, 10'-14' story height, 135 lbs/LF, 4000PSI	1718.14		$9.97	$119,582.54
	Cast-in-place concrete column, 16", square, tied, minimum reinforcing, 300K load, 10'-14' story height, 240 lbs/LF, 4000PSI	1718.14		$13.67	$164,082.37
	Cast-in-place concrete column, 20", square, tied, minimum reinforcing, 500K load, 10'-14' story height, 375 lbs/LF, 4000PSI	1718.14		$19.54	$234,526.11

	Cast-in-place concrete beam and slab, 7.5" slab, two way, 12" column, 25'x25' bay, 40 PSF superimposed load, 149 PSF total load	11400		$17.38	$208,620.00
	Flat slab, concrete, with drop panels, 6" slab/2.5" panel, 12" column, 15'x15' bay, 75 PSF superimposed load, 153 PSF total load	600		$0.74	$8,910.00
B1020	Roof Construction			$0.83	$9,960.00
	Roof, concrete, beam and slab, 25'x25' bay, 40 PSF superimposed load, 20" deep beam, 9" slab, 152 PSF total load	600		$0.83	$9,960.00
B2010	Exterior Walls			$297.74	$3,572,864.00
	Brick wall, composite double wythe, standard face/CMU back-up, 8" thick, perlite core fill, 3" XPS	86720		$297.74	$3,572,864.00
B2020	Exterior Windows			$63.72	$764,581.33
	Windows, aluminum, sliding, standard glass, 5' x 3'	1445.33		$63.72	$764,581.33
B2030	Exterior Doors			$2.97	$35,658.21
	Door, aluminum & glass, without transom, wide stile, hardware, 3'-0" x 7'-0" opening	0.33		$0.11	$1,315.86
	Door, aluminum & glass, without transom, non-standard, double door, hardware, 6'-0" x 7'-0" opening	0.16		$0.11	$1,361.38

	Door, aluminum & glass, sliding patio, tempered glass, premium, 6'-0" x 7'-0" opening	10.17		$2.75	$32,980.97
B3010	Roof Coverings			$2.38	$28,503.94
	Roofing, single ply membrane, EPDM, 60 mils, loosely laid, stone ballast	600		$0.08	$1,008.00
	Insulation, rigid, roof deck, extruded polystyrene, 40 PSI compressive strength, 4" thick, R20	600		$0.21	$2,526.00
	Roof edges, aluminum, duranodic, .050" thick, 6" face	542		$1.27	$15,284.40
	Flashing, aluminum, no backing sides, .019"	542		$0.25	$3,046.04
	Gravel stop, aluminum, extruded, 4", mill finish, .050" thick	542		$0.55	$6,639.50
C	Interiors		11.96 %	$81.27	$975,254.81
C1010	Partitions			$46.63	$559,563.73
	Concrete block (CMU) partition, light weight, hollow, 6" thick, no finish	3200		$2.77	$33,280.00
	Metal partition, 5/8"fire rated gypsum board face, 1/4" sound deadening gypsum board, 2-1/2" @ 24", same opposite face, no insulation	7466.66		$4.21	$50,549.33
	Furring 1 side only, steel channels, 3/4", 16" OC	6400		$1.38	$16,512.00

	Gypsum board, 1 face only, exterior sheathing, fire resistant, 1/2"	6400		$0.55	$6,592.00
	Add for the following: taping and finishing	6400		$0.36	$4,288.00
	1/2" fire rated gypsum board, taped & finished, painted on metal furring	86720		$37.36	$448,342.40
C1020	Interior Doors			$8.55	$102,545.46
	Door, single leaf, kd steel frame, hollow metal, commercial quality, flush, 3'-0" x 7'-0" x 1-3/8"	83.91		$8.55	$102,545.46
C1030	Fittings			$10.32	$123,817.54
	Cabinets, residential, base, hardwood, 1 top drawer & 1 door below x 24" W	61.07		$2.60	$31,179.23
	Cabinets, residential, wall, two doors x 48" wide	30.53		$1.76	$21,132.25
	Cabinets, residential, counter top-laminated plastic, stock, economy	1810.28		$5.96	$71,506.06
C2010	Stair Construction			$3.74	$44,838.62
	Stairs, steel, pan tread for conc in-fill, picket rail,12 risers w/ landing	3.55		$3.74	$44,838.62
C3010	Wall Finishes			$2.22	$26,698.66
	Painting, interior on plaster and drywall, walls & ceilings, roller work, primer & 2 coats	20266.66		$1.50	$18,037.33
	Ceramic tile, thin set, 4-1/4" x 4-1/4"	1066.66		$0.72	$8,661.33
C3020	Floor Finishes			$5.28	p$63,310.80

	Carpet tile, nylon, fusion bonded, 18" x 18" or 24" x 24", 24 oz	6360		$2.41	$28,874.40
	Carpet tile, nylon, fusion bonded, 18" x 18" or 24" x 24", 35 oz	3000		$1.30	$15,630.00
	Vinyl, composition tile, maximum	1440		$0.37	$4,406.40
	Tile, ceramic natural clay	1200		$1.20	$14,400.00
C3030	Ceiling Finishes			$4.54	$54,480.00
	Gypsum board ceilings, 1/2" fire rated gypsum board, painted and textured finish, 7/8"resilient channel furring, 24" OC support	12000		$4.54	$54,480.00
D	Services		16.32 %	$110.87	$1,330,432.39
D1010	Elevators and Lifts			$13.93	$167,172.41
	Traction, geared passenger, 3500 lb,15 floors, 10' story height, 2 car group, 350 FPM	0.33		$13.93	$167,172.41
D2010	Plumbing Fixtures			$6.67	$80,070.22
	Kitchen sink w/trim, countertop, PE on CI, 24" x 21", single bowl	10.17		$1.29	$15,421.66
	Laundry sink w/trim, PE on CI, black iron frame, 24" x 20", single compt	0.99		$0.15	$1,797.52
	Service sink w/trim, PE on CI, corner floor, 28" x 28", w/rim guard	1.24		$0.34	$4,065.52
	Bathroom, three fixture, 2 wall plumbing, lavatory, water closet & bathtub, stand alone	10.17		$4.90	$58,785.52

D2020	Domestic Water Distribution			$8.42	$101,029.66
	Electric water heater, commercial, 100< F rise, 50 gallon tank, 9 KW 37 GPH	10.17		$8.42	$101,029.66
D2040	Rain Water Drainage			$0.25	$3,035.17
	Roof drain, DWV PVC, 4" diam, diam, 10' high	0.41		$0.05	$602.07
	Roof drain, DWV PVC, 4" diam, for each additional foot add	62.06		$0.20	$2,433.10
D3010	Energy Supply			$8.24	$98,880.00
	Apartment building heating system, fin tube radiation, forced hot water, 30,000 SF area,300,000 CF vol	12000		$8.24	$98,880.00
D3030	Cooling Generating Systems			$9.49	$113,880.00
	Packaged chiller, air cooled, with fan coil unit, medical centers, 40,000 SF, 93.33 ton	12000		$9.49	$113,880.00
D4010	Sprinklers			$3.02	$36,276.37
	Wet pipe sprinkler systems, steel, light hazard, 1 floor, 10,000 SF	792		$0.25	$3,001.68
	Wet pipe sprinkler systems, steel, light hazard, each additional floor, 10,000 SF	11196		$2.60	$31,236.84
	Standard High Rise Accessory Package 16 story	0.07		$0.17	$2,037.85
D4020	Standpipes			$22.96	$275,550.00
	Wet standpipe risers, class III, steel, black, sch 40, 6" diam pipe, 1 floor	15		$20.06	$240,750.00

	Fire pump, electric, with controller, 5" pump, 100 HP, 1000 GPM	1		$2.58	$31,000.00
	Fire pump, electric, for jockey pump system, add	1		$0.32	$3,800.00
D5010	Electrical Service/Distribution			$24.20	$290,450.00
	Underground service installation, includes excavation, backfill, and compaction, 100' length, 4' depth, 3 phase, 4 wire, 277/480 volts, 2000 A	2		$8.65	$103,800.00
	Feeder installation 600 V, including RGS conduit and XHHW wire, 2000 A	200		$8.18	$98,200.00
	Switchgear installation, incl switchboard, panels & circuit breaker, 120/208 V, 3 phase, 2000 A	2		$7.37	$88,450.00
D5020	Lighting and Branch Wiring			$9.43	$113,188.00
	Receptacles incl plate, box, conduit, wire, 10 per 1000 SF, 1.2 W per SF, with transformer	12000		$3.81	$45,720.00
	Wall switches, 2.5 per 1000 SF	12000		$0.59	$7,080.00
	Miscellaneous power, 2 watts	12000		$0.56	$6,720.00
	Central air conditioning power, 3 watts	12000		$0.62	$7,440.00
	Motor installation, three phase, 460 V, 15 HP motor size	4		$0.87	$10,480.00
	Motor feeder systems, three phase, feed to 200 V 5 HP, 230 V 7.5 HP, 460 V 15 HP, 575 V 20 HP	400		$0.38	$4,548.00

	Incandescent fixtures recess mounted, type A, 1 watt per SF, 8 FC, 6 fixtures per 1000 SF	12000		$2.60	$31,200.00
D5030	Communications and Security			$4.24	$50,900.56
	Communication and alarm systems, fire detection, addressable, 100 detectors, includes outlets, boxes, conduit and wire	0.14		$0.97	$11,678.90
	Fire alarm command center, addressable with voice, excl. wire & conduit	1		$1.04	$12,425.00
	Communication and alarm systems, includes outlets, boxes, conduit and wire, intercom systems, 100 stations	0.11		$1.26	$15,082.76
	Communication and alarm systems, includes outlets, boxes, conduit and wire, master TV antenna systems, 30 outlets	0.11		$0.39	$4,693.90
	Internet wiring, 2 data/voice outlets per 1000 S.F.	10.8		$0.58	$7,020.00
E	Equipment & Furnishings		0.24%	$1.62	$19,381.41
E1090	Other Equipment			$1.62	$19,381.41
	Architectural equipment, appliances, range, 30" free standing, 1 oven, gas, average	10.17		$1.03	$12,408.58
	Architectural equipment, appliances, dish washer, built-in, 2 cycles, economy	10.17		$0.58	$6,972.83
F	Special Construction		0%		
G	Building Sitework		0%		

	SubTotal		100%	$679.26	$8,151,071.00
	Contractor Fees (GC,Overhead,Profit)		25.00 %	$169.81	$2,037,767.75
	Architectural Fees		6.00%	$50.94	$611,330.33
	User Fees		0.00%	$0.00	$0.00
	Total Building Cost			$900.01	$10,800,169.08

The table above shows total net cost including materials, contractor fees, architectural fees, labor and overhead.

6.4. Work Breakdown Structure

The project scope is work that should be done in order to get the desired output. Changes will occur, thus the project scope management involves the processes to manage the changes and to ensure that the project will be conducted on time and within the planned budget. The scope of the project is determined by work breakdown structure (WBS), which include alterations through formal procedures. WBS plays an important role in planning the whole framework of the construction project. It is a product-oriented grouping of the elements of the project in a graphical way for the organization and subdivision of the entire project scope (Tejaswini, Swetha, & Rajendra 2017). Therefore, WBS is an essential project tool, which requires significant planning and considerable thought to be developed and implemented, and also to minimize influence of changes of subsequent parts as it applies to the wide range of project activities. Moreover, WBS is considered as a base for planning, scheduling, estimation and control procedures. A comprehensive WBS increases the probability of the successful completion of the project.

The PMBOK Guide was followed to create the WBS for current residential building construction. The main 5 milestones were subdivided into appropriate processes. The Lucidchart application was used to design the WBS scheme.

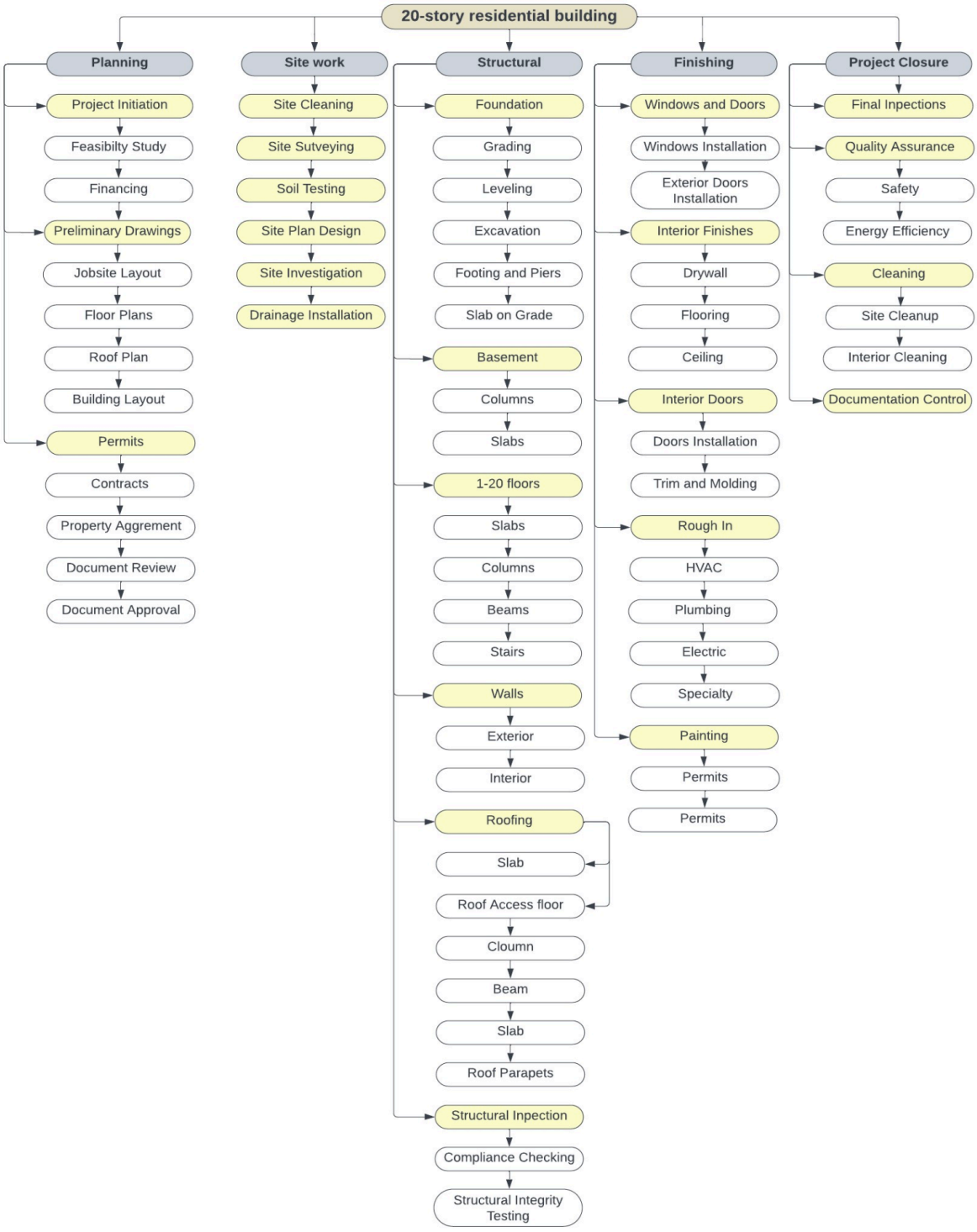

Figure 6.2. WBS for construction of residential building

6.5. Scheduling

Project scheduling is also one the important parts of the construction activities. To manage, organize and complete projects in a timely and financially manner with high quality results, clear scheduling is needed. Also, it influences the successful conduction of the construction, as proper schedule keeps the project on track, assigns responsibilities and resources to appropriate disciplines. It results in cost reduction, mitigation of time, budget and delays related risks (Darshana & Nagare, 2021).

To create an effective schedule and Gantt chart the Microsoft Project software was used. Due to its provided tools, simple interface, flexibility and convenience the detailed Gantt chart was designed. During the creation of it, non-working days and official holiday days in Los-Angeles were taken into consideration. Also, with the help of MS project the critical path was determined. It is shown in the red color sequence of the activities. The duration of the entire project is 669 days.

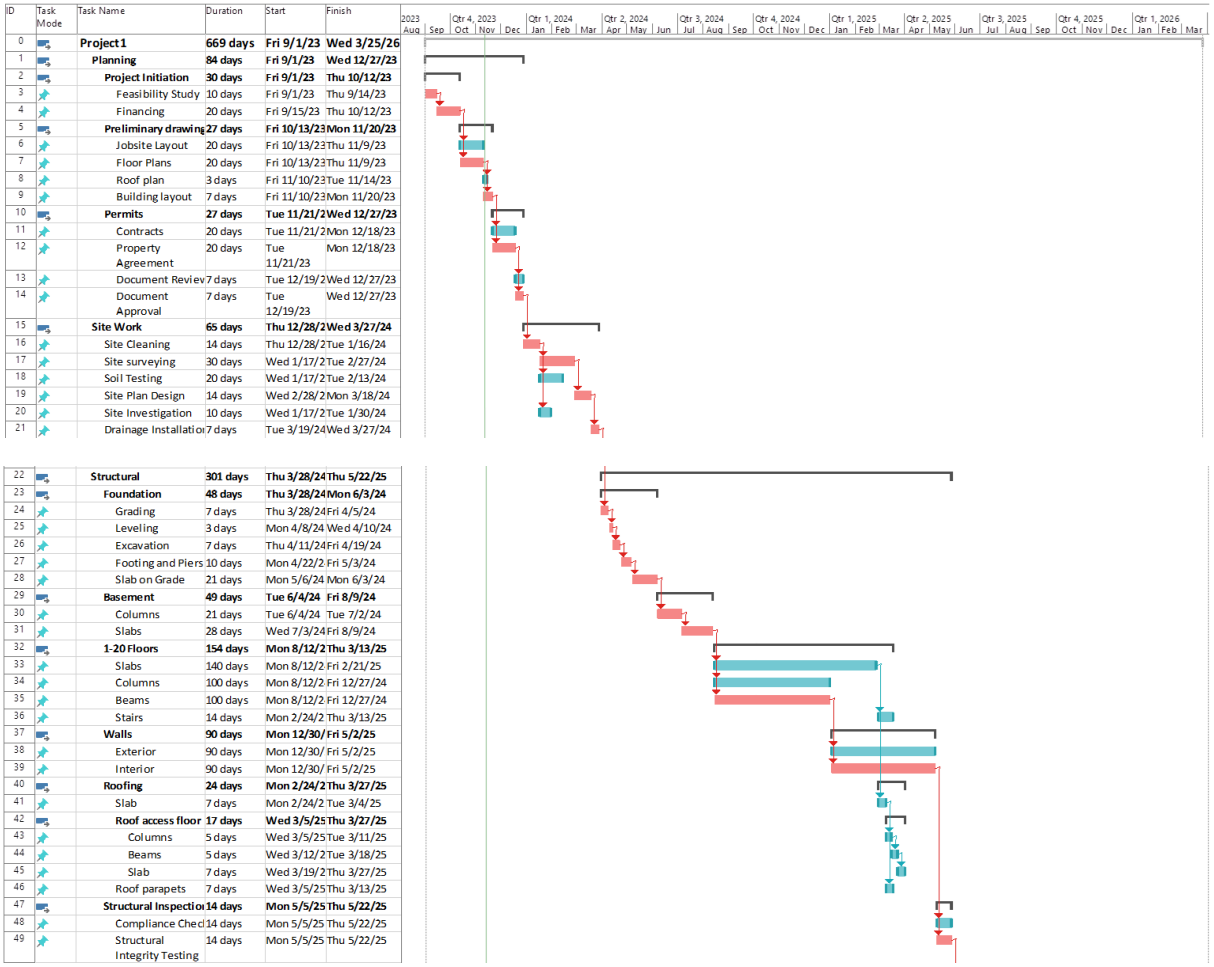

ID	Task Mode	Task Name	Duration	Start	Finish
0		**Project1**	**669 days**	**Fri 9/1/23**	**Wed 3/25/26**
1		**Planning**	**84 days**	**Fri 9/1/23**	**Wed 12/27/23**
2		**Project Initiation**	**30 days**	**Fri 9/1/23**	**Thu 10/12/23**
3		Feasibility Study	10 days	Fri 9/1/23	Thu 9/14/23
4		Financing	20 days	Fri 9/15/23	Thu 10/12/23
5		**Preliminary drawing**	**27 days**	**Fri 10/13/23**	**Mon 11/20/23**
6		Jobsite Layout	20 days	Fri 10/13/23	Thu 11/9/23
7		Floor Plans	20 days	Fri 10/13/23	Thu 11/9/23
8		Roof plan	3 days	Fri 11/10/23	Tue 11/14/23
9		Building layout	7 days	Fri 11/10/23	Mon 11/20/23
10		**Permits**	**27 days**	**Tue 11/21/2**	**Wed 12/27/23**
11		Contracts	20 days	Tue 11/21/2	Mon 12/18/23
12		Property Agreement	20 days	Tue 11/21/23	Mon 12/18/23
13		Document Reviev	7 days	Tue 12/19/2	Wed 12/27/23
14		Document Approval	7 days	Tue 12/19/23	Wed 12/27/23
15		**Site Work**	**65 days**	**Thu 12/28/2**	**Wed 3/27/24**
16		Site Cleaning	14 days	Thu 12/28/2	Tue 1/16/24
17		Site surveying	30 days	Wed 1/17/2	Tue 2/27/24
18		Soil Testing	20 days	Wed 1/17/2	Tue 2/13/24
19		Site Plan Design	14 days	Wed 2/28/2	Mon 3/18/24
20		Site Investigation	10 days	Wed 1/17/2	Tue 1/30/24
21		Drainage Installatio	7 days	Tue 3/19/24	Wed 3/27/24
22		**Structural**	**301 days**	**Thu 3/28/24**	**Thu 5/22/25**
23		**Foundation**	**48 days**	**Thu 3/28/24**	**Mon 6/3/24**
24		Grading	7 days	Thu 3/28/24	Fri 4/5/24
25		Leveling	3 days	Mon 4/8/24	Wed 4/10/24
26		Excavation	7 days	Thu 4/11/24	Fri 4/19/24
27		Footing and Piers	10 days	Mon 4/22/2	Fri 5/3/24
28		Slab on Grade	21 days	Mon 5/6/24	Mon 6/3/24
29		**Basement**	**49 days**	**Tue 6/4/24**	**Fri 8/9/24**
30		Columns	21 days	Tue 6/4/24	Tue 7/2/24
31		Slabs	28 days	Wed 7/3/24	Fri 8/9/24
32		**1-20 Floors**	**154 days**	**Mon 8/12/2**	**Thu 3/13/25**
33		Slabs	140 days	Mon 8/12/2	Fri 2/21/25
34		Columns	100 days	Mon 8/12/2	Fri 12/27/24
35		Beams	100 days	Mon 8/12/2	Fri 12/27/24
36		Stairs	14 days	Mon 2/24/2	Thu 3/13/25
37		**Walls**	**90 days**	**Mon 12/30/**	**Fri 5/2/25**
38		Exterior	90 days	Mon 12/30/	Fri 5/2/25
39		Interior	90 days	Mon 12/30/	Fri 5/2/25
40		**Roofing**	**24 days**	**Mon 2/24/2**	**Thu 3/27/25**
41		Slab	7 days	Mon 2/24/2	Tue 3/4/25
42		**Roof access floor**	**17 days**	**Wed 3/5/25**	**Thu 3/27/25**
43		Columns	5 days	Wed 3/5/25	Tue 3/11/25
44		Beams	5 days	Wed 3/12/2	Tue 3/18/25
45		Slab	7 days	Wed 3/19/2	Thu 3/27/25
46		Roof parapets	7 days	Wed 3/5/25	Thu 3/13/25
47		**Structural Inspectio**	**14 days**	**Mon 5/5/25**	**Thu 5/22/25**
48		Compliance Chec	14 days	Mon 5/5/25	Thu 5/22/25
49		Structural Integrity Testing	14 days	Mon 5/5/25	Thu 5/22/25

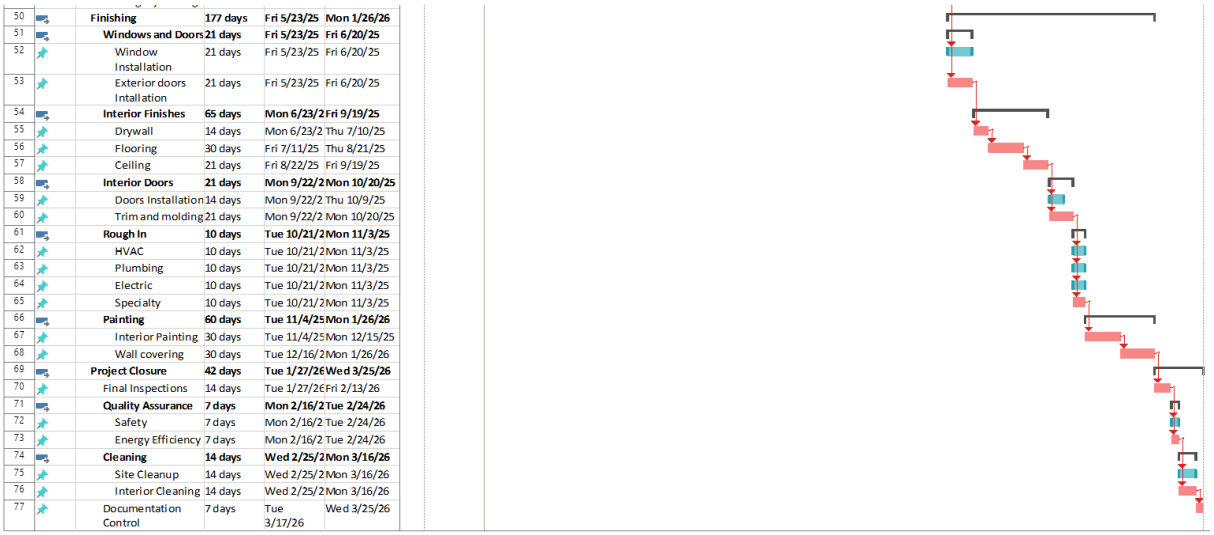

50	**Finishing**	**177 days**	**Fri 5/23/25**	**Mon 1/26/26**	
51	**Windows and Doors**	**21 days**	**Fri 5/23/25**	**Fri 6/20/25**	
52	Window Installation	21 days	Fri 5/23/25	Fri 6/20/25	
53	Exterior doors Intallation	21 days	Fri 5/23/25	Fri 6/20/25	
54	**Interior Finishes**	**65 days**	**Mon 6/23/2**	**Fri 9/19/25**	
55	Drywall	14 days	Mon 6/23/2	Thu 7/10/25	
56	Flooring	30 days	Fri 7/11/25	Thu 8/21/25	
57	Ceiling	21 days	Fri 8/22/25	Fri 9/19/25	
58	**Interior Doors**	**21 days**	**Mon 9/22/2**	**Mon 10/20/25**	
59	Doors Installation	14 days	Mon 9/22/2	Thu 10/9/25	
60	Trim and molding	21 days	Mon 9/22/2	Mon 10/20/25	
61	**Rough In**	**10 days**	**Tue 10/21/2**	**Mon 11/3/25**	
62	HVAC	10 days	Tue 10/21/2	Mon 11/3/25	
63	Plumbing	10 days	Tue 10/21/2	Mon 11/3/25	
64	Electric	10 days	Tue 10/21/2	Mon 11/3/25	
65	Specialty	10 days	Tue 10/21/2	Mon 11/3/25	
66	**Painting**	**60 days**	**Tue 11/4/25**	**Mon 1/26/26**	
67	Interior Painting	30 days	Tue 11/4/25	Mon 12/15/25	
68	Wall covering	30 days	Tue 12/16/2	Mon 1/26/26	
69	**Project Closure**	**42 days**	**Tue 1/27/26**	**Wed 3/25/26**	
70	Final Inspections	14 days	Tue 1/27/26	Fri 2/13/26	
71	**Quality Assurance**	**7 days**	**Mon 2/16/2**	**Tue 2/24/26**	
72	Safety	7 days	Mon 2/16/2	Tue 2/24/26	
73	Energy Efficiency	7 days	Mon 2/16/2	Tue 2/24/26	
74	**Cleaning**	**14 days**	**Wed 2/25/2**	**Mon 3/16/26**	
75	Site Cleanup	14 days	Wed 2/25/2	Mon 3/16/26	
76	Interior Cleaning	14 days	Wed 2/25/2	Mon 3/16/26	
77	Documentation Control	7 days	Tue 3/17/26	Wed 3/25/26	

Figure 6.3. Gantt Chart for the residential building construction

6.6. Risk management

Each construction project is associated with taking the risks, so contractors and owners should prepare for the potential occurrence of any cases. In order to avoid bankruptcy and stopping the project risk management analysis should be conducted. In the construction industry, the identification of risks is based on determining types of risks, their characteristics and estimation of probability. The effective risk management does not mean determining the risks after or during the construction processes, but including the protection against negative aspects of all risks and comprehensive analysis. After that maximum beneficial decisions will be taken using analytical and mathematical tools. Taking into account all parameters and probability of the risks the investors decide to preserve risk assurance, neutrality toward risk or aversion of it. The final assessment of the risk management also considers the impact of each risk on the environment (Pawel, 2021).

The table below shows types of risks, their description, probability and severity level and their mitigation measures. It should be noted that types of risks were identified by researching seismic conditions, governmental regulations and their frequency in previous residential projects construction in Los Angeles.

Table 6.3. Risk Assessment

Types of risks		**Description of the risks**	**ProTable 5.2.bability**	**Severity**	**Mitigation measures**

Design	D1	Inaccurate architectural and engineering designs	Medium	High	Effective collaboration between clients and leaders
	D2	Design changes during construction	Medium	High	Enhance interdisciplinary coordination during design
	D3	Non-compliance with building codes	Low	High	Regular code reviews
Financial	F1	Budget overruns	Medium	Medium	Define well the scope of the work
	F2	Fluctuations in cost of material and labor	Medium	Medium	Explore alternative or unconventional materials
	F3	Delays in securing financing	Low	Medium	Have a written record of your terms
Environmental	E1	Weather-related delays and disruptions	Medium	Medium	Include in contract documents about expected weather conditions
	E2	Environmental impact assessments and regulatory compliance	Medium	Medium	Investing in sustainable materials and techniques
	E3	Unforeseen environmental issues at the construction site	Low	High	Find any possible dangers
Schedule	Sc 1	Delays in obtaining approvals	Medium	High	Finalize clear and detailed plan and schedule
	Sc 2	Labor shortages	Medium	High	Improve recruitment strategies
	Sc 3	Changes in project scope	Medium	High	Manage changes continuously
Safety	S1	Construction site accidents and injuries	Medium	High	Provide safety trainings to workers
	S2	Lack of compliance with safety regulations	Medium	High	Implement policies to met non-compliances
	S3	Safety-related incidents (fire etc)	Low	High	Implement control measures
Geotechnical	G1	Unforeseen soil or foundation issues	Medium	Medium	Properly done construction surveys and studies

	G2	Landslides, subsidence, or soil erosion	Medium	Medium	Implement drainage system
	G3	Seismic risks in earthquake-prone areas	High	High	Strength connection between building connections
Labor	L1	Labor disputes and strikes	Medium	Medium	Establish healthy working environment
	L2	Shortages of skilled labor	Medium	Medium	Provide development programs
	L3	Worker productivity issues	Medium	Medium	Limit overtime work
Political and external	P1	Changes in government policies or regulations	Medium	High	Monitoring government policy changes
	P2	Geopolitical factors affecting the supply chain	Medium	High	Use predictive supply analytics
Change Management	C1	Scope changes initiated by the client	Medium	Medium	Get approval to any changes and understand its impact
	C2	Changes in project requirements	Medium	Medium	Make a detailed documentation and communicate with team
	C3	Inadequate change control processes	Low	Medium	Automate change management process

After identification of the risks the risk management matrix or risk control matrix was created. It helps to capture the likelihood of each risk and evaluate possible damage caused by them. The figure below represents propagation and severity of all identified risks. The levels were decided by 3 categories: low, medium and high. Most of the risks were evaluated as medium impact risks. Only one risk from geotechnical type of risk (Seismic risks in earthquake-prone areas) was indicated as high impact risk, which is associated with location of residential building in seismic zone.

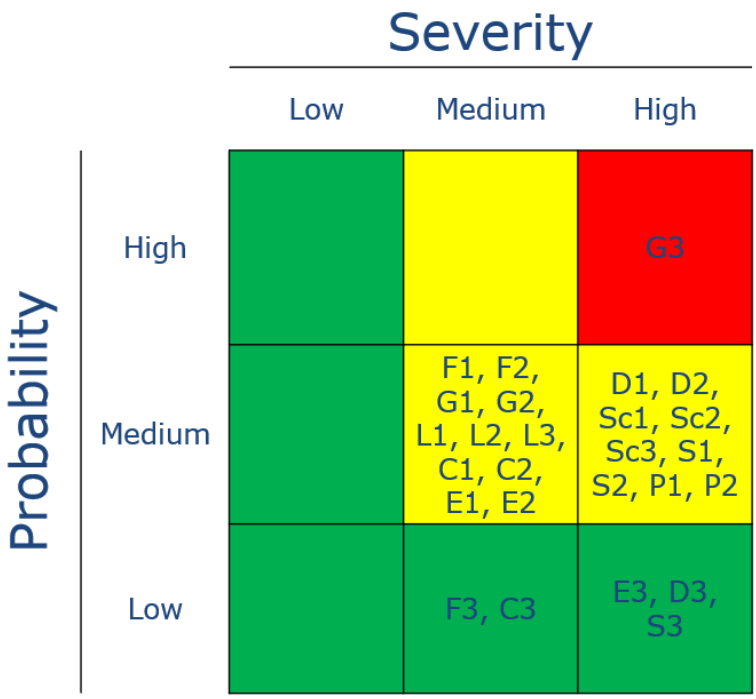

Figure 6.4. Risk Management matrix

6.7. Quality Management Plan

Quality control is necessary for any construction project. The main elements of the project's quality management strategy are as follows: Quality planning, according to the Project Management Institute (2017), includes creating standards and processes, figuring out what has to be done, setting quality targets, and working with the project team. Inspections, testing, and audits are performed as part of quality assurance to ensure that the work complies with the norms and specifications for quality. Any issues will be identified and fixed soon away, according to the Project Management Institute's 2017 report.

The process of fixing problems found during the quality assurance phase is known as quality control. This comprises determining the root cause of the problem, creating a solution, implementing it, and making sure the problem is fixed (ASQ Quality Glossary, 2022).

To guarantee that all project participants are aware of the quality standards and procedures, quality training is essential. It will be changed to become a project-specific quality management system that focuses on planning, assurance, control, and training. Every member of

the project team must be aware of and have access to the quality management system documentation (Project Management Institute, 2017).

Figure 6.5. Quality Management Steps

6.8. Procurement planning/ Stakeholder analysis

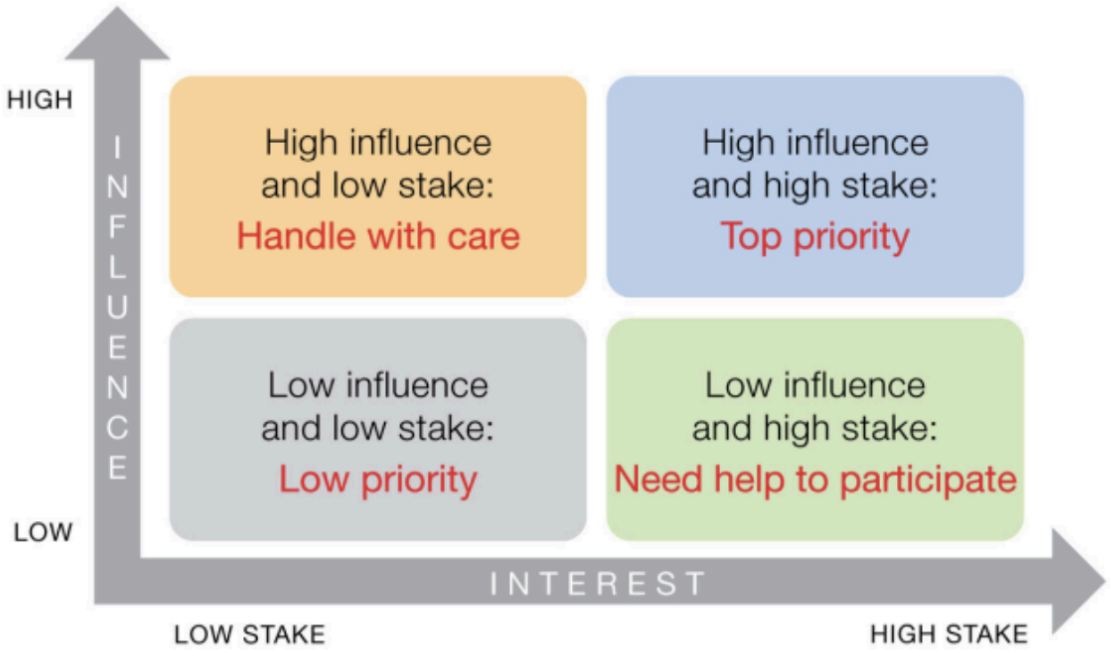

Figure 6.6. Interest-influence effect

Careful construction management is needed for the 12-story residential building project at 1952 Avenue of the Stars in Los Angeles, California. Two essential elements of construction management are organizing the procurement procedure and carrying out a stakeholder analysis. The Code of Practice for Project Management for Construction and Development states that procurement planning entails selecting qualified vendors, evaluating suppliers, and drafting purchase orders and contracts (CIOB, 2018). The project team must keep a careful eye on the procurement process to make sure supplies arrive on schedule, track suppliers' performance, and handle any possible problems.

To find out who is worried about the project, how much they care, how powerful they are, and how their actions could affect it, a stakeholder analysis is crucial. According to the Project Management Institute's Guide to the Project Management Body of Knowledge (PMI, 2017), a stakeholder analysis should be conducted in order to identify stakeholders, assess their interest and influence, and develop a management plan. For example, they need to plan how they will interact with stakeholders, collect data, and ask for and act upon their feedback.

By using thorough procurement planning and stakeholder analysis, the project team can ensure that supplies, machinery, and services are acquired on time and at a reasonable cost, as well as that all parties involved are kept informed and involved throughout the project. Figure X below displays the Stakeholders Map for Residential Building Construction.

Stakeholder Role	Contribution to Project	Interest	Influence
Property Owner	Project initiation	High	High
Architect	Residential building design	High	Moderate
Civil Engineer	Building design and construc	Moderate	Moderate
Construction Contractor	Project management	High	High
Subcontractors/Suppliers	Construction activities	Moderate	Moderate
Governmental Authorities	Approvals and inspections	Moderate	High
Financial Institutions	Funding support	Moderate	High
Utility Companies	Service provision	Low	Moderate
Environmental Consultants	Environmental compliance	Moderate	Low
Legal Advisors	Legal aspects of the project	Moderate	Low
Future Residents	Resident preferences	Moderate	Low

Figure 6.7. Stakeholder Matrix

6.9. Construction Safety

All parties participating in a building project should prioritize construction safety control since it is crucial for both the workers and the smooth operation of the construction operations. OSHA standards and other safety laws and ordinances should be adhered to when developing a residential structure. The special team must first create a safety plan, and employees must be informed of all risks, hazards, and safety measures. Additionally, the safety strategy must be updated as development progresses. Employees should also wear personal protective equipment and receive training on how to avoid or manage potential risks. In addition to worker safety, all site visitors should abide by safety regulations. Additionally, procedures on building sites

shouldn't endanger public safety. It has to do with the movement of materials, their inventory, loud noises, and other things (Almaskati, 2024).

Figure 6.8. Construction Safety Measures

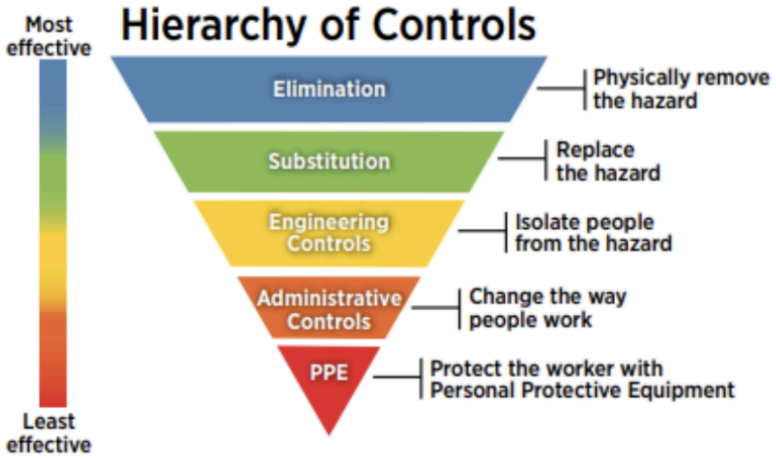

Figure 6.9. Hazard management hierarchy (Department of Labor Logo United Statesdepartment of Labor 2016)

OSHA's hierarchy of controls is typically used to categorize safety precautions according to their efficacy. Choosing the most effective risk avoidance strategy is beneficial. Professionals frequently use the hierarchy of controls as a framework. The degrees of controls are depicted in the above picture along with descriptions, namely for people protective equipment, engineering controls, administrative controls, substitution, and elimination (Almaskati, 2024).

The potential hazards on the building site are included in the table below along with an assessment of them. The results show that noise is the least dangerous risk among the others, while working at a height has the highest ranking.

Risk Description	Likelihood (1-5)	Severity (1-5)	Risk Score
Likelihood (1-5): 2			
Fire and Blast Hazards	2	4	8
Structural Failure	2	5	10
Noise Levels	2	2	4
Likelihood (1-5): 3			
Slips, trips, and falls	3	3	9
Insufficient Personal Protective	3	3	9
Temperature Extremes	3	3	9
Electrical Dangers	3	4	12
Entrapment Risks	3	4	12
Hazardous Material Storage	3	3	9
Hand-Arm Vibration Disorder	3	3	9
Likelihood (1-5): 4			
Working at elevated heights	4	4	16

Figure 6.10. Construction risk register

6.10. Construction site planning

Construction site layout planning is one of the crucial parts in planning processes of construction. It defines where different facilities at different phases of construction will be located. These facilities can be temporary or fixed, which are required for specific construction activities. The distribution and location of tools and facilities defined by space availability on the site. Also, the sizes and types of the facilities used during each construction stage can vary (Ganiyu et al., 2021).

The construction site planning for the current high-rise residential building is located in the intersection of West 12th and South Grand Avenue streets, thus it was important that the construction process should not interfere with traffic movement in these streets. It is 110 meters in length and 48 meters in width, which creates enough space for different stocks and roads for vehicle movement.

The building area is on the south side of the site opposite to all stockpiles. The equipment and motor park, reinforcement stockpile, material stockpile and excavated ground areas are located next to each other in a row on the north side of the construction site. The road connects all the stocks and the main office buildings for quick, safe and convenient transportation. However, the construction pit is in a safe distance from the road. The waste material stock and office buildings are located on the west side. However, waste material stock is placed far from all areas in order to prevent any discomfort and intervention for workers and construction processes.

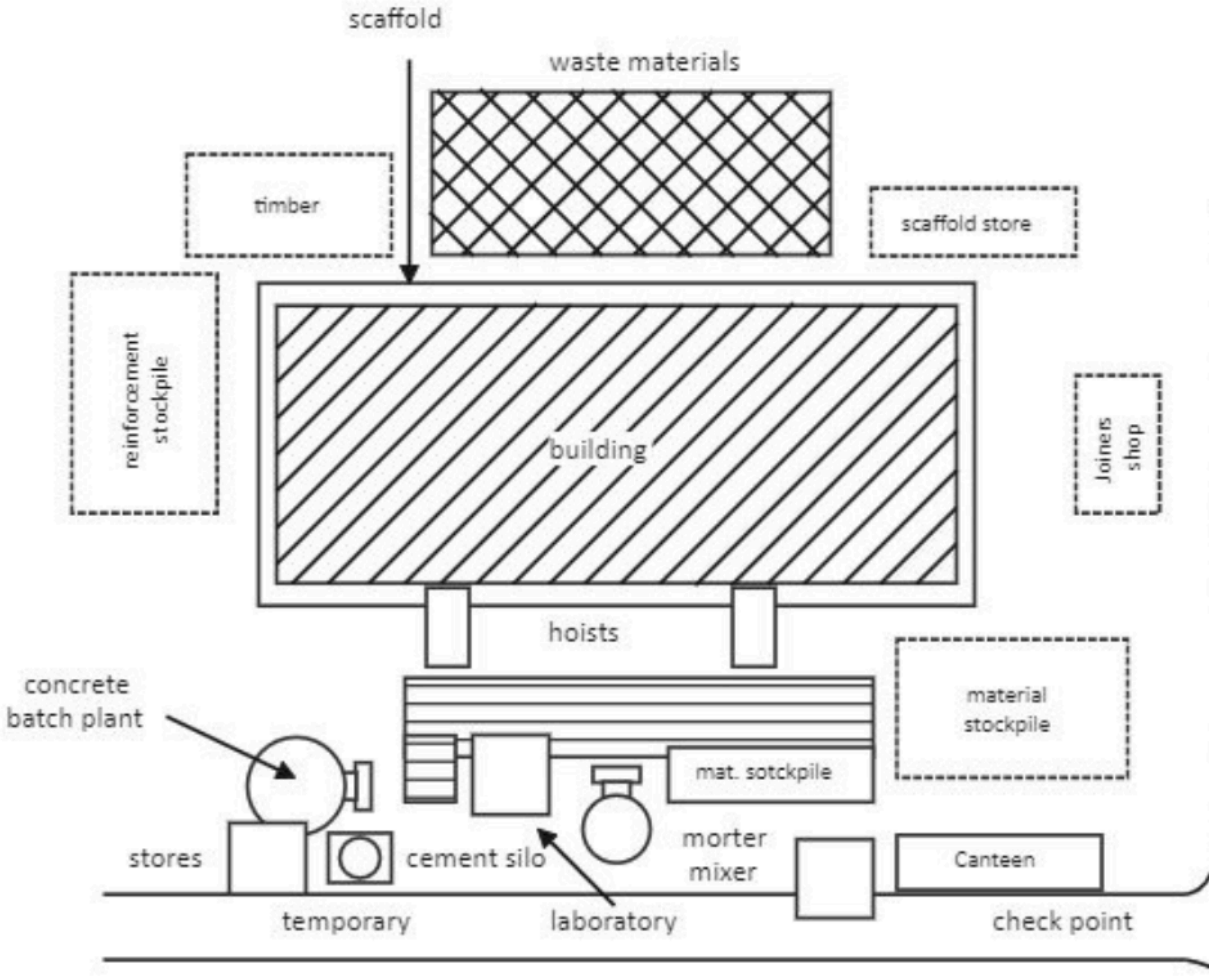

Figure 6.11. The construction site layout planning

7. Conclusion

This capstone project represents a tall order of multidisciplinary effort in designing and analyzing a 12-storey high-rise residential building located at 6435 Wilshire Blvd, Los Angeles, California. The main aim of this project is to deliver a structurally sound, environmentally sustainable, functionally optimized building that can meet regulatory standards and urban housing needs for a growing metropolis like Los Angeles. Fully integrated architectural, structural, geotechnical, environmental, and construction management considerations make sure that no area of modern high-rise design is overlooked.

By taking into consideration gravity and lateral loadings such as wind and seismic forces, the structural analysis was performed in SAP2000 to assure stability and strength in resisting lateral loads. The ultimate choice of the whole superstructure in reinforced concrete is very durable, offers good economy, and may be designed to behave well under seismic action - an important consideration in the highly hazardous zones of Los Angeles. Some of these innovative structural solution designs entail the gravity load-resisting system and the lateral force-resisting system, which really show advanced engineering principles applied to safety and efficiency requirements.

The geotechnical point of view was highly considered owing to poor soil characteristics and seismic hazards. On this basis, pile foundations were decided upon to ensure stability over a long period and reducing seismic hazards. This kind of foundation also accommodates the project's scale while optimizing feasibility in the urban environment. The geotechnical design gives safety to the building concerning liquefaction and ground motion.

Natural lighting, ventilation, and energy-efficient systems ensure leading architectural design, functionality, and sustainability. Mixed-use spaces, including commercial premises at the ground floor and residential units on higher levels, add an economic dimension and a value which would increase with community living. Three thoughtful layouts with terraces, recreational facilities, and means for emergency evacuation meet IBC 2024 and provide full support to comfort and safety for occupants.

The design process was driven by the principle of environmental sustainability: the project considers LEED certification goals, such as energy efficiency, water conservation, and sustainable materials. Site-specific management and drainage systems of stormwater will have lesser environmental impacts and at the same time address local regulations. This is a clear indication of how the project aims to reduce its carbon footprint andlong-term operational efficiencies.

The project, from the perspective of construction management, reflects a practical, well-thought-out execution strategy. For proper resource mobilization and mitigation of risks, it considers a well-worked-out detailed work breakdown structure and project schedule. Cost analysis, with acknowledgment of the limitation in data due to RSMeans 2018 values, projects the costs realistically. Therefore, the plan should provide room for flexibility to incorporate updated material costs and labor fees that would ensure the financial viability of the plan.

The project is not just a technological feat, but it is also an embodiment of good and responsible engineering practice. Ethical considerations played an important role in underlining integrity, transparency, and cooperation amongst team members. The adherence to national and international standards throughout the design process guarantees that the building meets the highest safety and sustainability benchmarks.

This capstone project embodies the meeting of innovation, sustainability, and functionality in a form that answers urban needs for housing. Advanced engineering tools combined with regulatory compliance and environmental stewardship make this high-rise residential building design exemplary for future urban development. While this project was successfully able to achieve its objected, the cost estimation could be refined, alternative materials further explored, and in-service performance monitoring implemented to make any future work adaptable and impactful. Conclusively, the discussed project will satisfy the demand for housing in Los Angeles while providing a guideline for how high-rise constructions can be sustainably and resiliently made.

8. Reference List

American Concrete Institute (ACI) (2023). *Building Code Requirements for Structural Concrete (ACI 318-19)*. American Concrete Institute, 2019. *Available at*: https://www.concrete.org

American Society of Civil Engineers (2017) *Minimum Design Loads and Associated Criteria for Buildings and Other Structures ASCE/SEI 7-16*. rep. American Society of Civil Engineers. Available at: https://ascelibrary.org/doi/book/10.1061/9780784414248 (Accessed: 23 September 2023).

American Society of Civil Engineers (ASCE). ASCE Hazard Tool. *Available at*: https://hazards.asce.org

Bay Area Council Economic Institute (2021) *The true cost of wildfires: analyzing the impact of wildfires on the California economy*. San Francisco, CA: Bay Area Council Economic Institute. Available at: http://www.bayareaeconomy.org/files/pdf/BACEI_WildfireImpacts_Nov2021.pdf (Accessed: 3 October 2024).

Benmokrane, B., El-Naggar, M., Yu, Y., & Jalal, F. (2021). *Design and Construction of Deep Foundations: Pile Foundations for Buildings and Structures*. CRC Press. https://www.routledge.com/Design-and-Construction-of-Deep-Foundations/Benmokrane-El-Naggar-Yu-Jalal/p/book/9780367895294

Bond, A., Harris, A. 2013. *Implementation and evolution of Eurocode 7*. In: Arnold, M., et al., eds. *Modern Geotechnical Design Codes of Practice*. Amsterdam: IOS Press, pp. 3–14.

California Building Standards Commission (2022). *California Building Code (CBC)*. *Available at*: https://www.dgs.ca.gov/BSC.

Coduto, D. P. (2001). *Foundation design: Principles and practices* (2nd ed.). Prentice Hall. Available at: https://www.pearson.com/en-us/subject-catalog/p/foundation-design-principles-and-practices/P200000005660

Chen, B., Jin, Y., Scaduto, E., Moritz, M.A., Goulden, M.L. and Randerson, J.T. (2021) 'Climate, fuel, and land use shaped the spatial pattern of wildfire in California's Sierra Nevada', *Journal of Geophysical Research: Biogeosciences*, 126(5), e2020JG005786. doi: 10.1029/2020JG005786.

Chudley, R., & Greeno, R. (2016). *Building Construction Handbook* (11th ed.). Routledge. https://www.routledge.com/Building-Construction-Handbook/Chudley-Greeno/p/book/9781138907096

Coduto, D. P. (2001). *Foundation Design: Principles and Practices* (2nd ed.). Prentice Hall. https://www.pearson.com/en-us/subject-catalog/p/foundation-design-principles-and-practices/P200000005660

Craig, R. F., & Knappett, J. A. (2012). *Craig's Soil Mechanics* (8th ed.). Spon Press. https://www.routledge.com/Craigs-Soil-Mechanics/Knappett-Craig/p/book/9780415561266 ity of Los Angeles, n.d. *Sewer system service requests*. Available at: https://data.lacity.org/City-Infrastructure-Service-Requests/Sewer-System/7aty-5ywx (Accessed: 3 October 2024).

Das, B. M. (2024). *Principles of Foundation Engineering* (10th ed.). Cengage Learning. "Lateral Earth Pressure: At-Rest, Rankine, and Coulomb." *Chapter 13. https://courses.minia.edu.eg/Attach/Earth%20pressure.pdf*

Das, B.M. and Sivakugan, N. (2019). *Principles of foundation engineering*. Boston, Cengage

Learning.

Darshana, P. K., Nagare, M. R. (2021) "Prepare Project Schedule using Microsoft Project." *International Journal of Research Publication and Reviews,* 2-8, pages 233-245.

Elsamny, M.K., Ibrahim, M.A., Gad, S.A. and Abd-Mageed, M. (2017) 'Experimental evaluation of bearing capacity and behaviour of single pile and pile group in cohesionless soil', *International Journal of Engineering Research & Technology (IJERT)*, 6(5), pp. 695-704. Available at: http://surl.li/wpgylc (Accessed: 26 October 2024).

Environmental Impact Analysis (2014) Utilities and Service Systems—Solid Wcaste. Available at https://planning.lacity.org/development-services/eir

Federal Emergency Management Agency (FEMA). *Guidelines for Design of Structures in High Seismic Zones*. FEMA P-1050, 2019. Available at: https://www.fema.gov.

Gould, F. E., & Joyce, N. E. (2009). *Construction Project Management* (3rd ed.). Pearson. Available at: https://www.pearson.com/store/p/construction-project-management/P100000638269

International Code Council (ICC) (2024). *International Building Code (IBC)* (2024). Available at: https://www.iccsafe.org

Irvine Geotechnical (2022). Geotechnical Report for Wilshire Boulevard Site. Available at: https://www.irvingeotech.com

Leadership in Energy and Environmental Design (LEED). Green Building Standards and Certification. *Available at*: https://www.usgbc.org

LoopNet (n.d.) *6435 Wilshire Blvd for lease*. Available at: https://www.loopnet.com/viewer/pdf?file=https%3a%2f%2fimages1.loopnet.com%2fd2%2ft0SowynEVti8LfbqNneNrwkPl2aVhY6SyBYaxfOIGlY%2f6435%2520Wilshire%2520Blvd%2520FOR%2520LEASE.pdf (Accessed: 9 September 2024).

LoopNet (n.d.) *6435 Wilshire Blvd, Los Angeles, CA 90048*. Available at: https://www.loopnet.com/property/6435-wilshire-blvd-los-angeles-ca-90048/06037-5510023051/ (Accessed: 8 September 2024).

LoopNet (n.d.) *6435 Wilshire Blvd, Los Angeles, CA*. Available at: https://www.loopnet.com/Listing/6435-Wilshire-Blvd-Los-Angeles-CA (Accessed: 9 September 2024).

Los Angeles City Planning (2022) *Los Angeles City Population Projections*. Available at: https://planning.lacity.org/ (Accessed: 25 October 2024).

Los Angeles Sewer and Stormwater Infrastructure (2023). *Available at*: https://www.lacitysan.org

Los Angeles City Planning Department (2023). Housing and Urban Development Statistics. *Available at*: https://planning.lacity.org

Los Angeles County Public Works (n.d.) *Water Supply*. Available at: https://pw.lacounty.gov/core-service-areas/water-resources/water-supply/#:~:text=Los%20Angeles%20Aqueduct&text=In%20Los%20Angeles%2C%20a%20223,capacity%20to%20the%20water%20system (Accessed: 21 September 2024).

Le Kouby, A., Dias, D., & Kastner, R. (2016). Numerical investigation of the group effect and installation sequence of piles. *Geotechnical and Geological Engineering, 34*(1), 31–45. Available at: https://doi.org/10.1007/s10706-015-9926-0

Los Angeles County Public Works, (n.d.). *Storm drain disclaimer*. Available at: https://pw.lacounty.gov/fcd/StormDrain/disclaimer.cfm?CFID=15756810&CFTOKEN=f1ea937f9966edc0-DF7CE277-D056-4F9F-30AD3D36D42D5BC5 (Accessed: 31 October 2024).

Mathai, R. (2020). Advantages of Reinforced Concrete in Structural Design. *Concrete Journal*, 54(3), 45–58.

Meteoblue, n.d. *Weather forecast for Los Angeles*. Available at: https://www.meteoblue.com/en/weather/week/los-angeles_united-states_5368361 (Accessed: 31 September 2024).

National Renewable Energy Laboratory (NREL). Energy Efficiency Strategies for High-Rise Residential Buildings. NREL Report No. 24342, 2021. *Available at*: https://www.nrel.gov.

NOAA National Data Buoy Center (n.d.) *Seabreeze*. Available at: https://www.ndbc.noaa.gov/education/seabreeze_ans.shtml (Accessed: 18 September 2024).

Northey, R. D., & Gribble, C. D. (2013). *Geology for Engineers and Environmental Scientists* (8th ed.). CRC Press. Available at: https://www.routledge.com/Geology-for-Engineers-and-Environmental-Scientists/Northey-Gribble/p/book/9780415315609

Nicolas, D., Monjurul, H., & Ming, L. (2018) "RSMeans-Guided Approach to Detailed Cost Estimating: A Residential Project Case." Available at: https://www.researchgate.net/publication/326016874_RSMeans-Guided_Approach_to_Detailed_Cost_Estimating_A_Residential_Project_Case

National Oceanic and Atmospheric Administration (NOAA). Climate Data for Los Angeles. Available at: https://www.noaa.gov

Poulos, H.G., Carter, J.P. and Small, J.C., 2001. Foundations and retaining structures – research and practice. In: *15th International Conference on Soil Mechanics and Geotechnical Engineering*.

Project Management Institute. *A Guide to the Project Management Body of Knowledge (PMBOK Guide)* (7th ed.). Project Management Institute.

Property Shark (n.d.) *6435 Wilshire Blvd, Los Angeles, CA 90048*. Available at: https://www.propertyshark.com/mason/Property/16421826/6435-Wilshire-Blvd-Los-Angeles-CA-90048/ (Accessed: 5 September 2024).

Sharma, N., Dasgupta, K. and Dey, A. (2020) 'Natural period of reinforced concrete building frames on pile foundation considering seismic soil-structure interaction effects', *Structures*, 27, pp. 1594-1612. doi: 10.1016/j.istruc.2020.07.010.

Sharp, J. (2021). Analysis of Los Angeles Urban Growth. *Urban Planning Quarterly*, 34(2), 101–110.

Smith, J. (2020). *Construction Planning, Equipment, and Methods* (9th ed.). McGraw-Hill Education.

SkyCiv (n.d.) *Tall building foundation design*. Available at: https://skyciv.com/technical/tall-building-foundation-design/ (Accessed: 5 October 2024).

Terzaghi, K., Peck, R. B., & Mesri, G. (1996). *Soil mechanics in engineering practice* (3rd ed.). John Wiley & Sons. Available at: https://www.wiley.com/en-us/Soil+Mechanics+in+Engineering+Practice%2C+3rd+Edition-p-9780471086581

Tomlinson, M. J., & Woodward, J. (2015). *Pile design and construction practice* (6th ed.). CRC Press. Available at: https://www.routledge.com/Pile-Design-and-Construction-Practice-Sixth-Edition/Tomlinson-Woodward/p/book/9781466592643Tokimatsu, K., & Seed, H. B. (1987). Evaluation of Settlements in Sands Due to Earthquake Shaking. *Journal of Geotechnical Engineering*, 113(8), 861–878.

Topographic Map, n.d. *Los Angeles*. Available at: https://en-gb.topographic-map.com/map-s4hdn/Los-Angeles/?center=34.03989%2C-118.26321&zoom=19 (Accessed: 11 November 2024).

U.S. Environmental Protection Agency (2021) *National Emissions Inventory (NEI)*. Washington, DC: U.S. Environmental Protection Agency. Available at: https://www.epa.gov/air-emissions-inventories/national-emissions-inventory-nei (Accessed: 16 October 2024).

Urbanize LA (n.d.) *Beverly Grove: Black Equities Group, 6435 Wilshire Apartments*. Available at: https://la.urbanize.city/post/beverly-grove-black-equities-group-6435-wilshire-apartments (Accessed: 10 September 2024).

Federal Highway Administration (FHWA). (2006). *Design and construction of driven pile foundations – Reference manual* (FHWA NHI-05-042). U.S. Department of Transportation. Available at: https://www.fhwa.dot.gov/engineering/geotech/pubs/nhi05042/

9. Appendix

9.1. Appendix A

Calculations of stiffness of moment frame on each level

Table 9.1. Calculations of stiffness of the moment frame.

							Transverse	Longitudinal
Floor	**Column size**	**Ic,cr, m4**	**Ib,cr, m4**	**Minor b, Ib,cr**	**D, kN/m**	**h, m**	**Cf, kN/rad**	**Cf, kN/rad**
1	0.65	1.04E-02	7.74E-04	0.00448	2741	4	109625	32888
2	0.65	1.04E-02	7.74E-04	0.00448	3601	3.5	126030	37809
3	0.60	7.56E-03	7.74E-04	0.00448	3545	3.5	124084	37225
4	0.60	7.56E-03	7.74E-04	0.00448	3545	3.5	124084	37225
5	0.55	5.34E-03	7.74E-04	0.00448	3464	3.5	121239	36372
6	0.55	5.34E-03	7.74E-04	0.00448	3464	3.5	121239	36372
7	0.50	3.65E-03	7.74E-04	0.00448	3343	3.5	117003	35101
8	0.45	2.39E-03	7.74E-04	0.00448	3160	3.5	110613	33184
9	0.45	2.39E-03	7.74E-04	0.00448	3160	3.5	110613	33184
10	0.40	1.49E-03	7.74E-04	0.00448	2885	3.5	100964	30289
11	0.35	8.75E-04	7.74E-04	0.00448	2478	3.5	86745	26024
12	0.30	4.73E-04	7.74E-04	0.00448	1921	3.5	67236	20171
13	0.25	2.28E-04	7.74E-04	0.00448	1260	3.5	44099	13230

Calculations of total lateral seismic force including torsional effect for each floor

Table 9.2. Calculation of seismic force on each frame including the torsional effect (Floor 2).

Transverse				**Longitudinal**			
Frame	Ftorsion, kN	Fdirect, kN	Ftotal, kN	Frame	Ftorsion, kN	Fdirect, kN	Ftotal, kN
A	21.5106	42.46	63.97	1	-1.6329	15.44	13.81
B	15.3647	42.46	57.82	2	-1.1664	15.44	14.27
C	9.2188	42.46	51.67	3	-0.6998	15.44	14.74
D	3.0729	42.46	45.53	4	-0.2333	15.44	15.21

E	-3.0729	42.46	39.38	5	0.2333	15.44	15.67
F	-9.2188	42.46	33.24	6	0.6998	15.44	16.14
G	-15.3647	42.46	27.09	7	1.1664	15.44	16.6
H	-21.5106	42.46	20.94	8	1.6329	15.44	17.07

Table 9.3. Calculation of seismic force on each frame including the torsional effect (Floor 3).

Transverse				**Longitudinal**			
Frame	Ftorsion, kN	Fdirect, kN	Ftotal, kN	Frame	Ftorsion, kN	Fdirect, kN	Ftotal, kN
A	37.2228	73.47	110.69	1	-2.8256	26.72	23.89
B	26.5877	73.47	100.05	2	-2.0183	26.72	24.7
C	15.9526	73.47	89.42	3	-1.211	26.72	25.5
D	5.3175	73.47	78.78	4	-0.4037	26.72	26.31
E	-5.3175	73.47	68.15	5	0.4037	26.72	27.12
F	-15.9526	73.47	57.51	6	1.211	26.72	27.93
G	-26.5877	73.47	46.88	7	2.0183	26.72	28.73
H	-37.2228	73.47	36.24	8	2.8256	26.72	29.54

Table 9.4. Calculation of seismic force on each frame including the torsional effect (Floor 4)

Transverse				**Longitudinal**			
Frame	Ftorsion, kN	Fdirect, kN	Ftotal, kN	Frame	Ftorsion, kN	Fdirect, kN	Ftotal, kN
A	72.2463	110.6	182.85	1	-5.4843	40.22	34.73
B	51.6045	110.6	162.2	2	-3.9174	40.22	36.3
C	30.9627	110.6	141.56	3	-2.3504	40.22	37.87
D	10.3209	110.6	120.92	4	-0.7835	40.22	39.43
E	-10.3209	110.6	100.28	5	0.7835	40.22	41
F	-30.9627	110.6	79.64	6	2.3504	40.22	42.57
G	-51.6045	110.6	59	7	3.9174	40.22	44.14
				8	5.4843	40.22	45.7

Table 9.5. Calculation of seismic force on each frame including the torsional effect (Floor 5)

Transverse				Longitudinal			
Frame	Ftorsion, kN	Fdirect, kN	Ftotal, kN	Frame	Ftorsion, kN	Fdirect, kN	Ftotal, kN
A	97.7759	149.68	247.46	1	-7.4223	54.43	47.01
B	69.84	149.68	219.52	2	-5.3016	54.43	49.13
C	41.904	149.68	191.59	3	-3.181	54.43	51.25
D	13.968	149.68	163.65	4	-1.0603	54.43	53.37
E	-13.968	149.68	135.71	5	1.0603	54.43	55.49
F	-41.904	149.68	107.78	6	3.181	54.43	57.61
G	-69.84	149.68	79.84	7	5.3016	54.43	59.73
				8	7.4223	54.43	61.85

Table 9.6. Calculation of seismic force on each frame including the torsional effect (Floor 6)

Transverse				Longitudinal			
Frame	Ftorsion, kN	Fdirect, kN	Ftotal, kN	Frame	Ftorsion, kN	Fdirect, kN	Ftotal, kN
A	127.2051	194.74	321.94	1	-9.6563	70.81	61.16
B	90.8608	194.74	285.6	2	-6.8974	70.81	63.92
C	54.5165	194.74	249.25	3	-4.1384	70.81	66.67
D	18.1722	194.74	212.91	4	-1.3795	70.81	69.43
E	-18.1722	194.74	176.56	5	1.3795	70.81	72.19
F	-54.5165	194.74	140.22	6	4.1384	70.81	74.95
G	-90.8608	194.74	103.87	7	6.8974	70.81	77.71
				8	9.6563	70.81	80.47

Table 9.7. Calculation of seismic force on each frame including the torsional effect (Floor 7)

Transverse				Longitudinal			
Frame	Ftorsion, kN	Fdirect, kN	Ftotal, kN	Frame	Ftorsion, kN	Fdirect, kN	Ftotal, kN
A	156.4606	239.52	395.98	1	-11.8771	87.1	75.22
B	111.7576	239.52	351.28	2	-8.4837	87.1	78.62

C	67.0545	239.52	306.58	3	-5.0902	87.1	82.01
D	22.3515	239.52	261.87	4	-1.6967	87.1	85.4
E	-22.3515	239.52	217.17	5	1.6967	87.1	88.8
F	-67.0545	239.52	172.47	6	5.0902	87.1	92.19
G	-111.7576	239.52	127.76	7	8.4837	87.1	95.58
				8	11.8771	87.1	98.98

Table 9.8. Calculation of seismic force on each frame including the torsional effect (Floor 8)

Transverse				**Longitudinal**			
Frame	Ftorsion, kN	Fdirect, kN	Ftotal, kN	Frame	Ftorsion, kN	Fdirect, kN	Ftotal, kN
A	187.1326	286.48	473.61	1	-14.2055	104.17	89.97
B	133.6662	286.48	420.14	2	-10.1468	104.17	94.03
C	80.1997	286.48	366.68	3	-6.0881	104.17	98.09
D	26.7332	286.48	313.21	4	-2.0294	104.17	102.14
E	-26.7332	286.48	259.74	5	2.0294	104.17	106.2
F	-80.1997	286.48	206.28	6	6.0881	104.17	110.26
G	-133.6662	286.48	152.81	7	10.1468	104.17	114.32
				8	14.2055	104.17	118.38

Table 9.9. Calculation of seismic force on each frame including the torsional effect (Floor 9)

Transverse				**Longitudinal**			
Frame	Ftorsion, kN	Fdirect, kN	Ftotal, kN	Frame	Ftorsion, kN	Fdirect, kN	Ftotal, kN
A	222.1491	340.08	562.23	1	-16.8636	123.67	106.8
B	158.678	340.08	498.76	2	-12.0454	123.67	111.62
C	95.2068	340.08	435.29	3	-7.2273	123.67	116.44
D	31.7356	340.08	371.82	4	-2.4091	123.67	121.26
E	-31.7356	340.08	308.35	5	2.4091	123.67	126.08
F	-95.2068	340.08	244.88	6	7.2273	123.67	130.89
G	-158.678	340.08	181.41	7	12.0454	123.67	135.71
				8	16.8636	123.67	140.53

Table 9.10. Calculation of seismic force on each frame including the torsional effect (Floor 10)

Transverse				Longitudinal			
Frame	Ftorsion, kN	Fdirect, kN	Ftotal, kN	Frame	Ftorsion, kN	Fdirect, kN	Ftotal, kN
A	255.5514	391.22	646.77	1	-19.3992	142.26	122.86
B	182.5367	391.22	573.75	2	-12.6478	142.26	129.61
C	109.522	391.22	500.74	3	-7.5887	142.26	134.67
D	36.5073	391.22	427.72	4	-2.5296	142.26	139.73
E	-36.5073	391.22	354.71	5	2.5296	142.26	144.79
F	-109.522	391.22	281.7	6	7.5887	142.26	149.85
G	-182.5367	391.22	208.68	7	12.6478	142.26	154.91
				8	17.707	142.26	159.97

Table 9.11. Calculation of seismic force on each frame including the torsional effect (Floor 11)

Transverse				Longitudinal			
Frame	Ftorsion, kN	Fdirect, kN	Ftotal, kN	Frame	Ftorsion, kN	Fdirect, kN	Ftotal, kN
A	290.174	444.22	734.39	1	-22.0275	161.53	139.51
B	207.2671	444.22	651.49	2	-15.7339	161.53	145.8
C	124.3603	444.22	568.58	3	-9.4403	161.53	152.09
D	41.4534	444.22	485.67	4	-3.1468	161.53	158.39
E	-41.4534	444.22	402.77	5	3.1468	161.53	164.68
F	-124.3603	444.22	319.86	6	9.4403	161.53	170.98
G	-207.2671	444.22	236.95	7	15.7339	161.53	177.27
				8	22.0275	161.53	183.56

Table 9.12. Calculation of seismic force on each frame including the torsional effect (Floor 12)

Transverse				Longitudinal			
Frame	Ftorsion, kN	Fdirect, kN	Ftotal, kN	Frame	Ftorsion, kN	Fdirect, kN	Ftotal, kN
A	326.0551	499.15	825.21	1	-24.7512	181.51	156.76
B	232.8965	499.15	732.05	2	-17.6795	181.51	163.83

C	139.7379	499.15	638.89	3	-10.6077	181.51	170.9
D	46.5793	499.15	545.73	4	-3.5359	181.51	177.97
E	-46.5793	499.15	452.57	5	3.5359	181.51	185.05
F	-139.7379	499.15	359.41	6	10.6077	181.51	192.12
G	-232.8965	499.15	266.25	7	17.6795	181.51	199.19
				8	24.7512	181.51	206.26

Table 9.13. Calculation of seismic force on each frame including the torsional effect (Floor 13)

Transverse				**Longitudinal**			
Frame	Ftorsion, kN	Fdirect, kN	Ftotal, kN	Frame	Ftorsion, kN	Fdirect, kN	Ftotal, kN
A	132.9145	261.58	394.5	1	-10.0897	95.12	85.03
B	105.6987	261.58	367.28	2	-7.2069	95.12	87.91
C	37.9756	261.58	299.56	3	-4.3242	95.12	90.8
D	-37.9756	261.58	223.61	4	4.3242	95.12	99.44
E	-105.6987	261.58	155.88	5	7.2069	95.12	102.33
F	-132.9145	261.58	128.67	6	10.0897	95.12	105.21

9.2. Appendix B

Calculations of total lateral wind forces including torsional effect for each floor

Table 9.14. Calculation of wind force on each frame for Case 2 including the torsional effect (Floor 2).

Case 2 (X-Axis)				Case 2 (Y-Axis)			
Frame	Ftorsion (kN)	Fdirect (kN)	Ftotal (kN)	Frame	Ftorsion (kN)	Fdirect (kN)	Ftotal (kN)
1	-1.5241	10.91	9.39	1	-0.4332	12.46	12.02
2	-1.0887	10.91	9.83	2	-0.3094	12.46	12.15
3	-0.6532	10.91	10.26	3	-0.1856	12.46	12.27
4	-0.2177	10.91	10.70	4	-0.0619	12.46	12.39
5	0.2177	10.91	11.13	5	0.0619	12.46	12.52
6	0.6532	10.91	11.57	6	0.1856	12.46	12.64
7	1.0887	10.91	12.00	7	0.3094	12.46	12.77

8	1.5241	10.91	12.44	8	0.4332	12.46	12.89

Table 9.15. Calculation of wind force on each frame for Case 2 including the torsional effect (Floor 3).

Case 2 (X-Axis)				Case 2 (Y-Axis)			
Frame	Ftorsion (kN)	Fdirect (kN)	Ftotal (kN)	Frame	Ftorsion (kN)	Fdirect (kN)	Ftotal (kN)
1	-1.6332	10.91	9.28	1	-0.4579	13.08	12.62
2	-1.1666	10.91	9.75	2	-0.3271	13.08	12.75
3	-0.6999	10.91	10.21	3	-0.1962	13.08	12.88
4	-0.2333	10.91	10.68	4	-0.0654	13.08	13.01
5	0.2333	10.91	11.15	5	0.0654	13.08	13.14
6	0.6999	10.91	11.61	6	0.1962	13.08	13.27
7	1.1666	10.91	12.08	7	0.3271	13.08	13.40
8	1.6332	10.91	12.55	8	0.4579	13.08	13.53

Table 9.16. Calculation of wind force on each frame for Case 2 including the torsional effect (Floor 4).

Case 2 (X-Axis)				Case 2 (Y-Axis)			
Frame	Ftorsion (kN)	Fdirect (kN)	Ftotal (kN)	Frame	Ftorsion (kN)	Fdirect (kN)	Ftotal (kN)
1	-2.2171	11.12	8.9	1	-0.6156	13.58	12.96
2	-1.5836	11.12	9.54	2	-0.4397	13.58	13.14
3	-0.9502	11.12	10.17	3	-0.2638	13.58	13.32
4	-0.3167	11.12	10.8	4	-0.0879	13.58	13.49
5	0.3167	11.12	11.44	5	0.0879	13.58	13.67
6	0.9502	11.12	12.07	6	0.2638	13.58	13.84
7	1.5836	11.12	12.7	7	0.4397	13.58	14.02
				8	0.6156	13.58	14.19

Table 9.17. Calculation of wind force on each frame for Case 2 including the torsional effect (Floor 5).

Case 2 (X-Axis)				Case 2 (Y-Axis)			
Frame	Ftorsion	Fdirect	Ftotal (kN)	Frame	Ftorsion	Fdirect	Ftotal (kN)

	(kN)	(kN)			(kN)	(kN)	
1	-2.3107	11.53	9.21	1	-0.6368	14.01	13.37
2	-1.6505	11.53	9.87	2	-0.4549	14.01	13.55
3	-0.9903	11.53	10.54	3	-0.2729	14.01	13.74
4	-0.3301	11.53	11.2	4	-0.091	14.01	13.92
5	0.3301	11.53	11.86	5	0.091	14.01	14.1
6	0.9903	11.53	12.52	6	0.2729	14.01	14.28
7	1.6505	11.53	13.18	7	0.4549	14.01	14.46
				8	0.6368	14.01	14.65

Table 9.18. Calculation of wind force on each frame for Case 2 including the torsional effect (Floor 6).

Case 2 (X-Axis)				Case 2 (Y-Axis)			
Frame	Ftorsion (kN)	Fdirect (kN)	Ftotal (kN)	Frame	Ftorsion (kN)	Fdirect (kN)	Ftotal (kN)
1	-2.392	11.9	9.51	1	-0.6552	14.39	13.73
2	-1.7086	11.9	10.19	2	-0.468	14.39	13.92
3	-1.0251	11.9	10.88	3	-0.2808	14.39	14.11
4	-0.3417	11.9	11.56	4	-0.0936	14.39	14.29
5	0.3417	11.9	12.24	5	0.0936	14.39	14.48
6	1.0251	11.9	12.93	6	0.2808	14.39	14.67
7	1.7086	11.9	13.61	7	0.468	14.39	14.85
				8	0.6552	14.39	15.04

Table 9.19. Calculation of wind force on each frame for Case 2 including the torsional effect (Floor 7).

Case 2 (X-Axis)				Case 2 (Y-Axis)			
Frame	Ftorsion (kN)	Fdirect (kN)	Ftotal (kN)	Frame	Ftorsion (kN)	Fdirect (kN)	Ftotal (kN)
1	-2.4644	12.24	9.78	1	-0.6716	14.73	14.05
2	-1.7603	12.24	10.48	2	-0.4797	14.73	14.25
3	-1.0562	12.24	11.18	3	-0.2878	14.73	14.44
4	-0.3521	12.24	11.89	4	-0.0959	14.73	14.63

5	0.3521	12.24	12.59	5	0.0959	14.73	14.82
6	1.0562	12.24	13.3	6	0.2878	14.73	15.01
7	1.7603	12.24	14	7	0.4797	14.73	15.2
				8	0.6716	14.73	15.4

Table 9.20. Calculation of wind force on each frame for Case 2 including the torsional effect (Floor 8).

Case 2 (X-Axis)				Case 2 (Y-Axis)			
Frame	Ftorsion (kN)	Fdirect (kN)	Ftotal (kN)	Frame	Ftorsion (kN)	Fdirect (kN)	Ftotal (kN)
1	-2.5298	12.55	10.02	1	-0.6865	15.03	14.35
2	-1.807	12.55	10.74	2	-0.4903	15.03	14.54
3	-1.0842	12.55	11.46	3	-0.2942	15.03	14.74
4	-0.3614	12.55	12.19	4	-0.0981	15.03	14.94
5	0.3614	12.55	12.91	5	0.0981	15.03	15.13
6	1.0842	12.55	13.63	6	0.2942	15.03	15.33
7	1.807	12.55	14.35	7	0.4903	15.03	15.52
				8	0.6865	15.03	15.72

Table 9.21. Calculation of wind force on each frame for Case 2 including the torsional effect (Floor 9).

Case 2 (X-Axis)				Case 2 (Y-Axis)			
Frame	Ftorsion (kN)	Fdirect (kN)	Ftotal (kN)	Frame	Ftorsion (kN)	Fdirect (kN)	Ftotal (kN)
1	-2.59	12.83	10.24	1	-0.70	15.32	14.62
2	-1.85	12.83	10.98	2	-0.50	15.32	14.82
3	-1.11	12.83	11.72	3	-0.30	15.32	15.02
4	-0.37	12.83	12.46	4	-0.10	15.32	15.22
5	0.37	12.83	13.2	5	0.10	15.32	15.42
6	1.11	12.83	13.94	6	0.30	15.32	15.62
7	1.85	12.83	14.68	7	0.50	15.32	15.82
				8	0.70	15.32	16.02

Table 9.22. Calculation of wind force on each frame for Case 2 including the torsional effect (Floor 10).

Case 2 (X-Axis)				Case 2 (Y-Axis)			
Frame	Ftorsion (kN)	Fdirect (kN)	Ftotal (kN)	Frame	Ftorsion (kN)	Fdirect (kN)	Ftotal (kN)
1	-2.6451	13.09	10.45	1	-0.7126	15.58	14.87
2	-1.8894	13.09	11.2	2	-0.509	15.58	15.07
3	-1.1336	13.09	11.96	3	-0.3054	15.58	15.27
4	-0.3779	13.09	12.71	4	-0.1018	15.58	15.48
5	0.3779	13.09	13.47	5	0.1018	15.58	15.68
6	1.1336	13.09	14.23	6	0.3054	15.58	15.89
7	1.8894	13.09	14.98	7	0.509	15.58	16.09
				8	0.7126	15.58	16.29

Table 9.23. Calculation of wind force on each frame for Case 2 including the torsional effect (Floor 11).

Case 2 (X-Axis)				Case 2 (Y-Axis)			
Frame	Ftorsion (kN)	Fdirect (kN)	Ftotal (kN)	Frame	Ftorsion (kN)	Fdirect (kN)	Ftotal (kN)
1	-2.6968	13.34	10.64	1	-0.7243	15.83	15.1
2	-1.9263	13.34	11.41	2	-0.5174	15.83	15.31
3	-1.1558	13.34	12.18	3	-0.3104	15.83	15.52
4	-0.3853	13.34	12.95	4	-0.1035	15.83	15.72
5	0.3853	13.34	13.72	5	0.1035	15.83	15.93
6	1.1558	13.34	14.49	6	0.3104	15.83	16.14
7	1.9263	13.34	15.26	7	0.5174	15.83	16.34
				8	0.7243	15.83	16.55

Table 9.24. Calculation of wind force on each frame for Case 2 including the torsional effect (Floor 12).

Case 2 (X-Axis)				Case 2 (Y-Axis)			
Frame	Ftorsion (kN)	Fdirect (kN)	Ftotal (kN)	Frame	Ftorsion (kN)	Fdirect (kN)	Ftotal (kN)
1	-2.7452	13.57	10.82	1	-0.7353	16.06	15.32

2	-1.9609	13.57	11.61	2	-0.5252	16.06	15.53
3	-1.1765	13.57	12.39	3	-0.3151	16.06	15.74
4	-0.3922	13.57	13.18	4	-0.105	16.06	15.95
5	0.3922	13.57	13.96	5	0.105	16.06	16.16
6	1.1765	13.57	14.74	6	0.3151	16.06	16.37
7	1.9609	13.57	15.53	7	0.5252	16.06	16.58
				8	0.7353	16.06	16.79

Table 9.25. Calculation of wind force on each frame for Case 2 including the torsional effect (Floor 13).

Case 2 (X-Axis)				Case 2 (Y-Axis)			
Frame	Ftorsion (kN)	Fdirect (kN)	Ftotal (kN)	Frame	Ftorsion (kN)	Fdirect (kN)	Ftotal (kN)
1	-2.1709	6.84	4.67	1	-0.58	8.08	7.5
2	-1.7264	6.84	5.11	2	-0.4143	8.08	7.67
3	-0.6203	6.84	6.22	3	-0.2486	8.08	7.84
4	0.6203	6.84	7.46	4	0.2486	8.08	8.33
5	1.7264	6.84	8.57	5	0.4143	8.08	8.5
6	2.1709	6.84	9.01	6	0.58	8.08	8.66

Table 9.26. Calculation of wind force on each frame for Case 4 including the torsional effect (Floor 2).

Transverse				Longitudinal			
Frame	Ftorsion (kN)	Fdirect (kN)	Ftotal (kN)	Frame	Ftorsion (kN)	Fdirect (kN)	Ftotal (kN)
1	-2.5614	9.36	6.8	1	-0.7684	9.35	8.58
2	-1.8296	9.36	7.53	2	-0.5489	9.35	8.8
3	-1.0977	9.36	8.27	3	-0.3293	9.35	9.02
4	-0.3659	9.36	9	4	-0.1098	9.35	9.24
5	0.3659	9.36	9.73	5	0.1098	9.35	9.46
6	1.0977	9.36	10.46	6	0.3293	9.35	9.68
7	1.8296	9.36	11.19	7	0.5489	9.35	9.9
8	2.5614	9.36	11.93	8	0.7684	9.35	10.12

Table 9.27. Calculation of wind force on each frame for Case 4 including the torsional effect (Floor 3).

Transverse				Longitudinal			
Frame	Ftorsion (kN)	Fdirect (kN)	Ftotal (kN)	Frame	Ftorsion (kN)	Fdirect (kN)	Ftotal (kN)
1	-2.6846	9.36	6.68	1	-0.8054	9.82	9.01
2	-1.9175	9.36	7.45	2	-0.5753	9.82	9.24
3	-1.1505	9.36	8.21	3	-0.3452	9.82	9.47
4	-0.3835	9.36	8.98	4	-0.1151	9.82	9.7
5	0.3835	9.36	9.75	5	0.1151	9.82	9.93
6	1.1505	9.36	10.51	6	0.3452	9.82	10.16
7	1.9175	9.36	11.28	7	0.5753	9.82	10.39
8	2.6846	9.36	12.05	8	0.8054	9.82	10.62

Table 9.28. Calculation of wind force on each frame for Case 4 including the torsional effect (Floor 4).

Transverse				Longitudinal			
Frame	Ftorsion (kN)	Fdirect (kN)	Ftotal (kN)	Frame	Ftorsion (kN)	Fdirect (kN)	Ftotal (kN)
1	-2.8135	9.54	6.73	1	-0.844	10.19	9.35
2	-2.0096	9.54	7.53	2	-0.6029	10.19	9.59
3	-1.2058	9.54	8.33	3	-0.3617	10.19	9.83
4	-0.4019	9.54	9.14	4	-0.1206	10.19	10.07
5	0.4019	9.54	9.94	5	0.1206	10.19	10.31
6	1.2058	9.54	10.75	6	0.3617	10.19	10.55
7	2.0096	9.54	11.55	7	0.6029	10.19	10.8
				8	0.844	10.19	11.04

Table 9.29. Calculation of wind force on each frame for Case 4 including the torsional effect (Floor 5).

Transverse				Longitudinal			
Frame	Ftorsion (kN)	Fdirect (kN)	Ftotal (kN)	Frame	Ftorsion (kN)	Fdirect (kN)	Ftotal (kN)

1	-2.8548	9.89	7.03	1	-0.8564	10.52	9.66
2	-2.0391	9.89	7.85	2	-0.6117	10.52	9.9
3	-1.2235	9.89	8.66	3	-0.367	10.52	10.15
4	-0.4078	9.89	9.48	4	-0.1223	10.52	10.39
5	0.4078	9.89	10.3	5	0.1223	10.52	10.64
6	1.2235	9.89	11.11	6	0.367	10.52	10.88
7	2.0391	9.89	11.93	7	0.6117	10.52	11.13
				8	0.8564	10.52	11.37

Table 9.30. Calculation of wind force on each frame for Case 4 including the torsional effect (Floor 6).

Transverse				Longitudinal			
Frame	Ftorsion (kN)	Fdirect (kN)	Ftotal (kN)	Frame	Ftorsion (kN)	Fdirect (kN)	Ftotal (kN)
1	-2.9467	10.21	7.26	1	-0.884	10.8	9.92
2	-2.1048	10.21	8.11	2	-0.6314	10.8	10.17
3	-1.2629	10.21	8.95	3	-0.3789	10.8	10.42
4	-0.421	10.21	9.79	4	-0.1263	10.8	10.67
5	0.421	10.21	10.63	5	0.1263	10.8	10.93
6	1.2629	10.21	11.47	6	0.3789	10.8	11.18
7	2.1048	10.21	12.32	7	0.6314	10.8	11.43
				8	0.884	10.8	11.68

Table 9.31. Calculation of wind force on each frame for Case 4 including the torsional effect (Floor 7).

Transverse				Longitudinal			
Frame	Ftorsion (kN)	Fdirect (kN)	Ftotal (kN)	Frame	Ftorsion (kN)	Fdirect (kN)	Ftotal (kN)
1	-2.9227	10.5	7.58	1	-0.8768	11.05	10.18
2	-2.0876	10.5	8.41	2	-0.6263	11.05	10.43
3	-1.2526	10.5	9.25	3	-0.3758	11.05	10.68
4	-0.4175	10.5	10.08	4	-0.1253	11.05	10.93
5	0.4175	10.5	10.92	5	0.1253	11.05	11.18

6	1.2526	10.5	11.75	6	0.3758	11.05	11.43
7	2.0876	10.5	12.59	7	0.6263	11.05	11.68
				8	0.8768	11.05	11.93

Table 9.34. Calculation of wind force on each frame for Case 4 including the torsional effect (Floor 8).

Transverse				Longitudinal			
Frame	Ftorsion (kN)	Fdirect (kN)	Ftotal (kN)	Frame	Ftorsion (kN)	Fdirect (kN)	Ftotal (kN)
1	-2.8306	10.76	7.93	1	-0.8492	11.28	10.44
2	-2.0218	10.76	8.74	2	-0.6066	11.28	10.68
3	-1.2131	10.76	9.55	3	-0.3639	11.28	10.92
4	-0.4044	10.76	10.36	4	-0.1213	11.28	11.16
5	0.4044	10.76	11.17	5	0.1213	11.28	11.41
6	1.2131	10.76	11.98	6	0.3639	11.28	11.65
7	2.0218	10.76	12.79	7	0.6066	11.28	11.89
				8	0.8492	11.28	12.13

Table 9.35. Calculation of wind force on each frame for Case 4 including the torsional effect (Floor 9).

Transverse				Longitudinal			
Frame	Ftorsion (kN)	Fdirect (kN)	Ftotal (kN)	Frame	Ftorsion (kN)	Fdirect (kN)	Ftotal (kN)
1	-2.8924	11.01	8.11	1	-0.8677	11.5	10.63
2	-2.066	11.01	8.94	2	-0.6198	11.5	10.88
3	-1.2396	11.01	9.77	3	-0.3719	11.5	11.13
4	-0.4132	11.01	10.59	4	-0.124	11.5	11.37
5	0.4132	11.01	11.42	5	0.124	11.5	11.62
6	1.2396	11.01	12.25	6	0.3719	11.5	11.87
7	2.066	11.01	13.07	7	0.6198	11.5	12.12
				8	0.8677	11.5	12.37

Table 9.36. Calculation of wind force on each frame for Case 4 including the torsional effect (Floor 10).

Transverse				Longitudinal			
Frame	Ftorsion (kN)	Fdirect (kN)	Ftotal (kN)	Frame	Ftorsion (kN)	Fdirect (kN)	Ftotal (kN)
1	-2.6922	11.23	8.54	1	-0.8077	11.7	10.89
2	-1.923	11.23	9.31	2	-0.5769	11.7	11.12
3	-1.1538	11.23	10.08	3	-0.3461	11.7	11.35
4	-0.3846	11.23	10.85	4	-0.1154	11.7	11.58
5	0.3846	11.23	11.62	5	0.1154	11.7	11.81
6	1.1538	11.23	12.39	6	0.3461	11.7	12.04
7	1.923	11.23	13.15	7	0.5769	11.7	12.27
				8	0.8077	11.7	12.5

Table 9.37. Calculation of wind force on each frame for Case 4 including the torsional effect (Floor 11).

Transverse				Longitudinal			
Frame	Ftorsion (kN)	Fdirect (kN)	Ftotal (kN)	Frame	Ftorsion (kN)	Fdirect (kN)	Ftotal (kN)
1	-2.3549	11.44	9.09	1	-0.7065	11.88	11.17
2	-1.682	11.44	9.76	2	-0.5046	11.88	11.38
3	-1.0092	11.44	10.43	3	-0.3028	11.88	11.58
4	-0.3364	11.44	11.11	4	-0.1009	11.88	11.78
5	0.3364	11.44	11.78	5	0.1009	11.88	11.98
6	1.0092	11.44	12.45	6	0.3028	11.88	12.18
7	1.682	11.44	13.12	7	0.5046	11.88	12.38
				8	0.7065	11.88	12.59

Table 9.38. Calculation of wind force on each frame for Case 4 including the torsional effect (Floor 12).

Transverse				Longitudinal			
Frame	Ftorsion (kN)	Fdirect (kN)	Ftotal (kN)	Frame	Ftorsion (kN)	Fdirect (kN)	Ftotal (kN)
1	-1.8556	11.64	9.78	1	-0.5567	12.05	11.5

2	-1.3254	11.64	10.31	2	-0.3976	12.05	11.66
3	-0.7953	11.64	10.84	3	-0.2386	12.05	11.81
4	-0.2651	11.64	11.37	4	-0.0795	12.05	11.97
5	0.2651	11.64	11.91	5	0.0795	12.05	12.13
6	0.7953	11.64	12.44	6	0.2386	12.05	12.29
7	1.3254	11.64	12.97	7	0.3976	12.05	12.45
				8	0.5567	12.05	12.61

Table 9.39. Calculation of wind force on each frame for Case 4 including the torsional effect (Floor 13).

Transverse				Longitudinal			
Frame	Ftorsion (kN)	Fdirect (kN)	Ftotal (kN)	Frame	Ftorsion (kN)	Fdirect (kN)	Ftotal (kN)
1	-1.2358	5.87	4.63	1	-0.3708	6.07	5.7
2	-0.9828	5.87	4.89	2	-0.2948	6.07	5.77
3	-0.3531	5.87	5.51	3	-0.1059	6.07	5.96
4	0.3531	5.87	6.22	4	0.1059	6.07	6.17
5	0.9828	5.87	6.85	5	0.2948	6.07	6.36
6	1.2358	5.87	7.1	6	0.3708	6.07	6.44

TABLE 12.15 Coefficients for Long Piles, $k_z = n_h z$

Z	A_x	A_θ	A_m	A_v	$A_{p'}$	B_x	B_θ	B_m	B_v	$B_{p'}$
0.0	2.435	−1.623	0.000	1.000	0.000	1.623	−1.750	1.000	0.000	0.000
0.1	2.273	−1.618	0.100	0.989	−0.227	1.453	−1.650	1.000	−0.007	−0.145
0.2	2.112	−1.603	0.198	0.956	−0.422	1.293	−1.550	0.999	−0.028	−0.259
0.3	1.952	−1.578	0.291	0.906	−0.586	1.143	−1.450	0.994	−0.058	−0.343
0.4	1.796	−1.545	0.379	0.840	−0.718	1.003	−1.351	0.987	−0.095	−0.401
0.5	1.644	−1.503	0.459	0.764	−0.822	0.873	−1.253	0.976	−0.137	−0.436
0.6	1.496	−1.454	0.532	0.677	−0.897	0.752	−1.156	0.960	−0.181	−0.451
0.7	1.353	−1.397	0.595	0.585	−0.947	0.642	−1.061	0.939	−0.226	−0.449
0.8	1.216	−1.335	0.649	0.489	−0.973	0.540	−0.968	0.914	−0.270	−0.432
0.9	1.086	−1.268	0.693	0.392	−0.977	0.448	−0.878	0.885	−0.312	−0.403
1.0	0.962	−1.197	0.727	0.295	−0.962	0.364	−0.792	0.852	−0.350	−0.364
1.2	0.738	−1.047	0.767	0.109	−0.885	0.223	−0.629	0.775	−0.414	−0.268
1.4	0.544	−0.893	0.772	−0.056	−0.761	0.112	−0.482	0.688	−0.456	−0.157
1.6	0.381	−0.741	0.746	−0.193	−0.609	0.029	−0.354	0.594	−0.477	−0.047
1.8	0.247	−0.596	0.696	−0.298	−0.445	−0.030	−0.245	0.498	−0.476	0.054
2.0	0.142	−0.464	0.628	−0.371	−0.283	−0.070	−0.155	0.404	−0.456	0.140
3.0	−0.075	−0.040	0.225	−0.349	0.226	−0.089	0.057	0.059	−0.213	0.268
4.0	−0.050	0.052	0.000	−0.106	0.201	−0.028	0.049	−0.042	0.017	0.112
5.0	−0.009	0.025	−0.033	0.015	0.046	0.000	−0.011	−0.026	0.029	−0.002

Based on *Drilled Pier Foundations*, by R. J. Woodward, W. S. Gardner, and D. M. Greer. McGraw-Hill, 1972.

Figure 9.1. List of coefficients for long piles

TABLE 12.16 Representative Values of n_h

Soil	n_h kN/m^3
Dry or moist sand	
Loose	1800–2200
Medium	5500–7000
Dense	15,000–18,000
Submerged sand	
Loose	1000–1400
Medium	3500–4500
Dense	9000–12,000

Figure 9.2. Values of n_h coefficient for different types of soils

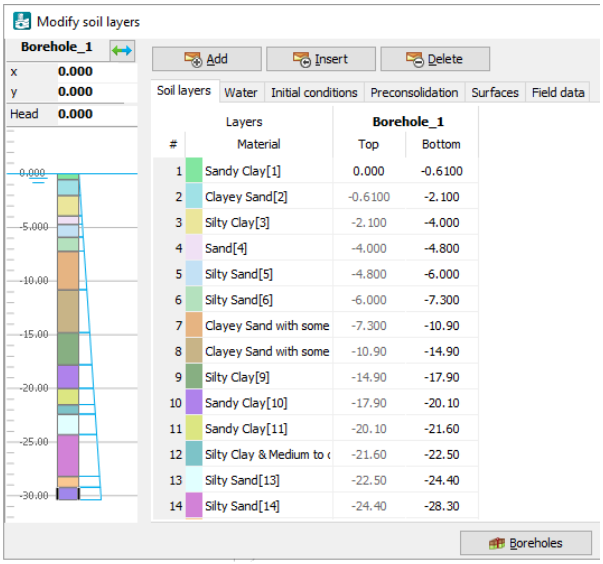

Figure 9.3. Soil profile input in Plaxis 2D and 3D

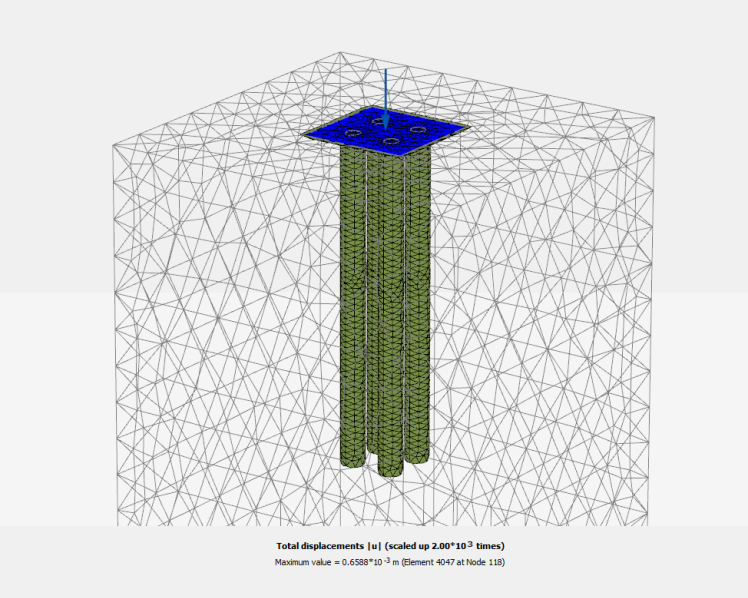

Figure 9.4. Software analysis of corner pile as a volume element

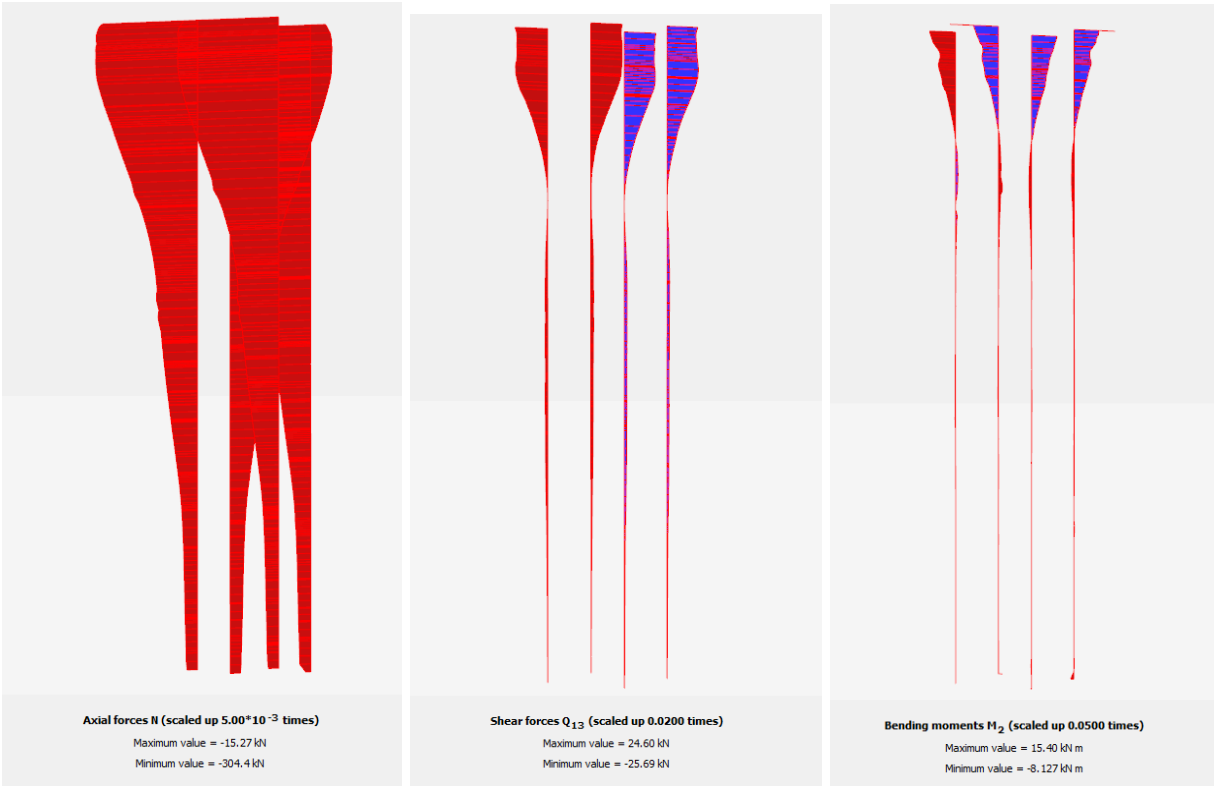

Figure 9.5. Axial and shear forces of pile volume element analysis

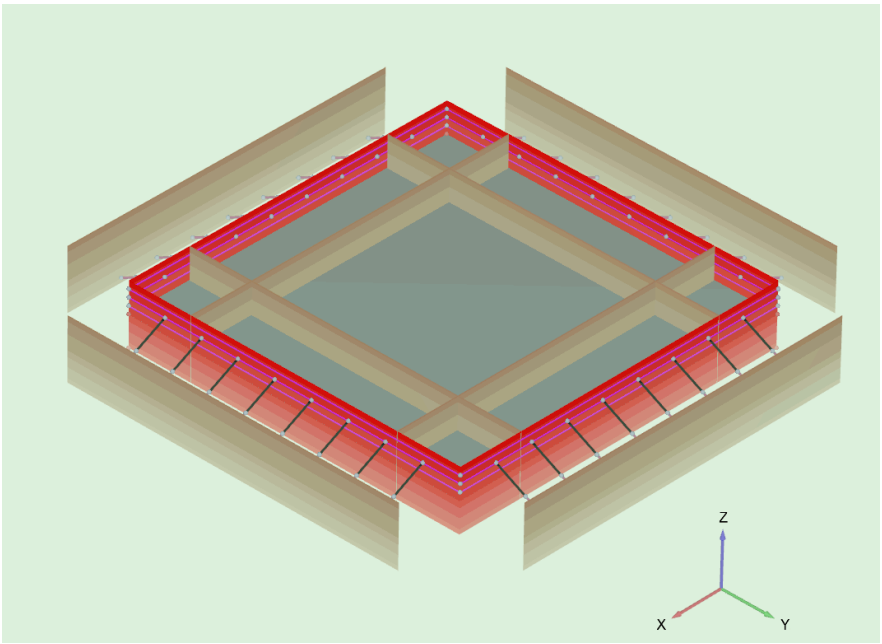

Figure 9.6. Excavation of the soil with the help of beams and sheet piles

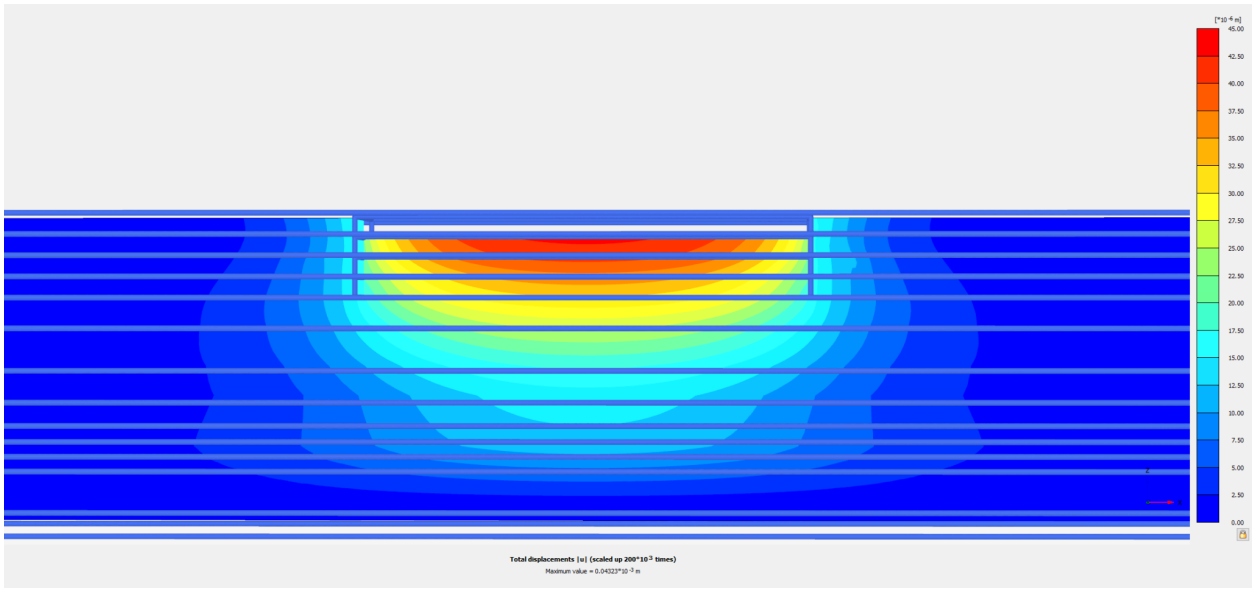

Figure 9.7. Total displacement of the excavation

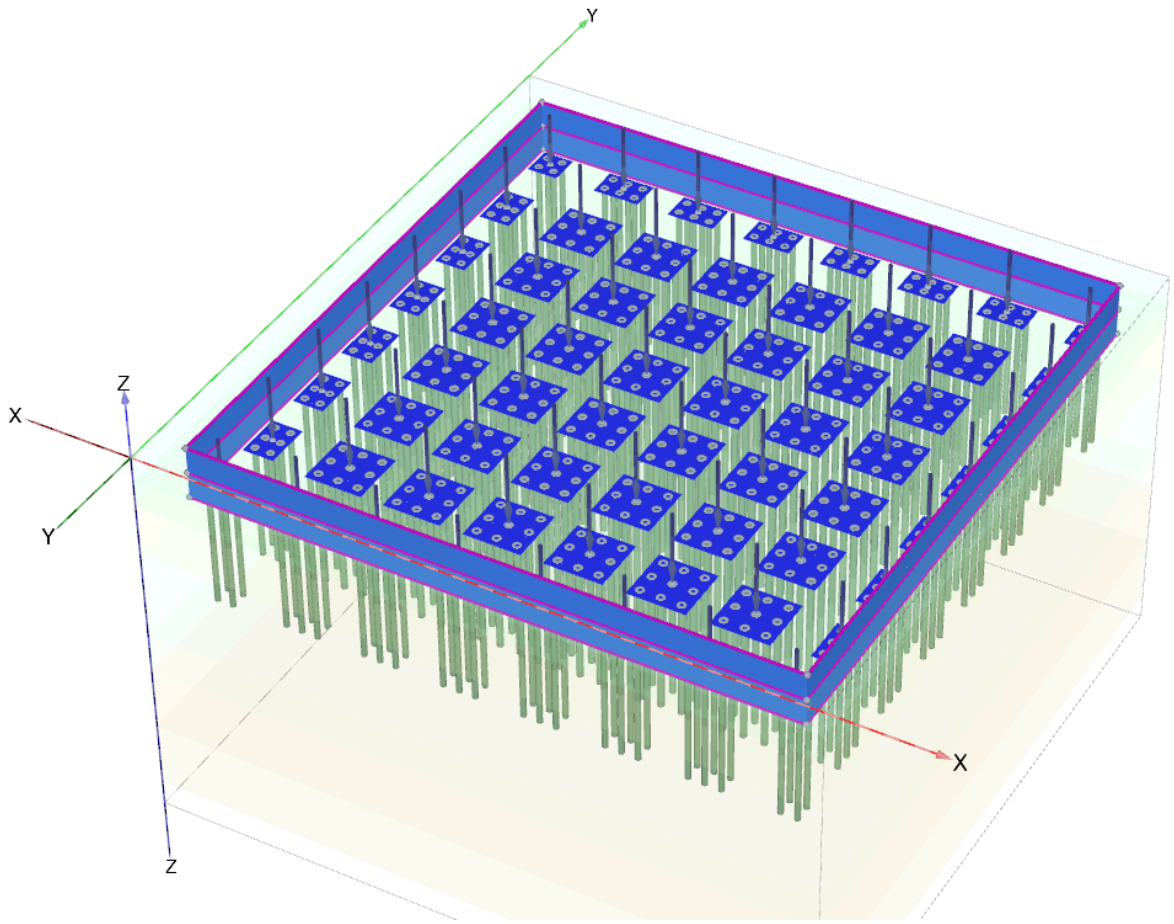

Figure 9.8. Sheet pile and group pile in Plaxis 3D